Volume 2 No. 1, 2007

CHEMISTRY JOURNAL OF MOLDOVA

General, Industrial and Ecological Chemistry

Editor-in-chief: Gheorghe DUCA

Academy of Sciences of Moldova
Institute of Chemistry
State University of Moldova

Volume 2 No. 1, 2007

CHEMISTRY
JOURNAL OF MOLDOVA

General, Industrial and Ecological Chemistry

Academy of Sciences of Moldova
Institute of Chemistry
State University of Moldova

Academy of Sciences of Moldova, Section of Biological, Chemical and Ecological Sciences, Institute of Chemistry
State University of Moldova, Department of Chemistry and Chemical Technology

CHEMISTRY JOURNAL OF MOLDOVA

General, Industrial and Ecological Chemistry

Editorial office address:
Institute of Chemistry, Academy of Sciences of Moldova, Str. Academiei, 3, MD-2028, Chisinau, Republic of Moldova
Tel: + 373 22 725490; Fax: +373 22 739954; e-mail: chemjm@cc.acad.md

ISSUE CONTENTS LIST WITH GRAPHICAL ABSTRACTS

RESEARCH DIRECTIONS AND THE MOST RELEVANT ACHIEVEMENTS OF CHEMISTRY RESEARCHERS IN THE REPUBLIC OF MOLDOVA FOR THE PERIOD OF 2004-2007

The first International Conference organized by the Chemical Society of Moldova has taken place in the early October 2003. Following are the most important research directions, objectives and realizations, achieved by different institutions involved in chemical research during the period of 2004-2007, presented in a very concise form.

The members of the Chemical Society of the Republic of Moldova perform investigations in various fields of modern chemistry: inorganic and bioinorganic, analytical and ecological, organic and bioorganic, physical and quantum chemistry. These investigations are performed in the 7 laboratories of the Institute of Chemistry of the Academy of Sciences of Moldova (ASM), the only one chemistry research institution in the country, as well as in other Academic Institutions (Institute of Genetics and Plant Physiology, Institute of Applied Physics, National Institute of Ecology) and University Centers like Scientific Center "Ecological and Applied Chemistry" from the State University of Moldova (the only one center of this profile in Moldova), at the Faculty of Chemistry and Chemical Technology of Moldova State University which includes the Chair of Inorganic and Physical Chemistry, Chair of Analytical and Organic Chemistry, Chair of Industrial and Ecological Chemistry, in other universities: Technical University of Moldova, State Medical and Pharmaceutical University "N. Testemițanu", State University of Tiraspol and State Agricultural University of Moldova. All the enumerated institutions are located in Chisinau. Certain research directions have been confirmed and gain ground in these institutions. Some of them locate scientific schools, recognized not only in Moldova but abroad too. Both fundamental and applied research is performed, that are important for the Moldovan National Economy.

The Republic of Moldova does not possess relevant minerals resources. The main branch of economy is agriculture and agricultural processing industry. Annually, the agricultural processing provides different wastes that can serve as renewable raw material for the production of different natural compounds. A part of these compounds are interesting as biologically active substances. The rest of them can be used and actually are used as raw material for the target synthesis of substances with potential applications in pharmaceutical, cosmetic, perfumery, food, wine and tobacco industries. Such investigations are realized in several institutions.

A positive evolution in the field of essential oil investigation and production is noticed in the recent years. This branch was almost destroyed after the disintegration of the Soviet Union. But the climatic conditions in Moldova are favorable for cultivation of essential oil producing plants.

Another research direction of primordial importance relates to ecology issues, first of all the problem of water resources which are rather limited in Moldova. Several scientific organizations work in this field and study different aspects of the problem: surface and underground waters, new technologies for purification of natural waters from undesirable contaminants are being elaborated (hydrogen sulfide, fluorine and iron salts, etc.), as well for treatment of residual waters.

One of the oldest research directions of chemical investigations, adopted broadly in several institution of Moldova, relates to the chemistry of coordination compounds.

The last 2-3 years have witnessed positive changes in the field of scientific research. But anyway, the science in general and chemical science in particular meets some difficulties, due to the absence of relevant equipment, limited access to the information, low level of salary. As a result, the field of research still remains a non-prestigious field of human activity for the younger generation. Under these circumstances it is very important for us to establish scientific collaboration with colleagues from abroad, including European Union, USA, Israel and other countries within collaborative bi- and multilateral projects (INTAS, NATO, CRDF/MRDA, Humboldt, DAAD, etc.). One of the basic priorities of this collaborations is establishing of new collaborative relationships with our colleagues from abroad and extinction of those existent, first of all in European Union in order to integrate in the 7-th framework program. We will update below in a concise way the basic directions of fundamental and applicative research, as well as the more important results achieved by each chemistry research unit from Moldova during the period of 2004-2007, after the first Conference of the Chemical Society of Moldova. It is intended to facilitate in such a way mutual contacts and collaborative relations with our colleagues from abroad. It is noteworthy mentioning that preparation of highly qualified specialists takes place in the same institutions that are involved in the chemistry research.

Institute of Chemistry of the Academy of Sciences of Moldova

Laboratory of Coordination Chemistry

A range of coordination compounds (~150) of 3d transition metals (such as V, Cr, Mn, Fe, Co, Ni, Cu, Zn) with such organic ligands as mono- and dicarboxylic acids, thiosemicarbazide, α-dioximes, bipyridile, imidazole, etc, have been synthesized and investigated. Using the template synthesis, mono-, bi- and polynuclear macrocyclic compounds with an open profile were obtained. New carboxylate classes and types have been obtained; among them were found compounds with such potential useful properties as single molecule magnets, ferro- and antiferromagnets, catalysts for the oxidation processes and stimulators of biosynthesis in microorganisms. The stimulator properties are characteristic for cobalt and copper compounds, i.e. cobalt (III) dioximates with fluorine containing anions and compounds of 3d metals with tetradentate ligands based on S-alkylisothiosemicarbazones of aromatic aldehydes and β-diketones. Some compounds demonstrated non-linear optical activity and can be used in optical electronics. A number of colored complexes of Ni(II) and Co(II) can serve as effective pigments for coloring the plastics.

(Head of laboratory, dr. hab. sci., prof. Bulhac I.)

Laboratory of Bioinorganic Chemistry

During the 2004 to 2006 period the laboratory of bioinorganic chemistry of the ASM continues to synthesize and study the homo- and heteronuclear oxo-carboxylates complexes containing d-, s- and f- metals. For the first time there were obtained a new set of tri-, tetra-, hexa-, nona, dodeca- and polynuclear complexes with the fragments $\{Fe_2MO\}$, $\{Fe_3LnO_2\}$, $\{Fe_4Ca_2O_2\}$, $\{Mn_{10}Fe_2O_{12}\}$, $\{Mn_{10}Ln_2O_9\}$, $\{Cu_2\}$, $\{Nd_2\}$, $\{Sm_n\}$, $\{Dy_n\}$, $\{Fe_3O(Fc)_6\}$, $\{(Ba_2Fe_2)_n\}$, $\{(FeSr_2)_n\}$), where M = s-, d-; Ln = f-elements; Fc = carboxyferrocenyl. The obtained complexes were studied by different physical methods: X-ray, IR, UV-VIS, EPR, luminescence and Mossbauer spectroscopy, thermogravimetry and magnetochemistry. By introduction of monodentate ligand with different affinity to coordinated metals in heterotrinuclear clusters with $\{Fe_2MO\}$ core and having the properties to form the intermolecular bonds it was demonstrated the possibility to localise the position of heterometal in this triangle.

Using the Schiff bases obtained by condensation of 3-formylsalycilic acid, 2-oxy-3-carboxynaftaldehide, oxy-acids of Krebs cycle with different ammines the new mono-, or polynuclear coordination compounds of d- and f- elements were synthesized and characterized.

The synthesized coordination compounds were tested with the purpose to obtain new biological active substances for biotechnology and physiology of plants. Several of the obtained compounds stimulated biomass accumulation of the strains of *Rhizopus arrhizus* F67, *Spirulina platensis*, as well as increasing the content of biologically active compounds like aminoacids, carotenoids, iron derivatives. Some of investigated substances showed growth stimulating properties for plants.

(Head of laboratory, corresponding member of the ASM, dr. hab. sci., prof. Turtă C.I.)

Laboratory of Quantum Chemistry and Chemical Kinetics

In the field of quantum chemistry the mechanism of the oxygen and phosphor molecules activation in the processes of coordination to the transition metals compounds in numerous important chemical reactions in chemistry, biology, medicine and the environment have been revealed. Using the vibronic theory of small molecules activation in the combination with the ab initio calculations a series of coordinative compounds of the transit metals (Mn, Fe, Co, Cu, Rh, Ir) with a variety of ligands (porphirines, phtalocianines, fenantroline, pyridine etc) have been studied.

It was demonstrated that the oxygen activation is due to the partial transfers of the charge to and from the dioxygen orbitals, and not to the total charge transfer. This explains why some compounds add the dioxygen in the reversible way, while in other cases the coordination is reversible. The results obtained contribute to the understanding of the dioxygen and phosphor activating processes.

Based on quantum chemical calculations the theory of the exchange interaction of the electrons transfer and the magnetic properties in poly-nuclear systems was developed.

(Head of laboratory, dr. hab. sci., prof. Ogurtsov I.Ya.)

Laboratory of Ecological Chemistry

During the period between 2004-2007 new methods for obtaining a number of adsorptive materials for environmental and health protection have been elaborated on the basis of secondary materials after grape processing. Their phisico-chemical properties have been studied. Carbonic adsorbents and catalysts have been obtained from vegetal byproducts (nutshells, peach and plum stones etc.). Adsorptive properties of cross linked adsorbents based on local diatomites and chemically modified ones have been studied. Technologies for underground and surface waters purification have been elaborated in order to eliminate hydrogen sulfide and nitrate contaminants. New plaster mixtures have been elaborated and implemented in the field of civil engineering. A new preparation has been obtained from the vinery wastes and it showed bold antifungal and antimicrobial properties.

(Head of laboratory, dr. hab. sci., prof. Lupaşcu T.)

Laboratory of Physico-Chemical Methods of Research and Analysis

An accumulation analysis method in adsorptive catodic stripping voltametry has been developed. The proposed procedure is performed in the presence of thiosemicarbaside derivatives, including application of modified carbon fiber electrodes. Methods have been elaborated for the determination of Cd, Cu, Pb, Ni in the food products and natural waters, including Nistru river. Investigations have been performed in order to evaluate the electrochemical behavior of systems metal - oxidation agent in the presence of new organic reagents for amplification of the analytical signal. Determination procedures have been elaborated using the method with anodic stripping for metals like Hg, Cd, Pb, Zn, Tl. Modification of the microelectrode by deposition of a nanolayer of mercury has led to a considerable method sensitivity and selectivity increase. Using this method it was possible to determine Tl in the Nistru river water and sediments and Cd in the soil samples.

(Head of laboratory, dr. Chiriac L.)

Laboratory of Organic Synthesis

The investigations in the field of organic synthesis revolve around the targeted synthesis of combinatorial libraries of heterocyclic bioactive compounds, based on the computational SAR studies. Following work is performed to estimate the match between forecasted and observed physiological effects. New heterocyclic compounds with cognition enhancing, anxiolitic and anticonvulsant properties have been prepared on the basis of benzoic acids hydrazides. A special attention has been paid to the synthesis of compounds with antituberculosis activity, a malady that poses problems both in the Republic of Moldova and other countries too. More then 40 new substances have been obtained from the 5-aryl-2-thio-1,3,4-oxodiazol series with this purpose and tested in the USA. The *in vitro* tests results have demonstrated a good correlation between forecasted and real activity. Four compounds with relevant activity have been selected for advanced studies. A number of compounds with psychotropic activity has been synthezed on the basis of izatine and oxazolidines. Two compounds from this series have shown higher activity then generic pharmaceuticals “Medazepam” and “Piracetam”. Derivatives of 1,3-imidazole and 1,2,4-thiazole with antifungal activity have been obtained.

(Head of laboratory, dr. hab. sci., Macaev F.Z.)

Laboratory of Terpenoid Chemistry

The field of natural product chemistry and synthesis has a long history in the Institute of Chemistry. Current efforts have been oriented to the synthesis of terpenes with specific structure and properties. The range of the investigated substrates spreads from monoterpenes to polyprenols. A special emphasize was placed on the synthesis of a series of sesquiterpenoids with drimanic structure (hydrocarbons, alcohols, ketones, lactones, esters and polyols). An original method for the fotodehydrogenation of α,β-unsaturated cyclic ketones to α,α-dienones has been elaborated.

The synthesis of austrodoral and austrodoric acid, natural norsesquiterpenoids of marine origine, has been performed for the first time. This work provided a new approach to the highly functionalized perhydrindane skeleton and confirmed the structure and stereochemistry of the corresponding natural compounds.

The natural bioactive diterpenoid ω-hidroxigeranylgeraniol has been obtained by two different approaches.

Onoceranic triterpenes have been prepared by a short and straightforward procedure from readily available homodrimanic compounds.

The method of cyclic terpenoids preparation by superacidic cyclization has been developed on more complex substrates. Investigation of ω-hidroxigeranylgeraniol derivatives cyclization has led to the elaboration of a new biomimetic procedure for the synthesis of sacculatanic diterpenoids. Studying the superacidic cyclization of linear sesterterpenic esters it was stated that the configuration of the internal double bond allows controlling the structural selectivity of the reaction, simulating the biogenetical behavior of natural polyprenols. It was demonstrated on the other hand that the superacidic cyclization reaction of the sesterterpenic derivatives can be also directed by a specific placement of a phenylsulfonyl group in the certain positions of the aliphatic chain.

It was established that the superacidic cylization of terpenoids can be realized in the ionic liquid medium. Substrates with functional groups stable to acidic conditions showed excellent results in these experiments.

(Head of laboratory, academician of ASM, dr. hab. sci., prof. Vlad P.F.)

Institute of Genetics and Plant Phisiology of the Academy of Sciences of Moldova

Laboratory of Natural Bioregulators

Natural products of steroid structure are studied for a long time in Moldova. A series of more then 50 steroidal glycosides of spirostanolic and furostanolic structures have been isolated from 3 species of plants of Solanaceae family (*Hyoscyamus niger L.*, *Physalis alkekengy L.*, and *Physalis leguminose L.*). These compounds contain as aglicones tigogenine, diosgenine and gitogenine, whyle their shugar chain in the C-3 position contains from 2 to 5 monozaharidic residues with linear or branched structure. Among the isolated spirostanolic oligozides there are compounds which

possess antibacterial, antimicrobial and antifungal activity. The preparation "Pacovirin" has been implemented in pharmaceutical production for the treatment of viral hepatitis. Some furostanolic glycosides showed plant growth regulator properties.

(Head of laboratory, dr. hab. sci., prof. Chintea P.C.)

Institute of Applied Physics of the Academy of Sciences of Moldova

Tadeusz Malinowski Laboratory of Physical Methods of Solid State Investigation

The laboratory is involved in structural study of different classes of chemical compounds. The basic priority is given to crystal engineering of supramolecular systems. New results oriented to the construction of heterometalic (d/f) complexes based on pyridine- carboxylic acids have been obtained during the recent years. These complexes are potential candidates for molecular electronic devices. Besides, bioactive binary and mixed complexes of transition metals with α-aminoacids have been investigated. The structure of layered systems with nano-dimentional cavities and channels has been studied with the perspective of obtaining on their basis of inclusion compounds with hydrogen, methane and other gases. The investigations of week interactions in host-guest complexes, especially those on the basis of crown ethers and azamacrocycles have been continued. The dependence structure-properties for the biologically active compounds and multi-component crystals including pharmaceutically active components is investigated too.

(Head of laboratory, dr. Simonov Yu.A.)

Laboratory of Materials Electrochemical Treatment

The main scientific activity has been concentrated on the problems of electrochemical dimensional micro- and nanotreatment and also to the development of methods of obtaining of the electrochemical coverings possessing unique functional properties. Essentially new method of determination of throwing power of electrolytes in controllable hydrodinamical conditions was proposed and investigated. Conditions of controlling micro- and macro distribution of current and rates of machining during electrochemical micromachining in presence of photoresist masks on nonuniform surfaces are developed, including under pulse conditions.

Influence of surface heat production on electrodeposition rate, on current density – deposition rate dependences; on technological parameters (first of all, for the case at chromium plating), including electrolyte throwing power and structure of the deposited layers were investigated for electrodeposition of chromium in standard chromic electrolyte and Co-W alloys in citrate electrolyte, at various bulk electrolyte temperatures and current densities of constant and pulse currents. It is shown, that the unipolar pulse current application increased the throwing power of standard chromic electrolyte.

The laboratory develops also cooperative projects with several IAP laboratories, Chisinau Technical University and foreign institutions. Electrochemical methods of obtaining nanocomposition, low-dimensioned objects and nanostructures with reference to the solution of problems of efficiency increasing of alternative energy sources and controlling of functional properties of surfaces were developed within these cooperations.

(Head of laboratory, corresponding member of the ASM, dr. hab. sci., prof. Dicusar A.I.)

Laboratory of Substances Electroflotation

The activation regularities of alluminium hydroxides and of some natural mineral sorbents from Moldova have been studied under different conditions, including electrical and thermal treatment and treatment with calcium oxide. The principles of tuning the properties of these adsorbents have been revealed. Active adsorbents with different broadly ranging structures and superficial properties have been obtained. The action of electrolysis gases on the superficial properties of mineral adsorbents has been studied. It is proposed to use these treated adsorbents for the elimination of some organic substances present in underground waters. Some toxic compounds have been eliminated from aqueous solutions by electrodialysis method. It was demonstrated that modified adsorbents can be utilized for the elimination of some noxious colorants and fluorine compounds from natural and residual waters. The mechanisms of fixing these compounds on the surface of the modified adsorbents have been clarified.

(Head of laboratory, dr. Zelenţov V.I.)

Institute of Ecology and Geography of the Academy of Sciences of Moldova

Laboratory "Quality of the Environment"

The ecological state of Moldova aquatic resources has been evaluated. Advanced methods and technologies have been elaborated for the liquid systems purification. The factors that cause equilibrium changes in the system water-suspensions and water quality parameters have been evaluated. Their autopurification capacity has been correlated to the organic substances content. The influence of natural waters alkalinity and acidity on the suspension and colloid substances coagulation has been determined. The current state of Prut river effluents has been estimated. It was shown

that industrial and agricultural pollutants are present in the boundary effluents and they inhibit the autopurification and nitrification processes. The local transboundary pollution burden has been calculated. A total number of 39 ISO standards have been recommended for implementation as national standards of water quality monitoring.

(Head of laboratory, dr. Tărîță A.)

State University of Moldova. Faculty of Chemistry and Chemical Technology

Research Center "Applied and Ecological Chemistry"
Laboratory "Redox and catalytic processes in food products and water" and Industrial and Ecological Chemistry Chair

A new procedure for tartaric acid and its derivatives obtaining from winery secondary products has been elaborated using liquid anionites for the tartaric acid extraction. The extraction process mechanism has been studied on model and real systems (wine yeasts, cognac winace) and a pilot-plant for tartaric acid production has been assembled.

N-nitrosoamines formation reaction as well as the nitrozation process inhibition have been studied by application of different natural and synthetic inhibitors, including those obtained from tartaric acid. Investigation of redox processes that take place in model and real systems has served for the elaboration of combating and prevention methods of their negative impact by natural biologically active substances promoted inhibition of nitrozation reactions that take place in food products, tobacco and humans. Electrochemical methods for nitrate and nitrite elimination has been elaborated for natural waters purification.

Following studies are also oriented on the elaboration of physico-chemical methods for diminishing the concentration of textile dies in residual waters.

(Scientific supervisor academician of ASM, dr. hab. sci., prof. Duca Gh., head dr. Gonța M.)

Laboratory "Electrochemical Processes and Ecologically Clean Production"

Methods for water purification have been elaborated and refined, basing on purification intensification by different physical actions. Study of photocatalitic and oxidoreductive degradative purification of water from organic persistent pollutants has been performed. There were elaborated electrochemical purification methods of natural and residual waters, as well as sorptive and membrane water conditioning technologies. Intensification of the pollutants destructive processes has been effected by microbiological and biochemical pathways. These approaches were considered in the production of alternative fuel sources like biogas from wastewaters and winery wastes. Electrochemical and chemo-catalitic processes for reduction of d-metals from solutions leading to alloys have been studied. The research has included also catalytic purification processes of different gaseous pollutants.

(Scientific supervisor academician of ASM, dr. hab. sci., prof. Duca Gh., head dr. Covalev V.)

Laboratory "Atmosphere Protection"

The influence of the homogeneous catalyst "Biofriendly" on the pollutant emissions originated from internal combustion engines has been studied. It was established that the content of carbon monoxide in the exhaust shows a 1.5-3 fold decrease, nitrogen oxides show a 1.3-1.6 fold decrease and methane shows a 1.4-1.6 fold decrease. The amount of smoke-black which contains carcinogenic hydrocarbons also decreases. The gasoline consumption is reduces by 10% and of the diesel fuel by 15%. Implementation of the homogeneous catalyst will lead to the improvement of the air basin in the Republic of Moldova.

Investigations of natural gas combustion in an electric field have been performed. It was demonstrated that application of a 12kV tension at 32mA improves the combustion yield by increasing flame temperature, reduces carbon monoxide content in the exhaust from 1.2% to 0.012% and saves 5% of fuel. A semiconducting sensor for the determination of carbon monoxide has been elaborated and tested.

(Scientific supervisor academician of ASM, dr. hab. sci., prof. Duca Gh., head dr. Crăciun A.)

Laboratory "Ecological Chemistry of Aquatic Systems"

Autopurification processes of both model and various field aquatic systems have been studied. Model studies included oxidation processes of some organic substances (benzoic and citric acids, cisteine and hydrochinone) catalized by Cu^{2+} and Fe^{3+} ions in the presence of oxygen and hydrogen peroxide. New methods for surface water quality estimation have been approved (redox state and autopurification kinetic parameters). New informational criteria for the estimation of ecological state of natural waters have been elaborated. The state of the Nistru river water has been investigated and traditional hydrochemical parameters as well as their redox state have been determined. It was confirmed that the redox

state of the natural waters and kinetic parameters can serve as indicators for the water quality estimation and forecasting dangerous consequences following the changes in the redox state and kinetic parameters. It was established that for the Nistru river waters season changes in the redox state is a characteristic feature and hydrogen peroxide concentration ($\sim 10^{-7}$) is not sufficient for an efficient realization of water autopurification processes which negatively influence the hydrobiota. The influence of some pesticides on water autopurification process has been investigated.

(Scientific supervisor academician of ASM, dr. hab. sci., prof. Duca Gh., head dr. Goreaceva N.)

Analytical and Organic Chemistry Chair

New thiosemicarbazones of 8-chinolinaldehyde have been obtained and new copper and palladium coordination compounds have been synthesized on their basis. Their biological activity and influence of substituents on the optical properties of copper complexes have been tested. The magnetic behaviour of copper binuclear complexes has been interpreted. It was established that the investigated thiosemicarbazones amplify their antibacterial properties on complexation with copper (II) and palladium (II). Membranes for potentiometric sensors have been created for the determination of perchlorates and nitrates. The target oriented transformation of S-methylthiosemicarbazone of salicylic aldehyde has been studied in the presence of sodium tetranitropalladate. The nitrosoamidation reaction has been described for the first time. The ligand assembled by thioamide group condensation is tridentate and condenses with the O,N,N atom set. Organic compounds have been obtained on the basis of isothiocyanatochalcones. A series of work relates to the synthesis and study of monomers and binary and ternary copolymers based on carbazolylmetacrilate with the aim of producing different organic semiconductors used in the optical information recording.

(Head of chair, dr. Dragalina G.)

Inorganic and Physical Chemistry Chair

There have been elaborated synthesis methods of new coordination compounds of Co, Ni, Cu and Zn with thio- and semicarbazones, hydrazones and Schiff bases of substituted salicylic aldehydes and pyridine-2-carboxialdehyde. New mono- and heterometalic coordination compounds of Bi (III) and Cr(III) have been obtained using as ligands nitrilotriacetic, β-hydroxiethyl-iminodiacetic, antranylodiacetic and ethylenediamine-tetraacetic acids with elements from s- and d-element blocks (Mg, Ca, Sr, Ba, Mn, Co, Ni, Cu, Zn etc.), their composition and structure have been established. The isomerisation mechanism of cobalt (II) octahedral complexes has been established. The biological activity of these substances has been tested. Some of compounds showed anticancer and antimicrobial activity. The heterometalic compounds of Bi (III) have high specific resistance (10^{14}-10^{15} Ohm·cm) and can serve as dielectric materials. Some chromium complexes can be used as molecular magnets.

A series on natural and synthetic adsorbents have been obtained and studied as selective catalysts for potable and residual water purification, stabilization of brute wines and juices.

(Head of chair, corresponding member of the ASM, dr. hab. sci., prof. Gulea A.)

Technical University of Moldova. Chair of Chemistry

Investigation of natural products is aimed to isolation of biologically active compounds from accessible natural sources. Efficient methods for the isolation and purification of hialuronic acid are considered. It is a biologically active compound found in different sources of animal origin with specific properties and could be used for production of new derivatives and compositions with potential application in food industry, pharmaceutical and cosmetics production. It is noteworthy mentioning that existing hyaluronic acid production and purification methods does not allow its broadly implementation.

Another research direction consists in the elaboration of technologies for preparation of iodine enriched products. Sunflower oils iodination product is used as iodine source. A procedure for the production of iodine fortified lactoacid products has been elaborated.

(Head of chair, dr. Verejan A.)

Tiraspol State University. Faculty of Chemistry and Biology

Chair of Chemistry

A series of more then 50 new Co(III) dioximates containing florous anions ($[BF_4]^{-1}$, $[PF_6]^{-1}$, $[SiF_6]^{-2}$, $[ZrF_6]^{-2}$, $[TiF_6]^{-2}$, $[AlF_6]^{-3}$ etc.) have been synthesized and studied. Dioximates have been obtained, where the complex cation charge is compensated simultaneously by two different anions. Some of the obtained compounds stimulated or stabililized biosynthetic processes in some fungal strains of genus *Rhizopus* and *Aspergillus* under unfavorable activity conditions.

The department participate in the realization of investigations of underground aquatic sources quality in

Chisinau, Ungheni and other rural localities. The content of a number of metals (Fe, Zn, Cu, Cr, Ni, Pb) and nitrates and mineralization degree has been determined.

(Head of chair, dr. Corobceanu E.)

N. Testemitanu Medical University of Moldova. Chair of Chemistry

The kinetics and reaction mechanism of catalytic homogeneous decomposition of hydrogen peroxides promoted by Mn(II) coordination compounds with *o*-fenantroline and α,α-dipyridil have been studied. The reaction mechanism has been suggested for these processes and further confirmed experimentally. It was demonstrated that the studied catalytic reactions proceed *via* a chain ion-molecular mechanism. The possibility of using the studied catalytic systems for determination of macro- and micro-quantities of Mn in homogenous phase has been demonstrated. The catalytic properties of coordination compounds of Fe(III) and Mn(III) with *o*-fenantroline and α,α-dipyridil has been studied in several periodate promoted redox reactions.

(Head of chair dr. hab. sci., prof. Tighineanu I.)

State Agricultural University of Moldova. Chair of Chemistry

The Chair of Chemistry has performed collaborative research jointly with the laboratory of quantum chemistry and chemical kinetics of the Institute of Chemistry of ASM. The process of white phosforus activation under the action of Ni and Cu coordination compounds has been studied. The secondary metabolites of red pepper *Capsicum Annuum L.* have been studied. The typical pepper metabolites like capsaitinosides, glycoalcaloids and steroid glycosides have been extracted and characterized.

(Head of chair, dr. Gorgos V.)

In summary, the results of the research activity in the field of chemistry have been materialized by publication of 440 articles in international editions and 235 papers in local editions. There were also 816 presentations at international conferences and 232 at local scientific meetings. 222 patents have been obtained. 15 Ph.D. and 2 habilitation theses have been successfully presented.

Academician Pavel F. VLAD
President of the Chemical Society of Moldova

Academician Gheorghe DUCA
President of the Academy of Sciences of Moldova

Academy of Sciences of Moldova
The Chemical Society of the Republic of Moldova
Department of Biological, Chemical and Ecological Sciences
Institute of Chemistry
State University of Moldova

The IInd International Conference of the Chemical Society of Republic of Moldova (ICOCSM-II) "Achievements and Perspectives of Modern Chemistry"

October 1-3, 2007
Chisinau, MOLDOVA

The Organizing Committee is glad to invite you to participate in the **IInd International Conference "Achievements and Perspectives of Modern Chemistry"** organized by the Chemical Society of the Republic of Moldova.

The conference will be hosted by the Institute of Chemistry of Academy of Sciences of Moldova on October 1-3, 2007.

The conference will produce a good opportunity to exchange ideas and experience in a wide spectrum of chemical research. Being an international and interdisciplinary one, ICOCSM-II will highlight the recent important scientific achievements in inorganic and physical chemistry, analytical chemistry and environmental protection, organic and bioorganic chemistry. The special attention will be paid to the compounds with the library of useful properties, e.g., molecular magnets, sensors, biologically active compounds.

SCIENTIFIC PROGRAM

Original fundamental and applied works will be submitted. Only the communications containing novel unpublished and significant results will be accepted. The Conference program will include Plenary Lectures, Oral Presentations and Posters. Scientific program will be organized around the following topics:

- Inorganic and physical chemistry;
- Analytical chemistry, chemical technology and environmental protection;
- Organic and bioorganic chemistry.

English is the official language of the conference.
No translation facilities will be provided.

ORGANIZING COMMITTEE

Pavel Vlad - Chairman
Tudor Lupascu - Co-chairman
Elena Gorincioi - Secretary
Aculina Arîcu
Ion Bulhac
Petru Chetruş
Galina Dragalina
Aurelian Gulea
Fliur Macaev
Ivan Ogurţov
Mihail Revenco
Yurii Simonov
Ion Toderaş
Constantin Turtă

PROGRAM COMMITTEE

Elena Gorincioi - Secretary
Tatiana Cazacu
Maria Cocu
Diana Dragancea
Carolina Edu
Marina Grinco
Veaceslav Kulciţki
Ana Lazarescu
Raisa Nastas
Sergey Pogrebnoi
Denis Prodius
Andrei Tikhonovschi
Marina Tcaci

INTERNATIONAL ADVISORY BOARD

Gheorghe Duca (Moldova) - Chairman
Ionel Haiduc (Romania) - Co-chairman
Freddy Adams (Belgium)
Vladimir Arion (Austria)
Sergey Andronati (Ukraine)
Irina Beletskaya (Russia)
Isaak Bersuker (USA)
Ivano Bertini (Italy)
Liviu Chibotaru (Belgium)
Wim Dehaen (Belgium)
Calin Deleanu (Romania)
Athina Geronikaki (Greece)
Vladislav Goncharuk (Ucraine)
Aede de Groot (Holland)
Vladimir Khripach (Belarus)
Fedor Lakhvich (Belarus)
Marcin Leonowicz (Poland)
Janusz Lipkowski (Poland)
Matei Macoveanu (Romania)
Andrei Malkov (UK)
Aurelia Meghea (Romania)
Raluca Mocanu (Romania)
Margareta Nicolau (Romania)
Galina Petukhova (Russia)
Sorin Rosca (Romania)
Bogdan Simionescu (Romania)

CONTACT INFORMATION

Dr. Elena Gorincioi – Conference Secretary
Institute of Chemistry, Academy of Sciences of Moldova
Academiei Str. 3, MD-2028, Chisinau, Moldova

Tel: (+373-22) 739963, Fax: (+373-22) 739954
E-mail: chemconf@cc.acad.md gorincioi_elena@yahoo.com

NANOSCOPIC MOLECULAR CLUSTER V_{15}: HIGH-FIELD EPR AND MAGNETIZATION AT ULTRA-LOW TEMPERATURES§

Boris Tsukerblat,[a] Alex Tarantul,[a] Achim Müller [b]

[a] *Department of Chemistry, Ben-Gurion University of the Negev, 84105 Beer-Sheva, Israel, e-mail: tsuker@bgumail.bgu.ac.il*
[b] *Fakultät für Chemie, Universität Bielefeld - 33501 Bielefeld, Germany, e-mail: a.mueller@uni-bielefeld.de*

In memory of Professor Yurii E. Perlin on the occasion of his 90 th birthday – to highlight his exceptional achievements and kudos

Abstract: In this paper we give a short overview of our efforts in the understanding of the magnetic properties of the fascinating nanoscopic cluster present in $K_6[V^{IV}_{15}As_6O_{42}(H_2O)]\cdot 8H_2O$ (hereafter V_{15}) exhibiting layers of magnetization. We analyze EPR and adiabatic magnetization of the V_{15} cluster with a triangular V^{IV}_3 array causing spin frustration. A model for V_{15} includes isotropic and antisymmetric (AS) exchange interactions in the general form compatible with the trigonal symmetry. Orientation of the AS vector (but not only its absolute value) is shown to play an important physical role in spin-frustrated systems. We were able to reach perfect fit to the experimental data on the stepwise dependence of magnetization vs. field at ultra-low temperatures. Furthermore, it was possible for the first time to estimate precisely two components of the AS vector coupling constant, namely, in-plane component and the perpendicular part. We show that only intramultiplet transitions in EPR are allowed when the vector of AS exchange is normal to the plane of vanadium triangle, meanwhile the in-plane part of AS exchange gives rise to a series of weak intermultiplet transitions. Experimental data on high-frequency EPR of V_{15} at low temperatures are discussed. The spin-vibronic effects in trimeric spin frustrated clusters are also studied and an important role of the interplay between the AS exchange and Jahn-Teller interaction is revealed. The results clarify the concept of spin-frustration in view of its magnetic and spectroscopic manifestations in metal clusters.

Keywords: nanoscopic molecular magnets; V_{15} cluster; antisymmetric exchange; Jahn- Teller effect.

1. INTRODUCTION

During the past decade growing attention has been attracted by a large unique cluster anion present in $K_6[V^{IV}_{15}As_6O_{42}(H_2O)]\cdot 8H_2O$ containing 15 ions V^{IV} (S_i=1/2) and exhibiting layers of different magnetizations [1–4]. The discovery of this fascinating system [1] opened a new trend in molecular magnetism closely related to the promising field of single molecule magnets that is expected to give a revolutionary impact on the design of new memory storage devices of molecular size and quantum computing. Studies of the adiabatic magnetization and quantum dynamics show that the V_{15} cluster exhibits the hysteresis loop of magnetization [5–10] of molecular origin and can be referred to as a mesoscopic system on the border line between classical and quantum world. The studies of the static magnetic susceptibility [3,4], energy pattern [11–18] and inelastic neutron scattering [19,20] showed that the low lying part of the energy spectrum is well isolated from the remaining spin levels and can be understood as a result of interaction between three moieties consisting of five strongly coupled spins giving rise to spin S_i=1/2 of each moiety. The three-spin model for the low lying excitations so far suggested [3,7] includes isotropic Heisenberg-Dirac-Van Vleck (HDVV) exchange interaction and AS exchange firstly proposed by Dzyaloshinsky [21] and Moria [22] as an origin of spin canting. The understanding of the role of the AS exchange in spin frustrated systems dates back to the seventies (see review article [23] and references therein). AS exchange was shown to result in a zero-field splitting of the frustrated ground state of the half-integer triangular spin systems, magnetic anisotropy, essential peculiarities of the EPR spectra and wide range of phenomena related to hyperfine interactions [23–35]. Some of the conclusions of these early papers have been mentioned later [17], in particular, those regarding the zero-field splitting and Kramers theorem (see [36]).

Hereunder we give a short overview of the magnetic interactions in V_{15} system with the emphasis on the manifestations of AS exchange. The three spin model is analyzed and applied to the study of energy level crossover in magnetic fields of different directions and to phenomena like low-temperature EPR, high field magnetization and structural instabilities arising from the spin-vibronic interaction and Jahn-Teller effect.

§ Material presented at the XV-th Conference "Physical Methods in Coordination and Supramolecular Chemistry", September 27 - October 1, 2006, Chişinău, Moldova

2. THE HAMILTONIAN, SYMMETRY PROPERTIES

The molecular cluster V_{15} has a distinct layered quasispherical structure within which fifteen V^{IV} ions ($s_i = 1/2$) are placed in a large central triangle sandwiched by two distorted (non-planar) hexagons [1,2] possessing $\mathbf{D}_3$ symmetry (Fig.1-3). Each subunit consisting of two spin-paired dimers and a spin of the triangle can be considered as an effective spin $s = 1/2$ placed in the central layer (Fig.1-3). This can be justified by consideration of the isotropic exchange parameters within the metal network J_1, J_2, J', J'' (see Fig.2,3) that have been firstly estimated in [3,4]. The parameter of the intradimer interaction in the hexagons is shown to be the leading one while the parameters J_1, J', J'' are significantly smaller and seem to be of the same order so that each spin of the central triangle is coupled to a pair of strongly coupled spins belonging to the lower and upper hexagons as shown in Fig.3. Each pentanuclear subunit consisting of two dimers (marked in bold in Fig.3) and a spin of the triangle can be considered as an effective spin $s = 1/2$ placed in the central layer so that the low lying part of the energy pattern of the system entire can be viewed as the result of spin coupling within the triangular cluster in which a relatively weak spin coupling appears through the interactions with the hexagons in their excited states. The energy pattern within the full spin space (Fig.4) is calculated with the use of our MAGPACK software [37], A Package to Calculate the Energy Levels, Bulk Magnetic Properties, and Inelastic Neutron Scattering Spectra of High Nuclearity Spin Clusters, based on the irreducible tensor operators (ITO) technique. Using this efficient tool specially designed for the study of high nuclearity clusters, one can show [36] that the ground state with total spin $S = 1/2$ and first excited state with $S = 3/2$ (Fig.4, box) are well isolated (about $400 cm^{-1}$) from the higher states thus justifying an effective triangle approximation. Although the exchange problem is tractable in full Hilbert space of 15 spins [4,14,17,18,36] ($2^{15} = 32768$ states) a model of a spin triangle proposed and substantiated in [3,4] and developed in [36] gives accurate and descriptive

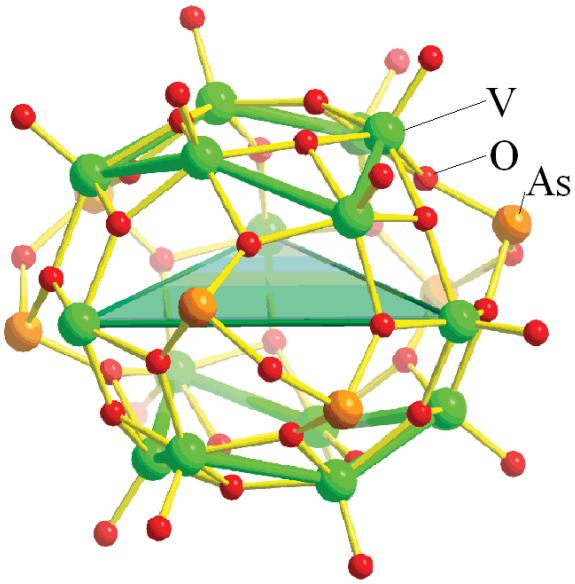

Fig. 1. The cluster anion $[V^{IV}_{15}As_6O_{42}(H_2O)]^{6-} = \{V_{15}As_6\}$: ball-and-stick representation without the central water molecule emphasizing the V_3 triangle [1].

results for the low lying set of the levels and can be applied at low temperatures providing a high accuracy of calculations for all thermodynamic and spectroscopic properties below 100K. In particular, this model allows to deduce the conclusions about the role of the AS exchange [36]. The isotropic superexchange can be described by the conventional HDVV Hamiltonian that represents a solid background for the consideration of the exchange interactions in transition metal clusters. For a symmetric triangle one finds the following Hamiltonian:

$$H_0 = -2J_0\left(\boldsymbol{S}_1\boldsymbol{S}_2 + \boldsymbol{S}_2\boldsymbol{S}_3 + \boldsymbol{S}_3\boldsymbol{S}_1\right), \qquad (1)$$

where $S_i = 1/2$ and J_0 is the parameter of the antiferromagnetic exchange $(J_0 < 0)$; for the sake of convenience we use a positive value $J = -J_0$ and the basis will be labeled as $|S_1S_2(S_{12})S_3SM\rangle \equiv |(S_{12})SM\rangle$, where $S_{12} = 0, 1$ is the intermediate spin in three-spin coupling scheme. The energy pattern includes two degenerate spin

doublets and a spin quadruplet separated by the gap 3*J*. The HDVV interaction is obviously magnetically isotropic that arises from its physical origin and mathematical structure of the HDVV Hamiltonian. To adequately describe EPR spectra and anisotropy of the magnetization on should take into account anisotropic magnetic interactions between the vanadium ions. First kind of such interaction is represented by the AS exchange introduced by Dzyaloshinsky [21] and Moria [22] as an origin of spin canting in non-collinear magnetic crystals. The Hamiltonian of AS exchange preserving trigonal symmetry is given by [36]:

$$\begin{aligned} H_{AS} &= D_n\left([\mathbf{S}_1\times\mathbf{S}_2]_Z+[\mathbf{S}_2\times\mathbf{S}_3]_Z+[\mathbf{S}_3\times\mathbf{S}_1]_Z\right)\\ &+D_l\left([\mathbf{S}_1\times\mathbf{S}_2]_X-\frac{1}{2}[\mathbf{S}_2\times\mathbf{S}_3]_X+\frac{\sqrt{3}}{2}[\mathbf{S}_2\times\mathbf{S}_3]_Y-\frac{1}{2}[\mathbf{S}_3\times\mathbf{S}_1]_X-\frac{\sqrt{3}}{2}[\mathbf{S}_3\times\mathbf{S}_1]_Y\right)\\ &+D_t\left([\mathbf{S}_1\times\mathbf{S}_2]_Y-\frac{\sqrt{3}}{2}[\mathbf{S}_2\times\mathbf{S}_3]_X-\frac{1}{2}[\mathbf{S}_2\times\mathbf{S}_3]_Y+\frac{\sqrt{3}}{2}[\mathbf{S}_3\times\mathbf{S}_1]_X-\frac{1}{2}[\mathbf{S}_3\times\mathbf{S}_1]_Y\right) \end{aligned} \quad (2)$$

Here the spin operators are related to the molecular frame, the parameter D_n is associated with the normal (Z-axis) component of AS exchange, D_l and D_t are those for the in-plane parts (see details in [36]) . The matrix of H_{AS} was explicitly calculated in the basis $|(S_{12})SM\rangle$ using the ITO technique [27, 38].

The analysis of the HDVV Hamiltonian (see review article [23] and references therein) revealed that the "degeneracy doubling" in the ground spin-frustrated state $(S_{12})S$ = (0)1/2,(1)1/2 is related to the exact orbital degeneracy so that the ground term is the orbital doublet ^2E in the trigonal symmetry. It was concluded [23] that the AS exchange acts within the $(S_{12})S$ = (0)1/2,(1)1/2 manifold like a first order spin-orbital interaction within ^2E term and gives rise to two doublets in agreement with the Kramers theorem [38].

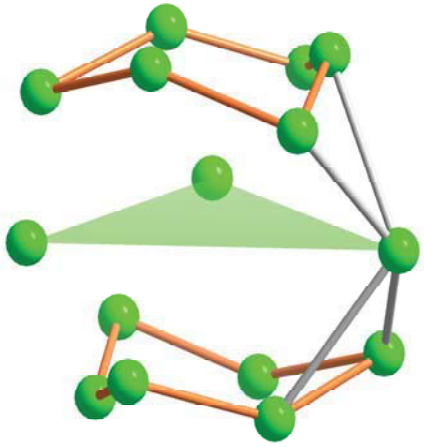

Fig. 2. Scheme of the V_{15} metal network [1] in the cluster anion $[V^{IV}_{15}As_6O_{42}(H_2O)]^{6-} = \{V_{15}As_6\}$.

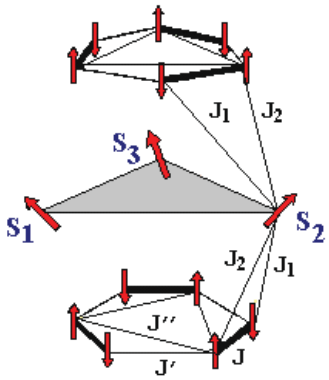

Fig. 3. Schematic structure of the metal network of the V_{15} cluster and pictorial representation of spin arrangement in the low energy states.

Within the pseudoangular momentum representation the basis $|(0)1/2,\pm1/2\rangle$, $|(1)1/2,\pm1/2\rangle$ of the irreducible representation *E* in trigonal point groups can be related to two projections $M_L=+1$ and $M_L=-1$ belonging to the fictitious orbital angular momentum *L*=1, the basis functions $u_{LM_L}(S,M_S)\equiv u_{M_L}(S,M_S)$ can be found as the circular superpositions [36]:

$$\begin{aligned} u_{\pm1}(1/2,\pm1/2) &= \mp1/\sqrt{2}\left(|(0)1/2,\pm1/2\rangle \pm i|(1)1/2,\pm1/2\rangle\right),\\ u_{\pm1}(1/2,\mp1/2) &= \mp1/\sqrt{2}\left(|(0)1/2,\mp1/2\rangle \pm i|(1)1/2,\mp1/2\rangle\right). \end{aligned} \quad (3)$$

Using this conception one can introduce the functions $U_S(M_J)$ belonging to a definite full spin S and projections $M_J = M_L + M_S$ of the full pseudoangular momentum, so that $U_{1/2}(\pm 3/2) = u_{\pm 1}(1/2, \pm 1/2)$ and $U_{1/2}(\pm 1/2) = u_{\pm 1}(\mp 1/2)$. The quantum numbers so far introduced correspond to the Russel-Saunders coupling scheme in axial symmetry. The level with $S = 3/2$ is an orbital singlet corresponding thus to $M_L = 0$, the components are labeled as $u_0(3/2, M_S) \equiv U_{3/2}(M_J)$ with $M_S = \pm 1/2$ and $M_S = \pm 3/2$, so that $M_J = \pm 1/2$ and $\pm 3/2$.

3. THE ENERGY PATTERN IN PARALLEL FIELD

Due to the actual axial symmetry of the system reflected in the pseudoangular momentum classification of the states, the matrix of the full Hamiltonian can be blocked into four second order matrices each corresponding to a definite projection M_J of the total pseudoangular momentum. The eigen-functions of the system are found as the superpositions of states with the same M_J originating from $S = 1/2$ and $S = 3/2$ multiplets that corresponds to the *jj*-coupling scheme in axial symmetry when $S = 1/2$ and $S = 3/2$ multiplets are mixed and M_L, M_S are no longer good quantum numbers so that the eigen-states are enumerated by quantum number M_J.

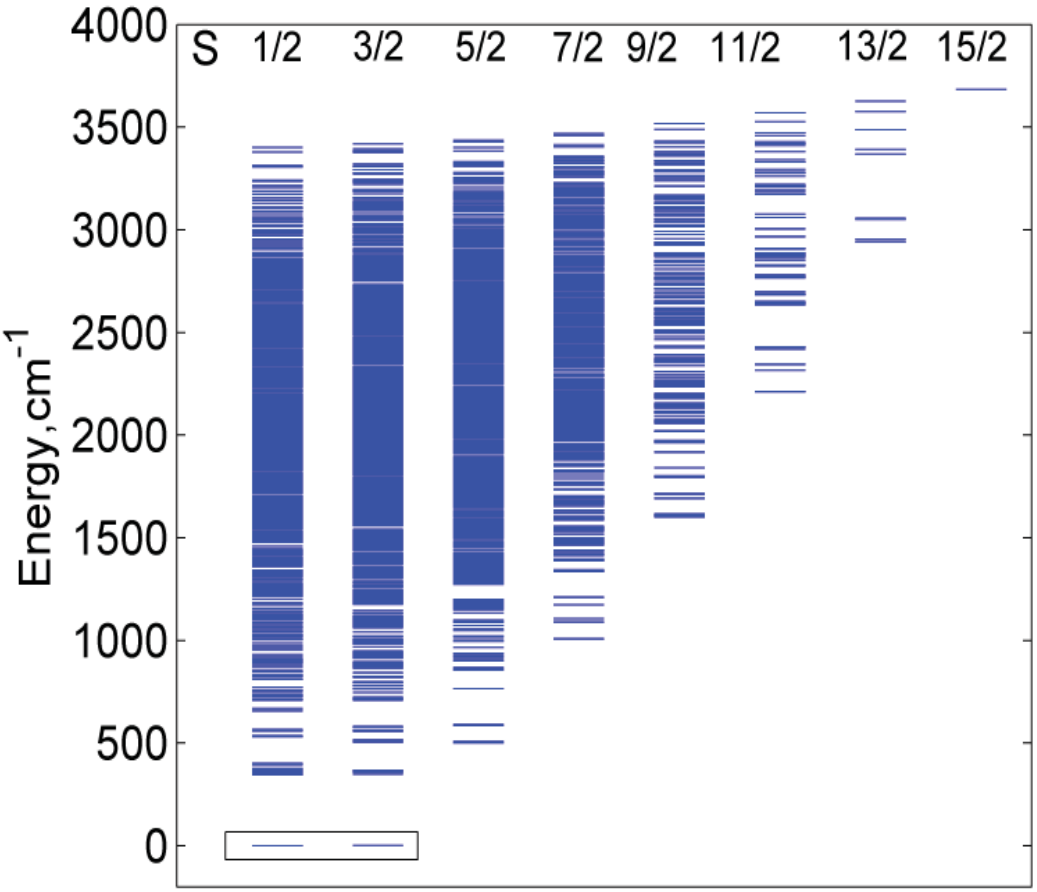

Fig. 4. Energy levels of the V_{15} cluster calculated with the parameters values from [3] . The levels are grouped accordingly to the total spin S. The calculation was performed using the MAGPACK software [37].

In absence of the field the full pattern consists of four Kramers doublets, two of them possess $M_J = \pm 1/2$ and two doublets with $M_J = \pm 3/2$. If the Zeeman interaction with the magnetic field $\boldsymbol{H} \parallel C_3$ axis (preserving thus axial symmetry) is also taken into account, the energy levels are enumerated by the definite values of M_J. This allows to

find the analytical solution for the energy levels providing an arbitrary interrelation between parameters (it is assumed that $g = g_{||}$) [36]:

$$\varepsilon_{1,2}(H) = -\frac{1}{4}\sqrt{\left(\sqrt{3}D_n \pm 2g\beta H + 6J\right)^2 + 3D_\perp^2} - \frac{\sqrt{3}}{4}D_n$$
$$\varepsilon_{3,4}(H) = -\frac{1}{4}\sqrt{\left(\sqrt{3}D_n \pm 2g\beta H - 6J\right)^2 + 9D_\perp^2} + \frac{\sqrt{3}}{4}D_n \mp g\beta H$$
$$\varepsilon_{5,6}(H) = \frac{1}{4}\sqrt{\left(\sqrt{3}D_n \mp 2g\beta H + 6J\right)^2 + 3D_\perp^2} - \frac{\sqrt{3}}{4}D_n$$
$$\varepsilon_{7,8}(H) = \frac{1}{4}\sqrt{\left(\sqrt{3}D_n \pm 2g\beta H - 6J\right)^2 + 9D_\perp^2} + \frac{\sqrt{3}}{4}D_n \mp g\beta H \qquad (4)$$

These levels are shown in Fig. 5. One can see that they do depend upon two effective parameters of AS exchange D_n and $D_\perp$ $\left(D_\perp^2 = D_t^2 + D_l^2\right)$ rather than upon three parameters D_n, D_l and D_t of the Hamiltonian. It is important that the "normal" part of the AS exchange operates only within the basis of two "accidentally" degenerate doublets $(S_{12})S = (0)1/2, (1)1/2$, meanwhile two "in-plane" contributions (terms of the Hamiltonian associated with the parameters D_l and D_l) lead only to a mixing of the ground spin doublets $(0)1/2, (1)1/2$ with the excited spin quadruplet $(1)3/2$ separated from two low lying spin doublets by the gap $3J$. AS exchange leads to the splitting of the two *S*=1/2 levels into two Kramers doublets with $M_J = \pm 1/2$ and $M_J = \pm 3/2$. Usually isotropic exchange is a leading interaction, so it is useful to develop the zero-field energies as series in $D_\perp^2/J$. The zero-field splitting of two spin doublets within this approximation $\Delta \equiv \varepsilon(M_J = \pm 3/2) - \varepsilon(M_J = \pm 1/2) \cong \sqrt{3}\, D_n - D_\perp^2/8J$ is the first order effect with respect to the normal component of AS exchange and contains also second order correction (always negative) arising from the mixing of $(S_{12})1/2$ and $(1)3/2$ multiplets through in-plane components of AS exchange. It can be said that in-plane components of the AS exchange are reduced by the isotropic exchange so that under the realistic conditions $|D_n|, |D_\perp| << J$ the parameter $D_\perp$ is effectively small. At the same time this part of AS exchange leads to the avoided crossing of the magnetic sublevels of S=1/2 and S=3/2 multiplets in high field, at the crossing points the in-plane components of AS exchange act as a first order perturbation [36]. The excited $S = 3/2$ level shows also a zero-field splitting but this splitting $\Delta_1 = D_\perp^2/8J$ is not affected by the parameter D_n and represents solely a second order effect with respect to the in-plane part of AS exchange. For this reason the zero-field splitting of the excited quadruplet is expected to be smaller (if D_n and $D_\perp$ are comparable) than the splitting of two *S*=1/2 doublets. The sign of Δ determines the ground state, in the cases of $\Delta > 0$ and $\Delta < 0$ the ground states are the doublets with $|M_J| = 1/2$ and $|M_J| = 3/2$ respectively. The Zeeman sublevels are enumerated by the quantum number M_J as shown in Fig. 5 in the case of $\Delta > 0$, the fine structure of *S*=3/2 is shown in the inset. According to the general symmetry rule the levels with the same M_J show avoided crossing, meanwhile those with different M_J exhibit exact crossing (Fig. 3).

4. EPR TRANSITIONS, DISCUSSION OF EXPERIMENTAL DATA

Within the pseudoangular momentum approach one concludes that the general selection rule $M_J \rightarrow M_J \pm 1$ for the linearly polarized $\boldsymbol{H}_{osc} \perp C_3$ microwave field defines the allowed transitions as shown in Fig. 5. Using the analytical solutions for the Zeeman energies, one can evaluate the resonance fields for the EPR transitions. Recently we have reported [39] the representative schemes of transitions and EPR spectra simulated for different microwave

frequencies, including those used in the high-frequency EPR experiments at ultra-low temperatures [40]. In all calculations we used g=1.96 and J = 0,847 cm^{-1} that is consistent with the experimental data [41]. The zero-field splitting in the ground manifold $|\Delta|$ is set to 0.14 cm^{-1}, as was found from inelastic neutron scattering [11,12]. Since the normal and in-plane contributions of AS exchange can not be discriminated directly from the experimental data on the inelastic neutron scattering, the ratio $D_\perp/D_n$ is varied (providing a fixed value of $|\Delta|$) in order to reveal the influence of different AS exchange components on the EPR pattern. The transformations of the spectrum with the increase of the ratio $D_\perp/D_n$ are also shown in the proposed EPR schemes [39] . We shall consider separately two cases: (*i*) $D_n \neq 0$, $D_\perp = 0$ and (*ii*) $D_n \neq 0$, $D_\perp \neq 0$. Since normal part of the AS exchange does not mix different spin levels one can discuss the case (*i*) within the Russel-Saunders scheme when the operator $\hat{S}_x$ does not change M_L. This implies the following selection rules for the linearly polarized microwave radiation that are strictly valid within the Russel-Saunders approximation: the EPR transitions $M_J \rightarrow M_J \pm 1$ are allowed with the conservation at the same time of the full spin S, projection of the orbital angular momentum M_L and for $M_S \rightarrow M_S \pm 1$ ($\Delta S = 0,\ \Delta M_L = 0,\ \Delta M_S = \pm 1,\ \Delta M_J = \pm 1$). The allowed intramultiplet transitions are schematically shown in Fig. 6 for three frequency domains: $h\nu < \Delta$, $\Delta < h\nu < 3J$ and $h\nu > 3J$. One can see that the spectrum consists of three lines, one line arises from three strong transitions **3, 4, 5** (marked bold) within S=3/2 multiplet with the resonance field $H_{\mathbf{3,4,5}} = h\nu/g\beta$ andthe two remaining lines correspond to two interdoublet transitions within two S=1/2 levels (Fig. 5, 6). It should be stressed that the intermultiplet ($S = 1/2 \leftrightarrow S = 3/2$) transitions are strictly forbidden when $D_\perp = 0$ as well as intradoublet transitions in the two S =1/2 levels split by AS exchange (this has been proved in [23–27]).

Two situations $h\nu < \Delta$ and $h\nu > \Delta$ within the case (*i*) are to be distinguished. Providing $h\nu < \Delta$ (Fig. 6a) two interdoublet transitions **1** and **1′** have the resonance fields $H_{\mathbf{1'}} = \left(\sqrt{3}D_n - h\nu\right)/g\beta$ and $H_{\mathbf{1}} = \left(\sqrt{3}D_n + h\nu\right)/g\beta$, so that the separation between these lines $H_{\mathbf{1}} - H_{\mathbf{1'}} = 2h\nu/g\beta$ increases with increase of the microwave frequency. The full spectrum is asymmetric with the line at $H_{\mathbf{3,4,5}} = h\nu/g\beta$ being closer to the line at $H_{\mathbf{1'}}$, the difference in the resonance fields $H_{\mathbf{1}} - H_{\mathbf{3,4,5}} = \sqrt{3}D_n/g\beta$ is independent of microwave frequency ν and $H_{\mathbf{1'}} - H_{\mathbf{3,4,5}} = \left(2h\nu - \sqrt{3}D_n\right)/g\beta$ increases with the increase of ν. At relatively high temperatures (when the full intensity follows the low $I \propto T^{-1}$) the ratio of the intensities of three lines is 1:3:1. In the case of $h\nu < \Delta$ the interdoublet transitions are **1**, **2** (Figs. 6b and 6c) with the resonance fields $H_{\mathbf{1}} = \left(h\nu + \sqrt{3}D_n\right)/g\beta$ and $H_{\mathbf{2}} = \left(h\nu - \sqrt{3}D_n\right)/g\beta$. In this case the spectrum consists of the central peak at $H_{\mathbf{3,4,5}} = \sqrt{3}D_n/g\beta$ and two equally spaced side-lines at $H_{\mathbf{1}}$ and $H_{\mathbf{2}}$ with the ratio intensities 1:3:1. It is remarkable that in the case under consideration the full width of the spectrum $H_{\mathbf{1}} - H_{\mathbf{2}} = 2\sqrt{3}D_n/g\beta$ is directly related to the AS exchange and independent of ν.

In the general case (*ii*) when both components of AS exchange are nonzero ($D_n \neq 0$ $D_t \neq 0$) different spin levels are mixed and the system can be adequately described by the *jj*-coupling scheme.Two new essential features of the EPR pattern arise from the mixing of S=1/2 and S=3/2 spin levels by the in-plane part of AS exchange. First, due to axial zero-field splitting $\Delta_1 = D_\perp^2/8J$ of the excited S=3/2 level the transitions **3, 4, 5** at $h\nu > \Delta_1$ have different resonance fields: $H_{\mathbf{3,5}} = \left(h\nu \mp \Delta_1\right)/g\beta$, $H_{\mathbf{4}} = g\beta$ and providing $h\nu < \Delta_1$ line **3** does not exist and line **5′** corresponds to $H_{\mathbf{5'}} = \left(\Delta_1 - h\nu\right)/g\beta$ (see Fig. 5, inset). This leads to a peculiar fine triplet structure of the central peak in the patterns of the EPR lines so far discussed. The second order effect of mixing through the in-plane AS exchange is relatively small in the wide range of the fields except of the vicinity of the avoided crossing points (Fig. 5) where the in-plane component of the AS exchange acts as a first order perturbation.

The second important consequence of the in-plane AS exchange is that this interaction allows new transitions (obeying the general selection rule $\Delta M_J = \pm 1$) that are forbidden in the Russel-Sauders scheme, namely, the

intermultiplet transitions 6-12 and 9′ as shown in Fig. 5. The intensities of these newly allowed transitions depend on the extent of the mixing of S=1/2 and S=3/2 multiplets in the magnetic field and in a wide range of the field they are relatively weak. The high-frequency ($\nu = 57.831$GHz and $\nu = 108$ GHz) EPR measurements at ultra-low temperatures between 0.5 and 4.2K for the parallel ($\boldsymbol{H} \,||\, C_3$) field have been recently reported [42]. The transmission spectrum observed at 2.1T represents a relatively broad slightly asymmetric peak that becomes broader when the temperature decreases (Fig. 7). Since the observed structureless EPR peak does not provide unambiguous information about the fine structure of the absorption we will discuss a simplest approximation in which only the normal part of the AS exchange is taken into account. Since the fine structure of the absorption line is unresolved it is

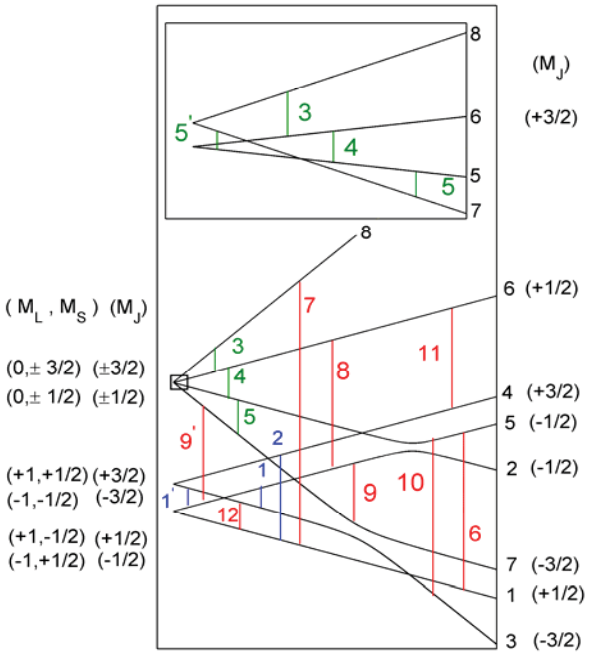

Fig. 5. Energy pattern of the V_{15} molecule within the three-spin model $(\text{the case } \Delta > 0)$ and allowed EPR transitions in the parallel ($\boldsymbol{H} \,||\, C_3$) field. Inset: magnified zero-field and Zeeman splitting of S=3/2 level ($\boldsymbol{H} \,||\, C_3$).

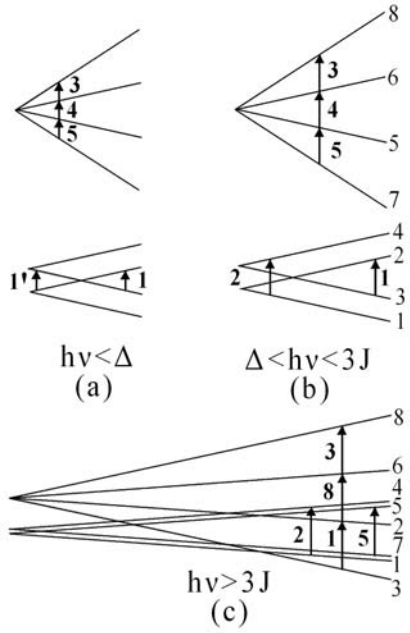

Fig. 6. Scheme of the EPR transitions in the case of $D_\perp = 0$: (a) $h\nu < \Delta$, (b) $h\nu > \Delta < 3J$, (c) $h\nu > 3J$.

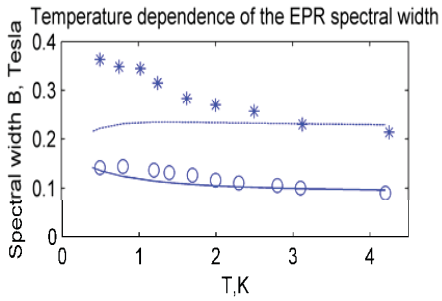

Fig. 7. Theoretical and experimental temperature dependence of the EPR spectral width for V_{15}. The theoretical curves are scaled at $T = 3K$, $J = 0.847\ cm^{-1}$, $\Delta = 0.14\ cm^{-1}$ ($\boldsymbol{H} \,||\, C_3$). Theoretical curves: 57.831 GHz (solid), 108 GHz (dashed); experimental data: 57.831 GHz (circles) 108 GHz (stars).

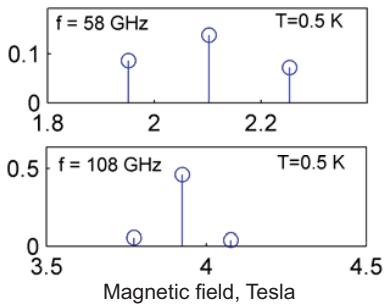

Fig. 8. Calculated EPR lines ($\boldsymbol{H} \,||\, C_3$) at $T = 0.5K$ for two frequencies. ($J = 0.847\ cm^{-1}$, $\Delta = 0.14\ cm^{-1}$).

reasonable to assume that the observed peak can be considered as an envelope of the broadened individual absorption lines arising from the allowed transitions. In the case of ν = 57.831 GHz (frequency region $\Delta < h\nu < 3J - \Delta/2$) the superposition involves the central lines **3,4,5** at $H_{3,4,5}$ = 2.11T and two sidebands **1** and **2** at H_1= 1.96T and H_2= 2.26T. At the frequency $\nu = 108$ GHz the full spectrum is assumed to consist of the central peak **1,3,8** and sidelines **2** and **5** ($H_{1,3,8}$ = 3.93T, H_2= 3.78T and H_5= 4.08T). In order to estimate approximately the role of the AS exchange in the broadening of the EPR peak we have calculated the central second moments of these discrete spectral distributions:

$$\left\langle \left(H - \overline{H}\right)^2 \right\rangle = \sum_{i=1}^{3} I_i \left(H_i - \overline{H}\right)^2 \Big/ \sum_{i=1}^{3} I_i , \tag{5}$$

$$\overline{H} = \sum_{i=1}^{3} I_i H_i \Big/ \sum_{i=1}^{3} I_i . \tag{6}$$

where I_i are the intensities of the lines at a given temperature and $\overline{H}$ is the center of the first moment (center of gravity) of the spectral distribution. The full width of the observed peak includes also contributions arising from the broadening of the individual lines. In order to take them into account, at least qualitatively, we have normalized the full width (obtained with the aid of Eqs. (5) and (6)) vs. temperature at $T = 3K$. As one can see the evaluated temperature dependence of the spectral width is in reasonable agreement with the experimental data at ν = 57.831GHz (Fig. 6). At the same time at $\nu = 108$ GHz probably the splitting of the lines due to AS exchange plays a secondary role in the broadening of the observed EPR peak, especially at ultra-low temperatures. This can also be illustrated by plotting of the EPR pattern at T = 0.5 K for two employed frequencies (Fig. 8). One can see that at low temperature the second moment at ν = 108 GHz is less than that for ν = 57.831 GHz due to lower intensity of the sidebands meanwhile the observed width is greater. Calculations of the second moments in a more general model when $D_\perp \neq 0$ give similar results but the smoothed line does not provide a reliable information about the interrelation between two components of AS exchange. In view of these results one might assume that the broadening of the EPR peak can be attributed to the spin-phonon interaction and also to the effects of lower symmetry that have been recently discussed [19]. More detailed information can be provided by the angular dependence of the high-frequency EPR and by the study of the mechanisms of relaxation. The hyperfine interaction is to be mentioned as an essential contribution to the broadening of the EPR line in the vanadium clusters.

5. ZEEMAN LEVELS IN PERPENDICULAR FIELD

In the important particular case when the in-plane of AS exchange is absent $(D_n \neq 0, D_l = D_t = 0)$ the special symmetry properties of the matrix of AS exchange allow to find the exact solution:

$$\begin{aligned}
\varepsilon_1 = \varepsilon_3 &= -\frac{3}{2}J - \frac{1}{2}\sqrt{(g\beta H)^2 + 3D_n^2} \ , \\
\varepsilon_2 = \varepsilon_4 &= -\frac{3}{2}J + \frac{1}{2}\sqrt{(g\beta H)^2 + 3D_n^2} \ , \\
\varepsilon_{5,6} &= \frac{3}{2}J \mp \frac{1}{2}g\beta H \ , \\
\varepsilon_{7,8} &= \frac{3}{2}J \mp \frac{3}{2}g\beta H \ .
\end{aligned} \tag{7}$$

In Eq. (7) H is the field in any direction in the plane, let's say $H = H_X$ and correspondingly g-factor $g \equiv g_\perp$. The levels ε_i (H) with i = 1, 2, 3, 4 are related to S=1/2 while i=5,6,7,8 are the numbers of Zeeman sublevels for S=3/2 (with $M = \mp 1/2$ and $M = \mp 1/2$) as shown in Fig. 9a in the case of the isotropic model. The energy pattern for the case

$D_n \neq 0, D_l = D_t = 0$ is shown in Fig. 9b. Three peculiarities of the energy pattern that are closely related to the magnetic behavior should be noticed: 1) the ground state involving two S=1/2 levels shows zero-field splitting into two Kramers doublets separated by the gap $\Delta = \sqrt{3}D_n$; 2) at low fields $g\beta H \leq \Delta$ the Zeeman energies are double degenerate and show quadratic dependence on the field:

$$\varepsilon_1 = \varepsilon_3 = -\sqrt{3}D_n/2 - (g\beta H)^2/4\sqrt{3}D_n,$$

$$\varepsilon_2 = \varepsilon_4 = -\sqrt{3}D_n/2 + (g\beta H)^2/4\sqrt{3}D_n. \quad (8)$$

This behavior is drastically different from that in the isotropic model and from the linear magnetic dependence in parallel field [23] and can be considered as a breaking of the normal AS exchange by the perpendicular field [23]; 3) the magnetic sublevels arising from S=3/2 (M = -1/2 and M = -3/2) cross the sublevels belonging to S=1/2 spin levels, no avoided crossing points are observed. At high field the levels $\varepsilon_{1,3}$ and $\varepsilon_{2,4}$ exhibit again linear magnetic dependence. One can see that strong perpendicular field restores linear Zeeman splitting but without zero-field splitting so that the perpendicular field reduces the normal part of AS coupling. This effect of reduction has been understood long time ago [23].

When the AS exchange in its general form is involved $(D_n \neq 0, D_l \neq 0, D_t \neq 0)$ the energy pattern shows new peculiarities (Fig. 9c). The low field part of the spectrum is not affected by the in-plane part of AS exchange and is very close to that in Fig. 9b due to the fact that the in-plane part of AS exchange is not operative within the ground manifold and the effect of S=1/2-S=3/2 mixing is small at low fields due to the large gap $3J >> |D_\perp|$. At the same time in the vicinity of the crossing points the effect of the normal AS exchange is negligible but the in-plane AS exchange acts as a first order perturbation giving rise to the avoided crossings as shown in Fig. 9c.

Let us note that at low fields far from anticrossing region the energies can be well described by Eq. (8) in the general case of AS exchange although they are deduced for a particular model when $(D_n \neq 0, D_l \neq 0, D_t \neq 0)$. In order to obtain three closely spaced low lying levels in the region of anticrossing field we will use the perturbation theory respectively to the in-plane part of AS exchange and the basis formed by three eigen-functions of H_0 whose eigen-values have crossing point at $g\beta H = 3J$, namely $|(0)1/2,-1/2\rangle, |(1)1/2,-1/2\rangle, |(1)3/2,-3/2\rangle$ (Fig. 9a). The secular equation can be solved due to some additional symmetry. The following approximate expressions were found [43,44] for the energy levels ε_i' in this region of the field:

$$\varepsilon_1' = -\frac{3}{2}J - \frac{1}{2}g\beta H, \quad (9)$$

$$\varepsilon_{3,7}' = -g\beta H \mp \frac{1}{8}\sqrt{(4g\beta H - 12J)^2 + 18D_\perp^2}, \quad (10)$$

These expressions give rather good accuracy and will be used in the description of the magnetization vs. field and temperature of V_{15} cluster.

6. TEMPERATURE AND FIELD DEPENDENCE OF MAGNETIZATION OF V_{15} -EFFECTS OF AS EXCHANGE

Let us consider some general features of the field dependence of magnetization related to the AS exchange by plotting the results of sample calculations. One can find the following expressions that work well at low field (Eq. (11)) and high field in the vicinity of anticrossing of the low lying levels (Eq. (12)) :

$$\mu(H) = \frac{g^2\beta^2 H}{2\sqrt{3D_n^2 + g^2\beta^2 H^2}}, \quad (11)$$

$$\mu(H) = g\beta + \frac{2g\beta(g\beta H - 3J)}{\sqrt{2(g\beta H - 3J)^2 + 18D_\perp^2}}. \quad (12)$$

Fig.9 (dashed line) shows $\mu(H)$ dependence in the framework of the isotropic model. The normal part of AS exchange results in the broadening of the low field step in $\mu(H)$ as shown by solid line. This broadening is closely related to the quadratic Zeeman effect in the low perpendicular field (see Fig. 9b). The in-plane part of the AS exchange leads to the broadening of the second step. When anticrossing in the region $H = 3J/g\beta$ appears due

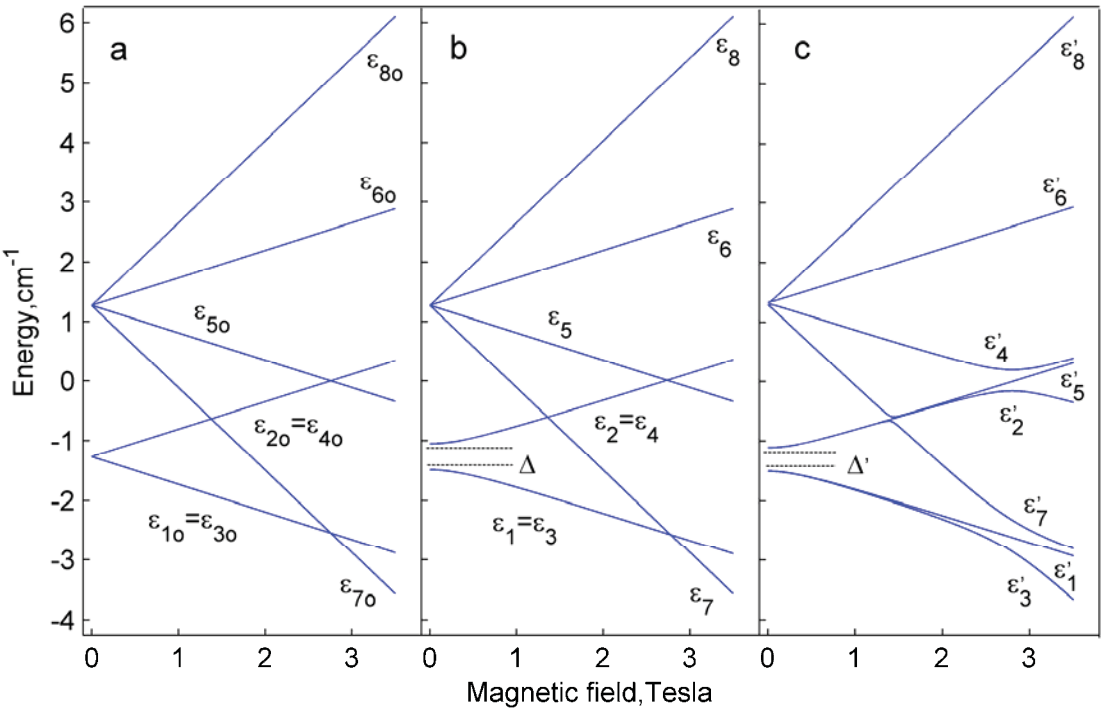

Fig. 9. Energy pattern of the triangular vanadium unit in the magnetic field applied in the plane ($\boldsymbol{H} \perp C_3$), $J = 0.847\ cm^{-1}$, $g = 2$. (a) $D_n = 0$, $D_\perp = 0$; (b) $D_n = 0.3J, D_\perp = 0$, (c) $D_n = 0.3J$, $D_\perp = 0.6J$.

to coupling of *S*=1/2, *M*=-1/2 *S*=3/2, *M*=-3/2 levels through in-plane AS exchange it obviously gives rise to a smoothed switch from S=1/2 to *S*=3/2 as shown in Fig. 9c. Fig. 10 schematically indicates that the first and the second steps of magnetization are affected by the two different parts of the AS exchange.

7. TEMPERATURE AND FIELD DEPENDENCE OF MAGNETIZATION - DISCUSSION OF EXPERIMENTAL DATA

The low-temperature adiabatic magnetization vs. field applied in the plane of the V_3 triangle ($\boldsymbol{H} \perp C_3$) exhibits steps whose broadening and shapes are temperature dependent (Figs. 10,11). Analysis of the experimental data in [41] has been performed in the framework of the HDVV model supplemented by a small quadrupolar anisotropy $\left(J_{XX} = J_{YY} \neq J_{ZZ}\right)$. Agreement between the calculated curves and experimental magnetization data proved to be quite good for T= 0.9 K and 4.2 K but the model fails to explain the low temperature data.

Modeling magnetization curves with consideration of the AS exchange gives perfect agreement for the whole range of temperatures including the lowest one. Such a modeling for the first time allowed us to estimate the AS exchange parameters. The best fit procedure gives the following set of parameters: $J = -0.855 cm^{-1}$, $g = 1.94$, $D_\perp = 0.238\ cm^{-1}$, $D_n = 0.054\ cm^{-1}$ (see [43,44]). The least mean square error value calculated for the whole sets

of the $\mu(H)$ curves is found to be $2.3 \cdot 10^{-3}$. The fit is well stable for the parameters J, g and $D_{\perp}$ but however, less stable with respect to D_n (see [44] for more details). To determine this parameter more accurately one needs low field

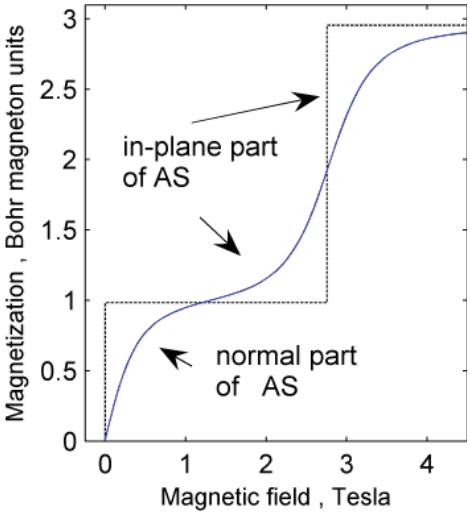

Fig. 10. Magnetization at T = 0 K in perpendicular field. Dashed line : $J = 0.847\ cm^{-1}$, $D_n = 0$, $D_{\perp} = 0$; Solid line: $J = 0.847\ cm^{-1}$, $D_n = 0.3J$, $D_{\perp} = 0.6J$.

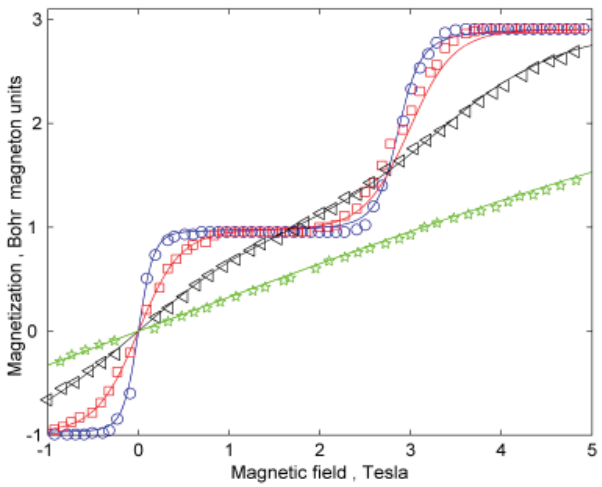

Fig.11. Experimental data (from ref [41]) and theoretical curves of static magnetization calculated with account for the isotropic and AS exchange interactions ($\boldsymbol{H} \perp C_3$). Experimental data : Circles- $T = 0.1\ K$, squares- $T = 0.3$K, triangles- $T = 0.9\ K$, stars– $T = 4.2\ K$. Solid lines- calculated.

data at ultra-low temperatures and additional data like EPR at low frequencies. Calculated curves (with the best fit parameters) and experimental data are in full agreement in the whole ranges of the temperature and field used in the experiments so far mentioned (Fig. 11).

8. VIBRONIC INTERACTION

Since the exchange multiplets are orbitally degenerate the role of the vibronic coupling (Jahn-Teller-JT-effect [45-47]) should be elucidated. We will use the semiclassic adiabatic approximation that gives a clear physical picture of the influence of the vibronic interaction on the magnetic characteristics. In the JT systems, in general, the electronic and vibrational states are mixed [45-47]. Nevertheless, in many important cases the adiabatic approach can serve as a relatively simple and at the same time powerful tool for the theoretical study of the JT systems. The question of the applicability of the semiclassic adiabatic approach to the vibronic problems in the JT systems is rather complicated in general (and will not be discussed here) and the thorough answer can be done with regard to a particular problem. The results of the semiclassic calculations of the magnetic moments in pseudo JT (mixed-valence) clusters vs. temperature were carefully tested by comparison with the results of quantum-mechanical evaluation [48]. The results exhibit very high accuracy of the semiclassic theory in a wide range of the temperature and coupling parameters including cases of intermediate and even weak coupling. The qualitative difference in the estimation of magnetic behavior between the semiclassic and dynamic approaches was intentionally found for a specific choice of the parameters when the ground vibronic levels belonging to different spin values are close. This conclusion is common for the thermodynamic (non-resonance) characteristics of the JT systems that are defined exceptionally by the partition function. Keeping in mind these results, in the present study we shall take advantage of the semiclassic adiabatic approach in order to reveal the influence of the vibronic coupling on magnetization in the presence of the AS exchange.

The symmetry adapted vibrations $A_1\left(Q_{A_1} \equiv Q_1\right)$ and double degenerate E type $\left(Q_{Ex} \equiv Q_x, Q_{Ey} \equiv Q_y\right)$ of an equilateral triangular unit can be expressed as

$$Q_1 = \tfrac{1}{\sqrt{3}}\left[-\tfrac{1}{2}\left(\sqrt{3}X_1 + Y_1\right) + \tfrac{1}{2}\left(\sqrt{3}X_2 - Y_2\right)\right],$$
$$Q_x = \tfrac{1}{\sqrt{3}}\left[-\tfrac{1}{2}\left(\sqrt{3}X_1 - Y_1\right) - \tfrac{1}{2}\left(\sqrt{3}X_2 + Y_2\right)\right],$$
$$Q_y = \tfrac{1}{\sqrt{3}}\left[\tfrac{1}{2}\left(X_1 + \sqrt{3}Y_1\right) + \tfrac{1}{2}\left(X_2 - \sqrt{3}Y_2\right) - X_3\right]. \quad (13)$$

The vibronic interaction arises from the modulation of the isotropic and AS exchange interactions by the molecular displacements. In fact, the exchange parameters are the functions of the interatomic distances so the linear terms of the vibronic Hamiltonian can be represented as:

$$H_{ev} = 2\sum_{ij} \boldsymbol{S}_i \boldsymbol{S}_j \sum_{\alpha=1,x.y} \left(\frac{\partial J_{ij}\left(R_{ij}\right)}{\partial R_{ij}}\right)_{\Delta R_{ij}=0} \cdot \frac{\partial R_{ij}}{\partial Q_\alpha} Q_\alpha \ , \quad (14)$$

$$H'_{ev} = \sum_{ij} \left[\boldsymbol{S}_i \times \boldsymbol{S}_j\right] \sum_{\alpha=1,x.y} \left(\frac{\partial \boldsymbol{D}_{ij}\left(R_{ij}\right)}{\partial R_{ij}}\right)_{\Delta R_{ij}=0} \cdot \frac{\partial R_{ij}}{\partial Q_\alpha} Q_\alpha \quad (15)$$

Here the summation is extended over all pairwise spin-spin interactions (*ij*= 12, 23, 31). Eqs. (14) and (15) are the contributions of the overall vibronic coupling relating to the isotropic and AS exchange interactions respectively. After all required transformations one can arrive at the following vibronic Hamiltonian H_{ev}:

$$H_{ev} = \lambda\left(\hat{V}_1 Q_1 + \hat{V}_x Q_x + \hat{V}_y Q_y\right) \quad (16)$$

where $\lambda \equiv \sqrt{6}\left(\partial J_{ij}\left(R_{ij}\right)/\partial R_{ij}\right)_0$ is the vibronic coupling parameter associated with the isotropic exchange and the operators $\hat{V}_\alpha$ are the following [49] (see [23,27] and references cited therein):

$$\hat{V}_1 = \sqrt{\tfrac{2}{3}}\left(\mathbf{S}_1\mathbf{S}_2 + \mathbf{S}_2\mathbf{S}_3 + \mathbf{S}_3\mathbf{S}_1\right), \quad (17)$$
$$\hat{V}_x = \tfrac{1}{\sqrt{6}}\left(\boldsymbol{S}_2\boldsymbol{S}_3 + \boldsymbol{S}_3\boldsymbol{S}_1 - 2\boldsymbol{S}_1\boldsymbol{S}\right),$$
$$\hat{V}_y = \tfrac{1}{\sqrt{2}}\left(\boldsymbol{S}_2\boldsymbol{S}_3 - \boldsymbol{S}_3\boldsymbol{S}_1\right).$$

By applying a similar procedure one can obtain the vibronic contribution associated with the AS exchange. The final expression is the following:

$$H'_{ev} = \hat{W}_1 Q_1 + \hat{W}_x Q_x + \hat{W}_y Q_y. \quad (18)$$

The operators $\hat{W}_\alpha$ are expressed in terms of the vector products of spin operators:

$$\hat{W}_1 = \boldsymbol{\lambda}_{12}\left[\boldsymbol{S}_1 \times \boldsymbol{S}_2\right] + \boldsymbol{\lambda}_{23}\left[\boldsymbol{S}_2 \times \boldsymbol{S}_3\right] + \boldsymbol{\lambda}_{31}\left[\boldsymbol{S}_3 \times \boldsymbol{S}_1\right],$$
$$\hat{W}_x = \tfrac{1}{2}\left(\boldsymbol{\lambda}_{12}\left[\boldsymbol{S}_1 \times \boldsymbol{S}_2\right] + \boldsymbol{\lambda}_{23}\left[\boldsymbol{S}_2 \times \boldsymbol{S}_3\right] - 2\boldsymbol{\lambda}_{31}\left[\boldsymbol{S}_3 \times \boldsymbol{S}_1\right]\right), \quad (19)$$
$$W_y = \tfrac{\sqrt{3}}{2}\left(\boldsymbol{\lambda}_{23}\left[\boldsymbol{S}_2 \times \boldsymbol{S}_3\right] - \boldsymbol{\lambda}_{31}\left[\boldsymbol{S}_3 \times \boldsymbol{S}_1\right]\right).$$

In Eq. (19) the values $\boldsymbol{\lambda}_{ij}$ are the vector coupling parameters defined as $\boldsymbol{\lambda}_{ij} = \left(\partial \boldsymbol{D}_{ij}\left(R_{ij}\right)/\partial R_{ij}\right)_0$. Under the condition of trigonal symmetry there are three parameters, namely, normal part $\lambda_n = \lambda_{ijn}$ and two perpendicular contributions $\lambda_t = \lambda_{ijt}$ and $\lambda_l = \lambda_{ijl}$ where the symbols *l* and *t* have the same meaning as in the definition of the AS exchange. As one can see the vibronic interaction appears due to dependence of the exchange parameters (isotropic and anisotropic)

upon the distances between the metal centers that means that the physical origin of the vibronic (or spin-vibronic) interaction is the modulation of the exchange interaction by the molecular or lattice vibrations. This leads to the fact that the matrix elements of the spin-vibronic interactions are expressed in terms of the two-particle operators. This is in line of the traditional theory of the JT effect but takes into account the feature of the exchange coupled systems. If an irrelevant *ab-initio* scheme for the evaluation of the exchange parameters as the functions of the distances is employed the corresponding derivatives (Eqs. (14) and (15)) with respect to the metal-metal distances can be calculated.

The evaluation of the vibronic matrices can be performed with the aid of the ITO approach [27, 38,50]. With this aim each pairwise interaction can be expressed in terms of the zeroth order and first order tensorial products of ITOs as:

$$\left(\boldsymbol{S}_i\,\boldsymbol{S}_j\right)=-\sqrt{3}\left\{\boldsymbol{S}_i^{(1)}\times\boldsymbol{S}_j^{(1)}\right\}^{(0)}, \tag{20}$$

$$\boldsymbol{\lambda}_{ij}\left[\boldsymbol{S}_i\times\boldsymbol{S}_j\right]=i\sqrt{2}\,\lambda_-\,e^{-i\phi}\left\{\boldsymbol{S}_i^{(1)}\times\boldsymbol{S}_j^{(1)}\right\}_1^{(1)}-i\sqrt{2}\,\lambda_+\,e^{i\phi}\left\{\boldsymbol{S}_i^{(1)}\times\boldsymbol{S}_j^{(1)}\right\}_{-1}^{(1)}-i\sqrt{2}\,\lambda_n\left\{\boldsymbol{S}_i^{(1)}\times\boldsymbol{S}_j^{(1)}\right\}_0^{(1)}$$

where $\left\{\boldsymbol{S}_i^{(1)}\times\boldsymbol{S}_j^{(1)}\right\}_m^{(k)}$ is the symbol of the tensor product [50] (rank κ, component m) of two spin ITOs $\boldsymbol{S}_i^{(1)}$ and $\boldsymbol{S}_j^{(1)}$ relating to the sites *i* and *j* $\phi=0,\ 2\pi/3,\ 2\pi/3$ for the sides 12, 23 and 31 of the triangle correspondingly, $\lambda_\pm=\mp\left(1/\sqrt{2}\right)\left(\lambda_l\pm i\lambda_t\right)$.

8. VIBRONIC MATRIX FOR THE GROUND STATE AND ADIABATIC SURFACES

In order to simplify our consideration and to get clear insight on the influence of the JT interaction on the magnetic properties we assume that the gap 3*J* exceeds considerably the vibronic coupling and AS exchange and therefore we include in the basis set only four low lying spin 1/2 states and exclude the full symmetric mode Q_1. In this view one should note that the role of A_1 mode is not a simple shift of the Q_1 coordinate. In fact, A_1 vibration is active in the pseudo JTE when a relatively small vibronic contribution of AS exchange is taken into account (a more detailed description will be given elsewhere). In the approximation so far assumed the matrix of the full Hamiltonian $H_{AS}+H_{ev}+H'_{ev}+H_{Zeeman}$ was obtained in [51]:

$$\begin{pmatrix}
\frac{1}{2}g_{||}\beta H_z+\frac{1}{2}\sqrt{\frac{3}{2}}\lambda Q_x & \frac{1}{2}g_{\perp}\beta H_x & \frac{\sqrt{3}}{2}\left(-iD_n+\frac{1}{\sqrt{2}}\lambda Q_y\right) & \frac{i}{2}\sqrt{\frac{3}{2}}\lambda_-\left(Q_x+iQ_y\right)\\
\frac{1}{2}g_{\perp}\beta H_x & -\frac{1}{2}g_{||}\beta H_z+\frac{1}{2}\sqrt{\frac{3}{2}}\lambda Q_x & -\frac{i}{2}\sqrt{\frac{3}{2}}\lambda_+\left(Q_x-iQ_y\right) & \frac{\sqrt{3}}{2}\left(iD_n+\frac{1}{\sqrt{2}}\lambda Q_y\right)\\
\frac{\sqrt{3}}{2}\left(iD_n+\frac{1}{\sqrt{2}}\lambda Q_y\right) & -\frac{i}{2}\sqrt{\frac{3}{2}}\lambda_-\left(Q_x+iQ_y\right) & \frac{1}{2}g_{||}\beta H_z-\frac{1}{2}\sqrt{\frac{3}{2}}\lambda Q_x & \frac{1}{2}g_{\perp}\beta H_x\\
-\frac{i}{2}\sqrt{\frac{3}{2}}\lambda_+\left(Q_x-iQ_y\right) & \frac{\sqrt{3}}{2}\left(-iD_n+\frac{1}{\sqrt{2}}\lambda Q_y\right) & \frac{1}{2}g_{\perp}\beta H_x & -\frac{1}{2}g_{||}\beta H_z-\frac{1}{2}\sqrt{\frac{3}{2}}\lambda Q_x
\end{pmatrix} \tag{21}$$

In the matrix representation of the full Hamiltonian the basis $\left|\left(S_{12}\right)SM\right\rangle$ is used with the following order of the basis spin functions: $\left|(0)\tfrac{1}{2},\tfrac{1}{2}\right\rangle$, $\left|(0)\tfrac{1}{2},-\tfrac{1}{2}\right\rangle$, $\left|(1)\tfrac{1}{2},\tfrac{1}{2}\right\rangle$, $\left|(1)\tfrac{1}{2},-\tfrac{1}{2}\right\rangle$. Since the system has axial magnetic anisotropy one can assume that the field is applied in a ZX plane ($H_y=0$). One sees that the vibronic interaction leads to a complicated combined JT and pseudo JT problem. The modulation of the isotropic exchange is expected to provide the dominant contribution to the vibronic interaction. To further simplify the solution of the problem and make it more obvious we put $\lambda_+=\lambda_-=0$ and $g_{||}=g_{\perp}=g$ (although the eigen-values of the vibronic matrix are found without these simplifying assumptions). The four eigen-values of the matrix are found as:

$$\varepsilon_{1,4}(\rho,\xi) = \mp\frac{1}{2\sqrt{2}}\hbar\omega\sqrt{2\xi^2 + 2\delta^2 + 3\upsilon^2\rho^2 - 2\sqrt{2}\,\xi\sqrt{3\upsilon^2\rho^2 + 2\delta^2\cos^2\theta}}$$

$$\varepsilon_{2,3}(\rho,\xi) = \pm\frac{1}{2\sqrt{2}}\hbar\omega\sqrt{2\xi^2 + 2\delta^2 + 3\upsilon^2\rho^2 + 2\sqrt{2}\,\xi\sqrt{3\upsilon^2\rho^2 + 2\delta^2\cos^2\theta}} \qquad (22)$$

The following dimensionless parameters are introduced: vibronic coupling parameter $\upsilon = (\lambda/\hbar\omega)(\hbar/M\omega)^{1/2}$, zero field splitting of the ground state $\delta = \sqrt{3}D_n/\hbar\omega \equiv \mathrm{D}/\hbar\omega$, applied field $\xi = g\beta H/\hbar\omega$ and the vibrational coordinates $q_\alpha = (M\omega/\hbar)^{1/2}Q_\alpha$, the angle θ is defined by $H_z = H\cos\theta$. Finally, ρ is the radial component in the plane $q_x\, q_y$ defined as usually: $q_x = \rho\cos\varphi$, $q_y = \rho\sin\varphi$. The adiabatic surfaces are axially symmetric (at an arbitrary direction of the applied field) respectively the C_3 axis complying with the actual axial symmetry of the AS exchange.

In the case of $\delta = 0$ and $\xi = 0$ one faces a two mode pseudo JT problem and one obtains simple expressions for a pair of the double degenerate surfaces that are quite similar to that in the pseudo JT $^2E \otimes e$ problem with spin-orbital interaction:

$$U_\pm(\rho)/\hbar\omega = \frac{\rho^2}{2} \pm \frac{1}{2}\sqrt{\delta^2 + \frac{3\upsilon^2\rho^2}{2}}\,. \qquad (23)$$

One can see that in the limit of the isotropic exchange model the surface represents a "Mexican hat" (Fig. 12a) with the

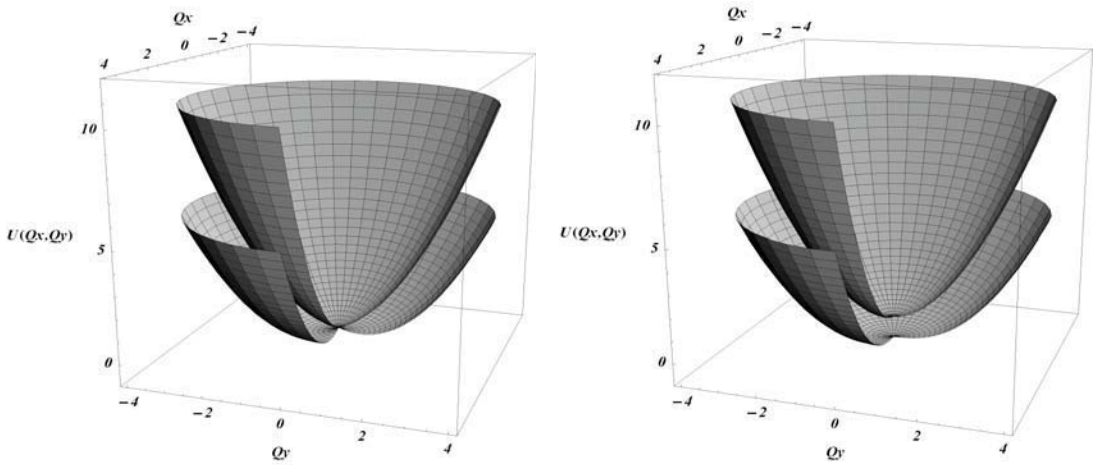

Fig. 12. Adiabatic potentials for the ground state of a triangular exchange system in the space of the double degenerate vibrations: (a) $\delta = 0, \upsilon = 2.0$; (b) strong AS exchange and/or weak vibronic interaction ($\delta = 1.0, \upsilon = 1.0$).

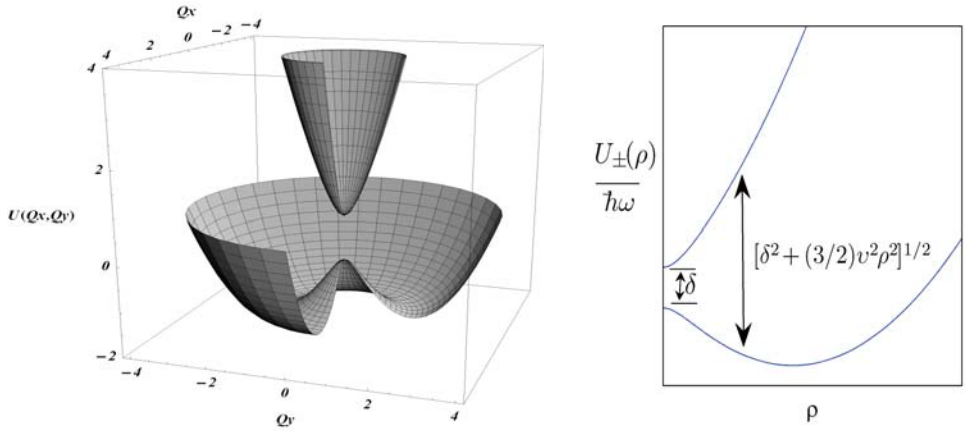

Fig. 13. The case of weak AS exchange and/or strong vibronic interaction ($\delta = 1.0, \upsilon = 3.0$).

Section of the adiabatic potentials in the case of JT instability, illustration for the zero-field splitting of the ground state in the vibronically distorted configurations conical intersection at $\rho = 0$ that corresponds to the basic JT $E \otimes e$ problem [23-25]: $U_{\pm}(\rho)/\hbar\omega = \rho^2/2 \pm \left(\sqrt{3}/2\sqrt{2}\right)|\upsilon|\rho$. This limiting case corresponding to the well known spin-phonon coupling Hamiltonian [49] (see for details [23, 27] and references cited therein) has recently been considered again in [48]. In general, the shape of the surfaces depends on the interrelation between the AS exchange and vibronic coupling that proved to be competitive. In the case of weak vibronic coupling and/or strong AS exchange $\upsilon^2 < 4|\delta|/3$ the lower surface possesses the only minimum at $q_x = q_y = 0 (\rho = 0)$ so that the symmetric (trigonal) configuration of the system proves to be stable. In the opposite case of strong vibronic interaction and/or weak AS exchange, $\upsilon^2 > 4|\delta|/3$, symmetric configuration of the cluster is unstable and the minima are disposed at the ring of the trough of the radius ρ_0:

$$\rho_0 = \frac{1}{2}\sqrt{\frac{3\upsilon^2}{2} - \frac{8\delta^2}{3\upsilon^2}}.$$

The radius ρ_0 decreases with the increase of AS exchange and vanishes at $|\delta| = 3\upsilon^2/4$ (defining thus critical value of the vibronic coupling υ_0). Example of this type of the pseudo JT surfaces is shown in Fig. 12b. The depth of the minima ring in the second type (respectively to the top in the low surface) depends on the interrelation between the JT constant and AS exchange and is found to be $\varepsilon_0 = \left(3\upsilon^2 - 4\delta^2\right)^2/48\upsilon^2$ while the gap between the surfaces in the minima points $3\upsilon^2/4$ is independent of the AS exchange. Fig. 13 shows the case of strong JT coupling (instability) and the cross-section of the adiabatic potentials.

10. INFLUENCE OF THE JAHN-TELLER EFFECT ON THE MAGNETIZATION

To clarify the physical situation let us assume that the motion of the system is confined to the bottom of the trough. Strictly speaking this is valid providing strong JT coupling but in all cases it gives clear qualitative results and transparent key expressions keeping at the same time good accuracy in the quantitative description. Providing $\rho = \rho_0' \equiv \sqrt{3/8}\,|\upsilon|$ (radius of the minima ring) the value $\sqrt{3\upsilon^2\rho^2/2}$ is simply the JT splitting $E_{JT} = 3\upsilon^2/4$ (gap between the surfaces in the minima points of the lower surface) one obtains for the Zeeman sublevels in the weak field range up to the second order terms with respect to the field ξ defined by the angle θ:

$$\frac{\varepsilon_{1,3}(\xi)}{\hbar\omega} = -\frac{1}{2}\delta\left(\rho_0'\right) \pm \frac{1}{2}\kappa_1(\theta)\xi - \kappa_2(\theta)\xi^2,$$
$$\frac{\varepsilon_{2,4}(\xi)}{\hbar\omega} = +\frac{1}{2}\delta\left(\rho_0'\right) \pm \frac{1}{2}\kappa_1(\theta)\xi + \kappa_2(\theta)\xi^2. \qquad (24)$$

where the eigen-values are denoted as $\varepsilon_i(\xi) \equiv \varepsilon_i(\rho_0', \xi)$ and the van Vleck coefficients $\kappa_1(\theta)$ (first coefficient) and $\kappa_2(\theta)$ (second coefficient) [53] can be directly related to the JT splitting and AS exchange by:

$$\kappa_1(\theta) = \sqrt{\frac{E_{JT}^2 + \delta^2\cos^2\theta}{E_{JT}^2 + \delta^2}},$$
$$\kappa_2(\theta) = \frac{\delta^2\sin^2\theta}{4\left(E_{JT}^2 + \delta^2\right)^{3/2}}. \qquad (25)$$

In order to reveal the influence of the JT coupling on the anisotropic properties of the AS exchange in more detail let us consider the effects of JT coupling in the two principal directions of the magnetic field. In the case of parallel field ($\boldsymbol{H}\|C_3$) one finds that $\kappa_1(0) = 1$ and $\kappa_2(0) = 0$ so that one obtains the linear Zeeman splitting in a pair of spin doublets in the parallel field but the role the zero-field splitting plays now the combined effective gap $\sqrt{E_{JT}^2 + \delta^2}$ instead of the initial one $|\delta|$ related to the AS exchange. In the case of perpendicular field $\boldsymbol{H} \perp C_3$ one obtains:

$$\frac{\varepsilon_{2,4}(\xi)}{\hbar\omega} = +\frac{1}{2}\sqrt{E_{JT}^2+\delta^2} \pm \frac{E_{JT}}{\sqrt{E_{JT}^2+\delta^2}}\ \frac{1}{2}\xi + \frac{\delta^2}{4\left(E_{JT}^2+\delta^2\right)^{3/2}}\ \xi^2 . \qquad (26)$$

Eq. (26) shows that the Zeeman pattern contains both linear and quadratic contributions. The role of the JT coupling can be understood by comparing the Zeeman picture so far obtained with that at $\upsilon = 0$. It is important that in the absence of the JT coupling the linear Zeeman terms disappear and the Zeeman energies contain only quadratic terms (with respect to the field). Thus Fig. 14a illustrates two degenerate pairs of the Zeeman levels in perpendicular field in the symmetric nuclear configuration. In a weak field range they are given by:

$$\frac{\varepsilon_1(\xi)}{\hbar\omega} = \frac{\varepsilon_3(\xi)}{\hbar\omega} = -\frac{|\delta|}{2} - \frac{\xi^2}{4|\delta|} \quad , \quad \frac{\varepsilon_2(\xi)}{\hbar\omega} = \frac{\varepsilon_4(\xi)}{\hbar\omega} = +\frac{|\delta|}{2} + \frac{\xi^2}{4|\delta|}. \qquad (27)$$

This can be referred to as the effect of the reduction of the magnetization in low magnetic field that is perpendicular to the axis of AS exchange [23,27]. The reduction of the Zeeman energy by the AS exchange gives rise to a small van Vleck type contribution to the magnetic susceptibility at low field $g\beta H << D_n$. An essential effect is that the JT interaction leads to the occurrence of the linear terms for the Zeeman energies at low field in plane of the triangle. This is shown in Figs. 14b-14d that illustrate transformation of the Zeeman levels under the influence of the vibronic coupling obtained with the aid of the general Eq. (22).

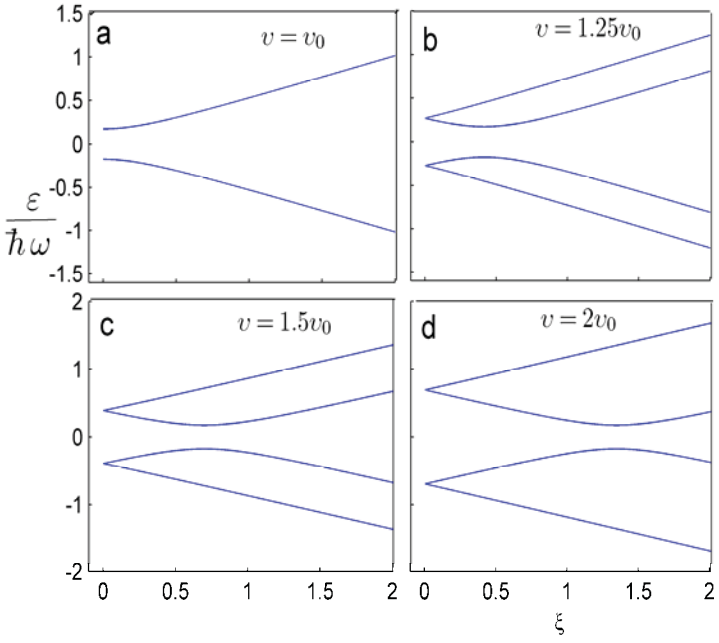

Fig. 14. Influence of the JT interaction (defined by the vibronic coupling parameter υ) on the Zeeman energy pattern in a perpendicular field.

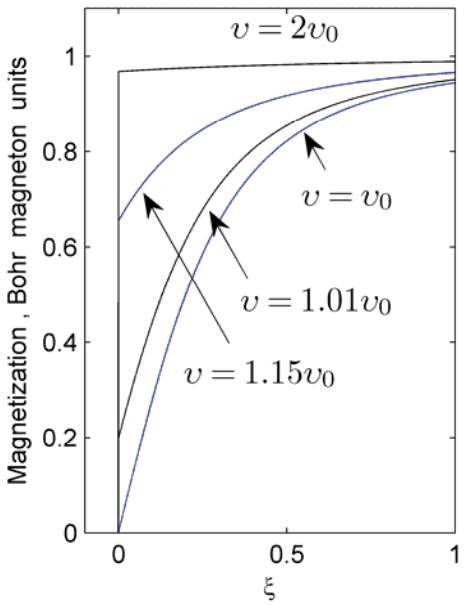

Fig. 15. Influence of the JT interaction on dependence of magnetization vs. perpendicular field ($\mathbf{H} \perp C_3$).

Fig. 15 illustrates the influence of the JTE on the field dependence of the magnetization of a triangular unit that is closely related to the influence of the vibronic coupling on the Zeeman pattern (Fig. 14). The magnetization vs. perpendicular field at *T*=0 is presented as a function of the vibronic coupling parameter υ that is assumed to satisfy the condition of instability $\upsilon^2 > \upsilon_0^2 \equiv 4|\delta|/3$. One can see that providing $\upsilon = \upsilon_0$ (and of course $\upsilon < \upsilon_0$ that corresponds to a symmetric stable configuration) the magnetization slowly increases with the increase of the field (due to reduction of the Zeeman interaction in the low field) then reaches saturation when the magnetic field is strong enough to break the AS exchange. Increase of the JT coupling leads to the fast increase of the magnetic moments in the region of low field and formation of the step in magnetization caused by the reduction of the magnetic anisotropy (appearance of the linear terms in the Zeeman levels). This observation is in line with the general concept of the reduction factors in the JT systems. On can see that the semiclassical approach is able to describe this effect. The height of the step depends on the interrelation between AS exchange and vibronic coupling and can be expressed as:

$$M(H=0)=\frac{g\beta}{2}\frac{E_{JT}}{\sqrt{E_{JT}^2+\delta^2}} \tag{28}$$

The height of the step increases with the increase of the vibronic coupling. Finally, when the JT coupling is strong enough ($\upsilon = 2\upsilon_0$) one can observe staircase like behavior of magnetization with the sharp step in which *M(H)* jumps from zero to *M(H* = 0) = gβ/2 at zero field (and T=0) that is expected for a magnetically isotropic system. The influence of the distortions caused by JT instability is very pronounced so that the step starts to appear even when $\upsilon = 1.01\,\upsilon_0$. Although the semiclassical description in this range of parameters loses its accuracy the qualitative results are able to draw an adequate physical picture. More accurate quantitative results in this area of vibronic coupling can be obtained by solving the dynamic pseudo JT problem. Another case of interest, strong magnetic field, is discussed in [47]. Numerical estimations [51] show that the vibronic JT parameters for V_{15} are small but the JT coupling is expected to be significant for copper(II) clusters. In fact, recently very large AS exchange was evoked in [54] in the study of unusual properties of tri- copper clusters. Very strong antiferromagnetic exchange interaction $\left(J=-650cm^{-1}\right)$ has been recently found [55] in a chloride-centered hexanuclear copper(II) cluster that can be a good candidate to test AS exchange in the excited states that exhibit degeneracy (E_1 and E_2 terms) and are expected to be JT active with the significant coupling constants.

SUMMARY

We have given a comprehensive analysis of the unique V_{15} molecular magnetic cluster within the three spin model assuming that the isotropic and AS exchange are acting in the equilateral spin-frustrated trimer. The energy levels behavior and crossover as well as the low-temperature magnetization were studied for different field directions and theoretically explained using pseudo angular momentum representations for the many-spin states. We have indicated the differences between the normal and in-plane parts of the AS exchange interaction and revealed the particular role played by the first at low fields and by the second one in the vicinity of intersection points. Afterwards using pseudo angular quantum numbers we have formulated the selection rules for the EPR transitions and have given comprehensive analysis of the EPR spectra at different frequencies. At the same time we have recognized the high-frequency temperature dependence of the spectral bandwidth as problem which can not be explained within the foregoing model and thus addressing us for studying additional phenomena like relaxation processes and hyperfine structure in vanadium clusters. We succeeded in fitting the results of our calculations to the experimental data for low-temperature magnetization and in this way for the first time precisely estimated the components of AS exchange vectors for the V_{15} molecule. JT instability is shown to eliminate spin frustration due to removal of the "accidental" degeneracy in course of the dynamical structural distortions. The influence of the vibronic interaction on the magnetization is revealed with the aid of the semiclassical adiabatic approach that provides qualitatively transparent results and gives numerical results with a good accuracy. The first and second van Vleck coefficients in the Zeeman energies are deduced as the functions of the direction of the field, AS exchange and vibronic coupling. The JT coupling is shown to be competitive to the AS exchange so that the increase of the vibronic coupling decrease the magnetic anisotropy of the system. On the other hand AS exchange tends to suppress to JTE. This is demonstrated by the theoretical modeling of the field dependence of the magnetization that clearly exhibits crucial role of the pseudo JT coupling in spin-frustrated systems. Furthermore we can conclude that we understand more about the physical contents of the concept of spin frustration and about frustrated systems integrated in complex systems. Therefore, we intend to extend this to other complex systems, e.g. where frustrated systems are interacting like double triangular cluster in $\{Mo_{57}\}\{V_3\}_2$ (see ref [56]). Structure-related magnetism of polyoxometalates from the standpoint of spin frustration in high-nuclearity metal clusters is highlighted in review article [57].

ACKNOWLEDGMENTS

Financial support from the German-Israeli Foundation (GIF) for Scientific Research & Development (grant G-775-19.10/2003) is gratefully acknowledged. A.M. thanks also the Deutsche Forschungsgemeinschaft, the Fonds der Chemischen Industrie, the European Union, and the Volkswagenstiftung.

REFERENCES

[1] A. Müller, J. Döring, Angew. Chem. Int. Ed. Engl. 27 (1988) 1721.
[2] D. Gatteschi, L. Pardi, A.-L. Barra, A. Müller, J. Döring, Nature 354 (1991) 465.
[3] A.-L. Barra, D. Gatteschi, L. Pardi, A. Müller, J. Döring, J. Am. Chem. Soc. 114 (1992) 8509.
[4] D. Gatteschi, L. Pardi, A.-L. Barra, A. Müller, Mol. Eng. 3(1993) 157.
[5] B. Barbara, J. Mol. Struct. 656 (2003) 135.
[6] I. Chiorescu, W. Wernsdorfer, A. Müller, H. Bögge, B. Barbara, Phys. Rev. Lett. 84 (2000) 3454.
[7] I. Chiorescu, W. Wernsdorfer, A. Müller, S. Miyashita, B. Barbara, Phys. Rev.B67 (2003) 020402(R).
[8] S. Miyashita, J. Phys. Soc. Japan, 65 (1996) 2734.
[9] H. Nojiria, T. Taniguchia, Y. Ajiro, A. Müller, B. Barbara, Physica B 346–347 (2004) 216.
[10] S. Miyashita, J. Phys. Soc. Japan, 64 (1995) 3207.
[11] V.V. Platonov, O.M. Tatsenko, V.I. Pils, A.K. Zvezdin, B. Barbara, Physics of the Solid State (Rus. Fizika Tverdogo Tela), 44 (2002) 2010.
[12] J. Kortus, M.R. Pederson, C.S. Hellberg, S.N. Khanna, Eur. Phys. J. D16 (2001) 177.
[13] J. Kortus, C.S. Hellberg, M.R. Pederson, Phys. Rev. Lett. 86 (2001) 3400.
[14] D.W. Boukhvalov, V.V. Dobrovitski, M.I. Katsnelson, A.I. Lichtenstein, B.N. Harmon, P. Kögerler, Phys. Rev. B70 (2004) 054417.
[15] H. De Raedt, S. Miyashita, K. Michielsen, Phys. Stat. Sol. (b) 241 (2004) 1180.
[16] S. Miyashita, H. De Raedt, K. Michielsen, Prog. Theor. Phys. 110 (2003) 889.
[17] H. De Raedt, S. Miyashita, K. Michielsen, M. Machida, Phys. Rev. B70 (2004) 064401.
[18] N.P. Konstantinidis, D. Coffey, Phys. Rev. B 66 (2002) 174426.
[19] G. Chaboussant, R. Basler, A. Sieber, S.T. Ochsenbein, A. Desmedt, R.E. Lechner, M.T.F. Telling, P. Kögerler, A. Müller, H.-U. Güdel, Europhys. Lett. 59 (2) (2002) 291.
[20] G. Chaboussant, S.T. Ochsenbein, A. Sieber, H.-U. Güdel, H. Mutka, A. Müller, B. Barbara, Europhys. Lett. 66 (3) (2004) 423.
[21] I.E. Dzyaloshinsky, Zh.Exp.Teor.Fiz. 32(1957)1547.
[22] T. Moria, Phys. Rev. 120 (1960) 91.
[23] B.S. Tsukerblat, M.I. Belinskii, V.E. Fainzilberg, Magnetochemistry and spectroscopy of transition metal exchange clusters, in: Soviet Sci. Rev. B, Harwood Acad. Pub. (1987), ed. M. Vol'pin, pp. 337– 482.
[24] M.I. Belinskii, B.S. Tsukerblat, A.V. Ablov, Phys. Stat. Solidi (1972) K71.
[25] M.I. Belinskii, B.S. Tsukerblat, Fizika. Tverdogo Tela (Rus), 15 (1973) 29.
[26] B.S. Tsukerblat, M.I. Belinskii, A.V. Ablov, Fizika. Tverdogo Tela (Rus), 16 (1974) 989.
[27] B.S. Tsukerblat, M.I. Belinskii, Magnetochemistry and Radiospectroscopy of Exchange Clusters, Pub. Stiintsa (Rus) Kishinev (1983).
[28] B.S. Tsukerblat, B. Ya. Kuavskaya, M. I. Belinskii, A. V. Ablov, V. M. Novotortsev, V.T. Kalinnikov, Theoretica Chimica Acta 38 (1975) 131.
[29] M.I. Belinskii, B.S. Tsukerblat, A.V. Ablov, Molecular Physics,28 (1974) 283.
[30] B.S. Tsukerblat, V.E. Fainzilberg, M.I. Belinskii, B. Ya. Kuyavskaya, Chem. Phys. Lett. 98 (1983) 149.
[31] B.S. Tsukerblat, B. Ya. Kuyavskaya, V.E. Fainzilberg, M.I. Belinskii, Chem. Phys. 90 (1984) 361; 90 (1984) 373.
[32] V. E. Fainzilberg, M.I. Belinskii, B. Ya. Kuyavskaya, B. S. Tsukerblat, Mol. Phys.,54 (1985) 799.
[33] B.S. Tsukerblat, I.G. Botsan, M.I. Belinskii, V.E. Faiinzilberg, Molec. Phys. 54 (1985) 813.
[34] V.E. Fainzilberg, M.I. Belinskii, B.S. Tsukerblat, Solid State Com. 36 (1980) 639.
[35] V.E. Fainzilberg, M.I. Belinskii, B.S. Tsukerblat, Mol. Phys., 44 (1981) 1177; 44 (1981) 1195; 45 (1982) 807.
[36] Tsukerblat, A. Tarantul, A. Müller, Phys. Lett. A 353 (2006) 48. 35
[37] J. J. Borras-Almenar, J.M.Clemente-Juan, E. Coronado, B.S. Tsukerblat, Inorganic Chemistry, 38 (1999) 6081; J. Comp. Chemistry, 22(2001)985.
[38] B.S. Tsukerblat, Group Theory in Chemistry and Spectroscopy, Academic Press, London,1994; Dover Pub. Inc, Mineola, New York, 2006.
[39] B. Tsukerblat, A. Tarantul, A. Müller , J. Chem. Phys., 125 (2006) 0547141.
[40] T. Sakon, K. Koyama, M. Motokawa, Y. Ajiro, A. Müller, B. Barbara, Physica B 346–347 (2004) 206.
[41] I. Chiorescu , W. Wernsdorfer, A. Müller, H. Bögge, B.Barbara, J.Magn. Magn. Mater., 221 (2000) 103.
[42] M. Machida, T. Iitaka, S. Miyashita, arXiv:cond-mat/0501439 v2 16 Jun 2005.
[43] A. Tarantul, B. Tsukerblat, A. Müller, *Chem. Phys. Let.*, 428 (2006) 36.
[44] A. Tarantul, B. Tsukerblat, A. Müller, *Inorg. Chem.,* 46 (2007) 161.
[45] R. Englman, *The Jahn–Teller Effect in Molecules and Crystals*, Wiley, London, 1972.

[46] I.B. Bersuker and V.Z. Polinger, *Vibronic Interactions in Molecules and Crystals*, Springer-Verlag, Berlin, 1989.
[47] I.B. Bersuker, *The Jahn-Teller Effect*, Cambridge University Press, 2006.
[48] J.J. Borrás-Almenar, E. Coronado, H.M. Kishinevsky, B.S. Tsukerblat, *Chem.Phys.Lett.* 217 (1994) 525.
[49] C.A. Bates and R.F. Jasper, *J.Phys.C: Sol. State Phys*., 4 (1971) 2341.
[50] A. Varshalovich, A. N. Moskalev and V. K. Khersonskii, *Quantum Theory of Angular Momentum*, World Scientific, Singapore, 1988.
[51] B. Tsukerblat**,** A. Tarantul, A. Müller, *J. Mol. Structure*, 838 (2007) 124.
[52] A.I. Popov, V.I. Plis, A. F. Popkov, A.K. Zvezdin, *Phys. Rev.B,* 69 (2004) 104418.
[53] O.Kahn, *Molecular magnetism*, VCH, NY, 1993.
[54] J. Yoon, L. M. Mirica, T. D. P. Stack, E.I. Solomon, *J.Am.Chem.Soc*., 126 (2004) 12586.
[55] A.A. Mohamed, A. Burini, R., Galassi, D. Paglialunga, J. R. Galán-Mascarós, K.R. Dunbar, J. P. Fackler, Jr. *Inorg. Chem*., 46 (2007) 2348.
[56] D. Gatteschi, R. Sessoli, W. Plass, A. Müller, E. Krickemeyer, J. Meyer, D. Sölter, P. Adler, *Inorg. Chem.***,** *3,* (1996) 1926.
[57] P. Kögerler, B. Tsukerblat, A. Müller, *Dalton Transactions* (to be published).

INVESTIGATION OF GRAPE SEED PROANTHOCYANIDINS. ACHIEVEMENTS AND PERSPECTIVES

V. Kulciţki, P. F. Vlad*, Gh. Duca, T. Lupaşcu
Institutul de Chimie al Academiei de Ştiinţe a Moldovei, str. Academiei 3, MD-2028, Chişinău, Republica Moldova
**E-mail: vlad_p@mail.md; Phone: 373 22 739775; Fax: 373 22 739775*

Abstract
The present paper provides an account of the basic technuques employed in the investigation of the grape seeds proanthocyanidins (condensed tannins). The importance and biological activity properties of these compounds are considered briefly in the introductory part, while isolation and structural investigation of grape seeds proanthocyanidins represent the basic part of the review. The references cover mostly the recent publications related to implementation of modern techniques of investigation, like high performance liquid chromatography (HPLC) and mass spectrometry (MS). Number of references – 68.

Keywords: polyphenols, proanthocyanidins, grape seeds, chromatography, MS, NMR.

Content

1. INTRODUCTION. GRAPE SEEDS TANNINS, BIOLOGICAL ACTIVITY AND APPLICATIONS.

Grape seeds condensed tannins (GST), called also proanthocyanidins, represent a group of natural products with polyphenolic structure. The interest towards these compunds is determined by several factors. First of all they posess a wide spectrum of biological activity, and their presence in the human diet is considered a preventing measure to avoid such severe pathologies like stroke and cancer. The beneficent intake of grape seeds tannins by humans is connected with moderate wine consumption. Grape seeds represent a byproduct of grape processing and they contain appreciable amounts of polyphenolic compounds. Provided the fact that valorification of the wine industry secondary products is one of the research priority directions recognized by Moldovan governement, several companies developed research programs directed to elaboration of efficient procedures for proanthocyanidins extraction from the grape seeds.

Historically, the first explored source of condensed tannins was the pine bark. One of the most preferable sources of these compounds in the recent years became the grape seeds, which are readily available in industrial quantities and a lot of different commercial grape seeds extracts are on the market as sources of grape seeds proanthocyanidins. Tannins are highly hydroxylated aromatic structures that form insoluble complexes with carbohydrates and proteins, a measure of their astringency is based on their ability to cause precipitation of salivary proteins. The polyphenolics, including proanthocyanidins, constitutes a considerable portion of the tannins found in wine, and in particular contribute heavily to the colour and flavour of red wines.

Oligomeric proanthocyanidin complexes are primarily known to be responsible for organolepthic properties of wine, including colour and astringency.[1,2,3,4] Besides, derivatives of flavan-3-ol are important natural antioxidants in living cells. Therefore, grape seeds proanthocyanidins are considered for their antioxidant activity first. The redox-potential of the phenolics is known to be sufficiently low, to interact easily with different oxidyzing species by different mechanisms, basically by a radical scavenging one.[5,6]

These compounds can also play an important role as repellents in plant protection against pathogens and different predators.[3] Literature data show that proanthocyanidins effect a protective action on DNA oxidative damage and have a benefical action to the preventive carcinogenesis inhibition.[7] Along with their antioxidant properties, proanthocyanidins can influence the release of nitrogen oxide by endothelial cells.[8] Basing on these mechanisms of action, these compounds have been reported to demonstrate antibacterial, antiviral, anticarcinogenic, anti-inflammatory, anti-allergic and vasodilatory actions. In addition, they have been reported to inhibit platelet aggregation, improve capillary permeability, diminish their fragility and to affect enzyme systems including phospholipase A2, cyclooxygenase, and lipoxygenase. The potential health benefit of proanthocyanidins was broadly recognized.[9] These varied biological activities have resulted in the phytopharmaceutical application of condensed tannins in reduction of edema, increased peripheral circulation, improvement in vision, treatment of diabetic retinopathy, prevention of cardiovascular disease, treatment of hypercholesterolemia, stabilization of connective tissue tone, reduced adverse allergic and inflammatory responses, and enhanced immune function and wound healing.[10] The well mediated "French paradox"[11] consists in the lower incidence of cardiovascular diseases, including fatal cases in France, compared with similar data for Great Britain or USA. It is explained by the regular wine consumption in France, that contributes to chronic inflammation inhibition and antiplatelet activity.[12]

Grape seeds proanthocyanidin extracts are used as active pharmaceutical components in different preparations (e.g. Leucoselect ™) for treatment of blood vessels fragility, increasing their walls stability, as well as for free radical quenching and superoxide ions inhibition.[13]

Basing on these data, grape seeds proanthocyanidins are of great interest as biologically active compounds with a broad spectrum of activity.

2. CHEMICAL STRUCTURE OF GRAPE SEED TANNINS

The composition of the grape seeds proantocianidins is very complex. The structural units that are on the basis of this complexity are two polyphenolic compounds: catechin **1** and *epi*-catechin **2**.

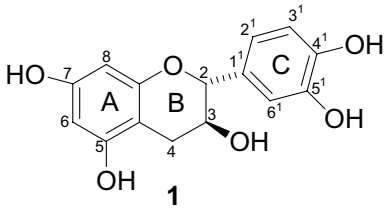

1

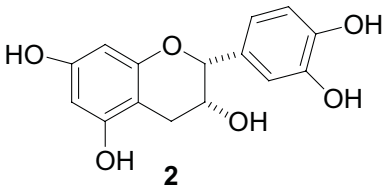

2

Oxidative condensation occurs between carbon C-4 of **1** or **2** and carbons C-6 or C-8 of the attached molecules. The resulting oligomers form a plethora of compounds differing in degree of polymerization (DP), linkage patterns and monomers sequence. Procyanidins B1-B4 (**3**-**6**), having the C4-C8 linkage, are the most common dimers.[14] Some oligomers and polymers have the C-3 hydroxil group esterified with galic acid.[8,14]

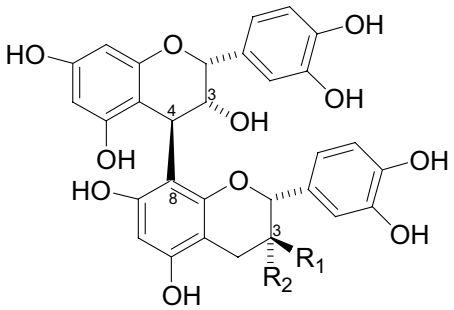

3 R_1=OH; R_2=H Proanthocyanidin B1
4 R_1=H; R_2=OH Proanthocyanidin B2

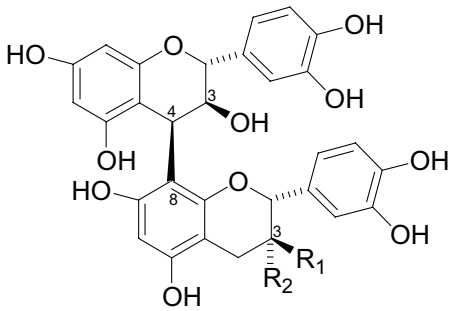

5 R_1=OH; R_2=H Proanthocyanidin B3
6 R_1=H; R_2=OH Proanthocyanidin B4

It is noteworthy mentioning that only few individual pure proanthocyanidins were isolated and characterized, ranging in structure up to tetramers.[13] Distribution of proanthocyanidins in grape seeds, including of white grapes, was studied by many authors.[13,15,16-19] Monomeric flavanols and their galates predominates in the water soluble procyanidins fraction obtained from grape seeds. Oligomers are represented mostly by B-type proanthocyanidins.[18,20] Their structure was investigated in the works.[11,21,22] A comparative study of flavan-3-ols composition was performed.[20] They were isolated from the seeds of 17 different varieties of Spanish grapes, including 10 red and 7 white samples. A total number of 27 proanthocyanidins were identified: (+)-catechin, (-)-epi-catechin, epi-catechin-3-O-galate, dimmers B-1 – B-7 (**3**)-

(**9**), trimers C-1 (**11**) and C-2 (**12**), along with a bunch of proanthocyanidins esterified with galic acid on C-3 hydroxyl group in B-cycle and on C-3' phenolic hydroxyl in C-cycle.

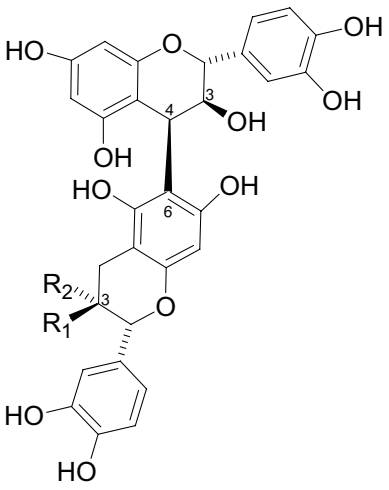

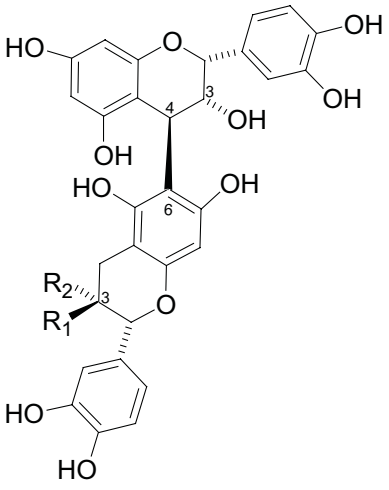

7 R_1=H; R_2=OH Proanthocyanidin B5
8 R_1=OH; R_2=H Proanthocyanidin B7

9 R_1=OH; R_2=H Proanthocyanidin B6
10 R_1=H; R_2=OH Proanthocyanidin B8

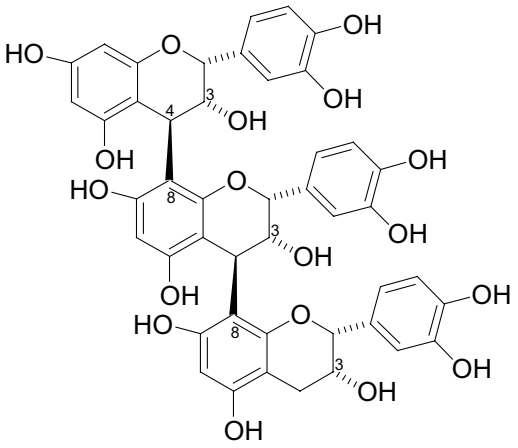

11 Proanthocyanidin C1

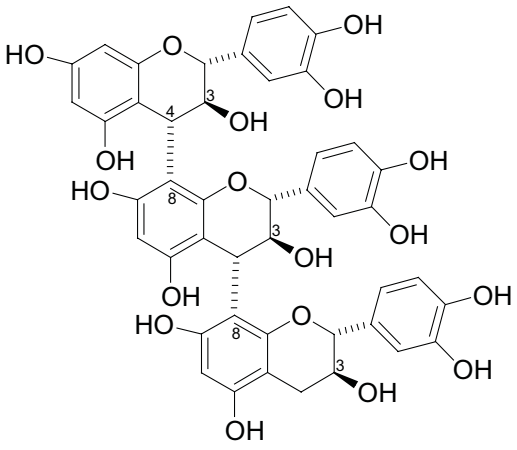

12 Proanthocyanidin C2

Among esterified compounds there are dimers and trimers of flavan-3-ol, some of them contain two galic acid residues. The B-2 dimer (**4**) predominates in the dimeric group. The described proanthocyanidins differ not only by the number and sequence of flavan-3-ol units, esterification patern, but also by different monomer junction (C-4 – C-8 and C-4 – C-6) and C-4 configuration (α or β). There is only one described tetramer in this work and it consists only of epi-catechin residues [epi-catechin (4β-8)- epi-catechin (4β-8)- epi-catechin (4β-8)- epi-catechin]. Isolation of individual polymeric tannins represents a very difficult task. All of the reported examples relate only isolation of fractions containing mixtures of several polymers.[13]

The mean degree of polymerisation (mDP) of flavan-3-ols can be different and the obtained data depend on the determination method. According to authors[1] high molecular weight proanthocyanidins can contain up to 20 flavan-3-ol units and these compounds are soluble in wine. A trigaloilated octamer was also reported.[23] Mass-spectrometric investigations[24] reported the polymerisation degree from 9 to 11 units. In the same time, basing on acidic hydrolysis experiments[25,26] higher values of 17 and 31 units were reported. A more detailed analysis of these data will be provided in the following discussion below.

3. EXTRACTION METHODS EMPLOYED IN THE GRAPE SEEDS TANNINS ISOLATION

Isolation of grape seeds proanthocyanidins includes seed grinding followed by extraction with a suitable solvent. Different solvents have been employed: acetone,[27,28] acetone-water mixture 70:30 in the presence of silicagel,[15] 60:40 at +4 °C,[1] 50:50 at room temperature,[2] methanol containing ascorbic acid (1g/l) at -20°C, followed by methanol-water

mixture (1:1) at -24°C and acetone-water mixture (75:25) all under nitrogen atmosphere.[20,29] Methanol in combination with other solvents was used for extraction of tannins too. Some examples include extraction with HCl-acidified methanol,[30] methanol-water mixture (75:25) at room temperature under ultrasound irradiation,[3] pure methanol at room temperature.[8] Aqueous ethanol was used for extraction of grape seeds tannins[5,31] and proanthocyanidins from *Rhodiola semenovii*.[32]

Proanthocyanidins are unstable compounds. They undergo facile oxidation by atmospheric oxygen. That's why some authors used antioxidants (SO_2, ascorbic acid) dissolved in extraction solvents employed in the grape seeds extraction. Other preventive actions include extraction under inert atmosphere (N_2), as well as grinding of the raw material under liquid nitrogen.[1] According to authors,[11] the mixture acetone-water is the best extraction solvent for grape seeds proanthocyanidins. Nevertheless, all of the enumerated solvents have the drawback to extract along with proanthocyanidins other accompanying compounds that make extraction laborious and lower the proanthocyanidins yield. There are no literature data reporting on selective solvent systems for proanthocyanidin extraction. On the other hand, it is known that lower molecular weight catechin oligomers are soluble in ethylacetate and this solvent showed notable selectivity for the extraction of some other natural compounds. In this context, authors[11] studied the extraction of grape seeds with ethylacetate as a method of preparative isolation of proanthocyanidins. It is noteworthy mentioning that the grape seeds were extracted without grinding, as a necessary condition to avoid concomitant extraction of ballast compounds. It turned out, though, that ethylacetate practically does not extract proanthocyanidins, due to a very low permeability of seeds wall for the non polar aprotic solvent. The solution of the problem included extraction with the mixture ethylacetate-water (90:10) and this mixture provided a selective extraction of proanthocyanidins according to a simple procedure which allowed preparative extractions in industrial quantities.

Another interesting extraction example[32] includes fractionation of an ethanol-water extract by successive extraction with diethyl ether and ethylacetate to provide more simple proanthocyanidin fractions. The etheric fraction included (+)-catechin (**1**), (+)-gallocatechin (**13**), (-)-epi-catechin (**2**), (-)-epi-catechin-gallate (**14**), (-)-epi-gallocatechin (**15**), (-)-epi-gallocatechin-gallate (**16**) and gallic acid (**17**). The ethylacetate fraction contained the following dimers: (+)-catechin-(4α-8)-(+)-catechin (**18**), (-)-epi-catechin gallate-(4β-8)-(-)-epi-catechin gallate (**19**) and (-)-epi-catechin-(4β-8)-(-)-epi-catechin gallate (**20**).

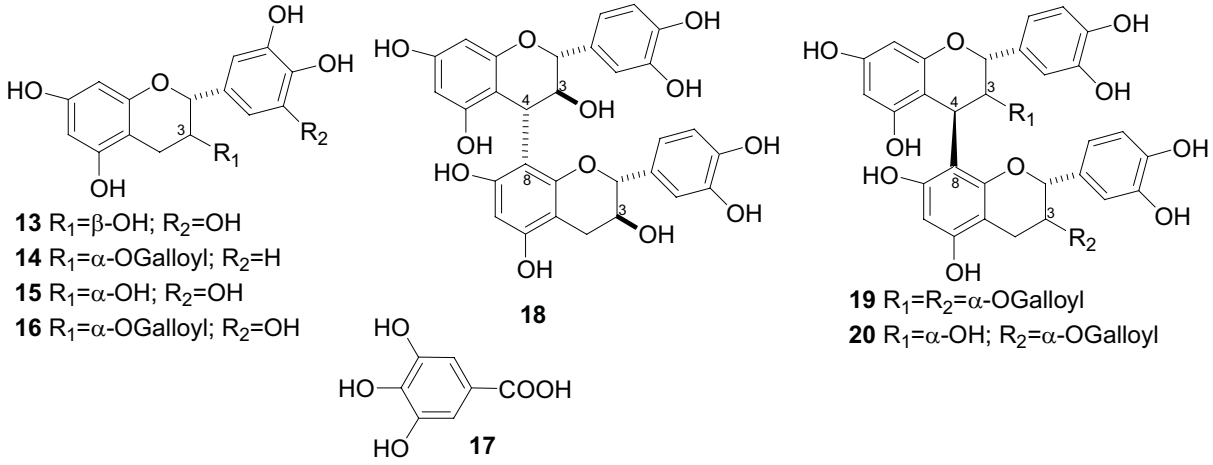

4. METHODS FOR PROANTHOCYANIDINS FRACTIONATION

Semipreparative fractionation of proanthocyanidins extracts is normaly performed by column chromatography. The separation procedure is based on the gel filtration-gel permeation chromatography (GPC). As the stationary phase Sephadex LH-20 is used most of all. For example Oszmianski and collaborators[15] used a column with Sephadex suspended in 96% ethanol. Elution of the column was performed with the same solvent. For a successful resolution of (+)-catechin and (-)-epichatechin the column was filled with a Sephadex slurry in water and elution was performed with a solution of acetic acid with the gradual increasing the acid concentration from 0 to 25%. Monitoring of the column eluate was performed by UV detection at 280nm. The further investigation of the obtained fractions was performed by HPLC. Degree of polymerisation of individual fractions was estimated by TLC. It has been noted that the mean degree of polymerisation can be established by gel filtration. In the other work, investigation of Leucoselect™[13] included dissolution of the sample in 90% ethanol, followed by fractionation on Sephadex LH-20. Elution was started with the same solvent, followed by a stepwise gradient of acetone in water (20%, 40%, 70% acetone). The obtained fractions were studied further by TSI/ESI MS, HPLC (GPC). A Sephadex column was used also for the fractionation of proanthocyanidins from *Rhodiola Semenovii*.[32] Fractionation of the mixture of proanthocyanidins on Sephadex was used

in other works too.[3,7] It is noteworthy mentioning that in the latter work[7] authors used the proanthocyanidin separation methodology described in earlier works.[33,34]

Fractionation of proanthocyanidins extract was performed also on columns with polyamide.[29,35] The TLC-grade polyamide was used for column chromatography in the work,[35] while commercial Macherey-Nagel, Duran (Germany) polyamide was used in the work.[29]

Preliminary fractionation of the grape seed extracts was based on adsorption chromatography using commercial Toyopearl TSK HW-40(F) gel (Tosoh corp., Tokyo).[8,1,2] The separation procedure has been described in the earlier work.[36] Monomers and oligomers have been eluted from the column with a mixture ethanol-water (55:45, v/v), containing 0.05% trifluoroacetic acid and polymeric proanthocyanidins with a mixture ethanol-water (60:40, v/v).[1] Fractogel TSK HW-40 (s) was used to fractionate a proanthocyanidin extract.[5] The origin of the stationary phase was not specified. Microcrystallic cellulose powder was also used for the column chromatography of proanthocyanidines.[32]

One should mention that the methodologies related to the separation of non-polar phenols from polymeric ones have been paid a lot of attention in the literature. But most of the methods are rather complicated, time consuming and lead to substantial amount of wastes. On the contrary, a very simple method has been elaborated on the basis of solid phase extraction (SPE) that allows a quick and efficient separation of phenolic compounds from grapes.[25] The method consists of the application of the sample solution on to a SPE cartridge (e.g. C_{18} Sep-Pak), followed by elution with solvents of different polarity. Low molecular weight components are separated from oligomers and higher polymers. A fractionation example of preliminary adsorbed on a SPE cartridge consists in elution of monomeric falavonols with diethyl ether and oligomeric with polymeric proanthocyanidins with methanol.[1] Authors[29] eluted from the SPE cartridge the phenoloxiacids with an aqueous buffer (pH=7), then monomeric and oligomeric flavan-3-ols have been eluted with ethylacetate, followed by a final wash with methanol to remove the polymeric proanthocyanidins. The fraction containing monomers and oligomeric flavan-3-ols was applied to SPE repeatedly to elute monomers with diethyl ether and oligomers with methanol. A similar fractionation of proanthocyanidines from wine was reported to produce 3 fractions of different polarity.[7] Phenoloxiacids were eluted with water, catechins, flavonols and anthocyanidins with ethylacetate while polymeric compounds were eluted with a mixture of methanol/acetone/water.

Fractions obtained after the preliminary fractionation are subjected as usual to a more rigorous separation procedure by HPLC methods.

5. CHEMICAL METHODS IN THE INVESTIGATION OF PROANTHOCYANIDINS

Chemical methods of investigation have been among the first approaches in the investigation of the chemical structure of complex polymeric polyphenolics from grape seeds. Most of these methods comprise a degradation of the polymeric structure under acidic conditions in the presence of a nucleophile. As the result, valuable information concerning proanthocyanidine structure can be obtained, including the mean degree of polymerisation, nature of monomeric flavanols and terminal groups. As nucleophilic agents benzylmercaptane[1,29,5,30,37-39] and floroglucinol[40] have been used in most of the investigations. In the case of the benzylmercaptane treatment extender units of the oligomer **I** provide flavan-3-ols thyoethers **II** and flavan-3-ols **III** from the terminal units. The mechanism of this cleavage is represented in the scheme below. Initial protonation of the pyran ring is followed by the nucleophilic attack of the sulphur compound and C4-C8 bond cleavage.

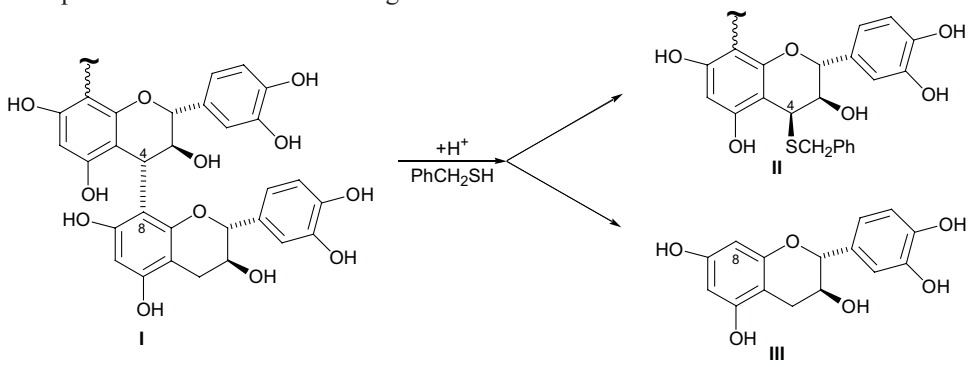

After acidic treatment in the presence of benzylmercaptane the reaction product can be treated with Raney-Ni[5] in order to remove the sulphur residue. Similar data are obtained after acidic hydrolysis in the presence of floroglucinol. The reaction is performed in methanol in the presence of sulphuric acid and excess floroglucinol. The method provide information on the flavan-3-ol units composition, conversion yield and mean degree of polymerisation.[3,40]

Proanthocyanidin cleavage was also performed under enzymatic catalysis, using phenol heterosidase.[5] The hydrolizate is analysed successively by HPLC. Proanthocyanidin structure was also evaluated by acidic

depolymerisation using hydrochloric acid in butanol,[41] total phenolics was determined by the well known Folin-Ciocalteau method and some other less common methods were also used. But all of the approaches lack reproducibility and specificity, due to the complex nature of the analytical matrix and side reactions that have been also reported.[13]

6. PHISICO-CHEMICAL METHODS IN THE INVESTIGATION OF PROANTHOCYANIDINS

Investigation of the grape seed condensed tannins following after rough fractionation was reported by different phisico-chemical methods of analysis. Classical chemical methods of investigation were followed by modern techniques, such as chromatographic (TLC, GLC, HPLC) and spectroscopic (UV-Vis, IR, MS, NMR) methods. But due to the high complexity of the studied mixtures of compounds, the most important information about the proanthocyanidin structure was obtained by HPLC and MS methods. Additionally, high field NMR spectroscopy has become also a powerful investigation tool, provided the fact that high performance NMR spectrometers (500 MHz and higher) has become routine equipment in modern laboratories. Basing on these considerations we will discuss below these modern methods of investigation and their implementation in the field of grape seeds condensed tannins chemistry.

6.1 HPLC methods

Along with the spectacular advent of HPLC, it was broadly use in the analysis of polyphenols of different botanical origins, including condensed tannins from wine, grapes and grape seeds. The power of this analytical method consists of the possibility to resolve highly polar compounds at ambient conditions, with no need of obtaining derivatives or sample heating. In the last decade several improvements have been made to the HPLC equipment which busted efficiently the overall method performance. First of all it is noteworthy mentioning the introduction of Diode Array Detectors in the UV-Vis monitoring of the separation process. They made it possible simultaneous monitoring of the column eluate on the whole spectral width, making possible “on the fly” registering of UV spectra of individual peaks and peak sections. This is a valuable information for peak identification and peak purity estimation,

The other breakthrough in HPLC is connected to the establishment of the interface between the HPLC and the mass spectrometer. It was possible to implement this hyphenated technique due to the development of efficient electro-spray ionization methods and narrow bore columns that reduced substantially the flow rates and peak volumes. In such a way the HPLC-MS method became the most versatile analytical technique for compounds ranging from low molecular weight to biopolymers.

Basing on these achievements, HPLC has found extensive applications in different areas of natural products research, including investigation of grape polyphenols. Two early pioneers of HPLC in oenology were Nagel and Wulf, who published a series of articles that were among the first applications of HPLC to phenolics analysis.[42-44] While initial HPLC studies tended to emphasize the novelty of the method, particularly its speed, oenologists soon began to apply the technique in monitoring the wine quality, including changes in flavonoid content during fermentation and aging of red wines.[44] The application of HPLC to the procyanidin content of ciders and wines was also reported,[45,46] as well as the anthocyanidin profile in wines across 10 years of aging.[47]

A comprehensive review on the HPLC of food flavonoids, including proanthocyanidins, has been published.[48] This review covers the period until 1999 but after that a lot of new papers relating HPLC separation of grape proanthocyanidins has been published.

For proanthocyanidins in foods, analysis by RP chromatography often has been the primary method of choice. HPLC–UV quantitative analysis of proanthocyanidins is typically carried out at 280 nm. However, UV detection is not specific for proanthocyanidins relative to other polyphenolic compounds. Fluorescence detection (excitation 276 and emission 316 nm) offers increased sensitivity and selectivity to procyanidins.[49] RP C18 columns have been used to separate monomers to trimers in the Spanish diet,[50] to tetramers in wine[51] and grape seed.[52,53] Proanthocyanidin oligomers do separate based on their degree of polymerization (monomers through tetramers) and as individual compounds, however, order of elution is not in accordance with molecular size. Furthermore, analysis beyond tetramers has not been achievable with RP chromatography because of retention time overlap and co-elution of higher oligomeric isomers.

Many reports relating to HPLC analysis of GST is connected to the investigation of their biological activity. Fitzpatrick and collaborators describe the isolation from grape seeds and characterization of some of the compounds responsible for endotheliumdependent relaxation of blood vessels activity[8]. Concord grape seeds were extracted with methanol and the compounds were analyzed by analytical and semipreparative HPLC after preliminary fractionation. A Waters HPLC system was employed in conjunction with a 481 UV/Vis detector, Radial Pak reverse phase Nova Pak C18 column, protected by a guard column of the same material. Elution was performed in the gradient mode, employing two

solvents. Mobile phase A was water, mobile phase B was 10% acetic acid in water. The gradient ran from 25% B up to 100% B isocratic over 55 min according to a complex profile. Flow rate was 1.0 mL/min and detection was made at 280 nm. The integral extracts showed a complex profile, with few well resolved identified peaks, except those of monomeric gallic acid, epicatechins and epicatechin galate. One fraction obtained after gel-permeation chromatography showed a satisfactory resolution of compounds possessing increased activity, and from this fraction an individual compound was isolated in a semi-preparative experiment. According to MS data it was a galloylated trimer, and the tentative structure **21** was proposed basing only on MS-MS experiment. Further investigations are necessary, in order to ascertain the stereochemistry of this proanthocyanidin compound.

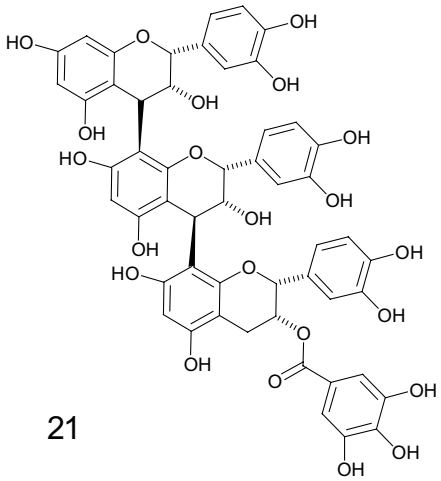

21

Leucoselect™ grape seed selected proanthocyanidins were analyzed by Peterlongo and collaborators[13]. HPLC - thermospray mass spectrometry allowed the detection of monomeric flavan-3-ols and dimeric proanthocyanidins in separate fractions of the commertial product obtained after GPC on Sephadex® LH-20. Separations were performed at room temperature on a SupelcoSil LC-18 column (250 x 4.6 mm i.d., particle size 5 μm). The solvent system was a linear gradient using MeCN (solvent A) and 0.3% phosphoric acid (solvent B) from 10% A to 60% A (complex profile) in 65 min. The flow-rate was 0.7 ml/min, the UV detector was set at 278 nm and the injection volume was 10 μl. Higher oligomers gave an unresolved band under these conditions.

A satisfactory resolution of GST up to trimers was reported on the HPLC of wine-like models[1]. Direct HPLC analyses were performed using a Waters Millenium HPLC-DAD system The column consisted of a Merck reversed-phase Lichrospher 100-RP 18 (250 mm x 4 mm i.d.) protected with a guard column of the same material and was equilibrated at 1mL/min in a mixture of solvent A (water/formic acid 95:5 v/v) and solvent B (acetonitrile/water/formic acid 80:15:5 v/v/v) in a 97/3 ratio. Elution was performed using a binary gradient starting from: isocratic 3% B to 90% B according to a complex profile. The elution was monitored on a Waters 996 photodiode array detector. Preliminary sample preparation consisted in the solid phase extraction procedure on Sep Pak tC18 cartridges. The main dimeric and trimeric forms were identified on the basis of their retention time and on the mass signals in a LC-ESI-MS experiment.

Monomeric flavan-3-ols and oligomeric proanthocyanidins from wines, grape seeds, and skins of Graciano, Tempranillo, and Cabernet Sauvignon varieties have been identified by means of HPLC/ESI-MS data and by comparison with the retention time and spectral features of flavan-3-ol reference compounds[29]. The HPLC followed a preliminary fractionation by polyamide column chromatography. The equipment used for the analysis consisted of a Konik Instruments UV-vis detector (Uvis 200), a Waters 717 Plus autosampler, and a Merck Hitachi L-6200A pump, coupled to a Konikron data treatment system. Separation was performed on a reversed-phase Merck (Darmstadt, Germany) C18 Lichrosphere 100 column (250mm x 4.6 mm, 5μm) at room temperature. For oligomeric procyanidins, a gradient consisting of solvent A (distilled water) and solvent B (water/acetic acid, 90/10, v/v) was applied at a flow rate of 1.0 mL/min from10% to 100%B (complex profile) followed by washing (methanol/water, 50/50, v/v) over a total period of 100min and reequilibration of the column for 20 min under initial gradient conditions. Detection was performed at 280 nm.

In the same work a Hewlett-Packard series 1100 chromatography system equipped with a diode array detector (DAD) and a quadrupole mass spectrometer (Hewlett-Packard series 1100 MSD) with an electrospray interface was used for HPLC/ESI-MS experiments. Separation was performed on a reversed-phase Waters Nova Pak C18 (300mm x 3.9mm, 4μm) column at room temperature. The solvent gradient described above for oligomeric procyanidins was applied at a flow rate of 0.7 mL/min. DAD detection was performed from 220 to 380 nm.

Reversed phase HPLC has been used for determination of some low molecular weight proanthocyanidins in Japanese foodstuffs and grape seeds extracts[54]. The experiment was performed on a Shimadzu HPLC apparatus, Class-VP Series, equipped with a SPD-M10AVP diode array detector. The column was a Develosil 300 ODS-HG-5, which

has a pore size of 300 Å. Unlike ordinary reversed-phase HPLC columns which has pore size of about 100 Å, using the column with the larger pore size made it possible to determine low molecular weight compounds (less than 1000), while higher molecular weight compounds have not been eluted. Grape seed tannins include compounds of high molecular weight (greater than 1000), therefore despite lower sensitivity the Develosil 300 column was used to determine all compounds in the studied objects.

The analysis conditions included a gradient elution performed at 35°C. Mobile phase A was the solution of phosphoric acid in water (1:1000, v/v) and the mobile phase B contained phosphoric acid in acetonitrile (1:1000, v/v). Starting the gradient with pure A it was arrived at 100% B in 61 minutes (complex profile), followed by a re-equilibration step. Detection was performed simultaneously with both DAD (set at 210 nm) and fluorescence detector (ex. 283 nm, em. 317 nm). The fluorescence detection proved to be the most sensitive in this case but it does not allowed detection of gallic acid under the reported detection conditions. Phosphoric acid has an absorbance at 210 nm, therefore the UV-HPLC chromatograms were corrected by subtracting the base line. Catechin, epi-catechin, B1 (**3**), B2 (**4**) and C2 (**12**) compounds have been determined. The other oligomers appeared in the chromatogram as a broad unresolved band.

A very interesting example of using RP HPLC in the analysis of GST was reported recently by Santos-Buelga and collaborators.[31] The methodology for the qualitative and quantitative characterization of wine proanthocyanidins was optimized using HPLC-MS. Chromatographic separations were performed both in analytical and semi-preparative versions.

The crude GST extract was fractionated on a Sephadex LH-20 column (500x30 mm) using ethanol as a solvent. The procyanidin dimers B2 (**4**), B1 (**3**), and B2-3-O-gallate along with the trimer EEC (EC-4,8-EC-4,8-C) were isolated from the obtained fractions by semipreparative HPLC. It employed a Waters 600 series pump and a Phenomenex 5 μm Ultracarb ODS20 (10x250 mm) column. The solvents were (A) acetic acid 5% and (B) methanol. The gradient used was from pure A to B according to a stepwise profile run for 60 min. Detection was carried out at 280 nm, and the peaks were collected by a fraction collector. The purity and identity of the isolated GST were checked by HPLC/DAD and LC-MS by comparison with standards previously obtained in these laboratories.

For analytical purposes analyses were carried out using a Hewlett-Packard 1100 chromatograph with a quaternary pump and a diode array detector (DAD) coupled to an HP Chem Station. A Waters Spherisorb S3 ODS-2 C8, 3 μm (4.6x150 mm) column was used thermostated at 30 °C. The mobile phase was (A) 2.5% acetic acid, (B) acetic acid/ acetonitrile (10:90, v:v), and (C) acetonitrile. The elution gradient was established from 100% A to 100%B, followed by 15%C in B to 50% C in B for a total of 40 min. Unfortunately, original chromatograms of wine samples are not provided in this paper. The results of checking the purity of individual GST are only presented.

Early separations of proanthocyanidins by normal phase chromatography were met with limited success but over time more understanding came about for example, increases in retention times were found to correspond with increasing degrees of polymerization. In the case of procyanidins, normal phase HPLC separation is based on hydrogen bonding interactions between silica hydroxyls with the larger oligomers having more extensive interactions and thus longer retention times.[55]

Normal phase HPLC, coupled with MALDI-TOF MS was used to characterize the proanthocyanidin composition of the grape seed extract.[56] A Phenomenex Luna 5 μm Silica column (250x4.6 mm) was used for all these analyses. Detection was made by UV at λ=280 nm. The ternary mobile phase consisted of (A) dichloromethane, (B) methanol, and (C) acetic acid and water (1:1 v/v). A complex series of linear gradients were used in the analysis over a 70 minutes period. The flow rate was kept at 1 mL/min and column temperature at 37 °C. The resolution of peaks was not excellent, but the most useful information provided in this paper is connected to the selective detection of certain mass fragments using the APCI in the MS detector.

A new normal phase chromatography method has been developed by Kennedy and Waterhouse.[57] It uses a binary gradient with mobile phases containing methylene chloride-methanol-formic acid-water, (A) 0:97:2:1 and (B) 83:14:2:1, both containing 20 mM heptanesulfonic acid. This method was used in a very recent paper from the same research group[7] for the analysis of GST. Additionally, a simple method to separate red wine nonpolymeric and polymeric phenols by SPE was devised. HPLC was used to monitor the obtained GST fractions. An HP 1090 apparatus with a Phenomenex Luna Silica 2 (particle size, 5 μm; 250x4.60 mm i.d.) column, protected by a guard column (10x4 mm) containing the same material was used to determine the nature of the phenolic compounds. The injection volume was 10 μL for each sample. Samples were analyzed at 280 nm. The elution conditions were as follows: 0.75 mL/min, linear gradients from 0 to 34% A in 30 min, from 34 to 100% A in 5 min, and 100% A for 10 min. The column was re-equilibrated with B for 10 min before subsequent injections. This method allowed separation of monomeric compounds from polymers.

Along with RP and normal phase HPLC, some papers relate on the use of gel filtration columns for analysis of GST. Gel permeation chromatography (GPC) could directly provide information on both degree of polymerization and average molecular weight. GPC analysis of proanthocyanidins has traditionally been carried out on acetylated derivatives. Derivatization was considered necessary because proanthocyanidins were too polar to be separated on currently available GPC columns. However, molecular weights determined by GPC were slightly higher compared to the ones obtained by degradation, due to the lack of suitable calibrating standards.

Kennedy and Taylor devised a method for gel permeation chromatography of GST[58] and this method was used latter on by the same authors to monitor the oxidative degradation of proanthocyanidins under basic conditions.[2] This method allowed measuring the size distribution to provide additional information on how oxidation affected the size of proanthocyanidins. Unfortunately, this method allowed the separation of proanthocyanidins only as broad bands, with no separate peaks of individual compounds.

A better resolution was achieved in the work of Peterlongo and collaborators[13]. GPC separations were carried out at room temperature on a PL Gel column 300=7.6 mm i.d. , particle size 5 mm, pore type 500 A (HP) connected to a pre-column 0.5-mm filter. The elution was isocratic using THF/aqueous LiBr 1.2 x 10^{-4} M 95:5 at a flow rate of 1.0 ml/min. Detection was at 280 nm. Acquisition time was 15 min. The analyzed polymers with decreasing molecular weights were eluted in succession. GPC analysis, performed as described was able not only to provide information on the composition of the extract, by evaluating the shape of the chromatographic profile, but also to allow a quantitative evaluation of the polyphenols in comparison to LeucoselectTM reference standard, thus ensuring constancy and reproducibility of biological effects.

6.2 Mass spectrometry methods

Mass spectrometry is a very powerful method for elucidation of the chemical structure of natural products. Its applicability is governed mostly by the ionization method employed for the transition of an uncharged inert molecule to an ion that is capable to be accelerated in the electromagnetic field. Electron impact ionization (EI) techniques historically are among the first ionization methods used in the investigation of polyphenolics from plants. It was used successfully to characterize monomeric phenolics, but its applicability to oligomers and polymers was limited because it required derivatization to increase their volatility. That's why fruit procyanidins have been acylated for EI analysis and this extra-step, along with the limited mass information available from this ionization technique severely limited its usefulness.

The development of liquid secondary ion mass spectrometry (LSI-MS) and fast atom bombardment mass spectrometry (FAB-MS) provided additional opportunities for structural identification of oligomeric polyphenolics with no need for derivatization and minimal manipulations required for the sample preparation. LSI typically uses cesium ions as the particle beam source, whereas FAB uses a neutral inert gas (argon or xenon). The sample is mixed into 1 to 2 μL of glycerol or other liquid matrix and applied to the tip of a sample probe, which is then introduced into the ion source chamber. One major role of the matrix, because of its low freezing point, is to keep the sample in a liquid state as it enters the high vacuum ion source. This matrix also reduces damage to the analyte caused by the high energy bombarding particle. The subsequent bombardment causes the ejection of a desorbed secondary ion beam containing positive and negative ions in addition to neutral species. The relative abundances are controlled by the source potentials, the analyte itself, and the nature of the support matrix. This is a relatively "soft" ionization procedures that produces abundant molecular ions with minimal structural fragmentation. The major advantage of FAB is that it is easy and fast to operate, while the spectra are simple to interpret. However, one of the major disadvantages of the FAB technique is that it requires a high concentration of the organic liquid matrix (typically 80 to 95% glycerol), overall giving only moderate sensitivity. Matrix cluster ions can, in some cases, dominate the mass spectrum. In addition, damage to the matrix caused by particle bombardment gives intense chemical background. It has been shown that discrimination in ionization efficiency of one analyte over another, due to differences in hydrophobicity and surface activity, causes problems when analyzing mixtures especially in quantitative applications. That's why the spectrum must typically be obtained from relatively pure samples.

This problem was successfully overcomed with the development of matrix-assisted laser desorption ionization (MALDI) mass spectrometry. Laser desorption techniques had existed since the early 1960s; however, their mass cut-off was relatively low. Low-energy nitrogen laser light, typically at 337 nm, in conjunction with a suitable matrix, normally a UV-absorbing organic molecule or a metal powder, could protect the analyte from degradation during the vaporization step, enabling the mass spectrometry of large biomolecules. In addition to allowing an increased mass range, MALDI has proven robust against sample contamination, although sample clean-up is still recommended. MALDI also primarily produces singly charged ions, allowing for the analysis of complex samples. When coupled to time-of-flight (TOF) spectrometers, which have no m/z limits, MALDI is an especially powerful mapping tool. The disadvantages of this method are connected to the impossibility of quantitative analysis. Another inherent disadvantage to MALDI is the inability to conveniently couple it to chromatography: techniques to couple liquid chromatography to MALDI have proven less successful, although various approaches have been devised.

An alternative soft ionization method to MALDI, thermospray ionization was introduced in the early 80-es for the coupling of analytical HPLC at conventional flow rates to a mass spectrometer. The effluent from the HPLC column is vaporized under reduced pressure by heating a stainless steel tube of 0.10 to 0.15 mm inner diameter. The resulting supersonic jet contains small droplets that vaporize further due to the hot gas in this low pressure region of the ion

source. Complete evaporation of the solvent from the liquid droplets produces gas phase ions from ionic compounds in the sample solution or from gas phase chemical ionization when an auxiliary filament or low-current discharge device is used. Ionization requires polar or charged species and volatile buffers. Thermospray is considered a soft ionization technique and induces only limited fragmentation of the analyte.

Another ionization method that has affected a tremendous impact over the last few years on the use of mass spectrometry in biological research is the electrospray ionization. It was the first method to extend the useful mass range of instruments to well over 50,000 Da. The sample is usually dissolved in a mixture of water and organic solvent, commonly methanol, isopropanol or acetonitrile. It can be directly infused, or injected into a continuous-flow of this mixture, or be contained in the effluent of an HPLC column or CE capillary. The ionization process starts with the sample nebulization step, which produces electrically charged droplets followed by liberation of the formed ions from the droplets in a combined process of solvent evaporation and Coulombic repulsion. Finally, the ions thus produced are swept from the atmospheric source region into the mass analyzer. The gradual thermal de-solvation leads to electrospray being a very "soft" ionization method. Unless the potential difference between the transfer capillary and the analyzer is increased, which results in collision-induced dissociations, there is minimal fragmentation of the analytes. An unique advantage of ESI to other methods is that the process leads to the formation of both singly and multiply charged ions and as a consequence of the multi-charging phenomenon, the instrument can be calibrated in the low m/z range, with no need of using sophisticated TOF techniques, using singly-charged calibrants with known exact masses. Major disadvantages are that spray formation is adversely affected even by moderate buffer and salt concentrations, and that mixtures of high mass samples can give overlapping charge state distributions that may be difficult to assign to individual components.

Mass spectrometry was used as a fast and direct method for elucidating the polyphenol constituents of grape seed extracts. In particular, the composition of various commercial extracts and of oligomeric and polymeric procyanidin fractions from grape seeds were determined by liquid secondary ion mass spectrometry (LSIMS) in negative ion mode.[59,33] Electrospray mass spectrometry ESI-MS was also used, directly or combined with liquid chromatography, for studying oligomeric and polymeric tannins contained in grape seeds; the negative ion ESI mass spectra showed the presence of a series of non-galloylated and galloylated oligomeric procyanidins up to trigalloylated octamer.[33]

During the last 7 years most of the reports on using MS methods are related to the hyphenated technique HPLC-MS. ESI was the ionisation method of choice in these studies. We will provide below the most recent examples reported in the literature devoted to investigation of GST.

ESI mass spectroscopy was reported in the work of Gabetta et al.[13] to identify and completely characterize the proanthocyanidin constituents of Leucoselect™ extract up to heptamers and their galates. The studied samples were injected into the spectrometer directly before and after fractionation procedure. In fact, each fraction was characterized by mass spectrum containing peaks corresponding to the protonated molecule $[M+H]^+$ for each polymeric constituent. Ions at m/z 579, 867 and 1155 are due to dimers, trimers and tetramers and ions at m/z 731, 1019 and 1307 corresponding to their monogallates. Ions at m/z 883, 1171 and 1459 corresponding to digallate derivatives of dimers, trimers and tetramers, respectively, and ions at m/z 1323 and 1611 corresponding to trigallate derivatives of trimers and tetramers, were also present. Fractions of higher oligomers showed ions at m/z 1443, 1731 and 2019 corresponding to pentamers, hexamers and heptamers; ions at m/z 1595, 1883 and 2171 corresponding to their monogallate derivatives; ions at m/z 1747 and 2035 corresponding to pentamer and hexamer digallate derivatives; and ions at m/z 1899 and 2187 corresponding to pentamer and hexamer trigallate derivatives. The last one was the largest polymeric proanthocyanidin detected in the mass spectra. No ions were detected above m/z 2200, or double charge peaks over the whole mass range. Ions corresponding to the loss of flavan-3-ol units were also present, showing that a certain degree of fragmentation took place even in ESI-MS conditions.

The thermospray ionization was also employed in this work in tandem with HPLC separation. Positive mass spectra have been acquired from m/z 160 to 1200 over a scan time of 1 s. Unlike ESI, TSI allowed only detection of monomeric flavan-3-ols and dimeric proanthocyanidins. The spectra contain only few ions, but they are useful for the identification. In this case catechin and epicatechin gave only the protonated molecule $[M+H]^+$ at m/z =291. Dimers give the protonated molecule $[M+H]^+$ at m/z =579, base peak being the flavan-3-ol protonated unit m/z =291. The presence of a peak at m/z =601 corresponding to the $[M+Na]^+$ ion, supports the molecular weight attribution. The dimer gallate gives a positive TSP mass spectrum showing, besides the protonated molecule $[M+H]^+$ at m/z =731, the ions corresponding to the loss of gallic acid residue at m/z =579 and to the loss of a flavan-3-ol unit at m/z =443.

Matrix-assisted laser desorption/ionization time-of-flight mass spectrometry was used to characterize the procyanidin composition of a grape seed extract.[56] Oligomers up to nonamers were observed. HPLC/ESI-MS was shown to separate the procyanidin isomers of the lower degree of polymerization but failed to resolve oligomers larger than pentamers. MALDI-TOF MS, on the other hand, allowed a rapid analysis of such complex mixtures. The individual oligomers of procyanidins in grape seeds were well resolved in MALDI-TOF MS spectra with their molecular weight determined with great accuracy. The dominating features of the spectra are two major series of ions separated by 152 Da. The first series was attributed to the sodium adducts of monomers and the oligomers composed purely of (+)-catechin and (-)-epicatechin, with the molecular weight of 290 + 288 (n - 1), n being the degree of polymerization. The second

series consists of ions with the molecular weight of 442 + 288 (n - 1), which are the sodium adducts of oligomers containing one galloylated unit, i.e., either a (+)-catechin gallate or an (-)-epicatechin gallate. Sodium was shown to originate from the grape seeds themselves and its presence greatly enhances the signal sensitivity.

The potential of the MALDI-TOF MS technique as a quantification tool was also discussed. Conditions for MALDI-TOF in terms of matrix selection and sample preparation have been optimized. 2,5-dihydroxybenzoic acid was shown to be the optimal matrix providing the broadest mass range with the least background noise. The relative intensity (sample intensity/internal standard intensity) of each oligomer showed a general increasing trend with increasing concentration. Application of MALDI-TOF as a quantitation tool is hampered though by the absence of individual standards of higher grape seeds proanthocyanidins.

Fractionated GST and individual compounds separated by RP HPLC were examined by electrospray Ion-Trap Mass Spectrometry in the negative ion mode.[8] The electrospray matrix was 80% MeOH/20% H_2O. In some cases MS/MS was also run on individual peaks in order to determine the proanthocyanidin structure of the compounds. Primary spectra showed categorical predomination of the molecular peaks $[M-H]^-$, and it was proved on an example of an individual HPLC peak, whyle MS/MS experiment provided a deeper fragmentation of the analized oligomer. Compounds up to pentamers (m/z 1441) have been detected in the analized extract.

A recent paper provided data concerning HPLC/ESI-MS fragmentation patterns of oligomeric procyanidins in grape and wine fractions obtained by polyamide column chromatography.[29] Along with the most abundant peaks of molecular ions $[M - H]^-$ (dimer m/z 577, dimer gallate m/z 729, trimer m/z 865), some peaks attributed to Retro-Diels-Alder (RDA) fission fragments originated from dimeric and trimeric procyanidins (ions with m/z 425 and m/z 713). An ion corresponding to its subsequent water elimination was only detected for dimeric procyanidins (m/z 407). Under the reported MS conditions, trimeric procyanidins only underwent one-stage RDA fission, since the characteristic ions (m/z 425 and 407) that resulted for the dimeric procyanidins were not observed. Some other MS fragments were tentatively attributed to different paths of fragmentation of different oligomers (up to trimers).

Although the molecular peaks in the ESI spectra are the most abundant, examining of minor ones also leads to very important conclusions about the GST structure. They can show additional information about the fragmentation path and sometimes the minor peaks correspond to multiple charged ions. This observation has led to important conclusions made in a recent work connected to the investigation of GST degree of polimerization.[24] Two fractions originated from a grape seeds extract were directly injected into the mass spectrometer under ESI conditions. The mean degree of polymerization of the investigated fractions, calculated on the basis of thyolisis experiments was 3 and 9 respectively. As it was expected, in the spectra acquired on the entire mass range (200-3000 Da) predominated the molecular ions of anthocyanidins and their galates, up to heptamers. The mean degree of polymerization (mDP) calculated on the basis of the MS experiment was in accordance with the thyolisis data for the fraction with the mDP=3. For the fraction with the mDP=9 there was a discrepancy between MS and thyolisis data. According to mass spectrum of this fraction, for the single charged series of molecular peaks $[M-H]^-$ the most abundant ions corresponded to proanthocyanidins with degree of polymerization 3 or 4 , much lower than that estimated from acid hydrolysis (mDP=8.9). A careful examination of the minor peaks in the spectrum of the fraction with mDP=9 showed that numerous ions could be assigned as doubly charged, based on the mass difference between isotopic peaks and these peaks were absent in the spectrum of the first fraction (mDP=3). Taking into consideration these ions, it was found that the highest value of polymerisation degree for this fraction was 13. Recording the spectra in a narrower m/z range with a higher resolution led to detection of triple charged ions $[M-3H]^{3-}$ having the maximum m/z =2890.5 that corresponds to the DP 28 with 4 galloylation and m/z =2947.7 that corresponds to the DP 27 with 7 galloylation units. The triple charged ions appeared to be eclipsed by more abundant single charged ones under low resolution condition of spectra aquisition.

The conclusion made in above discussed paper[24] has been confirmed by other studies of the low-molecular weight proanthocyanidine fraction isolated from wine samples. In their recent work Santos-Buelga and colaborators[3] used ESI MS to monitor the proanthocyanidin composition of wines at different maceration stages. Unlike in other studies, ionization was performed in the positive mode. No multiple charged ions have been detected and the molecular ions prevailed categorically over other fragments. Proanthocyanidins up to hexamers have been detected in the wine samples, even at advanced maceration stages.

In conclusion, we shall mention that mass spectrometry is a powerful method for investigation of grape seeds proanthocyanidins. Application of soft ionization techniques like MALDI-TOF or ESI allows monitoring exclusively molecular ions both in negative and positive modes. Higher molecular oligomers can be ionized more easily to produce multiple charged ions which can be distinguished by the distance between the isotopic peaks of the carbon.[60]

6.3. Miscellaneous methods

Investigation of grape seed proanthocyanidins included also other physicochemical methods, like thin layer chromatography (TLC) and Nuclear Magnetic Resonance (NMR) spectroscopy. But their power and usefulness are less satisfactory, compared to HPLC and MS methods.

The value of TLC is given by its simplicity, low cost and rapidity of analysis. Most of the recently reported examples of using TLC in the investigation of GST relate only to normal phase variant.[15,5,38,61] The resolution power of TLC, even on HPTLC plates, allows separation of proanthocyanidin mixture groups by molecular weight as bands. Consequently, the method can be successfully used to monitor preliminary fractionation of the natural extracts. In our opinion this method has a further potential, due to the continuous evolution of the stationary phases, especially in the reversed phase variant.

Nuclear Magnetic Resonance spectroscopy (NMR) has been used as a powerful tool in the structure elucidation of proanthocyanidins. But aplication of NMR, even at high operating frequencies required preliminary separation of individual compounds that is not always a trivial task. One of the first work in this field relates using of ^{1}H NMR to estimate the polymerization degree of proanthocyanidin mixtures.[62] ^{1}H and ^{13}C NMR spectroscopy techniques were used to estimate the degree of polymerization. In the absence of doubly linked A-type bonds, the average molecular weight can be determined directly from the ^{13}C NMR spectra by comparing the areas of the C3 resonances of the terminal and extender flavan-3-ol units, at 67-68 and 72-73 ppm, respectively.

A following report shows a complete and unambiguous assignment of the ^{1}H and ^{13}C NMR spectra of peracetylated catechin-(4-8)-catechin-(4-8)-catechin procyandin trimer, accomplished by reverse two-dimensional chemical shift correlation methods.[63] Two-dimensional NMR was the only analytical tool which used to check the identity of grapevine species, cultivars or clones.[64] The structure of the proanthocyanidin B-2 dimer was proved by two-dimensional heteronuclear NMR spectroscopy.[65] Identification of the peracetylated dimer B2 was also performed by ^{1}H and ^{13}C NMR.[5]

Another example of using of ^{1}H NMR to estimate the polymerization degree of proanthocyanidin mixtures was reported by Guyot and colaborators.[66] It was shown that by integrating the A-ring proton signals between 5.8 and 6.5 ppm in ^{1}H NMR spectra and comparing them to the intensity of the H4 signals of the terminal units between 2.4 and 3.0 ppm it is possible to derive the DP. This strategy was used latter by Schmidt and collaborators.[61]

Various phenolic compounds were synthesized in an aqueous-alcoholic solution containing (+)-catechin and glyoxylic acid which was used as a model of fruit-derived food browning that usually occurs during aging.[67] After purification by semi-preparative HPLC, the isolated compounds were subjected to homo- and heteronuclear proton and carbon NMR analysis including COSY, TOCSY, ROESY, HSQC and HMBC techniques. These experiments allowed the structural elucidation and complete ^{1}H and ^{13}C NMR assignment of the isolated compounds. The structure and conformation of two native procyanidin trimers in water have been determined using 2D NMR and molecular mechanics.[68]

7. CONCLUSIONS

To date, investigation of the structures of grape proanthocyanidins has been performed in different ways depending on the extension of the polymeric chain. In fact, only low molecular weight tannins up to tetramers can be isolated and characterized as pure compounds. Isolation of pure polymeric tannins is difficult. In most cases, only fractions corresponding to mixtures of several polymers can be obtained. Chemical methods must therefore be developed to separate individual proanthocyanidin molecules for identification while retaining them unchanged for simultaneous bioactivity testing. This problem represents a real challenge to chemical community.

Acknowledgements

This work was performed within the INTAS project 05-104-7505.

8. REFERENCES

[1] Vidal, S.; Cartalade, D.; Souquet, J.M.; Fulgrand, H.; Cheinier, V. Changes in Proanthocyanidin Chain Length in Winelike Model Solutions. *J. Agric. Food Chem.* **2002**, *50*, 2261-2266.

[2] Jorgensen, E.M.; Marin, A.B.; Kennedy, J. A. Analysis of the Oxidative Degradation of Proanthocyanidins under Basic Conditions. *J. Agric. Food Chem.* **2004**, *52*, 2292-2296.

[3] Gonzalez-Manzano, S.; Santos-Buelga, C.; Perez-Alonso, J.J.; Rivas-Gonzalo, J.C.; Escribano-Bailon, M.T. Characterization of the Mean Degree of Polymerization of Proanthocyanidins in Red Wines Using Liquid Chromatography-Mass Spectrometry (LC-MS). *J. Agric. Food Chem.* **2006**, *54*, 4326-4332.

[4] Peyrot des Gachons, C.; Kennedy, J. A. Direct method for determining seed and skeen proanthocyanidins extraction into red wine. *J. Agric. Food Chem.* **2003**, *51*, 5877-5881.

[5] de Freitas, V.; Glories, Y.; Laquerre, M. Incidence of Mollecular Structure in Oxidation of Grape Seeds Procyanidins. *J. Agric. Food Chem.* **1998**, *46*, 376-382.

[6] Uchida, S.; Edamatsu, R.; Hiramatsu, R.; Mori, A.; Nonaka, G.I.; Nishioka, I.; Ozaki, M. Condensed tannins scavenge active oxygen free radicals. *Med. Sci. Res.* **1987**, *15*, 831-832.
[7] Pinelo, M.; Laurie, V.F.; Waterhouse, A.L. A Simple Method To Separate Red Wine Nonpolymeric and Polymeric Phenols by Solid-Phase Extraction. *J. Agric. Food Chem.* **2006**, *54*, 2839-2844.
[8] Fitzpatrick, D.F.; Fleming, R.C.; Bing, B.; Maggi, D.A.; O'Malley, R.M. Isolation and Characterization of Endothelium-Dependent Vasorelaxing Compounds from Grape Seeds. *J. Agric. Food Chem.* **2000**, *48*, 6384-6390.
[9] Santos-Buelga, C.; Scalbert, A. Proanthocyanidins and Tannin-like Compounds – Nature, Occurrence, Dietary Intake and Effect on Nutrition and Health. *J. Sci. Food Agric.* **2000**, *80*, 1094-1117.
[10] Murray M, Pizzorno J. Procyanidolic oligomers. In: Murray M, Pizzorno J, eds. *The Textbook of Natural Medicine.* 2nd ed. London: Churchill Livingston; **1999**, 899-902.
[11] Pekic, B.; Kovac, V.; Alonso, E.; Revilla, E. Study of the Extraction of proanthocyanidins from grape seeds. *Food Chem.* **1998**, *61*(1-2), 201-206.
[12] Teissedre, P.L.; Waterhouse, A.L.; Frankel, E.N. Principal Phenolic Phytochemical in French Syrah and Grenache Rhone Wines and Their Antioxidant Activity in Inhibiting Oxydation of Human Low Density Lypoproteins. *J. Inter. Sci. de la Vigne et du Vin.* **1995**, *29*(4), 205-212.
[13] Gabetta, B.; Fuzzati, N.; Griffini, A.; Lolla, E.; Pace, R.; Ruffilli, T.; Peterlongo, F. Characterization of proanthocyanidins from grape seeds. *Fitoterapia.* **2000**, *71*, 162-175.
[14] da Silva J, Rigaud J, Cheynier V, et al. Procyanidin dimers and trimers from grape seeds. *Phytochemistry*. **1991**, *30*, 1259-1264.
[15] Oszmianski, J.; Sapis, J.C. Fractionation and Identification of Some Low Molecular Weight Grape Seed Phenolics. *J. Agric. Food Chem.* **1989**, *37*, 1293-1297.
[16] Lea, A.G.H.; Bridle, P.; Timberlake, C.F.; Singleton, V. The procyanidin of white grapes and wines. *Am. J. Enol. Vitic*. **1979**, *30*, 289-300.
[17] Romeyer, F.M.; Macheix, J.; Sapis, J. Changes and importance of oligomeric procyanidins during maturation of grape seeds. *Phytochemistry.* **1986**, *25*, 219-221.
[18] da Silva, R.J.M.; Bourzeix, M.; Cheynier, V.; Moutounet, M. Procyanidin composition of Chardonnay, Mauzac and Grenache blanc grapes. *Vitis*. **1991**, *30*, 245-252.
[19] da Silva, R.J.M.; Rosec, J.P.; Bourzeix, M.; Mourgues, J.; Moutounet, M. Dimer and trimer procyanidins in Carigan and Mourvedre grapes and red wines. *Vitis*. **1992**, *31*, 55-63.
[20] Santos-Buelga, C.; Francia-Aricha, E.M.; Escribano-Bailon, M.T. Comparative flavan-3-ol composition of seeds from different grape varieties. *Food Chem*. **1995**, *53*, 197-201.
[21] Kovac, V.; Bourzeix, M.; Heredia, N.; Ramos, T. Etude des catechines et proanthocyanidols de raisin et vins blancs. *Revue France d'Oenologie*. **1990**, *125*, 7-14.
[22] Kovac, V.; Alonso, E.; Revilla, E. The effect of adding supplementary quantities of seeds during fermentation on the phenolic composition of wines. *Am. J. Enol. Vitic*. **1995**, *46*, 363-367.
[23] de Freitas, V.; Glories, Y.; Bourgeois, G.; Vitry, C. Characterisation of oligomeric and polymeric procyanidins from grape seeds by liquid secondary ion mass spectrometry. *Phytochemistry*, **1998**, *49*, 1435.
[24] Hayasaka, Y.; Waters, E.J. Cheynier, V.; Herderich, M.J.; Vidal, S. Characterization of Proanthocyanidins in Grape Seeds Using Electrospray Mass Spectrometry. *Rapid Commun. Mass Spectrom.* **2003**, *17*, 9-16.
[25] Sun, B.S.; Leandro, C.; da Silva J.M.R.; Spranger, I. Separation of Grape and Wine Proanthocyanidins According to their Degree of Polymerization. *J. Agric. Food Chem*. **1998**, *46*, 1390-1396.
[26] Labarbe, V.; Cheinier, V.; Brossaud, F.; Souquet, J.M.; Moutounel, M. Quantitative fractionation of grape proanthocyanidins according to their degree of polymerization. *J. Agric. Food Chem*. **1999**, *47*, 2719-2723.
[27] Michaud, J.; Lacaze, P.; Masquelier, J. Fractionement des oligomers flavanolique du raisin. *Bull. Soc. Pharm. Bordeau*. **1971**, *110*, 111-116.
[28] Nonaka, G.J.; Miwa, N.; Nishioka, I.; Stilbene glycoside gallates and proanthocyanidins from *Polygonum multiflorum. Phytochemistry*. **1992**, *21*(2), 429-432.
[29] Monagas, M.; Gomez-Cordovez, C.; Bartolomea, B.; Laureano, O.; Ricardo da Silva, J.M. Monomeric, Oligomeric, and Polymeric Flavan-3-ol Composition of Wines and Grapes from Vitis vinifera L. Cv. Graciano, Tempranillo, and Cabernet Sauvignon. *J. Agric. Food Chem.* **2003**, *51*, 6475-6481.
[30] Geny, L.; Saucier, C.; Bracco, S.; Daviaud, F.; Glories, I. Composition and cellular localization of tannins in grape seeds during maturation. *J. Agric. Food Chem*. **2003**, *51*, 8051-8054.
[31] Darne, G.; Madero, T.J. Mise au point d'une methode d'extraction des lipides solubles totaux, des glusides solubles totaux et des composes phenoliques solubles totaux des organes de la vigne. *Vitis*. **1979**, *18*(3), 221-228.
[32] Kuliev, R.Z.; Akhmedov, U.; Khalmatov, Kh.Kh.; Kuliev, Z.A. Dimeric Proanthocyanidins from *Rhodiola semenovii*. *Chem. Nat. Comp.* **2004**, *40* (1), 94-95.

[33] Kantz, K.; Singleton, V.L. Isolation and Determination of Polymeric Polyphenols using Sephadex LH-20 and Analysis of Grape Tissue Extracts. *Am. J. Enol. Vitic*. **1990**, *41*, 223-228.
[34] Kantz, K.; Singleton, V.L. Isolation and Determination of Polymeric Polyphenols in Wines using Sephadex LH-20. *Am. J. Enol. Vitic*. **1991**, *42*, 309-316.
[35] da Silva J.M.R.; Rosec, J.P.; Bourzeix, M.; Heredia, N. Separation and Quantitative Determination of Grape and Wine Procyanidines by High Performance Reversed Phase Liquid Chromatography, *J. Sci. Food Agric*. **1990**, *53*, 85-92.
[36] Souquet, J. M.; Cheynier, V.; Brossaud, F.; Moutounet, M. Polymeric Proantocyanidines from Grape Skins. *Phytochemistry*. **1996**, *43*, 509-512.
[37] Prieur, C.; Rigaud, J.; Cheynier, V.; Moutounet, M. Oligomeric and polymeric procyanidins from grape seeds. *Phytochemistry*. **1994**, *36*, 781-784.
[38] Saucier, C.; Mirabel, M.; Daviaud, F.; Longieras, A.; Glories, Y. Rapid fractionations of grape seeds proanthocyanidins. *J. Agric. Food Chem*. **2001**, *49*, 5732-5735.
[39] Kennedy, J.A.; Matthews, M.A.; Waterhouse, A.I. Changes in grape seed polyphenol during fruit ripening. *Phytochemistry*. **2000**, *55*, 77-85.
[40] Kennedy, J.A.; Jones, G.P. Analysis of proanthocyanidins cleavage products following acid catalysis in the presence of excess floroglucinol. *J. Agric. Food Chem*. **2001**, *49*, 1740-1746.
[41] Porter, L.J.; Hrstich, L.N.; Chan, B.G. The conversion of procyanidins and prodelphinidins to cyanidin and delphinidin. *Phytochemistry*. **1986**, *25*, 223-230.
[42] Wulf, L.W.; Nagel, C.W. Analysis of phenolic acids and flavonoids by high-pressure liquid chromatography. *J. Chromatogr.* **1976**, 116, 271-279.
[43] Wulf, L.W.; Nagel, C.W. High-pressure liquid chromatographic separation of anthocyanins of *Vitis vinifera*. *Am. J. Enol. Vitic.* **1978**, *29*, 42-49.
[44] Nagel, C.W.; Wulf, L.W. Changes in anthocyanins, flavonoids and hydroxycinnamic acid esters during fermentation and aging of Merlot and Cabernet Sauvignon. *Am. J. Enol. Vitic*. **1979**, *30*, 111-116.
[45] Lea, A.G.H. High performance liquid chromatography of cider procyanidins. *J. Sci. Food Agric.* **1979**, *30*, 833-838.
[46] Lea, A.G.H. Reversed-phase gradient high-performance liquid chromatography of procyanidins and their oxidation products in ciders and wines, optimized by Snyder's procedures. *J. Chromatogr.* **1980**, *194*, 62-68.
[47] McCloskey, L.P.; Yengoyan, L.S. Analysis of anthocyanins in Vitis vinifera wines and red colour versus aging by HPLC and spectrophotometry. *Am. J. Enol. Vitic*. **1981**, *32*, 257-261.
[48] Merken HM, Beecher GR. Measurement of food flavonoids by high-performance liquid chromatography: A review. *J. Agric. Food Chem.* **2000**, *48*, 577–599.
[49] Lazarus SA, Adamson GE, Hammerstone JF, Schmitz HH. High-performance liquid chromatography/mass spectrometry analysis of proanthocyanidins in foods and beverages. *J. Agric. Food Chem*. **1999**, *47*, 3693–3701.
[50] de Pascual-Teresa S, Santos-Buelga C, Rivas-Gonzalo JC. Quantitative analysis of flavan-3-ols in Spanish foodstuffs and beverages. *J. Agric. Food Chem*. **2000**, *48*, 5331–5337.
[51] Carando S, Teissedre PL, Rascual-Martinez L, Cabanis JC. Levels of flavan-3-ols in French wine. *J. Agric. Food Chem*. **1999**, *47*, 4161–4166.
[52] Fuleki T, da Silva R.J.M. Catechin and procyanidin composition of seeds from grape cultivars grown in Ontario. *J. Agric. Food Chem*. **1997**, *45*, 1156–1160.
[53] Peng Z, Hayasaka Y, Iland PG, Sefton M, Hoj P, Waters EJ. Quantitative analysis of polymeric procyanidins (tannins) from grape (Vitis vinifera) seeds by reverse phase high-performance liquid chromatography. *J. Agric. Food Chem*. **2001**, *49*, 26–31.
[54] Nakamura, Y.; Tsuji, S.; Toogai, Y. Analysis of Proanthocyanidins in Grape Seed Extracts, Health Foods and Grape Seed Oils. *Journal of health Science*. **2003**, *49* (1), 45-54.
[55] Waterhouse AL, Ignelzi S, Shirley JR. A comparison of methods for quantifying oligomeric proanthocyanidins from grape seed extracts. *Am. J. Enol. Vitic*. **2000**, *51*, 383–389.
[56] Yang, Y; Chien, M. Characterization of Grape Procyanidins Using High-Performance Liquid Chromatography/ Mass Spectrometry and Matrix-Assisted Laser Desorption/Ionization Time-of-Flight Mass Spectrometry. *J. Agric. Food Chem*. **2000**, *48*, 3990-3996.
[57] Kennedy, J.A.; Waterhouse, A.L. Analysis of Pigmented High Molecular-Mass Grape Phenolics Using Ion-pair, Normal-Phase High-Performance Liquid Chromatography. *J. Chromatogr*. *A*. **2000**, 866, 25-34.
[58] Kennedy, J. A.; Taylor, A. W. Analysis of proanthocyanidins by high-performance gel permeation chromatography. *J. Chromatogr. A.* **2003**, 995, 99-107.
[59] Vivas, N.; Bourgeois, G.; Vitry, C.; Glories, Y.; de Freitas, V. Determination of the composition of commercial tannin extracts by liquid secondary ion mass spectrometry (LSIMS). *J. Sci. Food Agric.* **1996**, *72*, 309.

[60] Cheynier, V.; Doco, T.; Fulcrand, H.; Guyot, S.; Le Roux, E.; Souquet, J. M.; Rigaud, J.; Moutounet, M. ESI-MS analysis of polyphenolic oligomers and polymers. *Analysis*. **1997**, *25*, 32-37.

[61] Schmidt, B.M.; Howell, A.B.; McEniry, B.; Knight, C.T.; Seigler, D.; Erdman, J.W. JR.; Lila, M.A. Antiadhesion Components from Wild Blueberry (*Vaccinium angustifolium Ait.*) Fruits. *J. Agric. Food Chem.* **2004**, *52*, 6433-6442.

[62] Czochanska, Z.; Foo, L. Y.; Newman, R. H.; Porter, L. J. Polymeric proanthocyanidins. Stereochemistry, structural units and molecular weight. *J. Chem. Soc., Perkin Trans. 1*. **1980**, *1*, 2278-2286.

[63] Balas, L.; Vercauteren, J.; Laguerre, M. 2D NMR structure elucidation of proanthocyanidins: The special case of the catechin-(4-8)-catechin-(4-8)-catechin trimer. *Magn. Reson. Chem.* **1995**, *33*, 85-94.

[64] Forveille, L.; Vercauteren, J.; Rutledge, D.N. Multivariate statistical analysis of two-dimensional NMR data to differentiate grapevine cultivars and clones. *Food Chemistry*, **1996**, *57*, 3, 441-450.

[65] Khan, M.L.; Haslam, E.; Williamson, M.P. Structure and conformation of the procyanidin B-2 dimer. *Magn. Reson. Chem.* **1997**, *35*, 854-858.

[66] Guyot, S.; Le Guerneve, C.; Marnet, N.; Drilleau, J. F. Methods for determining the degree of polymerization of condensed tannins: A new ^{1}H NMR procedure applied to cider apple procyanidins. In *Plant Polyphenols 2: Chemistry, Biology, Pharmacology, Ecology*; Gross, Ed.; Kluwer Academic/Plenum Publishers: New York, **1999**.

[67] Es-Safi, N.E.; Le Guerneve, C.; Cheynier, V.; Moutounet, M. 2D NMR analysis for unambiguous structural elucidation of phenolic compounds formed through reaction between (+)-catechin and glyoxylic acid. *Magn. Reson. Chem.* **2002**, *40*, 693-704.

[68] Fouquet, E.; Laguerre, M.; Pianet, I. Structural and conformational analysis of two native procyanidin trimers. *Magn. Reson. Chem.* **2007**, *45*, 157-166.

SORPTION OF Ga (III) ON FLEXIBLE OPEN CELL POLYURETHANE FOAM OF POLYETHER TYPE IMPREGNATED WITH TRI-N-BUTHYL PHOSPATE

Lavinia Tofan[a], Doina Bilba[a], Carmen Paduraru[a] and Ovidiu Toma[b]*

[a] *Department of Environment Engineering and Management, Faculty of Chemical Engineering, "Gh. Asachi" Technical University of Iasi, 71 D.Mangeron Street, 700050 Iasi, Romania*

[b] *Department of Biochemistry, Faculty of Biology, "Al.I.Cuza" University of Iasi, 20A Bd. Carol I, 700505 Iasi, Romania*

** e-mail : otoma@uaic.ro; Tel. (+40 232) 201630 ; Fax (+40 232) 201472*

Abstract. The obtained results concerning the Ga (III) ion retention on flexible open cell polyurethane foam of polyether type pretreated with tri-n-butyl phosphate are presented. The influence of solution acidity, phases contact time, Ga (III) concentration and solution temperature have been investigated. The parameters of Ga (III) batch sorption have been optimized. On the basis of Langmuir isotherms, the sorption constants and the thermodynamic parameters, ΔG, ΔH and ΔS have been calculated.

Keywords: sorption, polyurethane foam, tri-n-butyl phosphate, gallium.

INTRODUCTION

The increasing demand for gallium in electronics industry has stimulated research on new materials and methods for the removal, recovery and determination of trace gallium in various natural and industrial samples. In this context, an alternative to the different ion - exchange resins can be represented by polyurethane foams [1]. Polyurethane foams have a wide range of applications in batch or dynamic separation and preconcentration of inorganic and organic species, gas and liquid chromatography and cells imunosorption [2,3].

Table 1

The main physical and chemical features of polyurethane foams

Character	Hydrophobic
Porosity	Large
Reversible swelling in	Water, HCl until 8M, H_2SO_4 until 4M , HNO_3 until 2M, glacial CH_3COOH, NH_4OH 2M, NaOH 2M, organic solvents (benzene, carbon tetrachloride, chloroform, acetone, alcohols)
Dissolution in	Concentrated H_2SO_4; concentrated HNO_3
Degradation by	Heating to 180 – 220^{0}C UV exposure
Anionic exchange capacity	Low
Surface area	High
Sorption rate of chemical species	Relative fast

The polyurethane foams can be efficiently used both in unloaded form [4-8] and after a physical or chemical treatment [9-15].The remarkable properties (Tab. 1) make flexible open-cell polyurethane foam of polyether type an ideal support for immobilizing by physical adsorption of various selective organic reagents and extractants [16]. Thus, the excellent properties of the flexible open-cell polyether of polyurethane foam type impregnated with the organic extractant tri-n-butyl phosphate (TBP) allowed quantitative separation of silver, gold, bismuth, cadmium, cobalt, chrome, copper, mercury, nickel, lead, palladium, tin, tantalum, thorium [9], and the concentration of iron from chloride media [17] and phenols from waters [18].

This paper deals with the experimental results of the retention of gallium ions on polyurethane foam of polyether type pretreated with TBP under specific conditions, giving the sorption isotherms and the values of thermodynamic amounts.

EXPERIMENTAL

Reagents and Chemicals

The stock solution of Ga(III) (1.584 mg/mL) was prepared by disolving $GaCl_3$ and was gravimetrically standardized (by precipitation with ammonia). Working solutions were freshly prepared by appropriate dilutions of the stock solution.

The "SPUMATIM" flexible open-cell polyurethane foam of polyether type was purified according to the procedure described in Fig. 1.

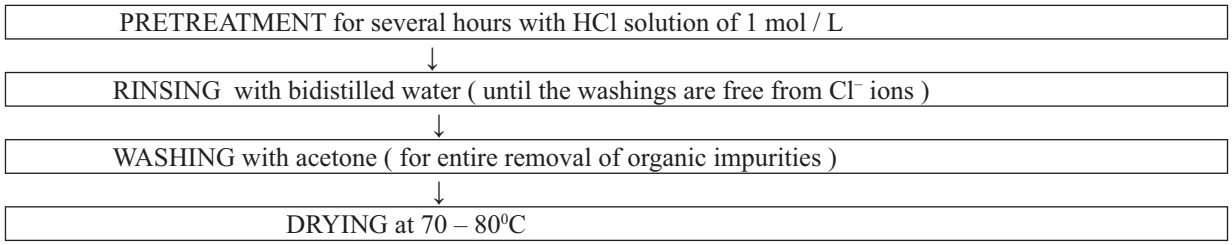

Fig.1. Scheme of polyurethane foam purification.

For foam impregnation, tri -n- butyl phosphate (Fluka, Buch, Switzerland) was used. An aqueous solution (0.5%) of rhodamine B was used for the spectrophotometric determination of gallium (III). All reagents were of analytical grade. Absorbance measurements were made on a S104D-WPA Linton Cambrige spectrophotometer.

Foam impregnation

In order to impregnation with TBP, the purified foam (cut into cubes of about 5mm edge) was equilibrated with the extractant agent. To ensure complete saturation, the cubes of foam were remained overnight in contact with TBP. Then, to remove the excess of TBP, the impregnated foam was washed several times with 4 mol/L HCl saturated with TBP. Finally, the TBP- polyurethane foam sorbent was dried and kept in a dessicator. The amount of TBP retained by the foam was of 5.1714 TBP/ g foam. This amount corresponds to an 83.8% content of TBP in the loaded foam.

General Sorption Procedure for Gallium

In the sorption systems under study batch conditions have been carried out. The weighed samples of about 0.1g of TBP- impregnated foam were equilibrated with volumes of 25 mL solution containing known and variable amounts of Ga (III) and HCl. After a determined time of contact, at constant temperature, the phases were separated. The Ga (III) content in supernatant was determined spectrophotometrically, with rhodamine B [19].

RESULTS AND DISCUSSION

Because of their various functional groups or heteroatoms, unloaded polyurethane foam sorbents which are not chemically inert, take part in the processes of sorption by virtue of their own structure. Thus, the retention of Ga (III) as $HGaCl_4$ on untreated polyether-type polyurethane foams was explained by a polyether extraction mechanism [20,21]. On the other hand, in the mechanism of the sorption by reagent- loaded polyurethane sorbents description, the nature of the physically or chemically imobilized reagent in the foam structure plays a leading role [2,9].

The selection of TBP as modifier agent for the cellular material has been determined by its double function: plasticizer which significantly increases the foam permeability and extractant with high solvation power in ionic association systems.

In order to establish the optimum conditions for Ga(III) sorption on flexible open cell polyurethane foam of polyether type loaded with tri-n-butyl-phosphate, the effect of solution acidity, phase contact time, Ga(III) concentration and solution temperature have been studied.

The effect of solution acidity on polyurethane foam-TBP-Ga (III) sorption systems is described by the means of Ga (III) distribution coefficients. The distribution coefficients (K_d) were calculated as ratio between moles of Ga(III) taken up per gram of TBP- loaded foam and moles of Ga(III) left in 1 mL solution at equilibrium.
Because the polyurethane foam is partially chemically destroyed in solutions with concentrations of HCl over 8 mol/L, the correlation is possible only in the range of HCl concentration 0- 8 mol/L [17].

It may be considered that in solutions with concentrations of 1-2 mol/L in HCl, the following equation describes rightly the Ga (III) retention equilibrium on TBP-loaded foam:

$$3[TBP.\ H_2O]_{foam} + [GaCl_3]_{aq} \rightleftharpoons [(TBP)_3.GaCl_3]_{foam} + 3[H_2O]_{aq}.$$

The solution acidity increase (4-6 mol/L in HCl) causes a mechanism of oxonium type for Ga (III) sorption (as $[GaCl_4]^-$ chlorocomplex):

$$[TBP\ .\ H_2O]_{foam} + [HCl]_{aq} \rightleftharpoons [TBP\ .\ HCl]_{foam} + [H_2O]_{aq}.$$

$$[TBP\ .\ HCl]_{foam} + [GaCl_4]^-_{aq} \rightleftharpoons [(TBPH)^+\ .\ GaCl_4^-]_{foam} + [Cl^-]_{aq}.$$

The dependence of Ga (III) distribution coefficients on hydrochloric acid concentrations until 8 mol/L is shown in Fig. 2.

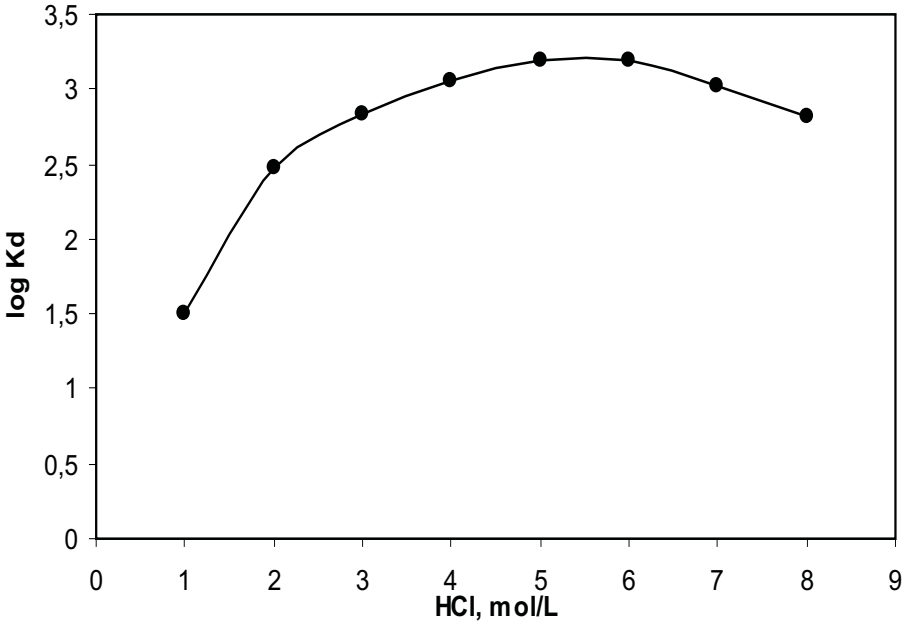

Fig. 2. The effect of HCl concentration (mol/L) on Ga (III) retention by polyurethane foam impregnated with TBP (C_0= 0.1584 mg Ga(III)/mL; shaking time = 1h).

The competitive effect of HCl extraction, predominantly to increase of medium acidity, determines a decrease in Ga (III) retention for HCl concentrations over 6 mol/L. This behavior is in good agreement with the proposed mechanism for extraction of Fe (III) from solutions 4 mol/L in HCl on polyurethane foam pretreated with TBP [17].

The experiments carried out in solutions 6 mol/L in HCl with an initial concentration of 0.1584 mg Ga (III)/mL revealed an increase of the Ga (III) retention degree with phase contact time increasing (Fig.3).

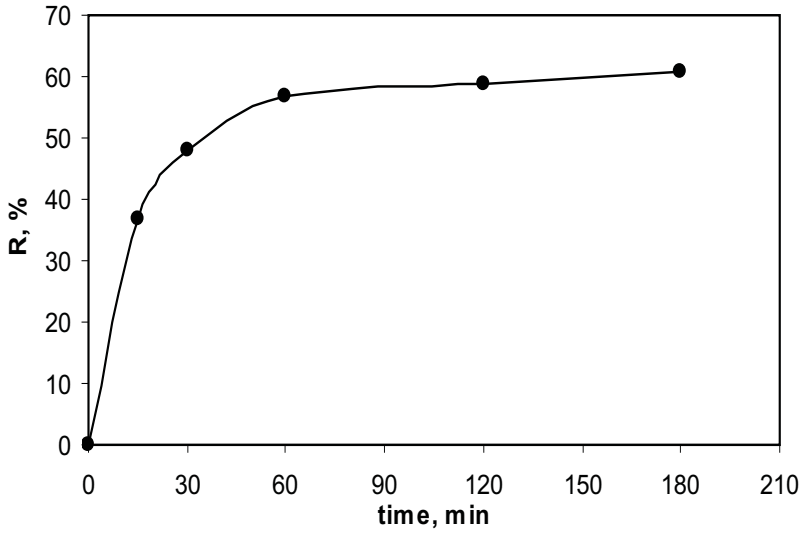

Fig. 3. The effect of phase contact time on Ga (III) retention by TBP-loaded polyurethane foam (C_0= 0.1584 mg Ga(III)/mL).

The equilibrium of Ga (III) sorption on polyurethane foam impregnated with TBP is reached after about 2h from phase contact.

The influence of the initial concentration (C_0) on Ga (III) sorption by TBP – polyurethane foam is giving in Fig. 4.

The amount of Ga (III) sorbed from solutions 6 mol/L in HCl, at two different temperatures, increases with increasing initial concentrations. This trend can be explained by assuming that surface sorption sites play a leading role in the systems under study. Higher initial concentrations might be closely associated with high values of the ratio between the initial number of Ga (III) mmoles and the finite number of surface active sites, thus resulting in an enhancement of the metal uptake.

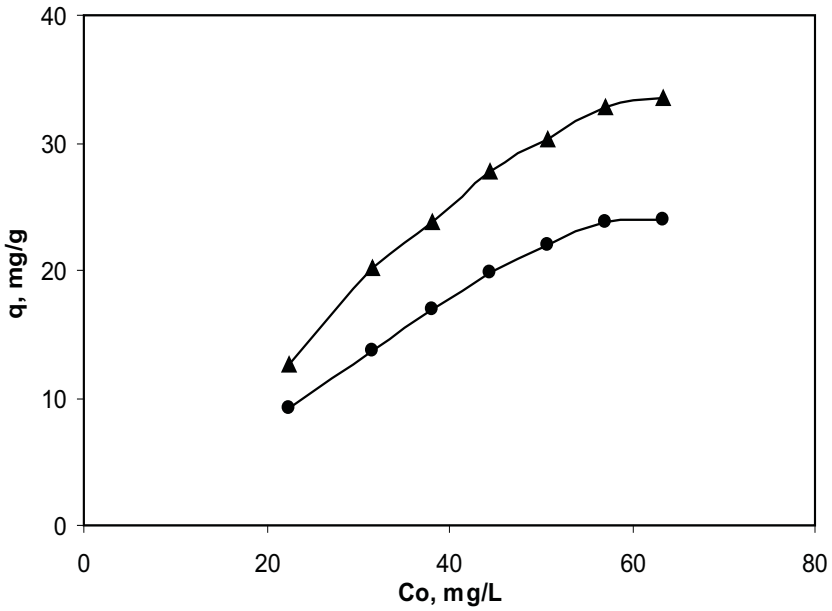

Fig. 4. The influence of initial concentration on Ga (III) - TBP – polyurethane foam sorption systems, at different temperatures (●)- 278 K; (▲)- 313 K.

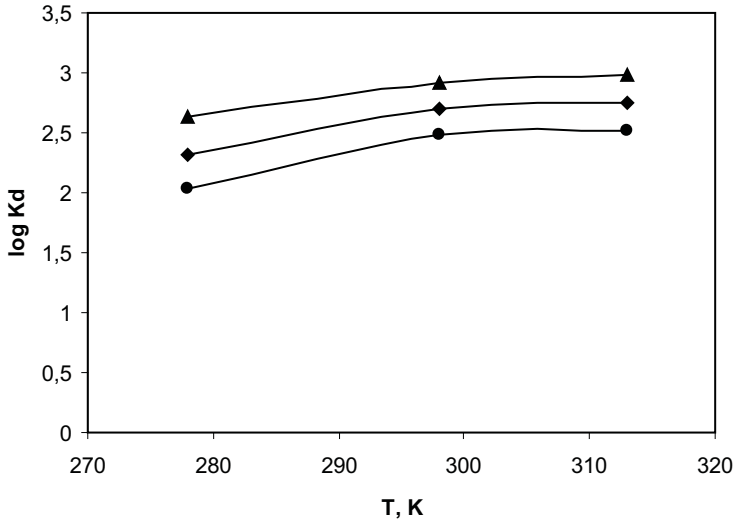

Fig.5. The effect of the temperature on Ga (III) retention by TBP – impregnated polyurethane foam, (●)-C_0 = 19 mg/L; (♦)- C_0 = 31.7 mg/L; (▲)- C_0= 44.3 mg/L.

The amount of Ga (III) sorbed from solutions 6 mol/L in HCl, at two different temperatures, increases with increasing initial concentrations. This trend can be explained by assuming that surface sorption sites play a leading role in the systems under study. Higher initial concentrations might be closely associated with high values of the ratio between the initial number of Ga (III) mmoles and the finite number of surface active sites, thus resulting in an enhancement of the metal uptake.

Fig. 5 presents the influence of temperature on Ga (III) retention by TBP – loaded polyurethane foam from solutions of different initial concentrations.

The lg K_d=f (T) curves in Fig. 5 have the same shape in all solutions. The high values of distribution coefficients (K_d) indicate a good affinity of the TBP–polyurethane foam toward Ga (III); with increasing temperature the retention of Ga (III) is higher, suggesting an endothermic chemical process.

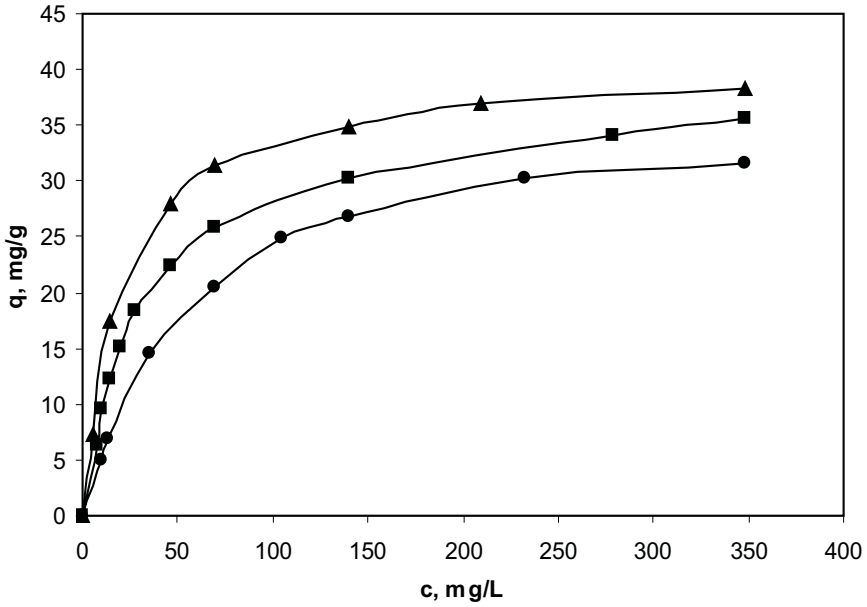

Fig. 6. Ga (III) isotherms of sorption on TBP loaded polyurethane foam, at different temperatures (•) –278 K; (■) –295 K; (▲) –313 K.

Plotting the variation of the retained amount of Ga (III) on solid phase (mg/g) versus the Ga(III) concentration left in solution at equilibrium (mg/L), at constant temperatures, the sorption isotherms represented in Fig. 6 are obtained.

The shape of isotherms in Fig.6 allowed a quantitative characterization of Ga (III) sorption. In this context, we used the equation of Langmuir type in linear form:

$$c/q = c/q_0 + 1/K_L.q_0$$

where: q is the amount of sorbed Ga (III) on solid phase (mg/g foam); c is the Ga(III) concentration in solution at equilibrium (mg/L); q_0 is the saturation sorption capacity (mmol/ g foam); K_L is a parameter related to the strength of the sorbed ion– sorbent binding (L/mol).

The sorption isotherm constants (q_0 and K_L) calculated from intercepts and slopes of corresponding linear Langmuir plots for Ga (III) sorption by untreated polyurethane foam and TBP- polyurethane foam at different temperatures, together with their correlation coefficients (R^2) are given in Tab. 2.

Table 2

Langmuir constants

T, K	R^2	q_0, mmol/g	K_L, L/mol
Polyurethane foam impregnated with TBP			
278	0.9994	0.5301	1262.87
295	0.9993	0.5535	2216.2
313	0.9999	0.5835	3424
Untreated polyurethane foam			
295	0.9952	0.4873	1526.7

Although Ga (III) is well retained on untreated foam, Tab. 2 points out that the analytical performances of the cellular material in sorption of Ga (III) traces were significantly improved by its impregnation with tri-n-butyl phosphate. Therefore the combination between the advantages of liquid extraction and chromatography techniques in TBP-loaded foam case result in sorption systems with high practical applicability.

As can be seen from Table II, on temperature increase, the saturation sorption capacity increases. This finding is in good agreement with viscosity water decrease on rising temperature, so that the penetrability of water and sorbed species in polyurethane sorbent pores is increased.

For a thermodynamic description in polyurethane foam-TBP-Ga (III)-HCl sorption systems the ΔG, ΔH and ΔS values were calculated (Tab. 3) by means of the following usual relations:

$$\Delta G = - RT \ln K_L$$
$$\ln K_L = \text{constant} - \Delta H / RT$$
$$\Delta S = (\Delta H - \Delta G) / RT$$

where R is gas constant and T is the absolute temperature .

Table 3

The thermodynamic parameters characteristic to Ga (III) sorption on polyurethane foam

T, K	ΔG, kJ/mol	ΔH, kJ/mol	ΔS, J/mol.K
Polyurethane foam impregnated with TBP			
278	- 16.496		132.42
295	- 18.883	20.317	132.88
313	- 21.967		132.53
Untreated polyurethane foam			
295	- 17.96	-	-

The negative values of free energy changes (ΔG) for all temperatures show a reasonable affinity of polyurethane foam against Ga (III) ions (spontaneous process of sorption). The positive value of ΔH (variation of enthalpy accompanying the Ga(III) sorption indicates an endothermic process, facilitated by higher temperatures. The positive entropy changes

(ΔS) characterize an increase in the disorder of the system on Ga(III) sorption by the polyurethane foam (probably due to the release of hydration water molecules surrounding the gallium ions).

We experimentally found that temperature rising contributes to a faster attainment of equilibrium, namely an increase of the sorption rate explained by an increase in Ga (III) diffusion rate from chlorhydric solutions to impregnated foam.

CONCLUSIONS

The affinity of flexible open cell polyurethane foam of polyether type for Ga (III) is improved by its impregnation with the organic extractant tri-n-butyl phosphate. If for untreated foam, Ga (III) retention may be explained by a polyether extraction mechanism, in the case of impregnated foam, the advantages of liquid-liquid extraction and chromatography techniques are combined.

The Ga (III) retention from solutions 6 mol/L in HCl on polyurethane foam pretreated with TBP is favored by the increase of phase contact time, the concentration of gallium in external solutions and the temperature.

REFERENCES

[1] Carvalho, M.S.; Neto, K.C.M.; Nobrega A.W.; Medeiros J.A., Se. Sci. and Technol. , 2000, 35(1), 57.
[2] Braun T.;.Navrati, J.D.; Farag, A.B., Polyurethane Foam Sorbents in Separation Science, CRC Press, Inc., Boca Raton, Florida, 1985.
[3] Dmitrienko, S.G.; Zolotov, Y.A., Russ. Chem. Rev. C/C of Uspekhi , 2002, 71(2), 159.
[4] Tofan, L.; Bilba, D.; Nacu, A., Mat. Plast. (Bucharest), 1994, 31, 245.
[5] Dmitrienko, S.G.; Pyatkova, L.N.; Zolotov, Y.A., J. Anal. Chem. , 2002, 57(10), 875.
[6] Abbas, M.N.; El-Assy, N.B.; Abdel Moniem, S., Anal. Lett. , 1989,22, 1555.
[7] Dmitrienko, S.G.; Shapovalova, E.N.; Kochetova, M.V.; Shpigun, O.A.; Zolotov, Y.A., J. Anal. Chem., 2002, 57(11), 1009.
[8] Dmitrienko, S.G.; Goncharova, L.V.; Runov, V.K.; Zakharov, V.N.; Aslanov, L.A., Russ. J. Phys. Chem., 1997, 71(12), 2014.
[9] Palagyi, S.; Braun, T., Elements and Inorganic Species on Solid Polyurethane Foam Sorbents in Preconcentration Techniques for Trace Elements, CRC Press, Boca Raton Ann Arbor London, 1993, pp 364.
[10] Tofan, L., Bilba, D. ; Nacu, A. ; Paduraru, C., Mat. Plast. (Bucharest), 1995, 32, 210.
[11] Elhossein, A.M.; Zaid, M.A.; El-Shahat, M.F., International Journal of Environmental and Analytical Chemistry, 2004, 12(15), 935.
[12] Saeed, M.M.; Ahmad, R., Radiochim. Acta, 2005, 93(6), 333.
[13] Matos, G.D.; Tarley, C.R.T.; Ferreira, S.L.C.; Arruda, M.A.Z., Ecletica Quimico , 2005, 30(1), 65.
[14] Moawed, E.A.; Zaid, M.A.A.; El-Shahat, M.F., Acta Chromatographica, 2005, 15, 220.
[15] Moawed, E.A., Acta Chromatographica, , 2004, 14, 198.
[16] Tofan, L.; Paduraru, C.; Bilba, D. ; Nacu, A., Bull.Polyt. Inst. (Jassy), 1996, 36, 31.
[17] Bilba, D.; Tofan, L.; Paduraru, C. ; Nacu, A., Rev. Roum. Chim., 1998, 43, 493.
[18] El-Shahaw, M.S.; Farag, A.B.; Mostafa, M.R., Sep. Sci. Technol. , 1994, 29(2), 289.
[19] Sandel, E.B., Colorimetric Determination of Traces of Metals, Interscience, New York, 1959, pp 475.
[20] Gesser, H.G.; Bock, E.; Baldwin, W.G.; Chow, A.; McBrideand, D.W.; Lipinski, W., Sep. Sci. Technol., 1976, 11, 317.
[21] Gesser, H.D.; Horsfall, G.A., J. Chim. Phys., 1977, 74, 1072.

USE OF CARBON CATALYSTS FOR OXIDATIVE DESTRUCTION OF WASTEWATERS

Svetlana S. Stavitskaya, Nikolai T. Kartel*

Institute for Sorption and Problems of Endoecology, NAS of Ukraine,
13, General Naumov street, 03164, Kyiv, Ukraine

Corresponding author: Tel/Fax +380 44 4529325; E-mail: nikar@kartel.kiev.ua

Abstract: The paper considers a possibility of using the catalytic action of the carbonaceous adsorbents modified by different ways for the purification of various solutions, natural and wastewaters. It has been found that the oxidative destruction of organic (phenols, dyes, pesticides, etc.) and inorganic (H_2S) contaminants in water solutions is considerably intensified in the presence of both ordinary activated carbons and especially, carbons with specially introduced catalytic additives. It is shown that the sewage treatment level is strongly affected by the amount and nature of a modifying agent introduced on the carbon surface.

Keywords: carbon, catalysis, oxidation, destruction, wastewaters.

1. INTRODUCTION

For effective removal of a number of organic contaminants from wastewaters it is often necessary to destroy them and to this end wastewaters are treatment with oxidizers [1-3]. Chlorination and ozonation are the most popular oxidative destruction methods. Ozone treatment at that is more preferable, owing to the ecologically cleaner method. The same advantage, i.e., the absence of the reduction by-products, is available when using molecular oxygen and hydrogen peroxide as oxidizers, however, the application of the latter two is rather limited, since in usual conditions they posses low reaction capability and are activated only in the presence of catalysts. Ions of metals having variable valence, for instance, can be used as catalysts. Data of paper [4] describe a positive experience in using oxygen in the presence of microquantities of iron, nickel, and chromium for wastewater purification from sulfur-containing compounds, oil products, and phenols. Hydrogen peroxide in the presence of Fe^{2+} and Fe^{3+} oxidizes 30-65% of organic contaminants from domestic sewage and in this case almost completely (by 98%) to CO_2 and also waters that do not contain phenols, organic solvents, etc. [2,4].

Some papers [3,5] indicate the expediency of using the oxidation-sorption method of purification from organic impurities, in which an oxidizer (ozone, chlorine, potassium permanganate) is introduced to the contaminated water and the water is filtered through a layer of activated carbon (AC). With such a method the increases in the purification level is usually much higher than during the summation of oxidation and sorption. As the authors of ref. [3] believe the improvement of the indices is attained, on the one hand, at the expense of greater sorption of the destruction products and, on the other hand, at the expense of more effective oxidation on surface, owing to the increase of the concentration of reacting substances on it. Although, ref. [3] contains a direct indication on the catalytic action of carbons, however, the phenomena described, most likely, are determined by catalytic actions of carbons, which, as well known, effectively accelerate many processes of oxidizing organic and inorganic substances by molecular oxygen and hydrogen peroxide both in the liquid and in gas phases [8-13]. However, the catalytic action of carbons, when considering the processes of the carbon-sorption purification of sewage from organic contaminants, in the majority of cases is not taken into account, although as it can be assumed the establishment of the catalytic phenomena and their controlled use can help in intensification of sewage treatment processes.

The present paper considers some possibilities of using the catalytic actions of various carbonaceous active materials modified by different methods for the sewage treatment.

2. RESULTS AND DISCUSSION

From the data of our previous papers [6,8-12] it follows that the catalytic actions of carbon materials to some degree could be controlled by changing the nature of their surfaces, by the introduction in their structure and in the surface of certain functional groups and compounds, ions, and complexes of metals. Proceeding from it, to perform the analysis of the oxidative destruction processes when removing impurities from waters solutions we used carbons with different chemical compositions of the surface (ordinary, oxidized, and nitrogen-containing), containing different surface functional groups and having catalytic active ions of metals (Fe(II), Fe (III), Ni (II), Co (II), Cr (III), etc.) bound into surface complexes or immobilized complexes of metals and other catalytic additives (CA). The main physical-chemical

characteristics of the used carbons are given in Tab. 1. It shows the data on porosity and ion exchange properties of carbons, on whose basis we prepared catalysts. As a rule, when preparing, for instance, the ion-substitution forms or during the impregnation by the catalytically active substances, the volume of sorption pores and, respectively, the volumes of micro- and mesopores some decrease. However, such decreasing is small, when using 1-2% of the pores filling and does not change the porosity nature substantially [11].

Table 1

Physical-Chemical Characteristics of Carbons

Catalyst sample	Volume of sorption pores, (W_s), cm^3/g	V_{meso}, cm^3/g	V_{micro}, cm^3/g	Specific surface area (S_{sp}), m^2/g	Static exchange capacity, mM/g	
					HCI	NaOH
AU-1	0.52	0.21	0.31	423	0.45	0.16
AU-2	0.48	0.28	0.30	-	0.46	0.14
AU-3	0.55	0.25	0.30	380	0.8	0.11
AU-4	0.65	0.20	0.45	520	0.20	2.50
AU-5	0.55	0.20	0.35	450	0.15	2.80
AU-6	0.35	0.15	0.20	-	0.10	2.70
AU-7	0.70	0.21	0.47	850	0.10	2.70
AU-8	0.90	-	-	-	0.20	1.00
AU-9	0.27	0.10	0.17	350	0.10	2.50
AR-3	0.45	0.15	0.30	418	0.45	0.21
SCN	0.68	0.28	0.40	630	0.67	0.12

The experiments were conducted using both model solutions of the known composition containing phenols, dyes, organic acids, pesticides, sulfides, and real, in particular industrial sewage with a set of different separately no identifiable organic contaminants.

Hydrogen peroxide and molecular oxygen were used mainly as oxidizers; in some cases (for comparison) we used oxidation by sodium hypochlorite and ozone.

We investigated the processes involving the removal of *phenol*, *methylene blue*, *congo red*, mixtures of *pesticides*, mixtures of *organic acids* after contact with oxidizers and individual activated carbons, both initial and modified (Tables 2 and 3, Fig. 1). For comparison, we also used homogeneous activators of hydrogen peroxide – the mixture of ions of two-or three-valence iron.

As could be expected, given the treatment with oxidizers the concentrations of organic substances some decreased. When in contact with AC as a result of adsorption we could observe a distinct removal of the mentioned substances. However, if in identical concentrations and temperature conditions and the same contact time we try to perform the simultaneous action of an oxidizer and adsorbent, the purification level is much higher (Tab. 2 and Fig.1).

Table 2

Removal of Organics from Model Solutions

Substance	Oxidizer	Carbon material	Catalyst	Purification level, %
Phenol	-	AR-V	-	25
	H_2O_2	-	-	15
		-	Fe (II) + Fe (III)	43
		AR-V	AR-V (CA) Fe (II) + Fe (III)	**88**
Congo red	-	AR-V	-	28
	H_2O_2	-	-	10
		-	Fe (II) + Fe (III)	31
		AR-V	AR-V (CA) Fe (II) + Fe (III)	**73**
Mixture of pesticides	-	AU-1	-	22
	H_2O_2	-	-	10
		-	Fe (II) + Fe (III)	31
		AU-1	AR-V (CA) Fe (II) + Fe (III)	**68**
Mixture of organic acids	-	AU-1	-	38
	H_2O_2	-	-	8
		-	Fe (II) + Fe (III)	18
		AU-1	AU-1 (CA) Fe (II) + Fe (III)	**55**

It is most likely, that it is achieved at the expense of the catalytic action of AC. This is also indicated by the fact that a similar, although much smaller increase in the purification level, is observed also in the presence of homogeneous activators, in particular, hydrogen peroxide – the mixture of Fe (III) – Fe (III) ions. However, ions adsorbed by carbons, as it follows from [12], should be more catalytically active. We could also observe a certain dependence of the purification level from the nature of carbons and type of modifying additives.

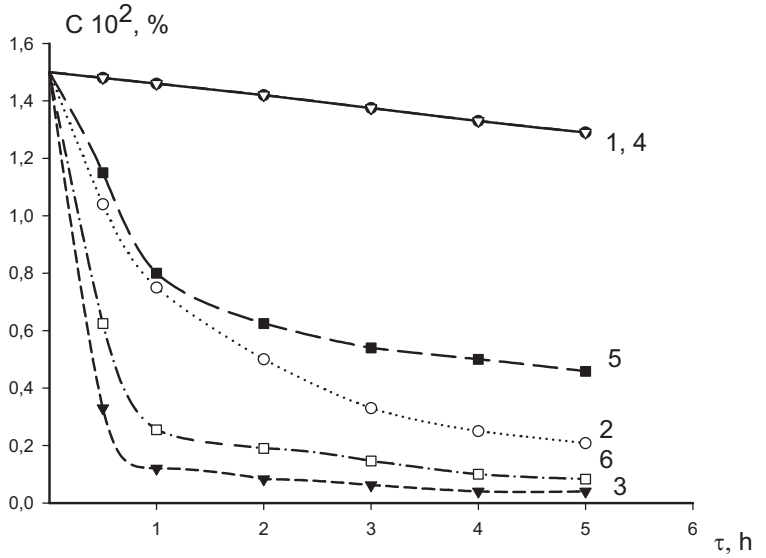

Fig. 1. Dependence of the content of *methylene blue* (1,2,3) and *phenol* (4,5,6) in the solution from contacting time with hydrogen peroxide (1,4), carbon SCN (2,5), and SCN + H_2O_2 system (3,6).

Indeed, earlier [8,9] it was shown that the catalytic oxidation by oxygen, for instance, of carbons is substantially affected by the nature of carbon and modifiers – ions of metals. The same factors also produce great influence on the oxidation of dibenzyl ester [6] and other similar processes.

As for the removal of organic substances from water solutions in the system "substance R + oxidizer (O_x) + AC", in particular, for cation substitution forms, the oxidative destruction may be following:

$$\text{AC } Me^{z+} + R + O_x\ (H_2O_2, O_2\ldots) \rightarrow \text{AC } Me^{z+}\ \begin{matrix}(H_2O_2)\\(HO_2^*)\\(R^*)(R)\end{matrix} + H_2O + \text{Oxidation products or } CO_2,$$

where the substance (R) being adsorbed and the oxidizer (O_x), for instance, H_2O_2, the radical HO_2^* or other radicals may hold the vacancies of the coordination sphere of the metal ion adsorbed in the surface complex. In this case we can ensure a tighter contact of reacting substances, which leads to the acceleration of the process. Such pattern of the process has been described in [13] for the catalytic regeneration of carbons.

Oxidative destruction in the processes investigated may take place both parallel to the formation of low-molecular products including carbon dioxide and water. The emergence of the destruction products is registered by the methods of IR- and UV-spectroscopy, while the excess amount of CO_2 in vessels, where the experiments were performed, by gas chromatography. The spectral and gas-chromatographic data were aimed, largely, to provide a qualitative confirmation of the described pattern of catalytic destruction. The qualitative determination of the destruction products and drawing a material balance in this case is difficult, due to the process complexity of the particular sorption of the destruction products.

The data obtained provided a basis to assume that the combination of sorption with catalytic oxidative destruction on modified AC with catalytic additives makes it possible to substantially intensify the process of sewage treatment. Respective experiments were performed with real sewage from several plants, which contained a sum of different organic impurities. The levels of contamination and treatment were determined by the COD (mg O/L) changes. In some cases we also determined the CO_2 amount in a closed space of the reaction vessels.

The experiments have shown that the combination of sorption on AC with catalytic destruction of impurities, in fact, much greater improves the process of purification (Tab. 3) in comparison with the effects of only oxidizers or only sorption purification. Destruction with such combined method occurs mainly till carbon dioxide and water. If the respective experiments are performed in dynamic conditions, as this is in the case of a lot of technological processes,

the volume of the solution purified till the breakthrough of the impurities to the filtrate increases essentially and the time of protective action become longer (Fig. 2). This makes it possible to refer this process as "catalytically prolonged sorption".

Table 3

Removal of Organics from Wastewaters

Mixture of organics	Oxidizer	Carbon material	Catalyst	Purification level, %
COD = 3490 mg O/L	-	AU-2	-	35
	H_2O_2	-	-	10
	O_2	-	-	5
	H_2O_2	-	Fe (II) + Fe (III)	19
		AU-2	-	32
			AU-2 (CA)	58
			(Fe (II) + Fe (III)) AU-2 (CA)	89
	O_2		(Fe (II) + Fe (III)) AU-2 (CA)	68
	H_2O_2	AU-3	AU-3 (CA) (Fe)	**92**
	O_2		AU-3 (CA)	85
COD = 2590 mg O/L	-	AU-2	-	33
	H_2O_2		AU-2 (CA)	**78**
	O_2	-	-	5
		AU-2	AU-2 (CA)	63
	O_3 (ozone-air mixture)	-	-	22
		-	-	18
	NaClO	AU-2	AU-2(CA)	52
	NaClO	AU-3	-	**78**
COD = 78 mg O/L	-	AU-3	AR-3 (CA)	**95**

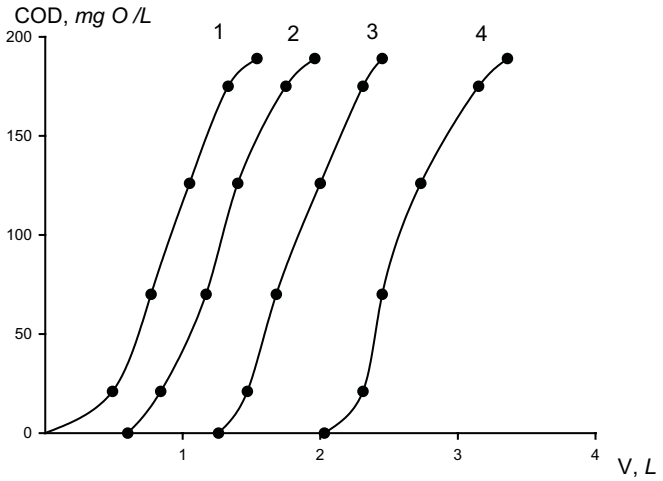

Fig. 2. Output curves of sorption of the mixture of organics from sewage on carbons AU-1 (1,2) and AU-4 (3,4) in the absence (1,3) and in the presence (2,4) of hydrogen peroxide and catalytic additives.

Activated carbons including those modified by cations of metals accelerate oxidation not only of organic but also inorganic substances including sulfuric compounds in the reduced from. These compounds, in particular, hydrogen sulfide are contaminants of natural and wastewaters encountered very often which necessitates their purification before use.

One of the ways to solve this problem is oxidation of sulfate forms by oxygen of air in the presence of catalysts. References [14] show that in addition to inorganic catalysts – caolinite, clinoptilolite etc. – the acceleration of hydrogen sulfide oxidation by oxygen of air may take place in the presence of carbon materials.

We have verified the use of carbon catalysts for the purification from hydrogen sulfide to the MPC level of the solutions modeling natural and wastewaters contaminated with these components. The content of natural sulfur was

within the range of 300 mg/L. The experiments were performed in alkaline and neutral media. As follows from Tab. 4, the purification of the solutions is taking place in the presence of activated carbons. The activity of carbon catalysts can be regulated by the change of the chemical nature of the surfaces of catalysts, by the introduction the surface complexes of these or other cations. For a given process nickel forms oxidized carbons appeared the most active.

Table 4

Purification of Water from Hydrogen Sulfide during Oxidation by Oxygen in the Presence of Carbon Catalysts

Catalyst	SCA*, mol O_2/ (g•min)	Purification level, rel. units**
Without catalyst	$4.0.10^{-6}$	1
AU-4-initial	$8.0.10^{-5}$	20
AU-4 (CA)	$4.0.10^{-4}$	1000
AU-5 (CA-1)	$1.0.10^{-4}$	250
AU-5 (CA-2)	$5.7.10^{-4}$	1430
AU-5 (CA-3)	$8.8.10^{-4}$	2200
Without catalyst	$1.0.10^{-6}$	1
AU-6 (CA-Cr)	$3.0.10^{-5}$	50
AU-6 (CA-Co)	$1.0.10^{-4}$	100
AU-6 (CA-Mn)	$1.7.10^{-4}$	170
AU-6 (CA-Fe)	$8.2.10^{-4}$	820
AU-6 (CA-Cu)	$1.6.10^{-3}$	1600
AU-6 (CA-Ni)	$3.4.10^{-3}$	3400

*SCA – specific catalytic activity; ** Level hydrogen sulfide removal was calculated in respect to the treatment of the same volume of water without catalyst.

3. CONCLUSIONS

The investigations conducted showed that the use of carbon catalysts in the oxidative destruction methods of wastewater treatment is promising both from organic and inorganic contaminants. On the basis of the obtained data it is possible to ascertain that the combination of adsorption with catalytic oxidative destruction on active carbons modified by catalytic additives allows essentially intensify a process of clearing wastewaters.

4. REFERENCES

[1] Сычев, Ф.Я.; Травин, С.О.; Дука, Г.Г.; Скурлатов, Ю.И., Каталитические реакции и охрана окружающей среды, Штиинца: Кишинев, 1983, 271.

[2] Селюков, А.В.; Травин, А.И., В кн.: Производство и потребление перекиси водорода. Труды Всесоюзной конференции, Ленинград, 1987, 46-50.

[3] Луценко, Г.Н.; Цветкова, А.И.; Свердлов, И.Ш., Физико-химическая очистка городских сточных вод, Стройиздат: Москва, 1984, 89.

[4] Котинав, В.Ф.; Котинав, И.В., Озонирование воды, Стройиздат: Москва, 1974, 112.

[5] Сидько, Р.Я.; Кержнер, Б.К.; Гончарук, В.В., Химия и технология воды, 1989, 11(10), 902-905.

[6] Ларина, А.А.; Ставицкая, С.С.; Тарковская, И.А., Катализ и катализаторы, 1992, 28, 48-53.

[7] Ставицкая, С.С.; Гоба, В.Е.; Картель, Н.Т., В кн.: Мікродомішки в воді. Матеріали міжнародного семінару, Київ, 2003, 65.

[8] Ставицкая С.С.; Тарковская, И.А.; Колотуша, Б.И., Украинский химический журнал, 1984, 50(9), 939-943.

[9] Лукомская, А.Ю.; Тарковская, И.А., Теоретическая и экспериментальная химия, 1986, 22(6), 25-28.

[10] Stavitskaya, S.S.; Strelko, V.V.; Kartel, N.T.; Tarkovskaya, I.A., In: Interfaces Against Pollution. Proceedings of the 3rd International Conference, Julich, Germany, 2004, 152.

[11] Тарковская, И.А.; Ставицкая, С.С.; и др., Химическая технология, 1991, 2. 14-19.

[12] Тарковская, И.А.; Шпота, Г.П., Теоретическая и экспериментальная химия, 1986, 22(5), 17-20.

[13] Тарковская\. И.А.; Гоба В.Е.; Томашевская, А.Н.; и др., Химия и технология воды, 1992, 14(5), 348-356.

[14] Ставицкая, С.С.; Тарковская, И.А.; Гороховатская, Н.В.; и др., Украинский химический журнал, 1990, 56(7), 723-726.

COMPOSITION OF MINERAL PHASES OF THE GHIDIRIM DIATOMITE

Vasile Rusu[a]*, Aliona Vrînceanu[a] and Igor Polevoi[b]

[a]*Institute of Chemistry of the Academy of Sciences of Moldova, Academiei str. 3, MD-2028 Chişinău, Republic of Moldova*
[b]*State University of Moldova, Mateevici str. 60, MD 2009, Chişinău, Republic of Moldova*
**E-mail: vrusumd@yahoo.com; Phone: 373 22 739731, Fax: 373 22 739954*

Abstract: Studies of the mineralogical composition of diatomite from the Ghidirim location of RM, as well as of the extracted clay phase are presented. The mineral phase of the diatomite contains a number of clay minerals, like montmorillonite (in a mixture with insignificant quantities of slightly chloritized montmorillonite), illite and kaolinite. Diatomite contains also non-clay components as fine-dispersed quartz and amorphous material, the more probable sources of which are opal, amorphous alumosilicates, aluminum and iron hydroxides. The applied procedure for separation of clay fractions by sizing settling in liquid media proves to be very useful, enabling possibilities for more accurate identification of the clay constituents of diatomic material. Procedure allows to separate very clean clay fraction especially rich in montmorillonite, which can be utilized itself as mineral adsorbent for practical purposes.

Keywords: diatomite, mineralogical composition.

1. INTRODUCTION

The Republic of Moldova is relatively rich in deposits of mineral adsorbents, including the diatomaceous earth, which possess appropriate physicochemical characteristics for usage in the technologies for clearing of juices, wines, vegetal oils, for a water treating, purification of waste waters etc. [1-6]. Significant deposits are localized along course of the Dniester, on the sector Naslavcea – Camenca. The properties of diatomites may vary over a wide range depending on the mineralogical, granulometrical, chemical composition and parameters of the porous structure. The diatomite from the Ghidirim location primarily is characterized by a macroporous structure allowing to be used basically in the processes of purification of systems containing components with large molecular sizes. Generally, depending on the mineralogical structure, diatomites can represent formations from well crystallized forms (christobalite) to quite amorphous forms (opal). Researcher's and practitioner's interests are concentrated actually on extension of the field of application of diatomites, as well as intensification of their usage efficiency through modification of the surface chemistry also the concentration of the diatomic phase by the elimination of impurities existing in the diatomic raw material. At the same time a common tendency is watched, particularly in the case when there is raised the problem for purification of diatomites from various impurities. More often, the question is mooted to cleanse the diatomic phase of all other phases, including clay minerals. In fact, the clay minerals which are present in the diatomic formations may be of a special interest for certain usages. Consequently, when the question is mooted to cleanse the diatomic formations the formulation should also include the proceeding of reutilization of the clay components.

Current work includes studies of the mineralogical composition of diatomite from the Ghidirim location of RM, as well as of the extracted clay phase, the furthermost purpose being synthesis of modified mineral adsorbents.

2. RESULTS AND DISCUSSIONS

2.1. Mineral-composition of diatomite

Figure 1 shows X-ray diffractograms of the Ghidirim diatomite, the integral sample containing all the characteristic constituents. Results demonstrate the presence of kaolinite and illite identified by the behavior of the basic reflexes of the samples before and after thermal treatment. Kaolinite is characterized by the presence of the basic reflexion (non-calcinated samples) localized at 7,1Å, depending on the degree of crystallization [7]. This reflex remains practically unchanged after the calcinations at 350ºC, but disappears after calcinations at 550ºC. For the studied diatomite a reflex at 7,08Å is registered for non-calcinated samples, persisting after calcinations at 350ºC and considerably decreasing in the intensity after calcinations at 550ºC. On its place a weak and diffuse reflex, asymmetric in the direction of low angles, is registered at about 6,97Å. Thus, the results show the presence of kaolinite in the studied diatomite. At the same time the behavior of the respective reflex after calcinations at 550ºC suggests the presence of some other clay components with special properties that will be discussed further.

Characteristic for illite is the presence of the basic reflex (non-calcinated samples) localized in the range of 9,9-10Å depending on the degree of crystallization [7]. This reflex remains essentially unchanged after calcinations at 350ºC and 550ºC. The intensity of this reflex increases after heat treatment in case when the studied material contains such minerals as montmorillonite, vermiculite or chlorite, due to the shift of basic reflexions of these minerals towards 10Å. The presence of illite in the studied diatomite is demonstrated by the presence of the 9,94Å reflex for non-calcinated samples, becoming much more intensive after calcinations at 550ºC.

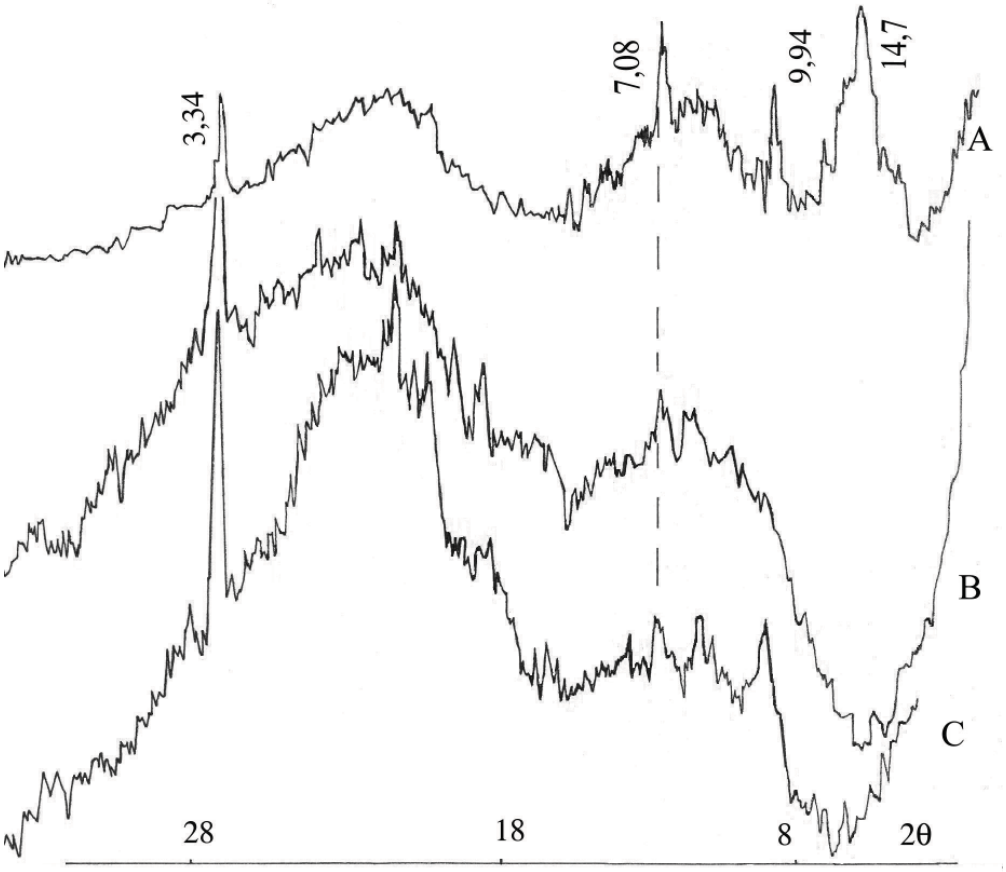

Fig. 1. X-ray diffractograms of the Ghidirim diatomite. Non-calcinated samples (A), after calcinations at 350ºC (B) and 550ºC (C).

After calcinations at 350ºC the basic line on diffractograms becomes arched and very diffuse in the range of 10-6Å,due to complex behavior of amorphous components (more probably, opal) which are present in diatomite material. Reflex of kaolinite (7,1Å) as well as reflexions of some new phases (7,69Å) are registered on the background of this diffuse band. This arching or the diffuse background considerably masks the illite reflex (10Å).

Identification of phases with reflexions in the range >10Å is more complicated. The basic reflex in the range of >10Å of the non-calcinated samples is registered at 14,7Å,with a diffuse "branch" in the range of 16-16,6Å. Calcinations at 350ºC "cleans" the >10 Å range,however the behavior of the 9,97Å reflex cannot be followed due to diffuse background in this range. Better intensification of the 9,97Å reflex is noted after calcinations at 550ºC.

Certain peculiarities of behavior of the reflexions in the range >10Å must be pointed especially, e.g. the presence of the 16-16,6Å "branch" for the non-calcinated samples, a strong decrease of the intensity of the main reflex 14,7Å and its shifting to 10Å after calcinations at 350ºC (on the background of the diffuse arching in the 10-6Å range), and slight intensification of residual reflexions in the range 13-14Å after calcinations at 550ºC. Such behavior of phases in the range >10Å suggests the presence of montmorillonite in a mixture with insignificant quantities of slightly chloritized montmorillonite [7]. The montmorillonite is identified by the presence of the main reflex 14,7Å and its contraction after calcinations leading to an intensification of the reflex 9,97Å. Following indications suggest the presence of the slightly chloritized montmorillonite. When Al-, Fe-hydroxy complexes are present in the interlayer spacing of montmorillonite, the mineral looses its normal contraction capacity after thermal treatment due to formation of associations closely bound to crystal packages. These formations represent intermediate systems between veritable 2:1 minerals (with characteristic properties) and Al-, Fe-chlorite being "intermediate" or intergrade minerals. The mentioned behavior of the reflexions in the range >10 Å demonstrates that the "intermediate" mineral in the studied diatomite is poorly chloritized and refers to slightly chloritized montmorillonite with Al-, Fe-hydroxy complexes being "insular" distributed in the interlayer spacing [7].

Characteristic for the slightly chloritized montmorillonite is the decrease of the reflex at 14Å after calcinations, shifting after 350ºC to smaller values or forming a diffuse band in the range of 12-14Å. Sometimes calcinations at 500-600ºC can produce an intensification of the reflex in the range of 12-14Å, depending on degree of chloritization of such

formations. The obtained results confirm the presence of slightly chloritized montmorillonite in the studied diatomite, which is indicated by the presence of the "branch" at 16-16,6Å for non-calcinated samples, strong decrease of the intensity of the main reflex at 14,7Å and its shift towards 10Å after calcinations at 350ºC (on the background of the diffuse arching 10-6Å), and intensification of the residual reflexes in the range of 13-14Å after calcinations at 550ºC.

Besides of mentioned clay minerals the studied diatomite contains also certain amounts of non-clay components. Particularly, the presence of fine-dispersed quartz is registered being identified by the presence of the main reflex at 3,34Å. Also, the presence of significant quantities of amorphous materials is registered being identified by arched band in the range of 5-2Å. More probably, such roentgen-amorphous materials in the diatomite are opal, amorphous aluminum and iron compounds, e.g. amorphous alumosilicates, hydroxides, hydroxy-complexes etc. However, further investigations are needed to more exactly identify the possible components of the amorphous material.

As a whole, the mineral phase of the Ghidirim diatomite contains a number of clay minerals, like montmorillonite (in a mixture with insignificant quantities of slightly chloritized montmorillonite), illite and kaolinite. Diatomite contains also non-clay components as fine-dispersed quartz and amorphous material, the more probable sources of which are opal, amorphous alumosilicates, aluminum and iron hydroxides etc.

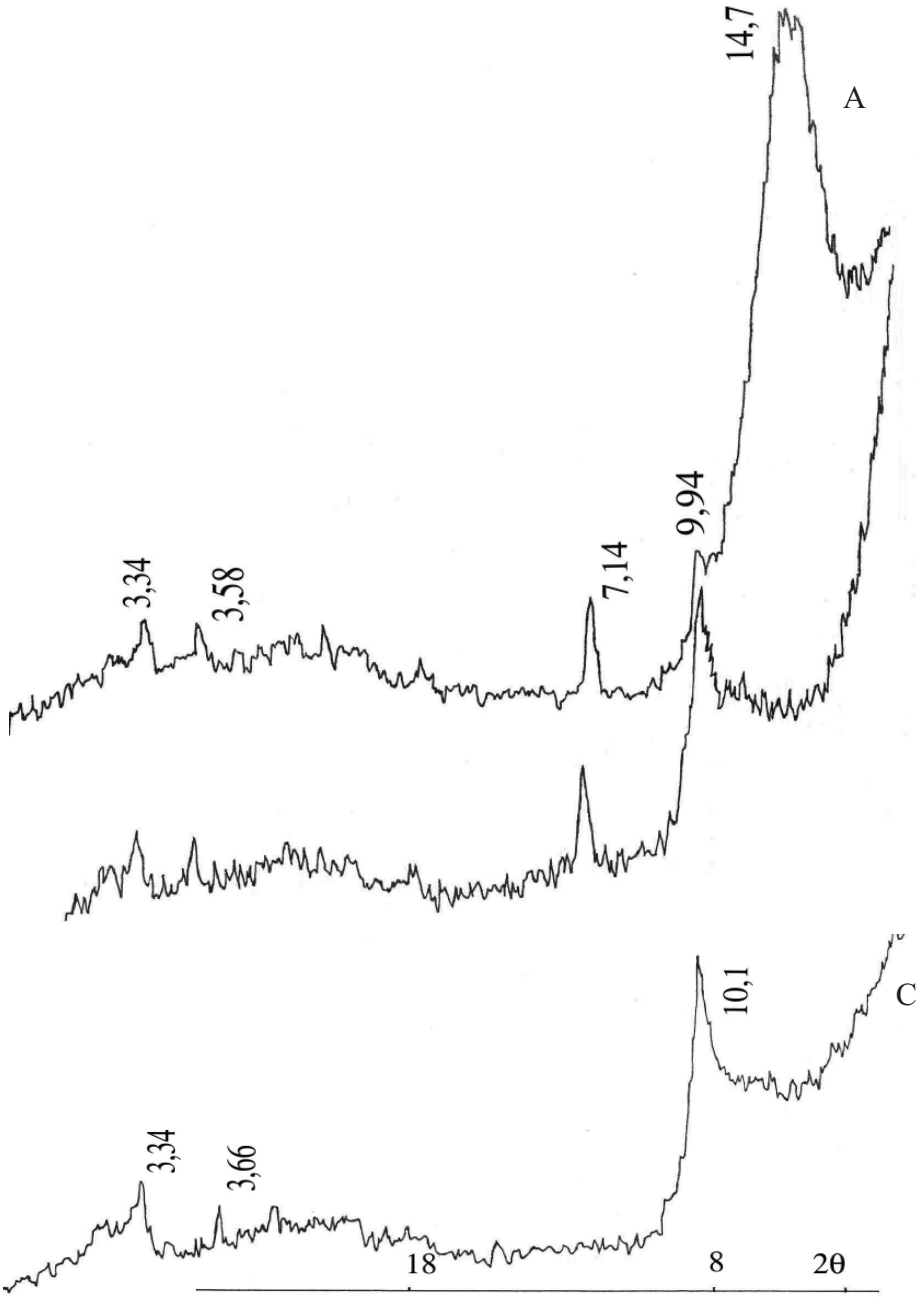

Fig. 2. X-ray diffractograms of the clay fractions extracted from the Ghidirim diatomite. The non-calcinated samples (A), after calcinations at 350ºC (B) and 550ºC (C).

2.2 Extraction of the clay fraction from the diatomite

Extraction of the clay minerals from the studied diatomite was performed using the method of sizing by settling in liquid media (distilled water) [7]. The procedure insures "mild" conditions for the extraction of clay constituents without their denaturing or destroying. For the extraction of different constituents from solid materials (soils, sediments, clay formations) are applied various chemical reagents (acids, bases, complexons etc.), however the degree of selectivity and effects on other components should be well-argued by individual investigations of each type of solid material [7]. Aqueous extraction applied in these studies are more easily to perform and, though sizing by settling in liquid media does not insure a complete extraction of all clay constituents from diatomite, such procedure, what is more importantly, does not alter natural chemical composition of clays. Fig. 2 shows diffractograms of the clay components extracted from the Ghidirim diatomite. Diffractograms of the integral diatomite, presented in figure 1, represents properly summary structure of the diatomic material, showing clay fraction on the background of the diatomic formation. Fig. 2 shows just the structure of the clay fraction separated from non-clay components, in consequence diffractograms are more "clean" showing distinctly reflexions of the clay minerals and their veraciously behavior on thermal treatment. The presence of montmorillonite, illite and kaolinit in separated clay fraction is uniquely demonstrated. Also, in this case the identification of the slightly chloritized montmorillonite is more veraciously proved by decreasing of the reflex in the range of 14Å after thermal treatment being shifted after 350ºC to the smaller values in the form of diffuse bands in the range of 12-14Å.

Though some quantities of fine-dispersed quartz also penetrate into the separated clay fraction, these quantities are matchless smaller compared to those which are contained in the initial diatomic material. It is very importantly that the separated clay fraction does not contain amorphous material extracted from the initial diatomic material.

Thus, the applied procedure of clay fraction separation by sizing settling in liquid media proves to be very useful enabling possibilities for more accurate identification of the clay constituents of diatomic material. Also, along with an accurate diagnostics of the clay minerals, it is very important that the applied procedure allows to separate very clean clay fraction especially rich in montmorillonite, which can be utilized itself as mineral adsorbent for practical purposes.

3. EXPERIMENTAL PART

The diatomite from the Ghidirim location of RM was used for investigations. The physical-chemical characteristics and parameters of the porous structure of this diatomite were described early [1]. Samples of diatomite containing all characteristic constituents (integral diatomic material) and separated clay fraction extracted by sizing settling in distilled water were studied. X-ray analysis was performed using the DRON-1 X-ray installation with CoKα radiation. There were used oriented preparations exposed to various thermal treatments in series (i) non-calcinated samples, (ii) samples after calcinations at 350ºC and (iii) samples after calcinations at 550ºC [7].

4. CONCLUSIONS

The performed analysis shows that the mineral phase of the Ghidirim diatomite contains a number of clay minerals, like montmorillonite (in a mixture with insignificant quantities of slightly chloritized montmorillonite), illite and kaolinite. The studied diatomite contains also non-clay components, some being well crystallized, for example fine dispersed quartz, as well as amorphous material, the more probable sources of which are opal, amorphous alumosilicates, aluminum and iron hydroxides.

The applied procedure for separation of clay fractions by sizing settling in liquid media proves to be very useful, enabling possibilities for more accurate identification of the clay constituents of diatomic material. Procedure allows to separate very clean clay fraction especially rich in montmorillonite, which can be utilized itself as mineral adsorbent for practical purposes.

5. REFERENCES

[1] Kerdivarenko, M.A. Moldavschie prirodnîe adsorbentî i tehnologhia ih primenenia. Kishinev: Cartea moldovenească, 1975, 190p. (rus.).
[2] Ropot, V.M.; Stratulat, G.V.; Sandu, M.A.; Lupashcu, F.G.; Rusu, V.I. i dr. Problemî cacestva, ispolyzovania i ohranî vodnîh resursov SSR Moldova. Kishinev: Stiința, 1991, 285 p. (rus.).
[3] Totok, G.T.; Rusu, V.I.; Ropot, V.M.; Bolotin, O.A. Recomendații na primenenie bentonitovîh glin MSSR dlea ocistchi prirodnîh vod. Utverjdenî Ministerstvom jilicyno-komunalynogo hozeaystva MSSR, ot 14.01.1986g. Kishinev: Stiința, 1986, 8p (rus.).
[4] Kerdivarenko, M.A.; Şeremet, N.V; Rusu, V.I. i dr. Izvestia Academii Nauk MSSR, seria biol. I him. nauk, 1990, No. 5, p.56-62 (rus.).
[5] Kerdivarenko, M.A.; Şeremet, N.V; Rusu, V.I. i dr. Izvestia Academii Nauk MSSR, seria biol. I him. nauk, 1991, No. 1, p.56-61 (rus.).
[6] Zelenţov, V.; Datco, T.; Dvornicova, E. Proceedings of Intern. Conf. "Mediul şi Industria", Bucureşti, 2005 (rom.).
[7] Rusu, V.; Lupaşcu, T. Chimia sedimentelor sistemelor acvatice. Proprietăți de suprafață. Modele fizico-chimice. Chişinău: IPE Elena VI, 2004, 272p. (rom.).

THE ROLE OF THE NATURAL ANTIOXIDANTS IN THE OXIHAEMOGLOBIN OXIDATION AND THE DIMINUTION OF NITRITE CONCENTRATION

Maria Gonța

Department of Ecological and Industrial Chemistry, State University of Moldova, 60 Mateevici, Chisinau, Republic of Moldova, Tel.: 57-75-53, E-mail: mvgonta@yahoo.com

Abstract: The paper includes the study of the inhibition of the process of methemoglobinization at oxidation with nitrites in the presence of sodium dihydroxyfumarate (DFH_3Na) and resveratrol (3,4',5-trihydroxystilben). The experimental study was carried out by treatment of the erythrocyte mass by hemolysis and exposure to nitrite. The kinetic investigations were carried out in following conditions: [Resv] = ($5\cdot10^{-5} – 1\cdot10^{-3}$) mol/l, [$DFH_3Na$] = $1\cdot10^{-6} – 5\cdot10^{-6}$ mol/l; [HbO_2]=$1\cdot10^{-3}$ mol/l; pH 7,1; t = 37^0C. The rate of transformation of HbO_2 in the presence of resveratrol and DFH_3Na was calculated from kinetic curves of consumption of the substrate and formation of MetHb obtained spectrophotometrically (λ_{max}= 540 nm for HbO_2 and λ_{max}=630 for MetHb). It has been found out that the introduction of resveratrol and DFH_3Na in the system $HbO_2 – NO_2^-$ causes the decrease of the autooxidation factor φ_{DFH3Na} approximately by 1.1 – 2.5 times and $\varphi_{resveratrol}$ by 1.1 – 1.7 times. The time of achievement of the maximum rate of oxidation of HbO_2 $d\zeta/d\tau$ (where ζ is the rate of transformation of HbO_2 in MetHb) increases while the phase of fast oxidation of HbO_2 decreases with increase of content of inhibitors. The process of interaction of nitrites with reducers (such as DFH_4, DFH_3Na, resveratrol and (+)-catechine) was carried out as well. It has been established that degree of diminishing of the concentration of nitrites in the system $RedH_2$-NO_2^- decreases as follows: DFH_4<DFH_3Na<Resv<(+)Catechol.

Keywords: nitrite, haemoglobin, inhibitor of methemoglobinization.

1. INTRODUCTION

In the specialized literature there are described groups of compounds that lead to MetHb formation (among them, different xenobiotics). The nitrates, the nitrites and nitric oxides play an important role in the MetHb formation; they penetrate in the human body via various ways: during the ingestion (food and water) and inhalation. The nitrates and the nitrites are indispensably joined with each other in the natural circuit of the nitrogen, but due to the chemical activity of the nitrite ion, their concentration in the environment is insignificant. Thus, the first stage of intoxication with nitrates is their reduction in nitrites. In all living beings, simultaneously with the common process of O_2 elimination, there occurs the self oxidation of HbO_2 in MetHb:

$$HbO_2 \rightarrow MetHb + O_2^{\bullet} \quad (1)$$

From the above reaction, we can observe that the radical of super oxide anion, with pragmatical properties is generated ($O_2^{\bullet}$). This radical was detected in HbO_2-$NaNO_2$ system, via the RMN method [1].

During the process of HbO_2 oxidation with NO_2^-, the oxygen from the haemoglobin molecule that appears as an auto catalyst in this process plays a great role. The authors of this work [2] suppose that after the process of oxide-reduction at the interaction of NO_2^- with $O_2^{\bullet}$ takes place the generation of nitrate oxide. Such a direction of the process is assured by the oxide-reducing potentials of NO_2^- and $O_2^{\bullet}$, accordingly +0, 99 and -0, 33 V. The $O_2^{\bullet}$ radical is not a direct oxidant of HbO_2, but it is compulsory in the process of autocatalysis.

Another important factor in the HbO_2 oxidation mechanism is the formation of $NO_2^{\bullet}$ at the initial stage of the oxidation process. The formation of this radical in the system was established by the use of amines (aniline), which imbibes the process of HbO_2 oxidation, due to the formation of N-nitrosamines with NO_2^- [3].

An important intermediary of the HbO_2 oxidation process with NO_2^- is H_2O_2, which forms as a result of $O_2^{\bullet}$ dismutation [2]. We established that H_2O_2 influence upon the HbO_2 oxidation reaction with NO_2^- depends on the initial concentrations of $[NO_2^-]_0$ and $[H_2O_2]_0$.

Knowing the mechanisms of the reactions between haemoglobin and different methemoglobinisants helps to elaborate methods of inhibition against haemoglobin oxidation.

HbO_2 oxidation with nitrites is being studied as a 2-stage process [4]: the slow process (lag period) and the fast process, (auto catalyst). The kinetic curves have a peculiar S-shape. There should be mentioned that the process of oxidation of the oxygenated form of HbO_2 and Hb with nitrites is different.

In order to decrease the degree of HbO_2 oxidation and diminish the concentration of oxidative particles that form in various systems it is necessary to use different antioxidants, especially natural ones.

The antioxidant activity of polyphenols

The polyphenols are characterized by their antioxidant activity and they can be used as well to reduce the oxidational degree of different substances.

The flavonoids constitute a large class of compounds present in plants, which contain a certain number of hydroxyl phenolic groups attached to the annular structure, endowing reducing properties. The antioxidant activity of phenols is determined by the presence of hydroxyl groups in B ring, in the positions 3' and 4' and in a lesser degree, by the hydroxyl group from B ring, in the position 4'. The phenols, especially the catehine, quercitin, kaemferol and their glycosides, are constituents of the green and black tea [5] and red wine [5]. The diets rich in fruits, vegetables and grapes are recommended against heart diseases accompanying various forms of cancer [7,8], methemoglobinemy, have anti-inflammatory and antimutagene effects [9] etc. These protecting effects have been attributed to the present antioxidants that include flavonoids, carotids and the vitamins C and B.

The researches performed *in vitro* established the antioxidant potential of the polyphenols as the parameter that determined the capture capacity of the free radicals, such as super oxide radicals, the singlet oxygen, hydroxyl radicals, peroxyl radicals, nitric monoxide and the peroxinitrite (they cause different pathologies). The chemical structures that contribute to the antioxidant activity of the polyphenols, including the neighbouring dihidroxi- or trihidroxi-structure, can cellar the ions o metal through the formation of complex and prevent the generation of free radicals. This structure also allows delocalizing the electrons, conferring high reactivity for destruction of free radicals.

The majority of polyphenolic constituents from the food products (flavonols – such as quercitin and kaempherol, flavones – such as luteolin, flavonols – such as catechin, antocynidins for instance, cyanidin and malvidin and their glycosides) present major efficiency, in comparison with the nutrient antioxidants: vitamins C, E, β-carotene, that are easily absorbed in the intestine [10].

Antocynidins and catechines have been tested *in vitro* for their inhibitional influence upon the cyclooxigenaze enzymes (COX) that provoke the multiplication of cancerogen cells and also upon the proliferation of cancer cells in human beings [5]. We established that cyanidine has the strongest inhibitory effect of the COX enzymes and it has hydroxyl groups 3',4' in B ring. The inhibitory activity decreased in the case of delphinidine and pelargonidine, that have 3', 4', 5'-trihidroxilic and 4'-hidroxilic groups in B ring, accordingly. From the point of view of the liaison between the structure and the activity, the number and the position of hydroxyl groups in auto cyanides B ring influence the inhibitory activity of these compounds. For catechine cis-, trans-isomery, epimerisation did not influence greatly the inhibitory activity on COX enzyme, but the presence of galloyl groups in catechine structure influenced more their inhibitory activity on the COX enzymes. Based on the obtained results during the inhibition of proliferation of cancer cells under the action of antocyanidins and catechines, we established that the degree of inhibition is higher for the galloyl derivatives of catechines [5] (gallocatechine – 95%, epigallocatechine – 100% and gallocatechingalate – 97%), but for antocyanidins, it represents almost 75%.

The degree of polymerisation has a greater influence on the inhibitory properties of the polyphenols and it augments together with the galloylation. The polyphenolic fractions extracted from the grapes with a different degree of polymerisation had a different antioxidant/antiradical and antiproliferative effect [6]. The polyphenolic solutions extracted from the grapes have been divided into 2 fractions having a different degree of polymerisation, with RP-HPLC. The antioxidant/antiradical activity determined via the DPPH test for the polyphenolic fraction from the grapes, composed of small, was higher than the fraction which included procyanide flavonols and oligomers with a greater molecular mass. Catherine A Rice-Evans et alt. [10] have studied the total antioxidant activity (TAA) and the antioxidant activity equal to Trolox (AAET) for the polyphenols that are contained in the green tea and red wine. AAET measures the concentration of the Trolox solution (mM) with a potential antioxidant equivalent at a standard concentration of the compound subjected to the research. The authors came to the conclusion that the antioxidant activity of the polyphenolic constituents of the green tea (Fig.1) in correlation with their content, according to their order of antioxidant activity, is: epigallocatechine (34%) ≈ epigallocatechingalate (32%) >> epicatehingallate (7%) ≈ epicatechine (6%) > catechine (1%) [10].

Through radio lithium generation of oxygen species in presence of different catechines, that are active constituents of the tea, we established that the DNA harm caused by these reactive particles, decreases at least in the presence of EGCG [11]. Thus, 66% from the antioxidant activity of the green tea is determined by epigallocatechine and epigallocatechine-gallate, which corresponds to the content of these compounds in the green tea (20,44% from 26,71% of the total number of polyphenols).

Based on the study of the total average antioxidant activity of the red wine, we established that 54,76% is determined by catechine and epicatechine contribution that represent almost 63,54% from the phenol constituents (191 and 82 mg/l accordingly) [10].

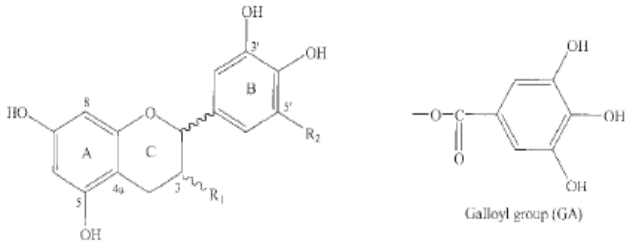

Fig. 1. The chemical structure of the catechines present in tea and in wine [5]. Catechine-(R_1 - OH, R_2 - H), gallocatechine-(R_1 - OH, R_2 - OH), catechingalate (R_1 - GA, R_2 - H), gallocatechingalate (R_1 - GA, R_2 - OH).

In various systems, the free radicals can form as a result of peroxide decomposition in presence of different metals: Fe^{2+}, Cu^{2+}, Cr^{3+} etc. As a result of H_2O_2 reduction through the Fenton reaction in presence of Cr^{3+} (which is toxic and causes genotoxicity), the $OH^{\bullet}$ radical is being formed:

$$Cr(III)+H_2O_2 \rightarrow Cr(IV)+OH^{\bullet}+OH^- \quad (2)$$

The hydroxyl radical formed *in vivo* produces oxidative harm to DNA, with the formation of 8-hydroxy-2-deoxyguanosine (8-OH-dG) that appears in this process as a biomarker [12]. Based on the study results, Silvia Lopez-Burillo et al. [12] established that the antioxidants inhibit the oxidative processes of DNA. Among the polyphenols studied in [12], the highest inhibitory effect is presented by (-)-epigallcatechine-3-gallate (EGCG) in concentration of 1 μM or more, which reduces the 8-OH-dG formation. Tea catechines can form stable compounds with Cu(II) and Cr(III) and as a result, $OH^{\bullet}$ radicals are generated [13]. But it was established that in the case of EGCG $OH^{\bullet}$ radicals are split up by the gallate group present in the complex and thus, the prooxidant effect of this compound is not manifested [14].

The green and black tea can inhibit lipoproteins' oxidation induced by Cu^{2+} [13], thus, it contributes to the prevention of arteriosclerosis and other heart diseases. The inhibition of this very process is determined by the fact that polyphenols can cellar the metals and decrease the concentration of active forms of the oxygen, which in its turn takes part at the protein oxidation.

2. MATERIALS AND METHODS

An inhibitor that was used in the, HbO_2–NO_2^- system is sodium dihidroxyfumarate (DFH_3Na). In order to establish the degree of inhibition, we studied the kinetic of the process of HbO_2 (λ_{max} = 540 nm) consumption and MetHb (λ_{max} = 630 nm) accumulation [15]. We counted the degree of transformation (η) after HbO_2 consumption, using the relation $\eta=D_0-D_\tau/D_0-D_\infty$ and the degree of MetHb formation according to the relation $\eta=D_\tau/D_\infty$. In concordance with the kinetic curves under the S-shape we measured the speed of the reaction as a derivative of the degree of conversion in time ($d\eta/d\tau$) [16].

The interaction of the sodium dihidroxyfumarate (DFH_3Na) and polyphenols with the nitrite ion was studied according to the variation of the nitrite concentrations in system with the use of Griess reagent [17]. We studied the influence of the reducer concentration on the speed of nitrite transformation reaction. DFH_3Na concentration has been varied within the following interval: 0 - $1\cdot10^{-3}$ M (C^1_{DFHNa}= 0 M, C^2_{DFHNa}= $1\cdot10^{-4}$ M, C^3_{DFHNa}= $5\cdot10^{-4}$ M, C^4_{DFHNa}= $1\cdot10^{-3}$ M). The reaction took place in the citrat-phosphate solution buffer with pH 2,6 at t = 37°C. the other reducers have been studied in the same interval of concentrations.

During the experiments, we used various reagents: (+) catechine (Fluka, 98%, HPLC), DFH_3Na, DFH_4 (Aldrich, 98%), resveratrol (Fluka, 98%, HPLC). There had been used the erythrocytes mass, collected from healthy donors, afterwards subjected to haemolysis during 18-20 hours.

3. RESULTS OF THE EXPERIENCES

The influence of sodium dihidroxyfumarate on the HbO_2 oxidation with NO_2^-

The formation of the MetHb in HbO_2 – NO_2^- system in presence of DFH3Na at t = 20°C, pH 7.2 (phosphate solution buffer), $[HbO_2]_0 = 5\cdot10^{-5}$ mol/l depending on various concentrations of DFH_3Na is presented in Fig.2. From the data of the experiments shown in Fig.2., at the variation of $[DFH_3Na]_0$ ($C^1_{DFH_3Na}$ = 0; $C^2_{DFH_3Na}$ = $2\cdot10^{-6}$ mol/l; $C^3_{DFH_3Na}$ = $3\cdot10^{-6}$ mol/l; $C^4_{DFH_3Na}$ = $4\cdot10^{-6}$ mol/l; $C^5_{DFH_3Na}$ = $5\cdot10^{-6}$ mol/l) the maximum concentration of MetHb is reached within t=30 min for $C^1_{DFH_3Na}$ and increases till t ≈ 60 min for$C^5_{DFH_3Na}$.

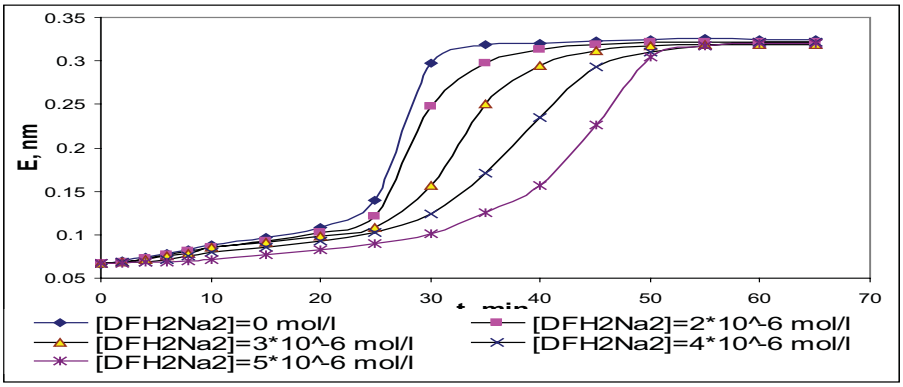

Fig. 2. The kinetic curves of MetHb formation in the HbO_2–NO_2^-–DFH_2Na_2 system, at the variation of DFH_2Na_2 concentration, phosphate solution buffer, pH = 7,2, t = 21ºC, λ = 630 nm, $[HbO_2]$ = 5*10^ -5 mol/l, $[NO_2^-]$ = 5*10^ -4 mol/l.

At the oxidation of HbO_2 with NO_2^- in presence of AAs the speed of the process after the curvature point in f($[AAs]_0$) varies in a lesser degree in comparison with the oxidation of HbO_2 with NO_2^- in presence of DFH_3Na, depending on its concentration. The influence upon the period of induction is peculiar for AAs. Contrary to this, the duration period of induction for the system with DFH_3Na is shorter, depending on its concentration, but the speed suffers a lot of changes after the curvature point of the autocatalytic process (Fig.2.)

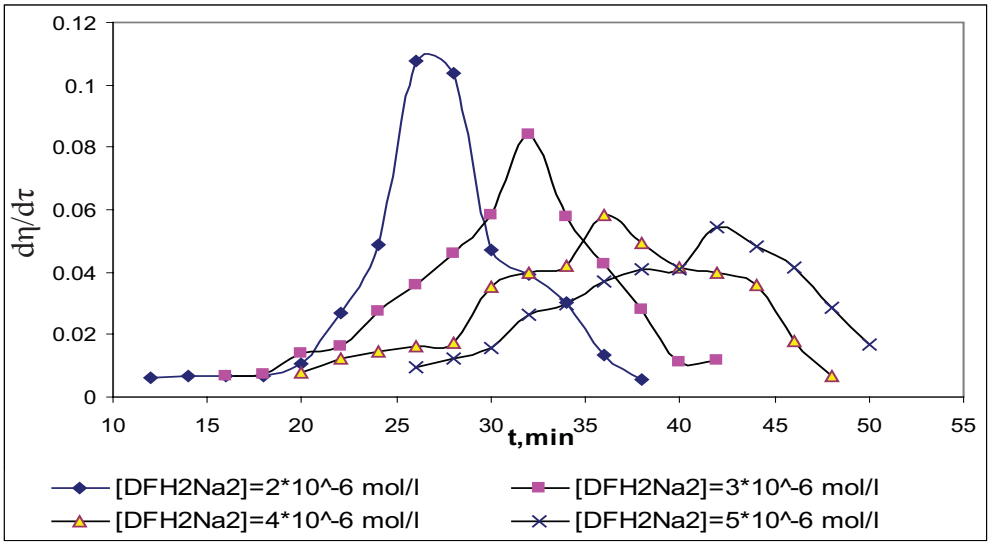

Fig.3. Speed variation (dη/dτ) depending on the time HbO_2–NO_2^- –DFH_2Na_2 system at variation of DFH_2Na_2 concentration, phosphate solution buffer, pH = 7,2, t = 21ºC, λ = 540 nm, $[NO_2^-]$ = 5*10^-4 mol/l, $[HbO_2]$ = 5*10^-5 mol/l.

Speed variation (dη/dτ) depending on time, measured on the basis of data obtained at λ=540nm and λ = 630 nm, depends on $[DFH_3Na]_0$. The maximum variation of the speed (dη/dτ) of MetHb formation in f(η) with the increase of $[DFH_3Na]_0$, reduces. We established that the position of the maximum of kinetic curve dη/dτ changes insignificantly depending on η and corresponds to the interval η = (0,5-0,7).

The change of maximum dη/dτ = f(η) towards the direction of smaller values of η for smaller concentrations of DFH_3Na, is determined by the presence in the reaction medium of $NO_2^{\bullet}$ radicals, with a higher concentration, which assures a greater contribution in the stage of process division, with the participation of this radical and with the reaching of the maximum speed. We observed that dη/dτ size depends on $[DFH_3Na]_0$ and increases when $[DFH_3Na]_0$ decreases. At $C^5_{DFH_3Na}$ we obtain dη/dτ almost twice smaller than in the case of $C^2_{DFH_3Na}$.

The angular coefficient of √η dependence on τ (factor of de auto acceleration φ = tgα) decreases when the concentration of the inhibitor increases. We can suppose that the catalyst concentration (H_2O_2), in the autocatalytic process diminishes when the DFH_3Na concentration increases, because the acceleration factor φ reduces, when DFH_3Na augments. [18, 19] Thus, we established that this inhibitor influence upon the division of the chain in HbO_2 oxidation, decreasing the speed of the auto acceleration process in the reactant medium.

The introduction in the $HbO_2 – NO_2^-$ - DFH_3Na system of H_2O_2 leads to the decrease of the inducing period from 25 min to ≈ 7 min [18]. If we compare the data of the experiment concerning the speed variation in the systems $HbO_2 – NO_2^-$ - DFH_3Na (Fig.3) and $HbO_2 – NO_2^-$ - $DFH_3Na – H_2O_2$, we will observe that the maximum variation of the speed in the system without H_2O_2 occurs at τ = 25 min, for $[DFH_3Na] = 2 \cdot 10^{-6}$ mol/l, and in presence of $[H_2O_2] = 5 \cdot 10^{-5}$ mol/l, fro the same concentration of the reducer– at τ = 7 min. The peroxide can interact with NO_2^- (3 reaction) and thus, there is formed the $NO_2^{\bullet}$ radical that keeps carrying the process.

$$H_2O_2 + NO_2^- + H^+ \rightarrow NO_2^{\bullet} + H_2O + HO^{\bullet} \quad (3)$$

Simultaneously with $NO_2^{\bullet}$ radical there forms $HO^{\bullet}$ radical that further participates in carrying of the reaction and in augmentation of the $NO_2^{\bullet}$ radical:

$$HO^{\bullet} + NO_2^- \rightarrow NO_2^{\bullet} + OH^- \quad (4)$$

In presence of the inhibitor, together with the increase of its concentration, the speed of HbO_2 oxidation reduces. The maximum variation of $d\eta/d\tau = 0{,}18$ speed for $[DFH_3Na]_0 = 2 \cdot 10^{-6}$ mol/l and it decreases up to 0,06 for $[DFH_3Na] = 5 \cdot 10^{-6}$ mol/l (Fig. 3). The speed of MetHb formation increases in presence of H_2O_2 due to the augmentation of the concentration of $NO_2^{\bullet}$ radical, that forms additionally to the interaction of H_2O_2 with NO_2^- and which is an oxidation agent of Fe^{2+} in Fe^{3+} from haem:

$$HbO_2 + NO_2^{\bullet} \rightarrow MetHb + O_2NOO^- \quad (5)$$

The action mechanism of the inhibitor is based on its interaction with $OH^{\bullet}$ radical that produces after the reaction (3) of more stable particles production [19]. The effect of inhibition will depend on the report of speed constants k_1/k_2, in which k_1 is the speed constant at the interaction of $OH^{\bullet}$- radicals with the inhibitor, while k_2 – speed constant of the reaction between $OH^{\bullet}$ and the nitrite ion (4th reaction). In the case when $k_1/k_2 > 1$, we obtain the effect of inhibition, i.e. the speed of the process that leads to Fe^{2+} oxidation in Fe^{3+} is lower than the speed generating radical oxidative particles, because these particles further interact with the inhibitor, not with the substrate. Based on the results presented in Fig.2., we consider that DFH_3Na can interact with both $OH^{\bullet}$ radical and $HO_2^{\bullet}$ radical, which form at the initial stage. Greater the concentration of the inhibitor, lower is the acceleration speed, as in this process the concentration of the peroxide has the role of catalyst and $[HO_2^{\bullet}]$ decreases. The speed of HbO_2 oxidation process decreases due to the reducing of $[NO_2^{\bullet}]$ after the reaction (4).

The effect of nitrite reduction with DFH_3Na and DFH_4

From the obtained data (Tab.1) we established that DFH_3Na the nitrate concentration decreases in the system and the speed of nitrate consumption is greater when DFH3Na concentration augments.

Table 1

The effect of nitrite reduction with DFH_3Na at pH 2,6; t = 37°C, $[NO_2^-]_0 = 1 \cdot 10^{-4}$ M

Nr.	$[DFH_3Na]_0$, 10^{-4}, M	W_{init}, 10^{-7} mol/l·s	NO_2^- reduction, % 30 min	$[NO_2^-]$, 10^{-5} mol/l 30 min
1	0,0	0,83	55,55	4,1
2	1,0	3,17	87,97	1,3
3	5,0	11,0	99,16	0,08
4	10,0	13,83	100,0	0

Based on the numeric curves, we calculated the speed constant (Fig. 4).

In Fig.4., there are presented the kinetic curves of nitrate consumption, depending on the DFH_3Na concentration. The nitrite concentration reduces during 1 min from 100 μM to 95 μM, 84 μM, 28 μM, 8 μM, corresponding for C_1, C_2, C_3, C_4 concentrations of DFH_3Na.

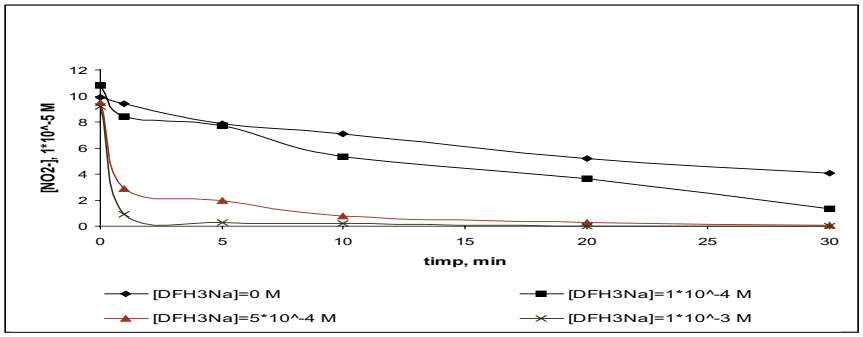

Fig. 4. The kinetic curves of nitrite consumption, depending on $[DFH_3Na]_0$, $[NO_2^-]_0 = 1 \cdot 10^{-4}$ mol/l, pH 2.6, t = 37°C.

If we increase DFH_3Na concentration from 100 μM to 1000 μM, NO_2^- concentration decreases from 95 μM to 8 μM, thus, we obtain the following: the augmentation of reducer concentration (10 times) leads to the decrease of NO_2^- concentration (almost 10 times). For DFH_3Na concentration of 100 μM the diminution of the nitrite content is slow, but when the $[DFH_3Na]$ increases the initial speed suddenly augments. The nitrite concentration reduces almost to 0 in 10 min for C^3_{DFHNa} and in 1 min for C^4_{DFHNa} (the rapport $[DFH_3Na]_0 : [NO_2^-]_0$ for C^3_{DFHNa} is 5, while for C^4_{DFHNa} it is 10). The higher the rapport, the greater the speed of the reaction. In the case when $[DFH_3Na]_0 = 0$, at pH 2,6 (citrate phosphate solution buffer), in the system there takes place the nitrite transformation into other forms (HNO_2, NO, N_2O_3, N_2O_4, NO_3^-), thus $[NO_2^-]$ reduces, which was determined by Griess method (kinetic curve for $C^1_{DFHNa} = 0$).

We also studied the kinetic of nitrite consumption in presence of dihidroxyfumarate acid (DFH_4). The experimental conditions have been the same as in the case of usage as a DFH_3Na reducer. The data concerning the nitrite consumption, obtained for different DFH_4 concentrations have been inserted in Tab.2.

Table 2

The effect of nitrite reduction with DFH4 at pH 2,6; t = 37°C, $[NO_2^-]_0 = 1 \cdot 10^{-4}$ mol/l

Nr.	$[DFH_4]_0$, 10^{-4}, M	W_{init}, 10^{-7} mol/l·s	NO_2^- reduction, % 30 min	$[NO_2^-]$, 10^{-5} mol/l 30 min
1	0,0	0,83	55,55	4,1
2	1,0	10,25	89,74	1,0
3	5,0	14,17	100,0	0
4	10,0	14,65	100,0	0

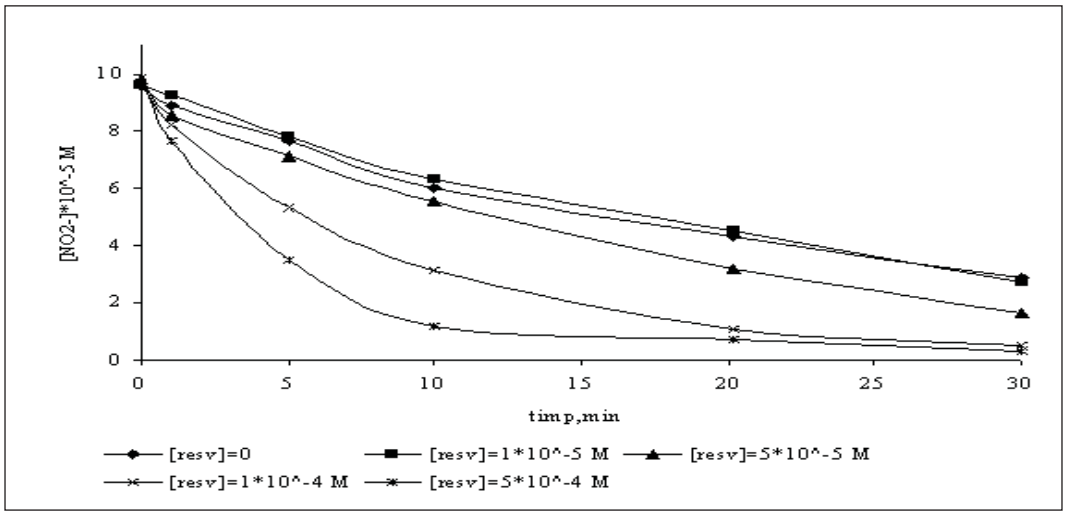

Fig.5. The kinetic curves of nitrite consumption depending on $[Resv]_0$, $[NO_2^-]_0 = 1 \cdot 10^{-4}$ mol/l, pH 2.6, t= 37°C.

In presence of DFH_4, the nitrite concentration reduces with a higher speed, in comparison with DFH_3Na. From table 2 we can observe that at $[DFH_4]_0 = 5 \cdot 10^{-4}$mol/l, the degree of NO_2^- transformation constitutes 100%.

Nitrite reduction with polyphenols

In the present study we researched the influence of rezveratrol and (+) catechine upon the process of nitrite reduction in the pattern sample.

One of the polyphenols, resveratrol (trans-3,5,4'-trihydroxystilben) (Resv), is a phytoalexine synthesized in certain plants, such as eucalyptus, spruce fir, lily. It is also tyo be found inmulberries and ground nuts, but the main natural source of Resv is *Vitis Vinifera*. It is synthesized as a response to fungi development in the grape-vine. The content of resveratrol in ground nuts varies from 0,02 to 1,79 μg/g, and the peel of fresh grapes contains almost 50-200 μg/g. A glass of red wine reaches between 600-700 μg of Resv and has a beneficent effect upon the prophylaxis of heart diseases, leukaemia and cancer.

In the present work we studied the variation of nitrite concentration depending on the Resv concentration (C^1_{Rezv} = 0 M, $C^2_{Rezv} = 5 \cdot 10^{-5}$ M, $C^3_{Rezv} = 1 \cdot 10^{-4}$ M, $C^4_{Rezv} = 5 \cdot 10^{-4}$ M, $C^5_{Rezv} = 1 \cdot 10^{-3}$ M) la pH 2,6 (citrate phosphate solution buffer

in the NO_2^-–Resv system). From the data presented in Fig.5, we observe that during 30 min the nitrite concentration reduces from 100 μM to 0 for C^3_{Rezv}, C^4_{Rezv} and C^5_{Rezv}. In the case of C^2_{Rezv} the nitrite concentration does not reduce up to 0, because the reducer concentration is lower in comparison with the nitrite concentration (50 μM and 100 μM accordingly). Thus, in the system we have a remnant concentration of nitrite after the whole Resv was consummated. In this system, the initial speed of transformation of nitrite (W_{NO2-}) is lower than in the case of DFH_3Na or DFH_4 (Fig.6.) and it is comparable with W_{NO2-} in (+)Ct presence.

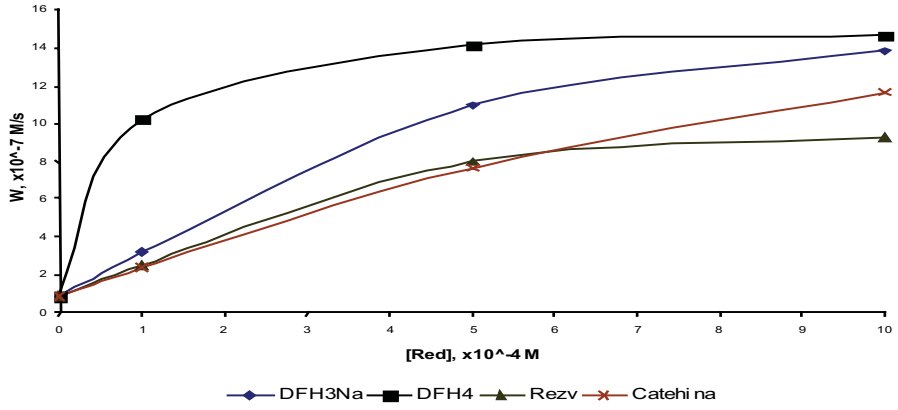

Fig.6. W_{NO2-} dependence based on $[RedH_2]_0$ at pH 2,6 (citrate-phosphate solution buffer), t = 37°C, $[NO_2^-]_0 = 1 \cdot 10^{-4}$ mol/l

PH of the reaction medium plays a great importance in the process of interaction of Resv with NO_2^-. This process was studied on different pH (1.0, 2.6, 3.0, 3.6, 4.0, 6.0) for $[NO_2^-]_0$ and $[Resv]_0$ of $1 \cdot 10^{-4}$ mol/l, in citrate phosphate solution buffer. We established that pH decrease augments the speed of reaction between Resv and nitrite.

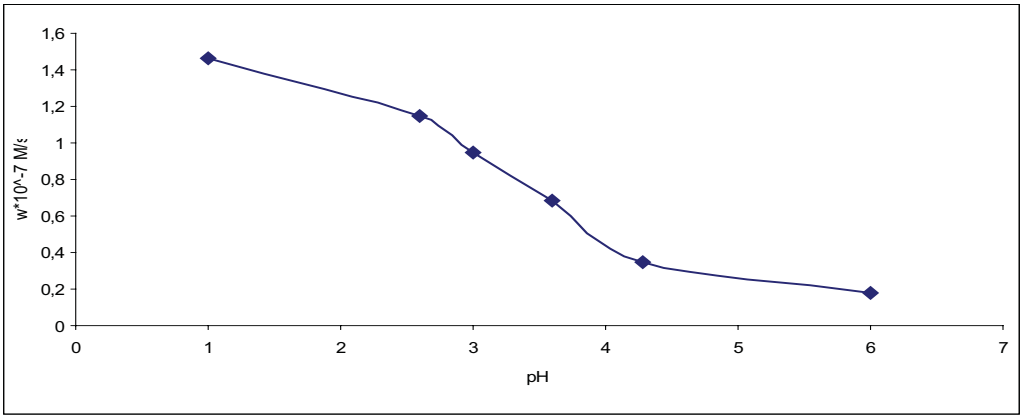

Fig.7. The initial variation speed of nitrites, depending on the pH for $[NO_2^-]_0 = 1 \cdot 10^{-4}$ mol/l, $[Rezv]_0 = 1 \cdot 10^{-4}$ mol/l and t = 37°

The nitrite concentration reduces for pH 1.0 from $1 \cdot 10^{-4}$ mol/l to ~ $0{,}77 \cdot 10^{-4}$M (in 5 min), i.e. with 53 μM, while at pH 3.0 with ~ 23 μM (the same period of time). Thus, less nitrite is used in the reaction, in the case of an increased pH. This may indicate that Resv is a less efficient inhibitor for an increased pH, because when the pH augments, a bigger quantity of nitrites remains in the system. We measured the initial variation speed of nitrites, depending on pH and we established that $W_{NO_2^-}$ decreases when pH increases (Fig.7).

Another inhibitor that was studied is (+) catechine ((+)Ct). The data obtained from the experiences on the reduction of NO_2^- with (+)Ct are presented in Tab. 3.

Table 3

The effect of nitrites reduction with (+) catechine, pH 2.6, t = 37°C, $[NO_2^-]_0 = 1 \cdot 10^{-4}$ mol/l

Nr.	$[(+)Ct]_0$, 10^{-4}, M	$W_{init,}$ 10^{-7} mol/l·s	Effect of reduction NO_2^-, % 30 min	$[NO_2^-]$, 10^{-5} mol/l 30 min
1	0,0	0,83	55,55	4,1
2	1,0	2,33	98,33	0,15
3	5,0	7,66	97,83	0,2
4	10,0	11,67	99,5	0,05

From the data presented in the table 3, we observe that the reduction speed of NO_2^- increases simultaneously with the (+)Ct concentration. For $[(+)Ct]=1 \cdot 10^{-3}$mol/l, NO_2^- concentration reduces with 99,5%. Thus, we can mark that (+)Ct reduces $[NO_2^-]$ when it interacts with NO_2^- in the reactive medium.

4. DISCUSSION

The variation of the concentration of nitrites in acid medium

In the system nitrite – citrate phosphate buffer (pH 2.6), the nitrite concentration decreases ($[RedH_2] = 0$ M). In this case, the quota of nitrites determined via Griess method, is almost 55%. The decrease of the $NO2^-$content in acid medium occurs in 2 ways: oxidation up to nitrates and the transformation into various volatile forms, agents of nitrosation. These forms are produced at the interaction of nitrite ions with the proton (H^+, H_3O^+), leading to the formation of nitrous acid. It has been demonstrated that the diminution of nitrite concentration is accelerated by pH reduction, and the effect of pH decrease leads to increase of HNO_2 concentration from the system, thus, the equilibrium emerges to the augmentation of NO, NO_2 and N_2O_4 concentrations [20]:

$$NO_2^- + H^+ \overset{k_1}{\rightleftarrows} HNO_2 \quad (6)$$

$$2HNO_2 \rightleftarrows N_2O_3 + H_2O \quad (7)$$

$$N_2O_3 \rightleftarrows NO + NO_2 \quad (8)$$

$$2NO_2 \rightleftarrows N_2O_4 \quad (9)$$

$$N_2O_4 + H_2O \rightarrow 2H^+ + NO_2^- + NO_3^- \quad (10)$$

Aerobian conditions:

$$2NO + O_2 \rightarrow N_2O_4 \quad (11)$$

Open system:

$$NO\ (aq) \rightleftarrows NO\ (g) \quad (12)$$

$$NO_2\ (aq) \rightleftarrows NO_2\ (g) \quad (13)$$

$$O_2\ (aq) \rightleftarrows O_2\ (g) \quad (14)$$

The main agents of nitrosation that form are N_2O_3, N_2O_4, and NO_2. At moderate acidity (pH 2 -5) all these agents are present in the reaction medium and are detected by [21], through spectrophotometric methods. At pH< 2 the closest agent is H_2O^+NO, which predominates in system ($HNO_2 + H^+ \leftrightarrow H_2O^+NO$). The speed for nitrite transformation depends on the initial concentration of NO_2^-, while the speed for its decreasing is determined by the equation [20]:

$$W = 1{,}1k_1a[NO] + 0{,}9k_La[NO_2^-] + k_5[N_2O_4]$$

At the introduction of SCN^- and Cl^- ions into the system, the speed of nitrite variation augments, because new formed species direct the equilibrium towards right:

$$HNO_2 + H^+ \rightleftarrows NO^+ + H_2O \quad (15)$$

$$NO^+ + SCN^- \rightleftarrows NOSCN \quad (16)$$

$$NO^+ + Cl^- \rightleftarrows NOCl \quad (17)$$

In citrate-phosphate solution buffer, the concentration of the nitrites reduces from $1\cdot10^{-4}$ mol/l to $1.5\cdot10^{-4}$ mol/l, while in presence of SCN^- and Cl^- ions, the variation of nitrite concentration reduces from $0.4\cdot10^{-4}$ mol/l to $0.3\cdot10^{-4}$ mol/l and ....accordingly.

The speed for nitrite transformation is greater in presence of SCN^- ions. The speed constant for the reaction (16) ($k_{10.2} = 3{,}4\cdot10^9$ $M^{-1}s^{-1}$) is pretty high and thus, the speed of NO_2^- concentration variation is greater than in presence of Cl^- ions with NOCl formation (reaction 17).

The influence of SCN^- ions upon the speed of NO_2^- transformation is determined by pH of the medium. The concentration of NOSCN complex decreases when pH (the interval 1.0-3.5) increases, because of the simultaneous reduction of $[NO^+]$.

The interaction of the reducers with the nitrites

The substrate interact cu nitric trioxide (III), formed from the nitrous acid obtained after the reaction (7). The reaction speed is of 2nd order after the concentration of the nitrite and of 1st order after the substrate concentration:

$$N_2O_3 + S \xrightarrow{k_8} S^+\text{-}NO + NO_2^- \quad (18)$$

$$W = k_{18}[N_2O_3][S] = k_{18}k_6[HNO_2]^2[S]$$

In the case when there are huge concentrations of substrate, the speed of the reaction can be represented via 2nd order after the nitrite and zero after the substrate:

$$W = k'[HNO_2]^2$$

In the system of reaction, DFH_4 acid and DFH_3Na interact cu the formed species (at pH of 2,6, N_2O_3 predominates) and thus, there takes place the reduction of concentration of nitrosation agents.

$$RedH_2 + H^+ + NO_2^- \rightarrow RedH^\bullet + H_2O + NO \quad (19)$$

$$RedH^\bullet + H_2O + NO + H^+ + NO_2^- \rightarrow Red + 2NO + 2H_2O \quad (20)$$

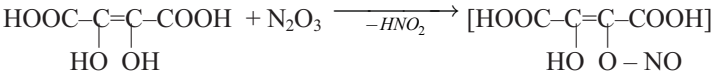

(21)

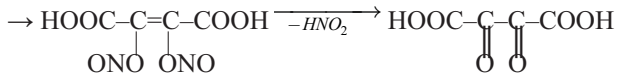

(22)

The nitrite reducers indicate that the nitrite concentration in the system reduces when their concentration increases. We used (+) catechine and resveratrol to perform the researches (Fig. 8.)

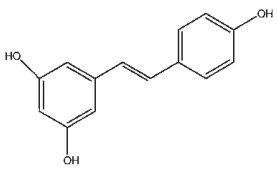

Fig. 8. The chemical structure of the resveratrol

In presence of SCN^- and Cl^- ions, the reducers interact with the nitrosyl NOSCN and NOCl species formed during the reaction (15) and (16), or with other species:

$$RedH_2+NOX \rightarrow HNO_2+Red+2NO+HX+H_2O \quad (23)$$

In the equation (23), NOX represents N_2O_3, NO^+, NOSCN, or NOCl. In presence of nitrosyl species, due to the catalytic effect, the nitrite consumption is greater, if compared with the system where there is only ClO_4^- or citrate-phosphate solution buffer.

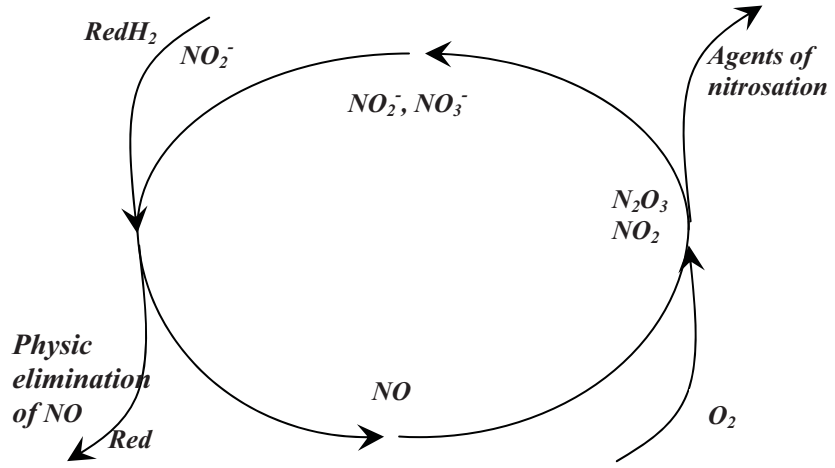

Fig. 9. Cycle of transformation of the nitrites in presence of $RedH_2$ (aerobian conditions).

This indicates that in presence of SCN^-, the reducers can become less effective inhibitors in various processes of nitrosation. The SCN^- ion is a stronger catalyst than Cl^-, this could be explained by the different equilibrium constants of the reaction (16) and (17).

As a result of the interaction of the reducers with different agents of nitrosation, the nitrite oxidation state changes, by reducing up to NO or oxidising up to NO_3^- [20]. The reduction of the nitrite concentration in the system during the reaction under the DFH_3Na or DFH_4 action is determined by the speed of transformation of NO_2^- into NO which further, in the gas phase, is removed. The nitric oxide, formed in aerobian conditions, can be recycled into agent of nitrosation or can be removed via mass transfer. The reduced speed of the mass transfer of NO reduces the inhibitory efficacy of the reducers, because in this case, due to the formation of a cycle, more $RedH_2$ inhibitor is consumed (Fig. 9).

In aerobian conditions, the reaction (11), that leads to the formation of Na_2O_4, will not take place, thus, the NO_2^- concentration, that transforms after the reactions (6) and (7) into nitrosation agents, will decrease.

As a result of the study of the process of interaction between NO_2^- and DFH_4 in aerobian and anaerobic conditions we established that the speed for NO_2^- diminution is greater, in absence of the oxygen. In this case, less DFH_4 is being consumed for the reduction of nitrite at their initial concentration and in the system; the concentration of nitrite reduces considerably.

The increase of the reaction speed simultaneously with pH reduction from 6,0 to 1,0 in Rezv-NO_2^- system is determined by the deviations of the equilibrium, depending on pH in equations (6) and (7) more towards right, thus, in the system, NO_2^-concentration decreases. But in this case, the stoichiometric rapport of the reducers consumed for the nitrite removal will increase.

From fig. 5 we can observe that at pH 1.0 the speed of NO_2^-d concentration is maximum and decreases while pH increases, in the established interval (almost 10 times) In aerobian conditions, the quantity of reducers that will be spent to remove the nitrite will be determined on one hand, by the rivalry between NO recycling and its transformation into nitrosation agent, and the removal of NO via mass transfer, on the other hand.

In conclusions, we may state that the degree of nitrite diminution in the $RedH_2$ – NO_2^- system decreases in the following manner: $DFH_4 < DFH_3Na <$ Resv < (+)Ct.

5. REFERENCES

[1] Jung F., Lassman G., Ebert B., Studiu Biophys.- 1981. - Vol.85. - V2. - p.139-140.
[2] KosakaH.,UozumM., Biochem.Biophys. Acta. – 1986. - Vol. 871. - N1., p.14-18.
[3] Tomoda A., Tsuji A., Yoneuama G. Biochem.J.- 1981. - Vol. 193. - N1. - p. 169-179.

[4] Shugaley I.V., Lopatina N.I., Umenskii I.V. Kinetics and mechanism of chain borning in the reaction of oxihemoglobin oxidation by nitrit. JOCh. – 1990. - T.60. - vol. 7. - c. 1650-1652.
[5] Navindra P. Seeram, Yanjun Zhang, and Muraleedharan G. Nair, Inhibition of Proliferation of Human Cancer Cells and Cyclooxygenase Enzymes by Anthocyanidins and Catechins, Nutrition and Cancer, 2003, 46(1), 101–106.
[6] Cecilia Matito, Foteini Mastorakou, Josep J. Centelles, Josep L. Torres, Marta Cascante, Antiproliferative effect of antioxidant polyphenols from grape in murine Hepa-1c1c7 Eur J Nutr 42 : 43–49, 2003, DOI 10.1007/s00394-003-0398-2.
[7] Brownson D.M., Arios N.G., Fugua B.K., Dnarmawardhane S.F., Mabry T.J., Flavonoid effects relevant to cancer, J.Nutr., Nov.1, 2002, 132(11): 3482S-4389.
[8] .Kyrtopoulos S.A, Pignatelli B., Kakanais G., Golematis B. and Esteve J.„Studies of gastric carcinogenesis. V. The effects of ascorbic acid on N-nitroso compound formation in human gastric juice *in vivo* and *in vitro* ", Carcinogenesis, 1991, vol.12 no.8 pp.1371 – 1376.
[9] Martırnezy C. Jimernez, Loarca-Pinaz G. and Dar vila Ortırzy G. Antimutagenic activity of phenolic compounds, oligosaccharides and quinolizidinic alkaloids from Lupinus campestris seeds, Food Additives and Contaminants, Vol. 20, No. 10 (October 2003), pp. 940–948 (Received 10 March 2003; revised 20 June 2003; accepted 14 July 2003).
[10] Rice-Evans C.A., Miller N.J., Paganga G., Structure-antioxidant activity relationships of flavonoids and phenolic acids, Free Rad. Biol & Medecine, vol.20, No.7, 1996, 933-955.
[11] Anderson R..E., Fisher L.J., Hara Y., Harris T., Mak W.B., Melton L.D., Pacher J.E., Green catechins partially protect DNA from OH· radical-induced strand breaks and base damage through fast chemical repair of DNA radicals, Carcinogenesis, vol.22, no.8, 2001, 1189-1193.
[12] Lopez-Burillo S., Tan D.-X., Mayo J.C., Sainz Rosa M., Manchester L.C. and Reiter R.J., Melatonin, xanthurenic acid, resveratrol, EGCG, vitamin C and a-lipoic acid differentially reduce oxidative DNA damage induced by Fenton reagents: a study of their individual and synergistic actions J. Pineal Res. 2003; 34:269–277.
[13] Chung S. Yang, Pins Maliakal, Xiaofeng Meng, Inhibition of carcinogenesis by TEA, Annu.Rev,Pharmacol. Toxicol., 2000, 42:25-54.
[14] Yamamotoa Y., Matsunaga K. and Friedman H., Protective effects of green tea catechins on alveolar macrophages against bacterial infections, BioFactors 21 (2004) 119–121 119.
[15] Duca Gh., Gonța M., Matveevici V., Iambarțev V. Impact des nitrites, nitrates et N-nitrosamines sur la sante et leur contenu dans les produits carnes // Actes du seminaire d'animation regionale (Region Europe Centrale et Occidentale SAR-2004). Chisinau: "Tehnica-Info". - 12-14 mai, 2004.- p. 43-48.
[16] Shugalei I.V., Lopashina N.I., Tzelinskii I.V., JOCh., 1988. Vol.58, 4 ed., p. 886-890.
[17] Mirvish S.S., Nitrate and nintrite concentration in human saliva for men and women at different ages and time of the day and their consistency over time, Eur. J. Of Cancer Prev., 2000, vol.9, p. 335-342.
[18] Gonța M. Inhibition of hemoglobin oxidation process in the presence of hydrogen peroxide, Mat. Conf. "Balance of scientific activity of USM, 2000-2002",Chişinău, 2003, p.70-71.
[19] Duca Gh., Gonța M. Impact of environment and methemoglobinemia, Mat. Conf. Scientific-practice, 2000, Chişinău: C.E.P Ştiința:2000, p.186-188.
[20] Lincht W.R., Tannenbaum S.R., Deen W.M., Use of ascorbic acid to inhibit nitrosation: kinetic and mass transfer considerations for an *in vitro* system, Carcinogenesis, Vol.9., 1988, 365-37.

INHIBITION OF *IN VITRO* NITROSATION OF NORNICOTINE

Porubin Diana

State University of Moldova, Department of Industrial and Ecological chemistry, 60, Mateevici, Chisinau, MD-2009, Republic of Moldova, tel.+37322577657, e-mail pdianamd@yahoo.com

Abstract. The inhibition of nornicotine nitrosation was studied. The concentration of nornicotine was 100 μM and nitrite 1000 μM. As inhibitors were used following compounds: ascorbic acid (as reference) (800, 1000, and 5000 μM), dihydroxyfumaric acid (1000 μM), (+)catechin (1000 μM), resveratrol (1000 μM), tartaric acid (1000 μM), quercetin (1000 μM), and grape seed extract (50, 100, 150 μg/ml). The best inhibitory effect was obtained for AAs at 5000 μM (90.7%), (+)Ct (95.5 %) and GSE at 150 μg/ml (96.1%). The small inhibitory effect was observed for TA – 22,5%.

Keywords: N-nitrosonornicotine, nitrosation, inhibition, grape seed extract, polyphenol.

1. INTRODUCTION

Smoking causes an estimated 430,000 deaths per year in the U.S., including 30% of all cancer deaths [1]. Lung cancer alone would kill over 150,000 people in the U.S. in 2000, and cigarette smoking is directly responsible for 87% of lung cancer mortality [1]. An understanding of nicotine metabolism provides a critical framework for deciphering the mechanisms by which tobacco products cause disease [2].

The reaction of nicotine with nitrous acid (derived from nitrite] results in the formation of three products, 4-(N-methylnitrosamino)-4-(3-pyridyl)-l-butanal(NNA), nitrosonornicotine (NNN), and 4-(N-methylnitrosamino)-1-(3-pyridyl)-l-butanone(NNK) [3].

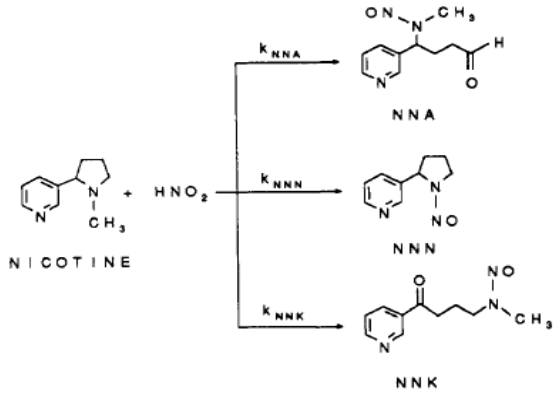

Reaction of nicotine and nitrous acid.

Humans, like rats, metabolize nicotine to nornicotine (0.4–2.7% of dose) and it is possible that nornicotine could also be concentrated in saliva [4].

Human exposure to nitrite occurs through diet, via reduction of dietary nitrate, and from endogenously produced nitric oxide [5,6].

N-Nitrosonornicotine (NNN) was the first tobacco specific nitrosamine (TSNA) for which tumorigenicity [7] and the occurrence in tobacco smoke [8] has been proven. NNK and NNN have been recently classified as “carcinogenic to humans” by the IARC [9].

Although enormous energies have been invested in treating existing cancer by chemotherapy, prevention of cancer is the preferred option. The reduction of human exposure to endogenously formed NOC, also as TSNA, as one of the ways of cancer chemoprevention, is possible through the use of inhibitors of the nitrosation process. Thus, ascorbic acid and ascorbate were shown to inhibit nitrosation by reacting with the nitrosating agents [10-13]. Polyphenolic compounds, which are present in high quantities in human foods and beverages derived from plant and fruits, are also potent blocking agents of NOC formation [14-17]. The polyphenols include a wide range of closely related compounds synthesized by plants; these include the flavonoids found in tea leaves (catechins), isoflavonoids in soybeans (genistein and daidzein), and stilbenes in red grapes (resveratrol). Each of these has been shown to have anticancer properties in cell culture models of cancer [18-20]. Because of the complexity of their action, the anticancer activity of polyphenols has yet to be clearly understood. Thus, complex polyphenols from grape seed extracts and red wine have been shown to possess in vitro antioxidant activity [21]; inhibit aromatase enzyme activity [22]; inhibit the

growth of cancer cells in cell culture [23,24]; and prevent or attenuate disease in various animal models of disease, including atherosclerosis [25], cataract formation [26], and skin cancer [27]. Some dietary polyphenols were shown to inhibit mutagenesis through inhibition of nitrosamine formation [28-32].

2. METHOD AND ANALYSIS

Chemicals. Nornicotine (NN), sodium nitrite, N-nitrosonornicotine (NNN), 5-methyl-*N*'-nitrosonornicotine (5-MeNNN), ethanol, ascorbic acid (AAs), dihidroxyfumaric acid (DFH_4), (+)catechin ((+)Ct), resveratrol (Resv), tartaric acid (TA), quercetin (Que), ammonium sulfamate were purchased from Sigma Chemical Co. (St. Louis, MO). Grape seed extract was ordered online www.wholehealtproducts.com

Equipment. The following main equipment was used for the analysis: SpeedVac centrifugal concentrator (Savant Instruments, Farmingdale, NY); HP 6890 gas chromatograph (Agilent Technologies, Wilmington, DE) interfaced to a model 543 Thermal Energy Analyzer (Orion Research, Beverly, MA); the separation was performed on a 30m x 0.25mm ID, 0.25µm film sickness, DB 1301 column (Agilent Technologies) and on a 15 m × 0.25 mm i.d. DB 5-MS column (0.25 µm film thickness) from J & W Scientific connected to a 2 m × 0.32 mm i.d. deactivated precolumn.

Method

For studying the inhibitory effect of NNN formation in watery system, the following compounds were used: ascorbic acid, dihydroxyfumaric acid, (+)catechin, resveratrol, tartaric acid, quercetin and GSE, vs control.

100 µM of NN to 1000 µM of $NaNO_2$ were used for control (without inhibitor). The same concentration of NN and $NaNO_2$ was used in the case of inhibitors, the ratio Inh: $NaNO_2$ = 1:1 for dihydroxyfumaric acid, (+)catechin, resveratrol, tartaric acid and quercetin, but for AAs the ratio was 1:0,5; 1:0,8; 1:1 and 1:5. For GSE we used the following concentration: 50, 100 and 150 µg/ml. Since inhibitors are not dissolvable in water, we considered to dissolve all reagents in ethanol (100%) The experiments have been done in the acid environment corresponding to that of gastric (pH 1-2), adding 100 µl HCl (1N) to each sample of 1 ml. The samples were kept for 1.5 hours in thermostat with shaker at temperature of 37°C.

After 1.5 hrs, the samples were kept in ice for stopping the reaction. To each samples 100 µl of ammonium sulfamate were added, for remaining nitrite destroying. After 15-20 min, 3 ml of KH_2PO_4 (pH 7) were added as buffer solution to each samples (1 ml).

Sample analysis includes several phases:

Internal standard: as internal standard used in a well-known concentration (20 ng), we used 5-MeNNN. Adding it to every sample excludes the error caused by NNN loses in the treatment process.

Sample work-up: in order to extract NNN from samples and its later purification, we used *ChemElut extraction cartridges* (packed with specially cleaned and sized diatomaceous earth), eluted 2 time with 4 ml methylene chloride ($MeCl_2$), collected in 15-ml centrifuge tubes and less in speed-vac to dryness (1.5 hrs).

Dry extract of NNN with internal standard were transferred with methanol to 200 µl plastic GC vials, and was less in speed-vac to dryness. The samples were re-dissolved adding 20 µl acetonitrile.

Analysis: after the samples have been purified, they have been analyzed. In this order, we used the GC-TEA (Gas Chromatography-ThermoEnergyAnalizer) method.

All samples have been analyzed twice, with duplicates.

3. RESULTS AND DISCUSSION

The standard curve for NNN and 5-MeNNN were analyzed. With these curves the concentration of NNN formed in system was calculate and re-calculate. (Fig.1.)

For all standard curves, high accuracy was obtained (R^2> 0,99).

Degree of nitrosation in all samples has an order of 10^{-4}- 10^{-5} % (Tab.1.).

In our study, AAs was used as reference, because ascorbic acid was shown to inhibit nitrosation over a pH range of 2–5 through a rapid reduction of nitrous acid to nitric oxide (NO) and formation of dehydroascorbic acid (Fig. 2) [23].

The experimental data showed that the degree of inhibition of NNN formation with Aas, as inhibitor, for the following concentration 800, 1000 and 5000 µM was 19.9, 31.6 and 90.7% vs control (Tab.1.). Medium recovery for these AAs concentration was 37%, for control – 94%. So, for rate Inh:Nitrite = 5:1, we have nearly complete inhibition of NNN formation.

It is possible that the same mechanism is involved in the inhibition of endogenous NNN formation by dihydroxyfumaric acid, observed in this study. DFH_4 showed a good inhibitory effect – 74.9% with 91%. Dihydroxyfumaric acid is formed by the oxidation of tartaric acid in the presence of iron (II) and hydrogen peroxide [33] and is found in grapes and secondary winery products. It was demonstrated that *N*-nitrosation of secondary amines in simulated gastric juice is effectively inhibited by dihydroxyfumaric acid [34,35], and the present study supports this finding. However, potential health effects of dihydroxyfumaric acid are unknown.

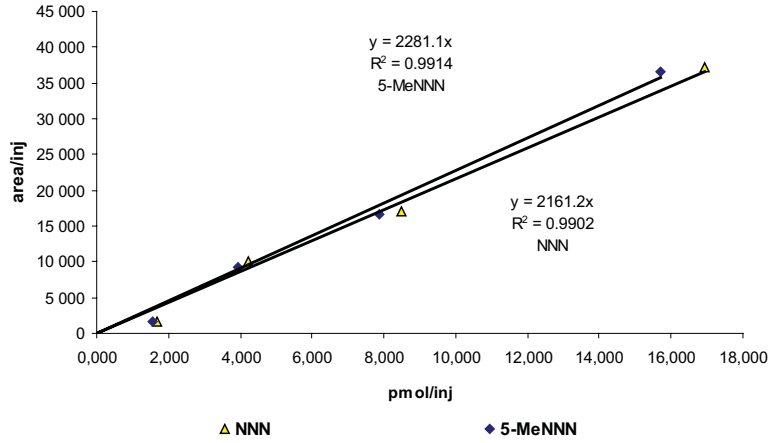

Fig. 1. Standard Curve for NNN and 5-MeNNN.

TA practically showed small inhibiting properties, only 22.5% from control (Tab.1.). The absence of double bond in the chemical structure of acid may be the cause of small inhibiting properties.

Polyphenolic antioxidants were shown to inhibit or catalyze formation of NOC, depending on their structure and reaction conditions [reviewed in 36]. In our study, we observed effective inhibition of nornicotine nitrosation in the presence of catechin, resveratrol, and quercetin with 95.5, 46.5, and 78.7% respectively (Tab.1.). Is interesting that Que is known as very good antioxidant, much better than catechin are, and it must be better inhibitor. It was found that inhibition of N-nitrosation is directly correlated with the scavenging (electron-donating) property for nitrogen-centered free radical [37]. Quercetin has an identical number of hydroxyl groups in the same position as catechin, but contains the 2,3-double bond in the C ring and 4-oxo function. This structure advantage confers an enhancement of the TEAC (total antioxidant activity in trolox equivalent) value to 7.7 mM compared to the saturated heterocyclic ring of catechin with approximately half the antioxidant activity (2,4 mM) [38]. We suppose that incomplete dissolution may be the blocking factor for better inhibitory effect. The effect of polyphenolic compounds on *N*-nitroso compound formation depends on pH, the nature of nitrosated amine, and the relative concentrations of nitrite and phenolics [36].

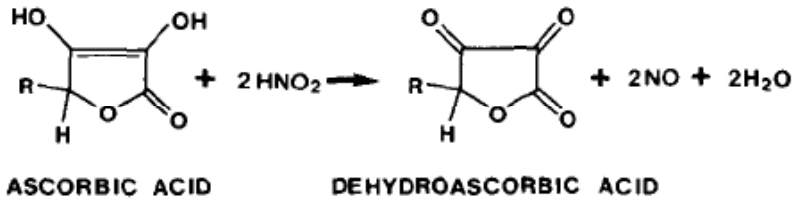

Fig. 2. Reduction of nitrous acid by ascorbic acid to NO and production of dehydroascorbic acid (ref. 23).

GSE showed a very good inhibitory effect in the nitrosation of nornicotine. We obtained 66.0, 93.2, and 96.1% of inhibition of NNN vs. control for the concentration of GSE 50, 100, and 150 mg/ml (Tab.1.). GSE used is naturally extracted, so there are no chemical or solvent residues. GSE contain a full 90% Oligomeric Proanthocyanidins, additionally, there is 56% of Grape Seed extract, 27% of Grape Skin Extract and 17% of Red Wine Extract. Oligomeric Proanthocyanidins, in fact anti-oxidants in general, are structured in such a way that they are able to donate electrons freely without altering their valence (their electrons are not paired) - what this means is that anti-oxidants can stabilize free radicals without themselves becoming dangerous [39]. They are a class of phenolic compounds, which take the form of oligomers or polymers of polyhydroxy flavan-3-ol units, such as (+)-catechin and (-)-epicatechin [40). Recently, epidemiological data have shown that red wine may reduce the mortality rate from coronary heart disease, the so-called ‘‘French paradox’’ [41.42]. Proanthocyanidins are the major polyphenols in red wine as well as in grape seeds, and they have potent antioxidant activity [43.44], inhibit low density lipoprotein oxidation [46], as well as a variety of biological activities [46-50].

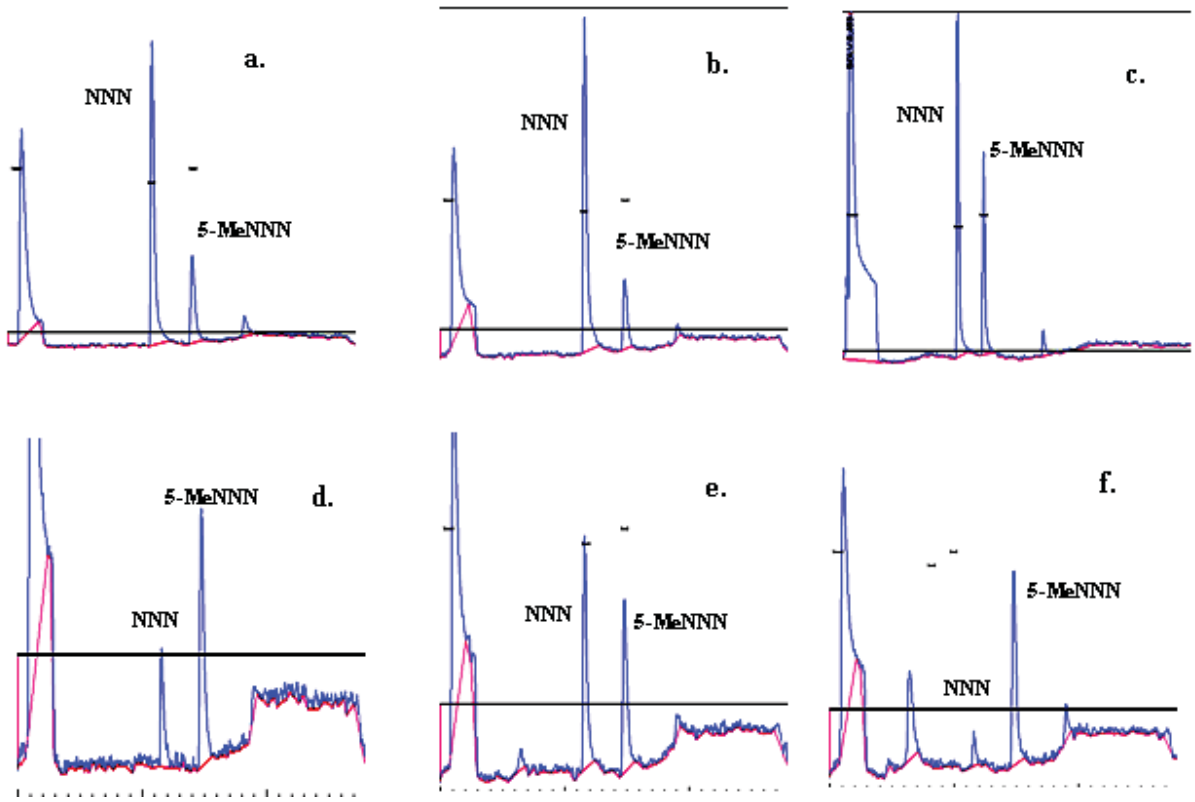

Fig. 3. GC-TEA traces of NNN and 5-MeNNN in the tested samples: (a) control $NN+NO_2^-$ (without inhibitor), (b-d) $NN+NO_2^-$ with 1000 µM AAs, DFH_4 and (+)Ct respectively; (e,f) $NN+NO_2^-$ with 50 and 150 GSE µg/ml respectively

In Fig.3. some GC-traces for sample are shown: control (without addition of inhibitor), with AAs, DFH_4, (+)Ct (each of 1000 µM) and GSE (50 and 150 µg/ml). Comparing the peaks area for NNN and 5-MeNNN in each trace with control, we can see an evident inhibitory effect of utilized compounds.

Table 1

Inhibitory effect of *in vitro* nitrosation of NN by different compounds

Sample	NNN of initial NN,%	NNN, pmol	Inhibition of NNN, %
Control	$3{,}12\cdot10^{-4}$	311,8	0,0
Aas, 800µM	$2{,}50\cdot10^{-4}$	249,7	19,9
Aas, 1000µM	$2{,}13\cdot10^{-4}$	213,3	31,6
Aas, 5000µM	$2{,}89\cdot10^{-5}$	28,9	90,7
TA, 1000µM	$2{,}42\cdot10^{-4}$	241,6	22,5
Rezv, 1000µM	$1{,}67\cdot10^{-4}$	166,8	46,5
DFH, 1000µM	$7{,}83\cdot10^{-5}$	78,3	74,9
Que, 1000µM	$6{,}64\cdot10^{-5}$	66,4	78,7
(+)Ct, 1000µM	$1{,}41\cdot10^{-5}$	14,1	95,5
GSE, 50µg/ml	$1{,}06\cdot10^{-4}$	106,1	66,0
GSE, 100µg/ml	$2{,}11\cdot10^{-5}$	21,1	93,2
GSE, 150µg/ml	$1{,}22\cdot10^{-5}$	12,2	96,1

4. CONCLUSION

The best inhibitory effect was obtained for AAs at the molar ratio AAs: NO_2^- = 5:1 (90.7%). From polyphenols (1:1 molar ration with nitrite), (+)Ct was the best result (95.5 %), DFH_4 and Que were the comparable inhibitory effect (74.9 and 78.7 % respectively). GSE at 100 and 150 µg/ml has shown a very good inhibition (93,2 and 96.1% respectively). The small inhibitory effect was observed for TA – 22,5%.

ACKNOWLEDGMENT

I thank Dr. S.S.Hecht and I.Stepanov at the University of Minnesota Cancer Center for help in the experiments and analysis. This study was supported by grant MTFP-1021A from the U.S. Civilian Research and Development Foundation to Diana Porubin.

5. REFERENCES

[1] American Cancer Society; Atlanta, G, 2000; pp.28–31.
[2] Hecht, S. S.;. Hochalter, J.B.; Villalta, P.W.; Murphy, Sh.E. PNAS, 2000, vol. 97, no. 23, p. 12493–12497.
[3] Caldwell, W. S.; Greene, J. M.; Plowchalk, D.R.; deBethizy, J. D., Chem. Res. Toxicol. 1991,4, 513-516.
[4] Benowitz,N.L.; Jacob, P.; Fong, I.; Gupta,S. J. Pharmacol. Exp. Ther., 268, (1994), 296–303.
[5] Assembly of Life Sciences. National Academy Press, Washington, DC, 1988, Ch. 8.
[6] Marletta,M.A. Chem. Res. Toxicol., 1, 1988, 249–257.
[7] Boyland, E.; Roe, F.J.C.; Gorrod, J.W. Nature 202, 1964, 1126.
[8] Hoffmann, D.; Hecht, S.S.; Ornaf, R.M.; Wynder, E.L. Science 1974, 186, p. 265–267.
[9] IARC (International Agency for Research on Cancer), Lyon, Press Release, 2004, No. 154.
[10] Shibata, A; Paganini-Hill, A; Ross, R.K; Henderson, B.E. Br. J. Cancer 1992, 66: p. 673-679.
[11] Mirvish, S.S. Am.J.Clin.Nutr., 1993, 57: 598-599.
[12] Mirvish, S.S. Cancer Res. (Suppl.), 1994, 54: 1948s-1951s.
[13] Dyke, G.W.; Craven, J.L; Hall, R.; Garner, R.C. Cancer Lett., 1994, 86: 159-165.
[14] Wu, Y.N; Wang, H.Z; Li, J.S; Han, C. Biomed. Environ. Sci., 1993, 6: 237-258.
[15] Helser, M.A; Hotchkiss, J.H; Roe, D.A. Carcinogenesis, 1992, 13: 2277-2280.
[16] Xu, G.P; Song, P.J; Reed, P.I. Eur. J. Cancer Prevent., 1993, 2: 327-335.
[17] Kurech, T; Kikugawa, K; Fukuda, S. J. Agric. Food Chem., 1980, 28: 1265-1269.
[18] Park, O.J.; Surh, Y.J. Toxicol. Lett., 2004, 150: 43-56.
[19] Barnes, S,; Peterson, T.G. Proc. Soc. Exp. Biol. Med., 1995, 208: 103-108.
[20] Mgbonyebi, O.P; Russo, J; Russo, I.H. Int. J. Oncol., 1998, 12: 865-869.
[21] Yamaguchi, F; Yoshimura, Y; Nakazawa, H; Ariga, T J. Agric. Food Chem., 1999, 47: 2544-2548.
[22] Eng, E.T ; Ye, J ; Williams, D ; et al Cancer Res., 2003, 63: 8516-8522.
[23] Agarwal, C; Sharma, Y; Zhao, J; Agarwal, R. Clin. Cancer Res., 2000, 6: 2921-2930.
[24] Sharma, G; Tyagi, A.K; Singh, R.P; et al. Breast Cancer Res. Treat., 2004, 85: 1-12.
[25] Zhao, J; Wang, J; Chen, Y; Agarwal, R. Carcinogenesis, 1999, 20: 1737-1745.
[26] Yamakoshi, J; Saito, M; Kataoka, S; Tokutake, S. J. Agric. Food Chem., 2002, 50: 4983-4988.
[27] Bomser J.A; Singletary K.W; Wallig M.A; Smith M.A.L. Clin. Cancer Res., 1999, 135: 151-157.
[28] Bartsch, H; Ohshima, H; Pignatelli, B. Mutat. Res., 1988, 202: 307-324.
[29] Pignatelli, B; Scriban, R; Descotes, G; Bartsch, H. Carcinogenesis, 1983, 4: 491-494.
[30] Pignatelli,B; Scriban, R; Descotes, G; Bartsch, H. Amer. Soc. Brewing Chem. J., 1984, 42: 18-23.
[31] Stich, H.F; Chan, P.K.L; Rosin M.P. Intern. J. Cancer, 1982, 30: 719-724.
[32] Stich, H.F; Dunn, B.P; Pignatelli, B; Ohshima, H; Bartsch, H. IARC Publ. 1984, No. 57, 213-222 .
[33] Wardman, P; Candeias L.P. Radiat Res, 1996;145:523-31.
[34] Gonta, M; Stepanov, I; Duca, Gh; et al. Intern. Conf. on Ecolog. Chem., Moldova, 2002:196-206.
[35] Duca, Gh; Gonța, M; Mahu, E; et al. Intern.Conf. Ecolog.Chem., Moldova, 2005:292-3.
[36] Bartsch, H; Ohshima, H; Pignatelli, B. Mutat. Res., 1988, 202: 307-324.
[37] Kono, Ya; Shibata, H.; Kodama Ya.; Sawa, Yo. Biochem.J., 1995, 312, 947-953.
[38] Rice-Evans, C.A; Miller, N.J.; Paganga, G. Free Rad Biol Med, 1996; 20: 933–56.
[39] www.wholehealthproducts.com (OPC Grape Seed Extract).
[40] Porter, L.J.; In: Harborne J.B. (Ed.). Chapman and Hall, London, 1986, 23–55.
[41] StLeger, A.S.; Moore, F.; Cochrane, A.L. Lancet, 1979, 1017–1020.
[42] Renaud, S.; De Lorgeril, M. Lancet, 1992, 339, 1523–1526.
[43] Ariga, T.; Hamano, M. Agricul. and Biol. Chem., 1990, 10, 2499–2504.
[44] Ricardo da Silva, J.M.; Darman, N.; Fernandez, Y.; Mitjavila, S. J. Agricul.and Food Chem., 1991, 39, 1549–1552.
[45] Teissedre, P.L.; Frankel, E.N.; Waterhouse, A.L.; Peleg, H.; German, J.G. J.Scien.Food Agricul., 1996, 70, 55–6.
[46] Arii, M; Miki, R; Hosoyama, H; Ariga, et al. Proceedings, Am.Assoc. for Cancer Res. 1998, 39,20.
[47] Dauer, A.; Metzner, P.; Schimmer, O.; Planta Medica, 1998, 64, 324–327.
[48] Saito, M.; Hosoyama, H.; Ariga, T.; Kataoka, S.; Yamaji, N. J.of Agricul. Food Chem., 1998, 46, 1460–1464.
[49] Yamakoshi, J.; Kataoka, S.; Koga, T.; Ariga, T. Atherosclerosis, 1999, 142, 139–149.
[50] Zhao, J.; Wang, J.; Chen, Y.; Agarwal, R. Carcinogenesis, 1999, 20, 1737–1745.

SPECTROSCOPIC PROPERTIES OF THE Ln-Ge COMPLEXES WITH DIETHYLENETRIAMINEPENTAACETIC ACID§

Sergiy Smola[a], Natalya Rusakova[a], Elena Martsinko[b], Inna Seifullina[b], Yuriy Korovin[a*]

[a]*A.V. Bogatsky Physico-Chemical Institute, National Academy of Sciences of Ukraine, 65080 Odessa, Ukraine*
[b]*I.I. Mechnikov Odessa National University, 65026 Odessa, Ukraine*
**Corresponding author: E-mail: lantachem@te.net.ua; fax +38 0482 652 012; tel: +38 0482 652 038*

Abstract: Four new heteronuclear lanthanide complexes with general formula [Ge(OH)(μ-HDTPA)LnGe(OH)(μ-DTPA)] (Ln = Sm – Dy) were synthesized and subsequently characterized by different physico-chemical methods. The structures of new compounds have been proposed. In considered complexes the 4f-luminescence of three-charged ions of samarium, europium, terbium and dysprosium is realized at UV-excitation. It is noteworthy that it is the first observation of 4f-luminescence in water solutions of heteronuclear *f-p*-complexes. The comparison of luminescent characteristics of hetero- and homonuclear landthanide complexes is described and discussed as well.

Keywords: Heteronuclear complexes; Lanthanides; Germanium; DTPA; Luminescence.

INTRODUCTION

The increasing number of the heteronuclear complexes involves the great interest in coordination chemistry. These species cause interest because of their properties which allow to consider them as perspective objects of researches both fundamental and applied orientation. Polyaminopolycarboxylic acids are the one of the most suitable organic ligands by means of which it is possible to receive heteronuclear species. In particular, the donor properties of diethylenetriaminepentaacetic acid (DTPA) allow to obtain the complexes internal coordination sphere of which includes simultaneously two different metals and more. However, the heteronuclear lanthanide complexes are studied much less in comparison with mononuclear ones, whereas lanthanide complexes with DTPA and its derivatives have attracted attention as potential contrast agents [1, 2]. The overwhelming number of works is devoted to *f-d*- and *f-s*-complexes. At the same time the data of *f-p*-complexes are singular [3, 4]. Therefore we reported the preliminary results to gain data on the spectroscopic properties of the lanthanide-germanium complexes with DTPA.

RESULTS AND DISCUSSIONS

Heterometallic complexes of samarium, europium, terbium and dysprosium with germanium have been synthesized by interaction of the complex acid $[Ge(OH)(H_2DTPA)]\cdot H_2O$ and the respective lanthanide acetates in aqueous solutions. The structure of these compounds was determined from the elemental, thermogravimetric, X-ray diffraction analysis, IR-spectroscopy.

On the basis of the results of elemental analysis it has been assumed that the ratio lanthanide : germanium : DTPA in obtained product equals 1 : 2 : 2. The XRD patterns were characterized by the interplanar distance personal set which differed from mononuclear germanium complex ones. No impurity phases were detected in them. Thus, on the basis of practically identical set of interplanar distances the conclusion that they were isostructural was made. According to thermogravimetric analysis dehydration starts at 60°C and ends at 210°C. The wide interval of this process up to high temperature is explained probably special expedient of water molecules packing due to the formation intra- and intermolecular hydrogen bonds that was mentioned for lanthanide complexes. Heteronuclear lanthanide complexes contain three water molecules in outer coordination sphere. Pyrolysis proceeds in one single sharp weight loss at 210-260°C (decarboxylation), while the formation of the inorganic residue is completed at 520-540°C.

The mode of ligand coordination in lanthanide-germanium complexes was determined from the IR spectroscopy data in comparison with IR spectrum of mononuclear germanium complex. The IR spectra of the heteronuclear complexes were characterized with the following bands: in vibration region νCH one (2990 cm^{-1}), that proves coordination of all three nitrogen atoms of H_5DTPA by metal ions; δGeOH (880 cm^{-1}), νGe-N (640 cm^{-1}), νC=O (1715 cm^{-1}) coordinated group COOH, ν_{as}C-O (1595 cm^{-1}), ν_sC-O (1400 cm^{-1}) groups COO-, bounded with f-metal; ν_{as}C-O (shoulder is about 1700 cm^{-1}) and ν_sC-O (1330 cm^{-1}) carboxylate ions bounded with germanium; wide band νOH with maximum about 3400 cm^{-1}. Thus, it can be concluded that saturation of germanium coordination number up to 6 occured at the expense of valence linkages with hydroxo- and three carboxylic groups, and also coordinate linkages to two nitrogen atoms of ligand. It was established that all DTPA donor centers are interlinked with metals in complexes. It corresponds to absence of inner sphere water molecules in these heteronuclear complexes.

§ Material presented at the XV-th Conference "Physical Methods in Coordination and Supramolecular Chemistry", September 27 - October 1, 2006, Chişinău, Moldova

All data analysis obtained with the help of different physico-chemical methods allow assuming that *p-f*-complexes are three nuclear ones. Coordinated polyhedron of germanium is the same as in complex acid $[Ge(OH)(H_2DTPA)]\cdot H_2O$. On the basis of obtained data and taking into account the coordination figures, oxidation degrees characterized typically for investigated metals (as well as isostructural of synthesized complexes), their structure schemes can be proposed as it is given in Fig.1. Coordination polyhedron of lanthanide is the "distorted octahedron" forming for account of tridentate coordination of two complex anions $[Ge(OH)DTPA]^{2-}$ and $[Ge(OH)HDTPA]^{-}$ with the closing of four glycine metal cycles.

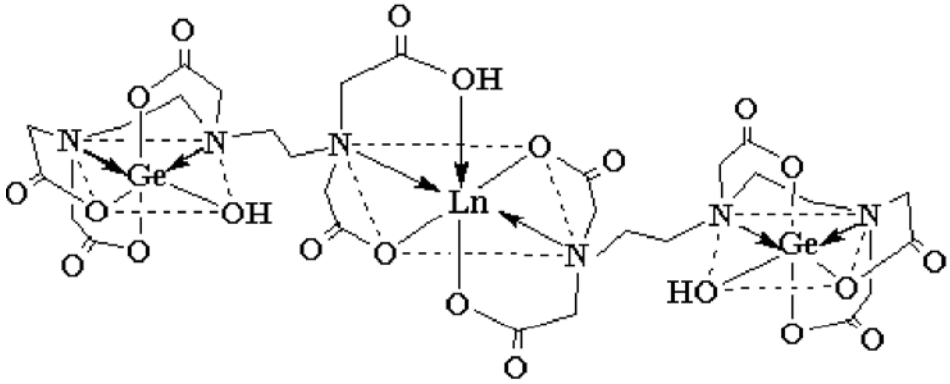

Fig 1. Structure of the lanthanide-germanium complexes (Ln = Sm - Dy).

The UV-Vis absorption spectra of heteronuclear terbium- and europium-germanium complexes have been shown in Fig. 2. Absorption spectrum of $Tb(Ge\text{-}DTPA)_2$ (Fig. 2a) were shifted hypsochromically as compared to Ge-DTPA spectrum and consisted of three bands (as well as for mononuclear complexes): intensive one at 195 nm and two less intensive bands within the range 255 – 260 nm and 350 nm. Samarium- and dysprosium-germanium complexes show the similar features. In contrast to previous, a new band in $Eu(Ge\text{-}DTPA)_2$ absorption spectrum appeared at 427 nm (Fig. 2b), that was not typically for Ge-DTPA. Other three bands noted in the ligand absorption spectrum shifted batochromically.

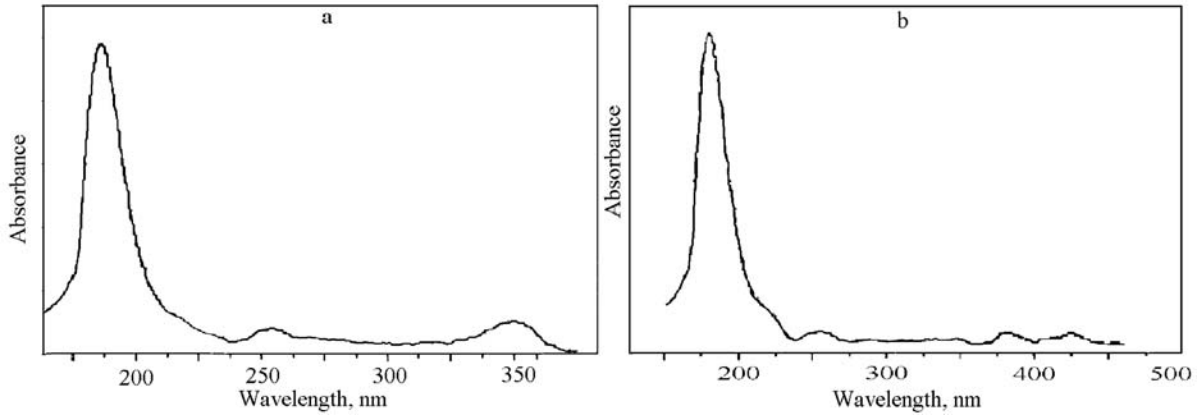

Fig 2. UV absorption spectra of $Tb(Ge\text{-}DTPA)_2$ (a) and $Eu(Ge\text{-}DTPA)_2$ (b) in H_2O.

The luminescent excitation spectra (Fig.3) of lanthanide complexes were measured at 298 K. The luminescence excitation spectrum of $Tb(Ge\text{-}DTPA)_2$ complex under the emission of 545 nm is shown in Fig 3a. In narrow-wavelength region there was one excitation peak with maximum at 235 nm. In long-wavelength region two strong excitation peaks were observed at 358 and 379 nm, which practically coincides with spectra of excitation of mononuclear complexes. Selected excitation under these wavelengths, the emission spectra show the similar luminescent position except for different luminescent intensities. The analogous picture is observed in excitation luminescence spectra of samarium and dysprosium heteronuclear complexes. Luminescence excitation spectrum of $Eu(Ge\text{-}DTPA)_2$ under the red emission of 617 nm is illustrated in Fig 3b. Unlike a mononuclear complex of europium which is characterized by two peaks with maxima at 310 nm and 400 nm, the excitation spectrum of $Eu(Ge\text{-}DTPA)_2$ consisted of three peaks in long-wavelength region at 310, 400 and 431 nm, situated separately.

The luminescent emission spectra of heteronuclear lanthanide complexes at room temperature are presented in Fig. 4 and 5. The increase of luminescence intensity for heteronuclear complexes in comparison with mononuclear complexes was observed (Tab. 1). Noteworthy, that the luminescence intensity of heteronuclear samarium, terbium or

dysprosium complexes at various lengths of excitation waves was higher (up to 1.8, 2.1 and 2.5 times, respectively), than in the mono-complexes. At the same time, the luminescence of heteronuclear europium complex was higher (up to 1.7 times) as compared to Eu-DTPA complex only in the excitation region of 310-330 nm.

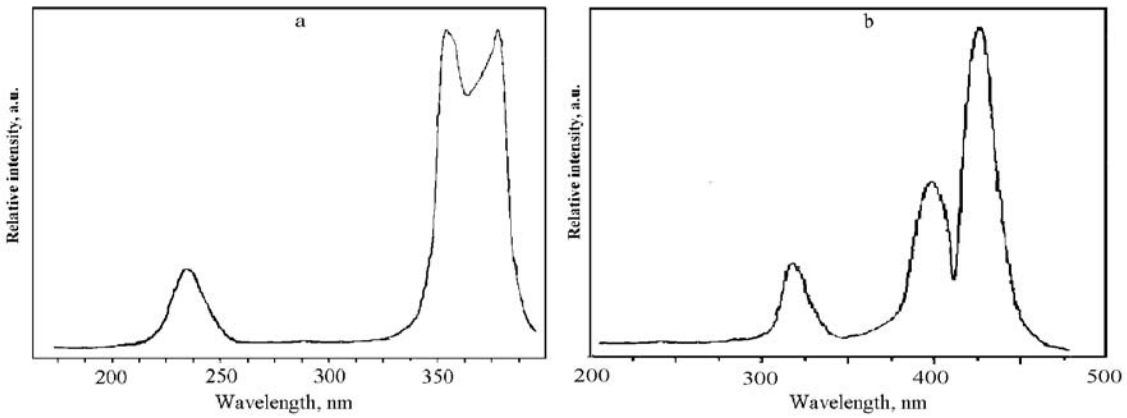

Fig. 3. Luminescence excitation spectra of $Tb(Ge\text{-}DTPA)_2$ (a) (λ_{em} = 545 nm) and $Eu(Ge\text{-}DTPA)_2$ (b) (λ_{em} = 612 nm) in H_2O.

The luminescence spectra of the terbium-germanium complex (Fig. 4a) registered under long (358 nm) wavelength show the similar emission of Tb^{3+} ion. Four main peaks were characterized emission originated from the $^5D_4 \rightarrow {}^7F_j$ (j = 6, 5, 4, 3) transition of Tb^{3+} ion. The strongest peak (λ_{max} = 547 nm; $^5D_4 \rightarrow {}^7F_5$ - transition) is corresponded to non-hypersensitive transition. Luminescence quantum yield increases in 2.1 times as compared to homonuclear complex (Tab. 1) Luminescence lifetime decreases – 570 μsec for $Tb(Ge\text{-}DTPA)_2$ and 750 μsec for Tb-DTPA complex.

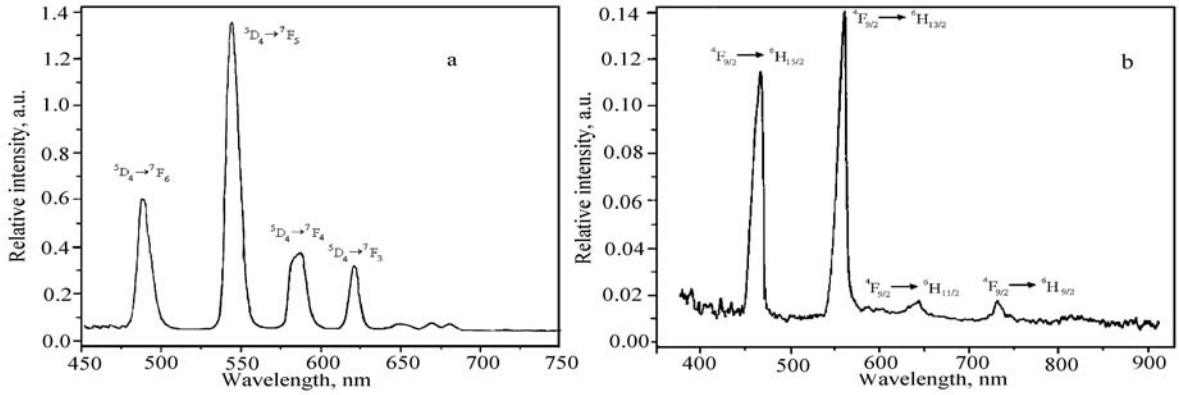

Fig. 4. Emission spectra of $Tb(Ge\text{-}DTPA)_2$ (a) (λ_{exc} = 358 nm) and $Dy(Ge\text{-}DTPA)_2$ (b) (λ_{exc} = 338) complexes (H_2O, 295 K).

The luminescence spectrum of $Dy(Ge\text{-}DTPA)_2$ (Fig 4b) show four apparent emission peaks ($^4F_{9/2} \rightarrow {}^6H_J$; J =15/2, 13/2, 11/2, 9/2) under the excitation 338 nm. The highest emission was the $^4F_{9/2} \rightarrow {}^6H_{13/2}$ hypersensitive transition. As it is shown in Tab. 1, terbium- and dysprosium-germanium complexes are characterized by the more strong emission than other heteronuclear lanthanide complexes for the more suitable energy match and more effective ligand-to-lanthanide ion energy transfer than Eu^{3+} and Sm^{3+}, which is confirmed by values of quantum yields and luminescence lifetimes for these complexes. So, the characteristic transition of terbium ion is not such sensitive as europium ion to the nearby environment. The increasing of luminescence quantum yield of heteronuclear complex up to 2.5 times in comparison with homonuclear dysprosium complex was observed (Tab. 1).

The low luminescence emission spectrum of samarium heteronuclear complex was measured (Fig. 5a), which under excitation wavelength 360 nm exhibits four predominantly characteristic emission corresponded to the $^4G_{5/2} \rightarrow {}^6H_J$ (J = 5/2, 7/2, 9/2, 11/2) transitions of Sm^{3+} ion. The 601 nm peak (non-hypersensitive transition $^4G_{5/2} \rightarrow {}^6H_{7/2}$) is the strongest. As it is shown in Tab. 1, almost twofold increasing of quantum yield in comparison with homonuclear dysprosium complex was observed.

The luminescence spectrum of europium complex under the excitation of 310 nm shows three emission peaks,

which correspond to the characteristic emission $^5D_0 \rightarrow {}^7F_J$ (J=1, 2, 4) transitions of Eu^{3+} ion, respectively. The 612 nm peak corresponding to hypersensitive transition ($^5D_0 \rightarrow {}^7F_2$) is the strongest and the band intensity ratio equals 1:2:1. Marginal changes of quantum yields were observed (Tab. 1), while luminescence lifetime increases in heneronuclear complex: 390 μsec for Eu-DTPA and 450 μsec for $Eu(Ge\text{-}DTPA)_2$.

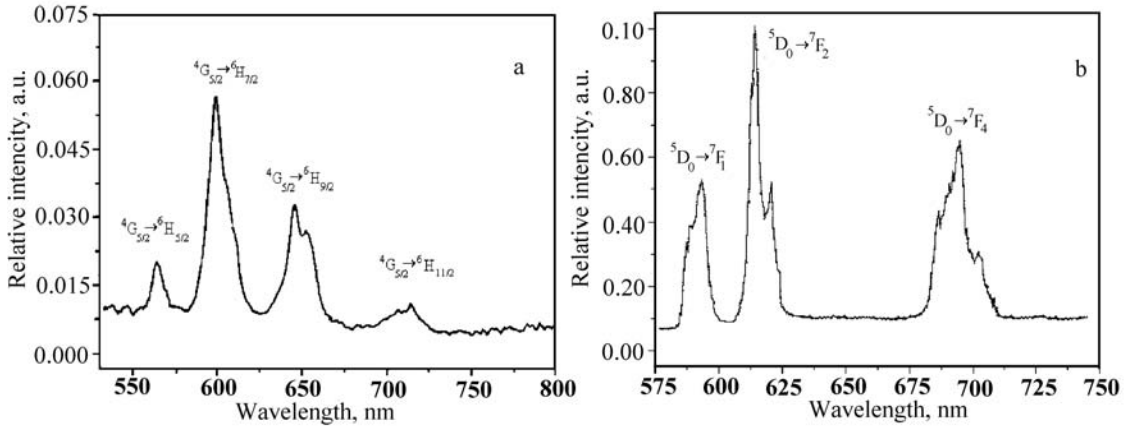

Fig. 5. Emission spectra of $Sm(Ge\text{-}DTPA)_2$ (a) (λ_{exc} = 360 nm) and $Eu(Ge\text{-}DTPA)_2$ (b) (λ_{exc} = 310 nm) complexes (H_2O, 295 K).

Table 1

Luminescent properties of $Ln(Ge\text{-}DTPA)_2$ complexes

Complex	Luminescence quantum yield φ[a]	φ_h/φ_m [b]	Lifetimes τ, μsec
$Sm\ (Ge\text{-}DTPA)_2$	0.0086	1.8	73
$Eu\ (Ge\text{-}DTPA)_2$	0.015	1.7	450
$Tb\ (Ge\text{-}DTPA)_2$	0.517	2.1	570
$Dy\ (Ge\text{-}DTPA)_2$	0.026	2.5	220

[a] Errors are ± 10 %.

[b] φ_h and φ_m - Luminescence quantum yield of heteronuclear and mononuclear complexes, respectively.

EXPERIMENTAL

General. Elemental analysis (C, H, N) was carried out by an Perkin-Elmer CHN-240 analyzer. All X-ray diffraction (XRD) measurements were made with DRON-2.0 powder diffractometer (CuK_α radiation). The thermogravimetric analysis was performed on a Paulik-Paulik-Erday Q-1500D derivatograph, under air atmospere, over the temperature range 20 – 500ºC at 5ºC/min speed of tests heating. The IR spectra were measured on a IR-75 spectrometer (KBr pellets). The UV-Vis absorption spectra were recorded with an Perkin-Elmer Lambda 9 spectrophotometer. The solvent (water) was used as a reference.

Synthesis

$Ln(CH_3COO)_3$ (Ln = Sm - Dy) and DTPA were purchased from Aldrich (Gillingham, Dorset) and used as received. Distilled and deionized water (18 MΩ cm^{-1}) was used throughout. The preparation of Ln complexes with DTPA was described previously [5]. The ligand $[Ge(OH)(H_2DTPA)]\cdot H_2O$ was synthesized according to [6].

$[Ge(OH)(\mu\text{-}HDTPA)SmGe(OH)(\mu\text{-}DTPA)]\cdot 3H_2O$. $Sm(CH_3COO)_3$ (0.33 g, 0.001 mol) and $[Ge(OH)(H_2DTPA)]\cdot H_2O$ (0.96 g, 0.002 mol) were dissolved in 40 ml of water. The solution was heated (~ 50ºC) with permanent stiring for 30 min. In two days the white precipitate was formed. The reaction product was separated on the filter, washed out by ethanol and ether and dried above anhydrous $CaCl_2$ up to a constant mass. Yield ~ 45%. Anal. Found, %: C, 30.29; H, 4.10; N, 7.64; Ge, 13.70; Sm, 13.59; Calcd. for $C_{28}H_{39}N_6O_{22}Ge_2Sm$, % C, 30.36; H, 3.52; N, 7.54; Ge, 13.03; Sm, 13.50.

$[Ge(OH)(\mu\text{-}HDTPA)EuGe(OH)(\mu\text{-}DTPA)]\cdot 3H_2O$ was synthesized following the similar procedure by the interaction of $Eu(CH_3COO)_3$ (0.33 g, 0.001 mol) and $[Ge(OH)(H_2DTPA)]\cdot H_2O$ (0.96 g, 0.002 mol). Yield ~ 48%. Anal. Found, %: C, 30.37; H, 4.02; N, 7.93; Ge, 13.37; Eu, 13.70; Calcd for $C_{28}H_{39}N_6O_{22}Ge_2Eu$, % C, 30.32; H, 3.52; N, 7.53; Ge, 13.02; Eu, 13.63.

$[Ge(OH)(\mu\text{-}HDTPA)TbGe(OH)(\mu\text{-}DTPA)\cdot 3H_2O$ was synthesized following the similar procedure using $Tb(CH_3COO)_3$ as a lanthanide salt (0.001 mol). Yield ~ 46%. Anal. Found, %: C, 30.59; H, 3.96; N, 7.80; Ge, 12.65; Tb, 14.65; Calcd for $C_{28}H_{39}N_6O_{22}Ge_2Tb$, % C, 30.13; H, 3.50; N, 7.49; Ge, 12.94; Tb, 14.17.

[Ge(OH)(μ-HDTPA)DyGe(OH)(μ-DTPA)]·3H_2O was synthesized following the similar procedure using $Dy(CH_3COO)_3$ as a lanthanide salt (0.001 mol). Yield ~ 36%. Anal. Found, %: C, 30.02; H, 3.92; N, 7.79; Ge, 12.28; Dy, 14.90; Calcd for $C_{28}H_{39}N_6O_{22}Ge_2Dy$, % C, 29.85; H, 3.46; N, 7.46; Ge, 12.90; Dy, 14.44.

The synthesized heteronuclear complexes of the composition [Ge(OH)(μ-HDTPA)LnGe(OH)(μ-DTPA)] are stable in air, soluble in water and insoluble in majority of the widespread used organic solvents.

Luminescence measurements. Excitation and luminescence spectra were recorded using an SDL-2 spectrometer designed for the study of excitation spectra and luminescence radiation over the range 200-800 nm for liquid and solid samples. The excitation source was a xenon lamp Xe-150. The spectrometer was also equipped with monochromators MDR-12 and MDR-23. The radiation of the sample was recorded at an angle of 90ºC to the exciting radiation. The luminescence lifetime (τ)data were obtained by means of a SDL-1 spectrofluorimeter (LOMO Association, St. Petersburg, Russia) with a LGI-21 nitrogen laser, with pulse duration of 8-10 ns at a wavelength of 337 nm and analyzed by iterative reconvolution and non-linear least-squares method [7]. The luminescence quantum yields (φ) were obtained by the method described by Haas and Stein [8] with the standards $[Ru(bipy)_3]^{2-}$ (φ = 0.028 in aerated water) for the Sm^{3+} and Eu^{3+} complexes and quinine sulphate (φ = 0.546 in H_2SO_4 1 N) for the Tb^{3+} and Dy^{3+} complexes. The measured values were corrected for the refractive indices. The triplet level position was obtained from phosphorescence spectra of gadolinium-germanium complex with DTPA at 77 K.

CONCLUSIONS

The interaction of [Ge(OH)(H_2DTPA)]·H_2O ligand with lanthanide salts leads to the formation of the new heteronuclear compounds with general formula [Ge(OH)(μ-HDTPA)LnGe(OH)(μ-DTPA)] (Ln = Sm – Dy). According to structure proposed lanthanide ions coordinate two complex anions $[Ge(OH)DTPA]^{2-}$ and $[Ge(OH)HDTPA]^{-}$ with the closing of four glycine metal cycles. The coordination polyhedron of lanthanide is the "distorted octahedron" while the germanium coordinated polyhedron was not changed. The spectroscopic properties of these complexes have been studied. The energy match between the ligand and lanthanide ions has been examined to predict that the energy transfer process exists between the ligand and Ln^{3+}. Terbium complex has the most efficient energy transfer. The increasing of luminescence intensity, quantum yields as compared to homonuclear lanthanide complexes with DTPA was observed. Since germanium is not the sensitizer of 4f-luminescence then it plays a role of original organizer for the structure of heteronuclear complexes.

REFERENCES

[1] Bianchi A., Calabi L., Corana F., Fontana S., Losi P., Maiocchi A., Paleari L., Valtancoli B. *Coord. Chem. Rev.* **2000**, 204, 309-393.
[2] Langereis S., Kooistra H.-A. T., van Genderen M. H. P., Meijer E. W. *Org. Biomol. Chem.* **2004**, 2, 1271-1274.
[3] Wullens H., Bodart N., Devillers M. *J. Solid State Chem.* **2002**, 167, 494-507.
[4] Stavila V., Gulea A., Popa N., Shova S., Merbach A., Simonov Yu., Lipkowski J. *Inorg. Chem. Commun.* **2004**, **7**, 634-637.
[5] Moeller T., Thompson L. C. *J. Inorg. Nucl. Chem.* **1962**, 24, 499 – 510.
[6] Seifullina I., Martsinko E., Iliukhin A., Sergienko V. *Russian J. Inorg. Chem*. **1998**, 43, 1509 - 1513.
[7] O'Connor D. V., Ware W.R., Andre J.C. *J. Phys. Chem.* **1979**, 83, 1333-1343.
[8] Haas Y., Stein G. *J. Phys. Chem.* **1971**, 75, 3668-3681.

STRUCTURE AND REDOX TRANSFORMATIONS OF IRON(III) COMPLEXES WITH SOME BIOLOGICALLY IMPORTANT INDOLE-3-ALKANOIC ACIDS IN AQUEOUS SOLUTIONS[§]

Krisztina Kovács [1], Alexander A. Kamnev [2]*, Alexei G. Shchelochkov [2], Ernő Kuzmann [1], János Mink [3], Tünde Megyes [3], Attila Vértes [1]

[1]*Research Group for Nuclear Techniques in Structural Chemistry, Hungarian Academy of Sciences; Laboratory of Nuclear Chemistry, Eötvös Loránd University, H-1518, Budapest 112, Hungary*
[2]*Laboratory of Biochemistry of Plant-Bacterial Symbioses, Institute of Biochemistry and Physiology of Plants and Microorganisms, Russian Academy of Sciences, 410049, Saratov, Russia*
[3]*Chemical Research Center of the Hungarian Academy of Sciences, H-1525, Budapest, P.O. Box 77, Hungary*
** Corresponding author. E-mail: aakamnev@ibppm.sgu.ru; Fax: +7-8452-970383*

Abstract: Interactions of a series of indole-3-alkanoic acids (with *n*-alkanoic acid side-chains from C_1 to C_4) with iron(III) in acidic aqueous solutions have been shown to comprise two parallel processes including complexation and redox transformations giving iron(II) hexaaquo complexes. The structure and composition of the reaction products are discussed, as analysed using a combination of instrumental techniques including ^{57}Fe Mössbauer, vibrational and ^{1}H NMR spectroscopies.

Keywords: indole-3-alkanoic acids, auxin phytohormones, iron(III) complexes, coordination structure, redox transformations

Introduction

Indole-3-acetic acid (IAA) and its close structural analogues, indole-3-carboxylic (ICA), indole-3-propionic (IPA) and indole-3-butyric (IBA) acids, are natural and synthetic phytohormones of the auxin series that regulate plant growth and development [1–3]. IAA (along with some other indolic auxins), being ubiquitous in plants, is also well documented to be synthesized by many soil microorganisms which exude it into soil [4], where it plays an essential role in plant-microbe interactions [5, 6]. Thus, within the soil and/or aquifer environment, auxin molecules can readily be subjected to chemical reactions involving different metal ions including iron [7], which is commonly ubiquitous in soil [8] and is one of the most important micronutrients for virtually all organisms [9]. In the biomedical field, prooxidant activity and cytotoxic effects of IAA and its derivatives upon peroxidase-catalysed oxidation have also been tested for potential novel applications in antitumour therapy [10, 11].

Earlier studies have shown [12–16] that both IAA and some other chemically and metabolically related organic substances of biological origin are capable of gradually reducing iron(III) in weakly acidic nitrate-containing aqueous media even under aerobic conditions. This could be of ecological significance since iron(III) has a poor biological availability, which is due to its full hydrolysis and extremely low solubility of ferric hydroxides in a wide pH range, whereas iron(II) species are more soluble and, therefore, more biologically available both for plants and for soil microorganisms. Note also that acidic soils are rather widely spread, comprising about 30% of only arable territories [17]. On the other hand, these processes can result in oxidative degradation of the organic biomolecules involved in plant-microbe interactions in soil [7]. Therefore, knowledge of the chemical processes is of interest both for basic research and in applied fields, particularly those related to agricultural and environmental biotechnology.

In the present work, chemical reactions are considered which occur between indole-3-alkanoic acids (with *n*-alkanoic acid side chains from C_1 to C_4) and iron(III) in acidic aqueous solutions under aerobic conditions, and their products are analysed using a combination of physicochemical instrumental techniques.

Results and Discussion

In order to follow *in-situ* redox processes involving iron species in aqueous solutions, ^{57}Fe Mössbauer spectroscopy is a very convenient and informative technique giving, in particular, direct quantitative information on the Fe(II)-to-Fe(III) ratio. As Mössbauer spectra can be obtained for solid matrices only (or, for non-solids, in a solidified state, e.g. rapidly frozen), aqueous solutions can be studied in the frozen state [18]. Note also that rapid freezing (e.g., by inserting small portions of a solution into liquid nitrogen) allows one to obtain a glassy solid that reflects the structure of the initial solution. Moreover, in such a frozen solution all processes are

[§] Material presented at the XV-th Conference "Physical Methods in Coordination and Supramolecular Chemistry", September 27 - October 1, 2006, Chişinău, Moldova

virtually ceased, so that by rapidly freezing a successive series of solution aliquots with their subsequent low-temperature Mössbauer spectroscopic measurements, one can obtain "snapshots" of the state of processes that have been "stopped" at certain successive time points [19]. Mössbauer spectra of iron(III)-containing aqueous solutions with different indole-3-alkanoic acids, filtered and rapidly frozen 15 min and 2 days after mixing, are shown in Figure 1, *a–h*. It can be seen that in the solutions which initially contained iron(III) only, already 15 min after mixing some certain amounts of iron(II) are present, which is distinctly evidenced by the appearance of a corresponding component doublet with a large quadrupole splitting (its position is indicated in Figure 1 by a square bracket above the upper spectrum) having varying intensity for different acids (cf. Figure 1, spectra *a* to *d*). The presence of the same iron(II)-related doublet with higher intensities is detected in the spectra of the mixtures obtained after 2 days (cf. Figure 1, spectra *e* to *h*). The Mössbauer parameters of the resulting Fe^{2+} species (i.e., isomer shifts $\delta = 1.39 \pm 0.01$ mm/s and quadrupole splittings $\Delta = 3.35 \pm 0.03$ mm/s) are typical of a hexaaquo coordination microenvironment [18].

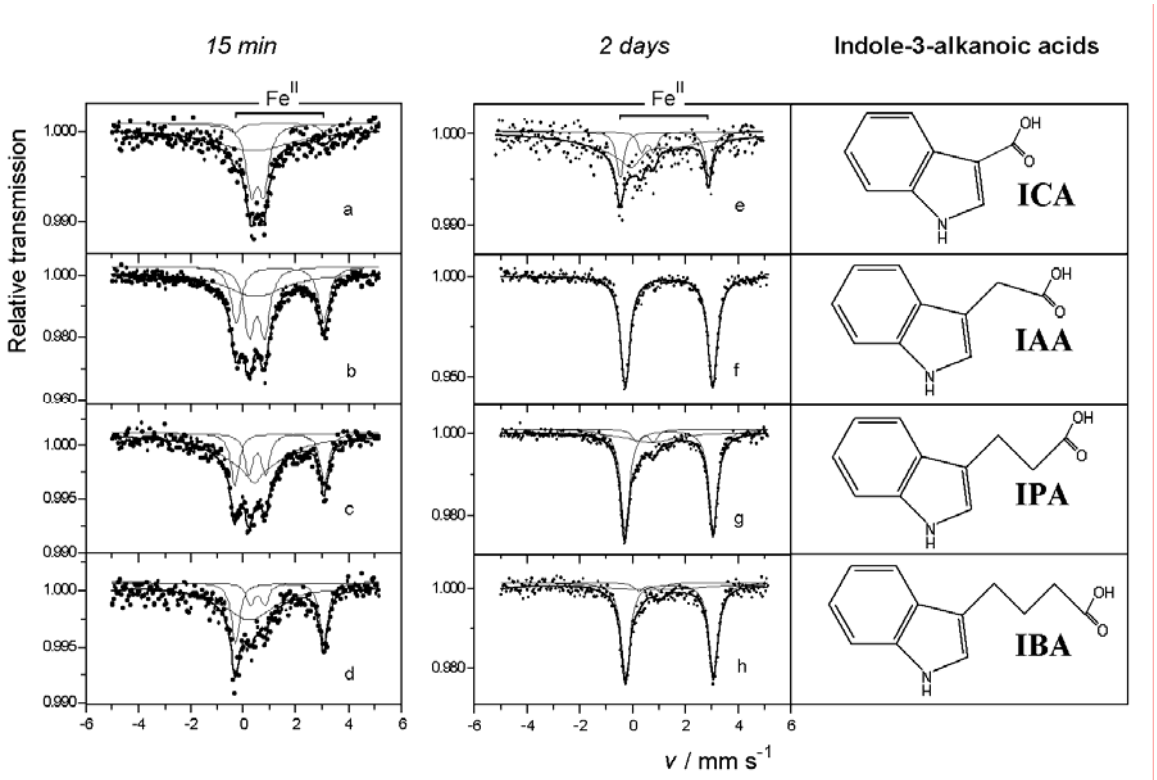

Figure 1. Mössbauer spectra of aqueous solutions of $^{57}Fe^{III}$ nitrate and indole-3-alkanoic acids (their structures are shown in the right-hand panel) filtered and rapidly frozen (at $T = 80$ K) 15 min (a–d) and 2 days (e–h) after mixing the reagents (1:3 molar ratio; final pH ~ 2 to 3). Spectra (a), (e) – indole-3-carboxylic acid (ICA); (b), (f) – indole-3-acetic acid (IAA); (c), (g) – indole-3-propionic acid (IPA); (d), (h) – indole-3-butyric acid (IBA). The position of the Fe^{II}-related doublets is indicated in the upper plots by square brackets.

Comparing the spectral intensities (cf. Figure 1, *e–h*) it can be seen that after 2 days of contact of the indolic acids with iron(III), in IAA solution there is ferrous iron only, as compared to the Fe–ICA, Fe–IPA or Fe–IBA systems where some remaining ferric iron is still detectable. This indicates a stronger reducing capability of IAA towards iron(III) in the series of indole-3-alkanoic acids, evidently related to the ease of the IAA side-chain decarboxylation [20–23]. Note also that both the relative and absolute intensities of the Fe^{II} component in ICA solutions (see Figure 1, spectra *a* and *e*) are less than those for the other acids, showing the least reducing capacity of ICA in the series. The other two components of the spectra (see Figure 1, spectra *a–h*, except spectrum *f*) represent iron(III) complexes with the corresponding ligands (doublets with $\delta = 0.52$ to 0.55 mm/s and $\Delta = 0.5$ to 0.6 mm/s), that remain in solution after filtering out the precipitated complexes, and residual mononuclear Fe^{3+} ions (evidently partly hydrolysed at weakly acidic pH, which give a very broad single line).

The iron(III) doublets (with $\delta = 0.52$ to 0.55 mm/s and $\Delta = 0.5$ to 0.6 mm/s) exhibit the parameters typical for high-spin Fe^{3+} in distorted octahedral coordination. The Mössbauer spectra of the corresponding solid complexes filtered out of the aqueous solutions (for IAA, IPA and IBA) all gave an intensive symmetric quadrupole doublet with similar parameters ($\delta = 0.52 \pm 0.01$ mm/s, $\Delta = 0.60 \pm 0.05$ mm/s at $T = 80$ K), and Mössbauer spectra of those complexes redissolved in acetone showed the same pattern in the frozen acetone solutions [24] reflecting the possibility of their molecular dissolution. In the frozen acetone solutions (at

concentrations of each of the complexes 0.1 M and 0.01 M, using ^{57}Fe-enriched samples in the latter case to enhance the intensity of the spectra), the lack of a magnetic structure (due to fast spin-spin relaxation) provides evidence that the iron(III) species have a dimeric structure [16, 18]. This result is in good agreement with the data of elemental analyses, FTIR and FT-Raman spectroscopic results (including those for deuterated samples) for the solid complexes filtered out of the solutions, indicating a μ-$(OH)_2$-bridged structure: $[L_2Fe<(OH)_2>FeL_2]$ (where L is the deprotonated IAA, IPA or IBA moiety) [24]. It has to be noted that in the case of ICA, the data of elemental analyses pointed to the possibility of the presence of a mixture of solid products which should be studied in more detail separately.

In the case of Fe^{III}–IAA complex dissolved in methanol, a solution X-ray diffraction study was also performed [24]. Analysis of the data for Fe^{III}–IAA complex as well as, by analogy (considering the closely related Mössbauer, FTIR and FT-Raman spectroscopic results), for the corresponding IPA and IBA complexes, can be interpreted using the general structure represented in Figure 2. Each iron atom in a complex is surrounded by six oxygen atoms in a slightly distorted octahedral symmetry as follows: four from two deprotonated IAA carboxylate ligands (in the bidentate coordination) and two from the dihydroxo bridge linking the two iron atoms. Nevertheless, it should be noted that under different conditions, a monomeric poorly water-soluble Fe(III)–IAA complex was obtained from aqueous solution which gave different spectroscopic images owing to its different structure [15].

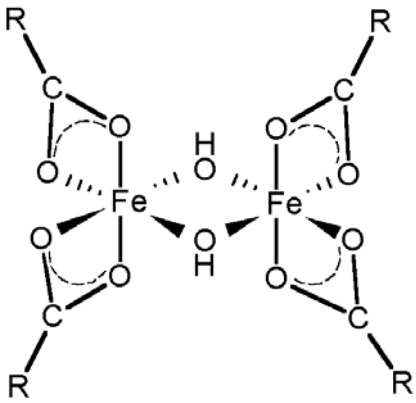

Figure 2. Schematic representation of solid Fe(III) complexes with IAA, IPA and IBA.

Thus the parameters of the spectra in Figure 1 suggest the existence of two parallel reactions between Fe^{3+} and the ligands (L); namely, both a redox transformation yielding Fe_{aq}^{2+} ions and Fe^{3+}–L complex formation take place, as shown in the following scheme.

$$Fe^{3+} + L \rightarrow \begin{cases} Fe^{III} \text{ complex (precipitate and/or dissolved form)} \\ Fe_{aq}^{2+} + \text{[oxidised L product(s)]} \end{cases}$$

While enzymatic oxidation of auxin phytohormone catalysed by plant peroxidases, regarding its mechanism and products, has been under intensive investigation owing to basic interest [21–23] as well as possible biomedical applications (see, e.g. [10, 11] and references therein), chemical oxidation products of auxins are much less studied [25]. Owing to the sophisticated nature of these chemical process involving radical products and/or intermediates [26], this seems to be not an easy and straightforward task.

Some products of aerial oxidation of indole-3-acetic acid in the presence of Fe^{III} were isolated and studied using FTIR spectroscopy, ^{1}H NMR and chromatography-mass spectrometry. The formation of oxindole-3-acetic acid was shown, which formed a poorly soluble complex with Fe^{III} similar to that with indole-3-acetic acid [15] by the coordiantion mode; in particular, giving a similar FTIR spectrum [27]. From the reaction medium, using extraction with isobutanol and further chromatographic separation, two other oxidation products were isolated. One of the products gave an intensive FTIR absorption band of carbonyl (1649 cm^{-1}), a couple of bands at 2925 and 2856 cm^{-1} (aliphatic C–H stretching vibrations) and a band at 3403 cm^{-1} (N–H or O–H stretching vibrations). Its ^{1}H NMR spectrum in deuterated acetone showed a group of signals of the oxindole moiety (7.2–8.4 p.p.m.), a singlet of the >N–H proton (10.01 p.p.m.), a quadruplet (3.2–3.7 p.p.m.) of the proton in the position C3 of the oxindole moiety split at neighbouring protons of the $–CH_3$ group. Finally, the latter three magnetically equivalent protons gave a doublet (split at the vicinal C3 proton) at 1.2 p.p.m. Altogether these data provide evidence for the formation of 3-methyl-2-oxindole as an oxidation product (Figure 3). Traces of the

other extracted product gave a mass spectrum which suggests that the oxidation product was formed by further oxidative splitting of the pyrrolin-2-one cycle [7].

It should be noted that both oxindole-3-acetate and 3-methyl-2-oxindole, which were found to be formed in the course of chemical oxidation of indole-3-acetic acid in the presence of Fe^{III} (see Figure 3), had earlier been reported among products of both its enzymatic [28, 29] and electrochemical oxidation [25] at physiological pH (along with 3-methylene-2-oxindole), i.e. under different conditions and involving different electron transfer modes. Nevertheless, the exact mechanism of chemical oxidation of IAA, in particular, under environmentally relevant conditions has to be elucidated in more detail, which requires further investigations.

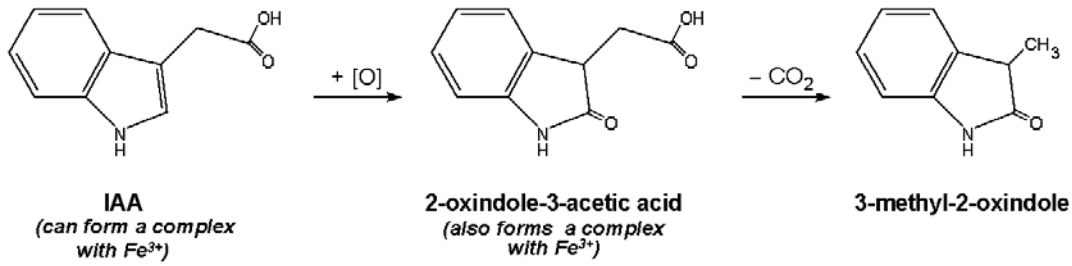

Figure 3. Scheme and some products of chemical oxidation of indole-3-acetic acid in aqueous solution under aerobic conditions in the presence of iron(III).

Conclusions

Iron(III) ions were shown to be gradually reduced by each of the indole-3-alkanoic acids with *n*-alkanoic side-chains C_1 to C_4 in acidic aqueous media under aerobic conditions using Mössbauer spectroscopic measurements in rapidly frozen solutions. The parameters of the Mössbauer spectra indicate that there are two parallel processes, *viz* iron(III) complexation and redox transformations. Within the series of the indole-3-alkanoic acids, indole-3-carboxylic acid showed the least reducing capability towards iron(III). After 2 days, indole-3-acetic acid showed virtually a complete reduction of iron(III) to iron(II), whereas iron(III) was still detectable in solutions of the other acids, along with iron(II). Mössbauer parameters of the frozen solutions provide evidence that the resulting iron(II) species is the hexaaquo complex. The solid complexes formed were found to have a dimeric μ-dihydroxo-bridged structure, that was confirmed using a combination of spectroscopic techniques for indole-3-acetic, indole-3-propionic and indole-3-butyric acids. Among the products of chemical oxidation of indole-3-acetic acid in the presence of iron(III) under aerobic conditions, oxindole-3-acetate and 3-methyl-2-oxindole were detected using vibrational and ^{1}H NMR spectroscopic measurements. The same substances had earlier been reported to be found among the products of enzymatic and electrochemical oxidation in circumneutral media, i.e. under different conditions and involving different electron transfer modes.

Experimental

Mössbauer measurements in aqueous solutions were performed using materials prepared from ^{57}Fe-enriched iron (ca. 90% ^{57}Fe) dissolved in nitric acid at elevated temperature. The stock solution was 0.01 M with regard to iron(III), with pH 0.9. The indole derivatives used (ICA, IAA, IPA, IBA) were dissolved in water adding KOH to the solutions up to pH 6–7. The concentration of the ligands after mixing was 0.03 M. Addition of iron(III) nitrate to an indolic acid in solution (up to the 1:3 metal-to-acid molar ratio) resulted in the colour change of the solutions and the formation of cocoa-brown precipitates indicating complexation of Fe^{3+} with the indole-3-alkanoic acids. The final pH values of the mixtures were around 2.5 (measured using an OP-211 laboratory pX/mV meter, Radelkis, Hungary).

The solutions were filtered after 15 min or 2 days, rapidly frozen in liquid nitrogen, and Mössbauer spectra of the rapidly frozen filtrates were recorded. For analysing the precipitates filtered out after 15 min, the resulting solids were dried on the filter paper at room temperature for a few days and placed in a cryostat cooled with liquid nitrogen. All Mössbauer spectra were recorded at liquid nitrogen temperature (ca. 80 K) using a conventional constant-acceleration Mössbauer spectrometer with a ^{57}Co(Rh) source using a "cold-finger" cryostat filled with liquid nitrogen. The spectrometer was calibrated using α-Fe foil at room temperature, which is the reference for all isomer shifts reported in this paper. Statistical treatment of the Mössbauer spectra was performed with the assumption of Lorentzian line shapes in order to calculate isomer shifts (δ, mm/s), quadrupole splittings (Δ, mm/s), line widths (full width at half maximum, Γ, mm/s) and partial resonant absorption areas (S_r, %) for all spectral components. ^{1}H NMR spectra were obtained on a Bruker AC-300 spectrometer (300 MHz), with $Si(CH_3)_4$ as an internal standard, in deuterated acetone solutions. All other measurements and experimental details were as described elsewhere [7, 16, 24, 27].

Acknowledgements

The material of this paper was presented as part of the invited lecture at the XV International Conference "Physical Methods in Coordination and Supramolecular Chemistry" (Chişinău, Moldova, 27 September – 1 October, 2006). A.A.K. is grateful to the organisers of the Conference and personally to Dr. Marina Fonari and Professor Constantin Turta for their helpful attention and hospitality; partial support for the visit from the Russian Foundation for Basic Research (by RFBR travel grant 06-03-42956) is also acknowledged. This work was supported by The Hungarian Science Foundation (OTKA Grant T043687), NATO (Expert Visit Grants LST.EV.980141 and CBP.NR.NREV.981748; Collaborative Linkage Grant LST.CLG.977664), Russian Academy of Sciences' Commission (Grant No. 205 under the 6th Competition-Expertise of research projects), as well as under the Agreements on Scientific Cooperation between the Russian and Hungarian Academies of Sciences for 2002–2004 and 2005–2007.

References

[1] Marumo, S. Auxins. In Takahashi, N. (Ed.), *Chemistry of Plant Hormones*, CRC Press, Inc.: Boca Raton, Flo. (U.S.A.), 1986; Chapter 2, pp. 9-56.
[2] Weyers, J.D.B.; Paterson, N.W.; New Phytol. 2001, 152, 375-407.
[3] Teale, W.D.; Paponov, I.A.; Palme K.; Nat. Rev. Mol. Cell Biol. 2006, 7, 847-859.
[4] Patten, C.L.; Glick, BR.; Can. J. Microbiol. 1996, 42, 207-220.
[5] Lambrecht, M.; Okon, Y.; Vande Broek, A.; Vanderleyden, J.; Trends Microbiol. 2000, 8, 298-300.
[6] Somers, E.; Vanderleyden, J.; Srinivasan, M.; Crit. Rev. Microbiol. 2004, 30, 205-240.
[7] Kamnev, A.A.; Kovács, K.; Shchelochkov, A.G.; Kulikov, L.A.; Perfiliev, Yu.D.; Kuzmann, E.; Vértes, A.; In *Metal Ions in Biology and Medicine*, Vol. 9; Alpoim, M.C.; Morais, P.V.; Santos, M.A.; Cristóvão, A.J.; Centeno, J.A.; Collery, Ph. (Eds.), John Libbey Eurotext: Paris, 2006; pp. 220-225.
[8] Cornell, R.M.; Schwertmann, U. The Fe Oxides: Structure, Properties, Reactions, Occurrences, and Uses, VCH: New York, 1996.
[9] Sigel, A.; Sigel, H., Eds. *Metal Ions in Biological Systems*, Vol. 35. *Iron Transport and Storage in Microorganisms, Plants, and Animals.* New York: Marcel Dekker, 1998, 824 pp.
[10] Tafazoli, S.; O'Brien, P.J.; Chem. Res. Toxicol. 2004, 17, 1350-1355.
[11] Veitch, N.C.; Phytochemistry, 2004, 65, 249-259.
[12] Kamnev, A.A.; Kuzmann, E. In *Spectroscopy of Biological Molecules: Modern Trends. Annex;* Carmona, P.; Navarro, R.; Hernanz, A., Eds. UNED Press: Madrid, 1997, pp. 85-86.
[13] Kamnev, A.A.; Kuzmann, E.; Biochem. Mol. Biol. Int. 1997, 41, 575-581.
[14] Kamnev, A.A.; Kuzmann, E.; Perfiliev, Yu.D.; Vankó, Gy.; Vértes, A.; J. Mol. Struct. 1999, 482-483, 703-711.
[15] Kamnev, A.A.; Shchelochkov, A.G.; Perfiliev, Yu.D.; Tarantilis, P.A.; Polissiou, M.G.; J. Mol. Struct. 2001, 563-564, 565-572.
[16] Kovács, K.; Kamnev, A.A.; Kuzmann, E.; Homonnay, Z.; Szilágyi, P.Á.; Sharma, V.K.; Vértes, A.; J. Radioanal. Nucl. Chem. 2005, 266, 513-517.
[17] Von Uexkull, H.R.; Mutert, E.; Plant Soil, 1995, 171, 1-15.
[18] Vértes, A.; Nagy, D.L., Eds. Mössbauer Spectroscopy of Frozen Solutions. Akad. Kiadó: Budapest, 1990.
[19] Krebs, C.; Price, J.C.; Baldwin, J.; Saleh, L.; Green, M.T.; Bollinger, J.M., Jr.; Inorg. Chem. 2005, 44, 742-757.
[20] Savitsky, P.A.; Gazaryan, I.G.; Tishkov, V.I.; Lagrimini, L.M.; Ruzgas, T.; Gorton, L.; Biochem. J. 1999, 340, 579-583.
[21] Gazaryan, I. G.; Lagrimini, L.M.; Ashby, G. A.; Thorneley, R.N.F.; Biochem. J. 1996, 313, 841-847.
[22] Harrod, J.F.; Guerin, C.; Inorg. Chim. Acta 1979, 37, 141-144.
[23] Hinman, R.L.; Lang, J.; Biochemistry (USA), 1965, 4, 144-158.
[24] Kovács, K.; Kamnev, A.A.; Mink, J.; Németh, Cs.; Kuzmann, E.; Megyes, T.; Grósz, T.; Medzihradszky-Schweiger, H.; Vértes, A.; Struct. Chem. 2006, 17, 105-120.
[25] Hu, T.; Dryhurst, G.; J. Electroanal. Chem. 1997, 432, 7-18.
[26] Candeias, L.P.; Folkes, L.K.; Dennis, M.F.; Patel, K.B.; Everett, S.A.; Stratford, M.R.L.; Wardman, P.; J. Phys. Chem. 1994, 98, 10131-10137.
[27] Shchelochkov, A.G.; Kamnev, A.A.; Tarantilis, P.A.; Polissiou, M.G.; In *Metal Ions in Biology and Medicine*, Vol. 7. Khassanova, L.; Collery, Ph.; Maymard, I.; Khassanova, Z.; Etienne, J.-C., Eds., John Libbey Eurotext: Paris, 2002, pp. 37-40.
[28] Gazaryan, I.G.; Chubar, T.A.; Mareeva, E.A.; Lagrimini, L.M.; Van Huystee, R.B.; Thorneley, R.N.F.; Phytochemistry 1999, 51, 175-186.
[29] Niwa, T.; Ishii, S.; Hiramatsu, A.; Osawa, T.; Biosci. Biotechnol. Biochem. 2003, 67, 1870-1874.

INTERACTION OF QUADRUPLE BONDING RHENIUM UNIT WITH FREE RADICALS§

Shtemenko A.V., Tretyak S.Y., Golichenko A.A.
Ukrainian State Chemical Technology University, 49005 Ukraine Dnepropetrovsk, Gagarina av.8
E–mail: ashtemenko@yahoo.com Phone: +38(0562)47–06–72. Fax: +38(0562)47–33–16.

Abstract: The interaction of cis-$Re_2(RCOO)_2Cl_4$, trans-$Re_2(RCOO)_2Cl_4$, $Re_2(RCOO)_3Cl_3$ and $Re_2(RCOO)_4Cl_2$ (where R - alkyl group) with 1,3,5-triphenylverdazyle radical in 1,2-dichlorethane was investigated. It is discovered, that gradual substitution of halogenide ligands by carboxylates in dirhenium(III) clusters led to slowing down of reaction with a radical due to different influence of these ligands on parameters of rhenium - rhenium bond. Presented data showed perspectivity of Re_2^{6+}-substances applications as therapeutic agents due to their low toxicity and antiradical properties that occured by δ-component of quadruple Re-Re bond electron transition.

Keywords: rhenium, cluster, quadruple bond, free radical, antiradical activity.

INTRODUCTION

It was revealed earlier, that a majority of dirhenium(III) halocarboxylates synthesized by us had low toxicity and different kinds of biological activity [1-5]. The binuclear cluster Re_2^{6+}- fragment is a part of these compounds and includes multiple rhenium – rhenium bond with δ-component [6], which plays the role of free radical "scavenger" [3] by virtue of minor energy δ-δ* cleavage (0,615 eV [7]). One of the specific problems is the search and investigation of substances displaying simultaneously antihemolytic and antiradical activity as the activation of free - radical processes accompany most pathological states [8]. In this connection therefore an actual study of interaction of derivatives cluster Re_2^{6+} with stable free radicals is both important and preferential. The interaction of a series of dirhenium(III) derivatives with 1,3,5-triphenylverdazyle radical (Vd) was investigated. The Vd-radical was synthesized according to procedure [9], subsequently upgraded by the writers. The 1,2-dichlorethane was selected as a solvent for carrying out investigations, since parent compounds possess good solubility. Also it possesses low electron-donating properties (DN ($SbCl_5$) = 0) [10], therefore the solvent does not react with a radical.

Vd-radical transfers to triphenylverdazyle-cation upon transition of an electron (Fig.1).

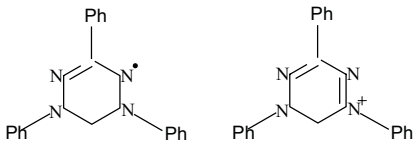

Vd - radical Vd - cation

Fig.1. 1,3,5-triphenylverdazyle radical and its cation.

Such type of transition may be explored with the help of electronic absorption spectra(EAS), as the maximum absorption is characteristic for Vd-radical at 13900 cm^{-1} and 25000 cm^{-1}, and for cation -18180 cm^{-1} [9]. With the help of EAS it is also possible to show the availability of a quadruple bond rhenium - rhenium in dirhenium(III) halocarboxylates in the visible region using δ-δ* -electron transition [11,12]. Thus, the electronic spectroscopy is a reliable method for studding transmutations in system Vd - derivatives – Re_2^{6+}.

The interaction of a Vd-radical with all possible structural types dirhenium(III) halocarboxylates ($Re_2(RCOO)_4Cl_2$, $Re_2(RCOO)_3Cl_3$, cis-$Re_2(RCOO)_2Cl_4$, trans-$Re_2(RCOO)_2Cl_4$, where R - alkyl group) was studied by EAS spectroscopy.

Study of interaction of Vd-radical with dihalotetra-μ-carboxylates of dirhenium(III)

The compounds $Re_2(RCOO)_4Cl_2$ (where R = C_2H_5, C_3H_7, i-C_3H_7, $C_{10}H_{15}$) (Fig.2) were selected for investigation. The structure and properties of these compounds were learnt earlier [13, 14].

§ Material presented at the XV-th Conference "Physical Methods in Coordination and Supramolecular Chemistry", September 27 - October 1, 2006, Chişinău, Moldova

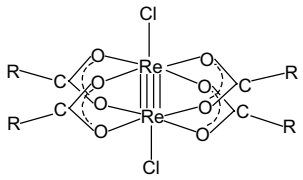

(where R - alkyl group)

Fig. 2. Structure of dirhenium(III) dihalotetra-μ-carboxylates.

Interaction of dihalotetra-μ-acetate of dirhenium(III) with a Vd-radical was not investigated, because this compound is not dissolved in most organic solvents.

Investigation of dihalotetra-μ-carboxylates of dirhenium(III) (R = C_2H_5, C_3H_7, i-C_3H_7, $C_{10}H_{15}$) has allowed the calculation of dependence of reaction rate from the length of alkyl groups and their bifurcation in cluster dirhenium(III) compounds. Study of a derivative of 1-adamantanecarboxylic acid (R=$C_{10}H_{15}$) was stipulated by the uniqueness of adamantane-group structure (Fig.3) This ligand belongs to the class of carcass ligands, which represents by itself three soldered cyclohexane rings in conformation chair (Fig.3).

It has a very high induction effect, even greater, than that of tert-butyl group that confirmed higher values of electrical dipole moments for adamantane derivatives. An example of that was showed earlier on chlorides of this group: μ($C_{10}H_{15}Cl$) = 2,32D, and μ($(CH_3)_3CCl$) = 2,13D [15,16].

Fig. 3 Structure of adamantane group.

A mixture of 0,0079g $Re_2(C_3H_7COO)_4Cl_2$ ($9{,}9\cdot10^{-6}$ mol) and 0,0062g Vd ($2{,}07\cdot10^{-5}$ mol) was soluble in 25ml 1,2-dichlorethane and recorded EAS of an obtained solution in time. As a result, disappearance of maximums characteristic for parent compounds (Fig.4) and appearance of a maximum absorption at 18180 $см^{-1}$ in EAS describing formation of Vd – cation, which took place. Tetracarboxylate derivatives reacted with a radical within 30-35 days.

The changing EAS (Fig.4) confirms the transfer of electrons from a Vd-radical to Re_2^{6+}- group, thus the Re-Re bond's order is decreased.

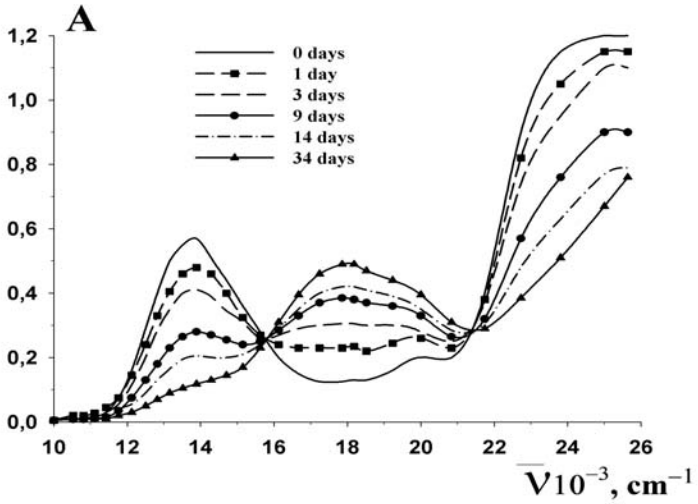

Fig. 4. EAS in 1,2-dichlorethane Vd with $Re_2(C_3H_7COO)_4Cl_2$.

As was displayed previously in results of the kinetic investigation [17], the reaction rate decreased when increase of induction effect in carboxylate group [J ($C_{10}H_{15}$-) > J (i-C_3H_7-) > J (C_3H_7-) > J (C_2H_5-)]. Thus for adamantane derivative it is observed to have the least reaction rate with a Vd-radical. Increasing of branching of alkyl groups (for example, C_3H_7 and i-C_3H_7) lead to decreasing of the reaction constant, that is in accord with the major induction effect of the branched group i-C_3H_7.

Study of interaction of a Vd-radical with trihalotri-μ-carboxylates of dirhenium(III)

Interaction of compounds $Re_2(RCOO)_3Cl_3$ [6] (Fig.5) with 1,3,5-triphenylverdazyle radical in 1,2-dichlorethane was investigated.

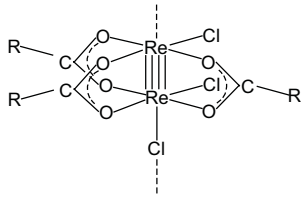

(where R = alkyl group)

Fig. 5. Structure of $Re_2(RCOO)_3Cl_3$.

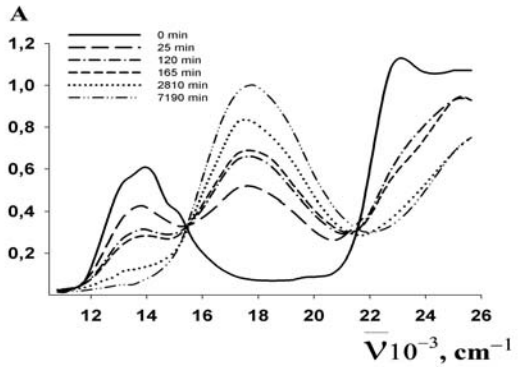

Fig. 6. EAS in 1,2-dichlorethane Vd with $Re_2(RCOO)_3Cl_3$.

0,0026g $Re_2(C_2H_5COO)_3Cl_3$ ($3{,}7\cdot10^{-6}$ mol) and 0,0023g Vd ($7{,}6\cdot10^{-6}$ mol) is dissolved in 1,2-dichlorethane, then obtained solutions is mixed and recorded change EAS in time (Fig.6).

The spectral data (fig.6) show that in time absorption maximum at 13890 $см^{-1}$ disappear and the maximum of absorption at 18180 $см^{-1}$ appears and is increased in intensiti, that confirms conversion of Vd-radical to Vd-cation [9]. Similar results were obtained for other trihalotri-μ-carboxylates of dirhenium(III). Interaction of a Vd-radical with tricarboxylate derivatives took place within several days (Fig.6).

Study of interaction of a Vd-radical with cis-tetrahalodi-μ-carboxylates of dirhenium(III)

Cis-tetrahalodi-μ-carboxylates of dirhenium(III) (Fig.7) are stable enough in solid state in air for a long time and soluble in many organic solvents and inorganic acids [11].

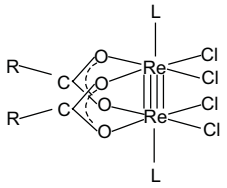

(where L = DMFA, R - alkyl group)

Fig. 7. Structure of cis-$Re_2(CH_3COO)_2Cl_4\cdot2DMFA$.

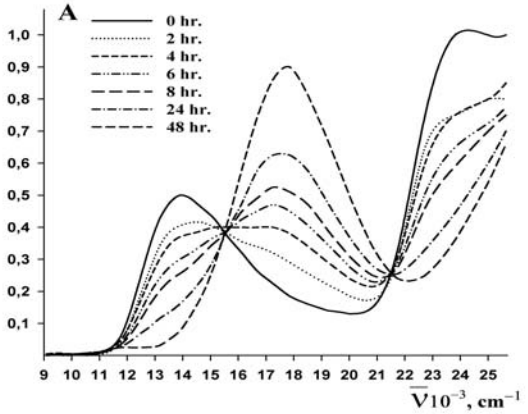

Fig. 8. EAS in 1,2-dichlorethane Vd with cis-$Re_2(CH_3COO)_2Cl_4\cdot2DMFA$.

0,0044g cis-$Re_2(CH_3COO)_2Cl_4 \cdot 2DMFA$($5{,}6 \cdot 10^{-6}$ mol) and 0,0035g Vd ($1{,}1 \cdot 10^{-5}$ mol) were dissolved in 12ml of 1,2-dichlorethane, then mixed obtained solutions and record change EAS in time. The interaction of a Vd-radical with cis-tetrahalodi-μ-carboxylates of dirhenium(III) in dichlorethane took place within days. The disappearance of absorption maximum in parent compounds took place in visible region and appearance of absorption maximum of Vd – cation (Fig.8) confirmed complete finishing of the reaction.

Study of interaction of a Vd-radical with trans-tetrahalodi-μ-carboxylates of dirhenium(III)

Trans-tetrahalodi-μ-carboxylates of dirhenium(III) (Fig.9) represents a significant interest both from the theoretical and applied aspects [18,19].

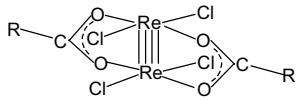

(where R = alkyl group)

Fig. 9. Structure of trans-$Re_2(RCOO)_2Cl_4$.

The interaction of 0,0062g of a Vd-radical ($20{,}7 \cdot 10^{-6}$ mol) with 0,0073g of a trans-$Re_2(RCOO)_2Cl_4$ ($10{,}6 \cdot 10^{-6}$ mol) in 25 ml of dichlorethane took place within several seconds, which was confirmed by the EAS data. The compounds were separately dissolved in 1,2-dichlorethane. Trans-$Re_2(RCOO)_2Cl_4$ and Vd-radical have, accordingly, blue (absorption maximum at 12500 and 16129 $см^{-1}$) and green colour (absorption maximum at 13900 $см^{-1}$) (fig.10). After mixing of both compounds, the colour of the resultant solution then immediately changed to violet.

Such conclusion is confirmed by EAS data (Fig.10), which clearly indicates the disappearance of maximums, specific for parent compounds and appearance of a maximum absorption at 18180 $см^{-1}$ describing formation of Vd – cation.

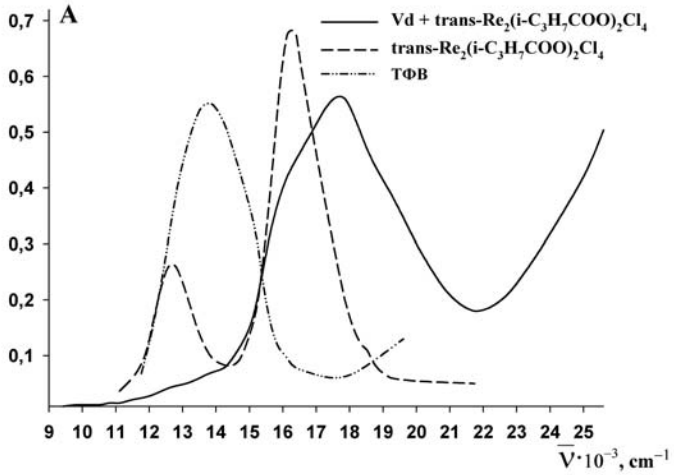

Fig. 10. EAS in 1,2-dichlorethane Vd with trans-$Re_2(i\text{-}C_3H_7COO)_2Cl_4$.

CONCLUSIONS

The interaction of all possible structural types of halocarboxylate derivatives of the cluster Re_2^{6+} with 1,3,5-triphenylverdazyle radical was studied. The reaction finished completely due to interaction of the compounds with twofold molar excess of a Vd-radical [20]. In these conditions disappearance of absorption bands, which were relevant to origin substances and appearance of Vd – cation bands took place in electronic absorption spectra. Disappearance of the maximum absorption, which characterizes δ-δ* -electron transition confirmed cleavage of δ-component of quadruple bond Re-Re.

Analysis of the obtained results shows that binuclear cluster fragment Re_2^{6+} actively reacted with Vd-radical, however the rate of such interaction strongly depends on the charge ratio and ligand environment of the cluster Re_2^{6+}.

It was shown, that a gradual substitution of halogenide ligands by carboxylates in dirhenium(III) clusters led to the slowing down of the reaction with a radical due to different influence on these ligands by the parameters of rhenium - rhenium bond. The least reaction rate is showed for tetracarboxylate derivatives. Besides, the reaction rate decreased with an increase of induction effect of alkyl groups. This fact may be explained by stronger pressing-in of electronic density to rhenium – rhenium bond, for which the effect of conjugation with COO- group and formation of pentamerous cycle was observed together with strengthening of the bond.

Presented data showed positive future prospects for application of Re_2^{6+}-substances applications as therapeutic agents due to their low toxicity and antiradical properties that occurred by δ-component of quadruple Re-Re bond electron transition.

REFERENCES

[1] Олійник С.А., Штеменко Н.І., Горчакова Н.О. та ін. Современные проблемы токсикологии. 2001, 1, 11–15.
[2] Eastland G.W. Jr, Yang G., Thompson T. Methods. Find. Exp. Clin. Pharmacol. 1983, 7, 435-438.
[3] Олійник С.А, Штеменко Н.І., Пірожкова І. В. та ін. Доповіді НАН України. 2001, 7, 176-180.
[4] Штеменко Н.И., Пирожкова–Паталах И.В., Штеменко А.В., Голиченко А.А. Укр.биохим.журнал. 2000, 3, 77–81.
[5] Штеменко Н.І., Олійник С.А., Штеменко О.В. та ін. Доповіді НАН України, 2001, 6, 194–198.
[6] Cotton F.A., Walton R.A. Oxford: Clarendon Press. 1993, 780.
[7] Bursten B.E., Cotton F.A., Fanwick P.E., Stanley G.G. J.Am.Chem.Soc. 1983, 105, 3082-3087.
[8] Гриневич Ю.П., Олійник С.А., Штеменко Н.І., Штеменко О.В. Укр.біохім.журн. 2003, 1, 50–56.
[9] Полумбрик О.М. Химия вердазильных радикалов; Наукова думка: Киев, 1984; с.25-46.
[10] Гутман В. Химия координационных соединений в неводных средах; Мир: Москва, 1970; с.30.
[11] Shtemenko O.V., Bovykin B.A. Rhenium and Rhenium Alloys; TMS Publication: Pensilvania, 1997; pp.189 – 197.
[12] Штеменко А.В., Голиченко А.А., Кожура О.В. Вопросы химии и хим. технологии. 2000, 2, 21–24.
[13] Cotton F.A., Oldham C., Robinson W.R. Inorg. Chem. 1966, 10, 1798-1804.
[14] Shtemenko A.V., Golichenko A.A., Domasevitch K.V. Z. Naturforsch. 2001, 4/5, 381–385.
[15] Багрий Е.И. Адамантаны : получение, свойства, применение; Наука: Москва, 1989; с.188-190.
[16] Мажейка И.Б., Янковская И.С., Полис Я.Ю. Ж.общ.химии. 1971, 7, 1633-1635.
[17] Голиченко А.А., Третяк С.Ю., Штеменко А.В. Вопросы химии и хим. технологии. 2006, 6, 22-24.
[18] Штеменко А.В., Багиров Ш.А., Котельникова А.С. и др. Журн. неорган. химии. 1981, 1, 111-114.
[19] Shtemenko O.V. Rhenium and Rhenium Alloys; TMS Publication: Pensilvania, 1997; pp.173 – 178.
[20] Штеменко А.В., Голиченко А.А., Третяк С.Ю. Вопросы химии и хим. технологии. 2005, 5, 37–39.

THE STRUCTURE OF THE TETRA-POTASSIUM SALT OF CALIX[4]ARENE DIHYDROXYPHOSPHONIC ACID§

Adina N. Lazar,* [a] Oksana Danylyuk,[b] Kinga Suwinska,[b] and Anthony W. Coleman[a]

[a] *Institut de Biologie et Chimie des Protéines, CNRS UMR 5086, 7 passage du Vercors, F-69367 Lyon cedex 07, France*
[b] *Institute of Physical Chemistry, Polish Academy of Sciences, Kasprzaka, 44/52, PL-01 224 Warszawa, Poland*
** E-mail: a.lazar@bo.ismn.cnr.it; Fax: +48 22 343 33 33*

Abstract: The solid-state structure of the tri-potassium calix[4]arene dihydroxyphosphonate salt is presented. In this structure, two potassium cations bridge between layers of dimeric calixarene diphosphonate units and two other potassium cations bridge along the face of the layers. The ubiquitous dimeric association of the calixarenes shows the highest interdigitation value so far observed. As expected, the cations are solvated and are complexed exo with respect to calixarene crown. The octahedral coordination sphere of the potassium cations is formed by two phosphonate groups of the calixarenes and four water molecules. Electrostatic forces represent the major element of interaction in the solid-state system.

Keywords: Calixarenes, cation binding, electrostatic interactions.

INTRODUCTION

Complexation of small molecules or ions by calixarenes is a subject of wide interest, which has been the basis for a large body of work in the past few years. The calixarenes have been widely used in binding various metal cations [1-3], aromatic ammonium and alkyl cations [4,5] or acetylcholine [4-6].

An extraordinary versatility has been shown by these macromolecules as metal binding agents, supramolecular systems being formed with metals belonging to all groups in the periodic table [7-9]. Previous studies showed that calix[4]arenes are efficient binders for different alkali and alkaline-earth cations. Small cations, like such as Li^+ and Na^+ are complexes as guest molecules in the aromatic cavity of the calixarene *(endo* complexation), whereas the larger ones (Rb^+ and Cs^+) do not fit in the calixarene cavity, existing as complexes *exo* with respect to the aromatic core.

Nevertheless, the complexation of the cations depends not only on their size, but also on the nature of the solvent used. Thus, for apolar solvents, in the case of neutral calixarene molecules, the complexation of cations is *endo*. For polar solvents, the complexation is *exo*, the cation being located outside the cone of the host molecule, close to the oxygen atoms of the lower rim [4].

The recognition properties can be fine-tuned through modification of the phenolic lower rim. Substitution at the phenolic oxygens are performed in order to render the host molecules more soluble or more complimentary with respect to guest molecules.

A large range of ion-complexing calix[n]arenes have been studied, since Mc Kervey [5], but no such abilities have been yet reported for the calix[4]arene dihydroxyphosphonic acid. This water-soluble calixarene derivative has proved to have strong complexation capacity with regard to organic amonium cations. Thus a wide variety of packing motifs have been observed in the solid state complexes of this derivative with both aromatic and aliphatic ammonium cations [10-12]. It is obvious that the anionic aspect of the calix[4]arene dihydroxyphosphonic acid facilitates the non-covalent interactions with positively charged molecules.

In this paper we present the first example of a metal cation, potassium, complexed by calix[4]arene dihydroxyphosphonic acid.

EXPERIMENTAL SECTION

Crystal Growth

Calix[4]arene dihydroxyphosphonic acid (**1**) was synthesised according to the literature [13]. A solution of 0.01M of **1** was prepared in methanol. In order to set up the pH of this solution at a neutral value (pH 7), careful neutralisation was applied, using KOH.

Crystals were grown from this solution, by slow evaporation at room temperature.

X-Ray diffraction

The intensity data were collected with a Nonius KappaCCD diffractometer (MoKα radiation λ = 0.71073 Å, 100(2) K). All the collected data were corrected for Lorentz and polarisation effects but not for absorption. The

§ Material presented at the XV-th Conference "Physical Methods in Coordination and Supramolecular Chemistry", September 27 - October 1, 2006, Chişinău, Moldova.

direct methods technique and Fourier techniques (SHELXS-86) [14] were employed in order to solve the structure and the refinements were done on $|F|^2$ (SHELX-97) [15]. H-atoms were placed in geometric positions. Crystallographic data for the structures in this paper have been deposited with the Cambridge Crystallographic Data Centre as supplementary publication. CCDC reference number 285773. Copies of the data can be obtained, free of charge, on application to CCDC, 12 Union Road, Cambridge, CB2 1EZ, UK fax: +44(0)-1223-336033 or e-mail: deposit@ccdc.cam.ac.uk].

RESULTS AND DISCUSSION

In this paper we present the first result of cations binding by calix[4]arene dihydroxyphosphonic acid, where the major driving force is the attraction between oppositely charged molecules.

Table 1

Crystal data of the complex of 1 with potassium cations

Compound	C4diP-K
Formula	$C_{28}H_{24}O_{10}P_2{\cdot}2K{\cdot}CH_3OH{\cdot}11H_2O$
FW	890.83
Temperature, K	100 (2)
Color	Colorless
Crystal size, mm	0.25 × 0.15 × 0.10
Crystal system	Monoclinic
Space group	$P2_1/c$
a, b, c Å	15.5758(7); 13.0023(7); 19.385(1)
β °	111.067(4)
V, Å^3	3663.5 (3)
Z	4
ρ_{calc}, Mg·m^{-3}	1.615
F(000)	1872
μ(MoKα) mm^{-1}	0.437
θ range for data collection,°	2.18 to 18.92
Reflections collected	23811
Absorption correction	none
Data / restraints / parameters	2869 / 0 / 536
Goodness-of-fit on F^2	1.08
Final R indices [I>2σ (I)]	R = 0.089, wR = 0. 216
R indices (all data)	R = 0.129, wR = 0. 238
Refinement method	Full-matrix least-squares on F^2

In the solid state structure of calix[4]arene dihydroxyphosphonic acid (Fig. 1a) with potassium cations, two molecules of **1** interact with six K^+ cations (Fig. 1b).

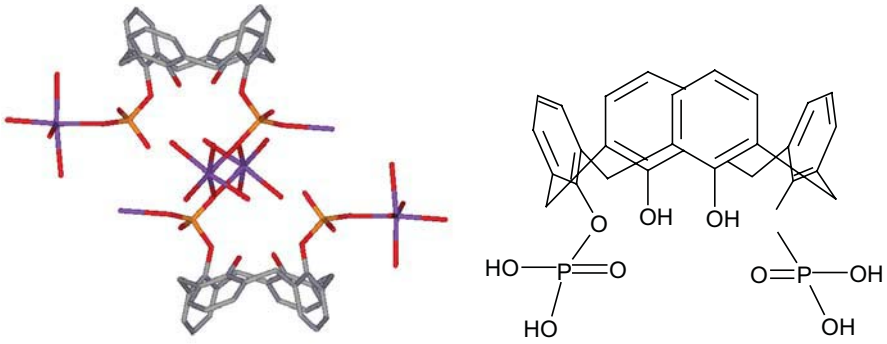

(a) (b)

Fig. 1: (a) Scheme of **1**; (b) Dimeric unit of the complex of **1** with K^+; solvent molecules are excludes for the simplicity of the figure.

As in all the other structures implying the calix[4]arene dihydroxyphosphonic acid, the characteristic generic motif is the dimeric association of two molecules of calixarene (Fig. 2a).

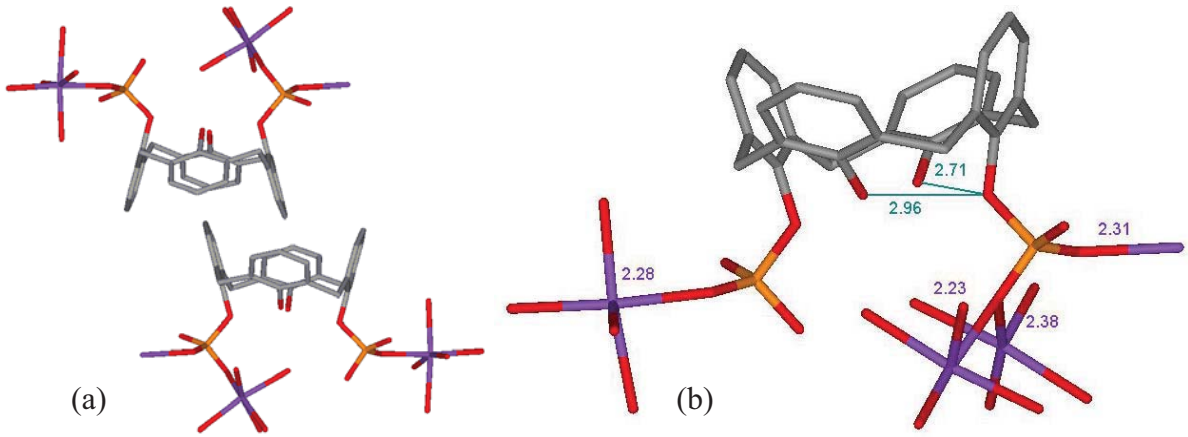

Fig. 2: (a) Interdigitation of the neighboring molecules of **1**, (b) Intramolecular H-bonds in **1**, (in green) and the electrostatic interactions with K^+ (values in blue).

Here, the interdigiting angle is 163.3° and represents the highest value of interdigitation with respect to the previously reported structures:158.8° in the case of uncomplexed dimer [16] or 161° in the complex with 4,4' bipyridine [17].

The strong electrostatic interactions involving the phosphonate oxygens determine an opening of the hydrophobic core. The angles between opposite aromatic rings of **1** being of 30.9(4)° and 105.2(4)°, notably bigger than in the case of uncomplexed calix[4]arene dihydroxyphosphonic acid, the latter structure presenting cone angles of 20.87° and 77.97°. As a consequence, the intramolecular hydrogen bonds between the phenolic oxygens are shorter than in the reference structure: 2.71(1) and 2.96(1) compared to 2.92(2) and 3.05(1) Å, respectively (Fig. 2b).

From a general point of view, the complex adopts a 1-D architecture based on layers of dimeric units characteristic to dihydroxyphosphonic calixarene, held together by the K^+ cations ion-paired with the deprotonated oxygen atoms of the phosphonate groups (Fig. 3). Thus, infinite bridges of electrostatic interactions are connecting the dimeric units of **1**. A stepped like organization is observed, as represented in Fig. 3a, with distances between the layers of 15.6 Å and between each dimeric unit of 13.0 Å. A perpendicular view to this motif shows the parallel packing of these sheets of dimers (Fig. 3b).

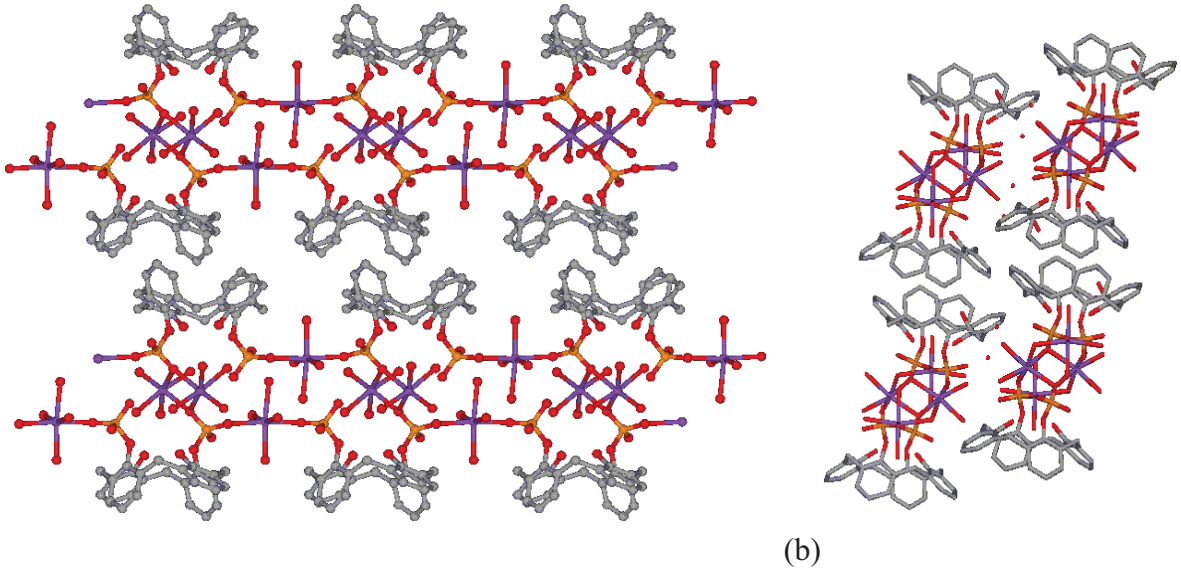

Fig. 3: (a) - View of the packing along **c** axis; (b) - View of the double chains along **b** axis.

The electrostatic interactions between the phosphonate oxygens and K^+ are multiple, the closed distances being: 2.24(1), 2.285(9), 2.31(1), and 2.38(1) 2.88(1) Å (see Fig. 2b). Eight water molecules are coordinated to the complex, by electrostatic interactions. Some of them form hydrogen bonds with phenolic oxygens or to oxygens of the phosphonate groups of **1**, while some other are hydrogen bonded between them (see Tab. 2).

Table 2

Selected interactions:

Interaction	Water···water	Water···K^+	OH···Water	OP···Water	OP···K^+
Electrostatic	-	K1···O1W 2.28(1) K1···O2W 2.25(2) K1···O3W 2.27(1) K1···O4W 2.33(2) K2···O5W 2.32(1) K2···O6W 2.31(1) K2···O7W 2.32(1) K2···O8W 2.43(1)	-	-	K1···O2A 2.88(1) K1···O4A 2.386(1) K1···O4A 2.238(3) K2···O2C 2.285(9) K2···O2A 2.31(1)
H-bonds	O1W···O4W 3.09(2) O2W···O3W 2.97(2) O2W···O4W 2.87(2) O3W···O4W 3.18(2) O5W···O8W 3.09(1) O7W···O8W 3.15(2) O10W···O11W 2.71(3)	-	O3C···O7W 2.67(2) O3A···O5W 2.89(1) O3A···O9W 2.74(2) O3A···O10W 2.64(3) O3C···O2W 2.62(1) O3C···O4W 3.06(3)	O4C···O5W 2.68(2) O4C···O11W 2.61(1) O2C···O8W 2.71(2) O2A···O6W 3.19(2) O4A···O1W 3.14(1) O4A···O3W 3.18(2) O4A···O4W 3.19(2)	-

Three other water molecules, plus a methanol molecule hydrogen bond with phenolic oxygens or with the coordinated solvent molecules. Selective values of non-covalent interactions are presented in Tab. 2.

CONCLUSION

Apparently simple, the solid state structure of calix[4]arene dihydroxyphosphonic acid presents a high degree of complexity, from the point of view of non-covalent interactions present in the complex, of the architecture achieved and of the effective cationic binding. As expected, ion pairing between phosphonate oxygen atoms and potassium cations dominate the forces driving the structural integrity.

ACKNWLEDGEMENTS

This research was partially supported by the Polish Ministry of Science and Information Society Technologies (Grant 4 T09A 068 25).

REFERENCES

[1] P. C. Kearney, L. S. Mizoue, R. A. Kumpf, J. E. Forman, A. McCurdy, D. A. Dougherty*, J Am Chem Soc.,* , **1993**, 115, 9907.
[2] A. Ikeda, S. Shinkai, *Chem Rev*., **1997**, 1713.
[3] A. Ikeda, S. Shinkai S, *J. Am. Chem. Soc*., **1994**, 116, 3102.
[4] S. Kumar, G. Hundal, D. Paul,M. S. Hundal, H. Singh, *J. Org. Chem*., **1999**, 64, 7717.
[5] F. Arnaud-Neu, G. Barrett, D. Corry, S. Cremin, G. Ferguson, J. F. Gallagher, S. J. Harris, M. A. McKervey M. J. Schwing-Weill*,, J Chem Soc Perkin 2*, **1997**, 575.
[6] R. Arnecke, V. Böhmer, R. Cacciapaglia, A. D. Cort, L. Mandolini, Tetrahedron, **1997**, 53, 4901.
[7] G. Arena, A. Casnati, A. Contino, G. G. Lombardo, D. Sciotto, R. Ungaro, *Chem Eur J.,* **1999**, 5, 738.
[8] V. Bohmer *, Kluwer Academic, Dordrecht*, **1991**.
[9] J. Vicens, Z. Asfari, J.M. Harrowfield, *Calixarenes 50th Anniversary: Commemorative Volume, Kluwer Academic, Dordrecht,* **1995**.
[10] A. W. Coleman, E. Da Silva, F. Nouar, M. Nierlich, A. Navaza, *J. Chem. Soc. Chem. Commun.,* **2003**, 7, 826.
[11] B. Rather, B. Moulton, M. J. Zaworotko, F. Perret, N. Morel-Desrosiers, E. Da Silva, A. W. Coleman, *Crystal Engineering*, **2003**, 6, 15.
[12] A. N. Lazar, A. Navaza, A. W. Coleman, *Chem. Commun.,* **2004**, 1052.
[13] V. I. Kalchenko, J. Lipkowski, Y. A. Simonov, M. A. Vysotsky, K. Suwinska, A. A. Dvorkin, V. V. Pirozhenko, I. F. Tsimbal, L. N. Markovsky.- *Zh. Obshch. Khim*., **1995**, 65, 1311-1320.
[14] G. M. Sheldrick, *Acta Cryst. A*, **1990**, 46, 467-473.
[15] G. M. Sheldrick*,, SHELXL-97. Program for the Refinement of Crystal Structures. Univ. of Goettingen, Germany*. **1997.**
[16] Lipkowski, Y. Simonov, V. I. Kalchenko, M. A. Vysotsky, L. N. Markovsky, *Anales de Quimica Int. Ed.*, **1998**, 94, 328-331.
[17] A. N. Lazar, N. Dupont, A. Navaza, A. W. Coleman, *Crystal Growth and Design*, **2006**, 6, 669-674.

A THIOLATO-BRIDGED OCTANUCLEAR COPPER(I,II) MIXED-VALENCE COMPLEX WITH N,N,S-TRIDENTATE LIGAND[§]

Takanori Kotera, Tsukasa Sugimoto, and Masahiro Mikuriya*

Department of Chemistry and Open Research Center for Coordination Molecule-Based Devices, School of Sciecne and Technology, Kwansei Gakuin University, Sanda, Hyogo 669-1337, Japan
**junpei@ksc.kwansei.ac.jp, TEL +81-79-565-8365, FAX +81-79-565-9077*

Abstract: Thiolato-bridged complex $[Cu^{I}_{4}Cu^{II}_{4}(peampt)_{4}Cl_{8}]\cdot 2H_{2}O$ (Hpeampt = 1-(2-pyridylethyl)amino) methylpropane-2-thiol) has been synthesized and characterized by the elemental analysis, IR and UV-vis spectroscopies and magnetic susceptibility measurement. The X-ray crystal structure analysis of this complex shows a localized mixed-valence octanuclear cage structure made up of four trigonal-bipyramidal $Cu^{II}N_{2}SCl_{2}$, two trigonal $Cu^{I}S_{2}Cl$, and two tetrahedral $Cu^{I}S_{2}Cl_{2}$ coordination sites. Temperature dependence of magnetic susceptibility (4.5—300 K) shows that a fairly strong antiferromagnetic interaction is operating between the four Cu^{II} ions.

Keywords: thiolato-bridged complexes; mixed-valence complexes; copper complexes; octanuclear complexes.

INTRODUCTION

Thiolato-bridged metal complexes with organic thiolic ligands have attracted much attention during the several decades because of their utilities as model complexes in relation to ubiquitous metal-cysteine centers of biologically important metal enzymes [1-3]. For example, thiolato-bridged copper species have been focused from a view of model compounds for nitrous oxide reductase and cytochrome c oxidase and these sites are interesting mixed-valent copper cluster with the spin-delocalized state [2]. However, isolation of thiolato-bridged metal complexes was generally hampered by the presence of undefined and undesired byproducts caused by electron-rich thiolato sulfur having a great affinity for various metal ions. Formation of discrete thiolato-bridged metal complexes could be expected to be feasible by the use of tridentate chelate ligands which have N,N,S-donor set by virtue of the chelating effect. Thus, we synthesized thiolic ligands such as 2-[(2-aminoethyl)amino]ethanethiol (Haeaet), 2-[(3-aminopropyl)amino]ethanethiol (Hapaet), 2-[(2-pyridylmethyl)amino]ethanethiol (Hpmaet), and 2-{[2-(2-pyridyl)ethyl]amino}ethanethiol (Hpeaet) and initiated a systematic study on thiolato-bridged metal complexes with these chelate ligands.

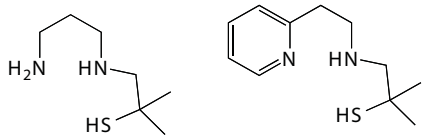

Hapampt Hpeampt

Scheme 1. N,N,S-tridentate thiolic ligands.

We isolated dinuclear nickel(II) complexes [4] and unique tetranuclear palladium(II) complexes [5] by reactions with nickel(II) and palladium(II) salts, repectively. In the case of zinc(II), linear and cyclic trinuclear and chain polynuclear complexes were obtained by these ligands [6]. Linear trinuclear structure consisting of octahedral-tetrahedral-octahedral coordination environments seems to be most favorable pattern in our systems and we isolated such species for the cases of Zn^{II}, Cd^{II}, Mn^{II}, Fe^{II}, Co^{II}, and Ni^{II} [7-11]. We explored a facile synthetic method of trinuclear heterometal complexes by using one-pot reaction of Hapaet [11]. After getting these experiences, we tried to make copper systems of our thiolic ligands and obtained a polymeric compound of $apaet^{-}$ which could not be crystallized [12]. By the use of a similar NNS-chelating ligand containing methyl groups at the β-position, 1-[(3-aminopropyl)amino]-2-methylpropane-2-thiol (Hapampt), we could successfully isolated a hexanuclear mixed-valence complex with unique $Cu^{I}_{3}Cu^{II}_{3}$ cluster in copper systems [12,13]. This may be ascribed to the presence of the methyl groups of the thiolic ligand to stabilize the mixed-valence state. We can expect formation of different type of copper complexes, if we introduce pyridyl group to this promising methyl-group-attached thiolic ligand, because it is known that pyridyl group is softer than the amino group. In this study, we synthesized a new thiolic ligand, 1-[(2-pyridylethyl)amino]methylpropane-2-thiol (Hpeampt) and examined the reactions with copper(II) ion in the hope of attaining to make mixed-valence species.

[§] Material presented at the XV-th Conference "Physical Methods in Coordination and Supramolecular Chemistry", September 27 - October 1, 2006, Chişinău, Moldova.

RESULTS AND DISCUSSION

In the case of the reaction of Hapampt ligand with copper(II) ion, a mixed-valent species, $[Cu^{I}_{3}Cu^{II}_{3}(apampt)_{3}Cl_{6}]\cdot 2H_{2}O$ (**1**), was formed. The X-ray crystal structure analysis shows a hexanuclear cage structure, where each apampt^{-} ligand is bonded to one copper(II) ion to form two adjacent chelates with six- and five-membered rings and each thiolato-sulfur is further bound to one copper(I) ion [12].

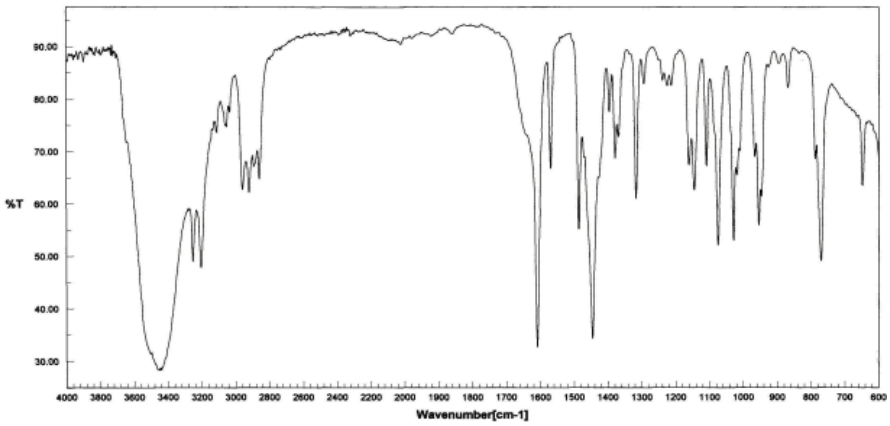

Fig. 1. Infrared spectra of $[Cu^{I}_{4}Cu^{II}_{4}(peampt)_{4}Cl_{8}]\cdot 2H_{2}O$ (2).

The localized mixed-valence structure was also supported by the electronic spectra and the magnetic susceptibility data. From the structural similarity, it can be considered that the peampt^{-} ligand is capable of forming two adjacent six- and five-membered chelate rings like the apampt^{-} ligand. Therefore it was expected to obtain similar mixed-valent complexes to the hexanuclear cluster **1**, although we can expect something different feature for product from reaction of the present thiolic ligand with copper(II) ion. Reaction of Hpeampt with copper(II) chloride dihydrate in methanol resulted in deprotonation of the thiolic ligand and gave black crystals of thiolato complex (**2**).

Table 1

Crystallographic data for $[Cu^{I}_{4}Cu^{II}_{4}(peampt)_{4}Cl_{8}]\cdot 2H_{2}O$ (2)

	$[Cu^{I}_{4}Cu^{II}_{4}(peampt)_{4}Cl_{8}]\cdot 2H_{2}O$ (2).
Empirical formula	$C_{44}H_{72}Cl_{8}Cu_{8}N_{8}O_{2}S_{4}$
Formula weight	1665.35
Temperature / K	293
Crystal dimensions /mm	0.1 × 0.1 × 0.05
Crystal system	monoclinic
Space group	$P2_{1}/c$ (No. 12)
a / Å	12.829(11)
b / Å	24.24(2)
c / Å	12.494(11)
α / °	90
β / °	116.952(17)
γ / °	90
V / Å^{3}	3464(5)
Z	2
$d_{calcd.}$ /gcm^{-3}	1.597
μ / mm^{-1}	2.873
Diffractometer	Bruker SMART APEX CCD
No. of reflection	11909
No. of observation	3633
Refl./Parameter ratio	10.7
*R*1, w*R*2 [$I > 2\sigma(I)$][a]	0.1291, 0.3039
Goodness-of-fit on F^2	1.282

[a] $R1 = \Sigma||F_o|-|F_c||/\Sigma|F_o|$; $R_w = [\Sigma w(F_o^2-F_c^2)^2/\Sigma w(F_o^2)^2]^{1/2}$.

In the infrared spectrum of **2**, the absorption bands due to the peampt^{-} ligand appear as a set of absorption bands in a similar frequency region to that of the free thiol with lacking the ν(SH) band as shown in Fig. 1. The presence of

H_2O is suggested from the broad band around 3449 cm^{-1} attributable to the ν(OH) band of the crystal water molecules. Unfortunately, all of the crystals were twinned and we failed to obtain a satisfactory quality of crystallographic data for this complex, despite of many attempt to get good quality of single-crystals, and therefore a more detailed analysis of the structure of **2** could not be performed. However, we can find that the preliminary X-ray crystal structure reveals an octanuclear structure with formulation of $[Cu^{I}_4Cu^{II}_4(peampt)_4Cl_8]\cdot 2H_2O$ that is distinctly different from **1**. The elemental analysis and the IR data also support this formulation. Crystal data and details concerning data collection are given in Tab. 1. An ORTEP drawing of **2** with atom-labeling scheme is shown in Fig. 2.

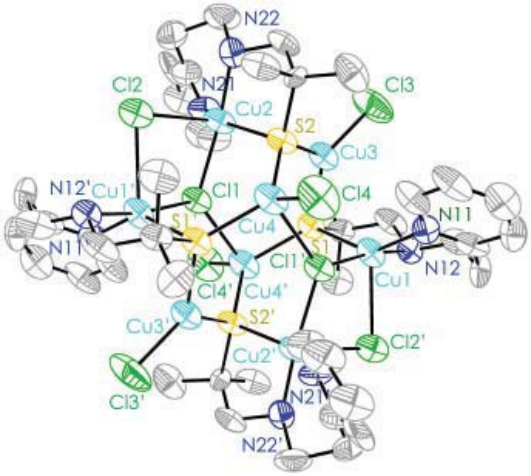

Fig. 2. ORTEP drawing of the structure of $[Cu^{I}_4Cu^{II}_4(peampt)_4Cl_8]\cdot 2H_2O$ (2) showing the 50% probability thermal ellipsoids and atom labeling scheme. Water molecules are omitted for clarity.

Selected bond distances and angles are listed in Table 2. The octanuclear molecule has a crystallograophically inversion center. The Cu1 (Cu1') atom is coordinated to the pyridyl-nitrogen N11 (N11'), amino-nitrogen N12 (N12'), and thiolato-sulfur S1 (S1') atoms of peampt⁻ in a *meridional* form, forming two adjacent six- and five-membered chelate rings. The Cu2 (Cu2') atom is also coordinated to the pyridyl N21 (N21'), amino N22 (N22'), and thiolato S2 (S2') of the thiolic ligand in a similar mode.

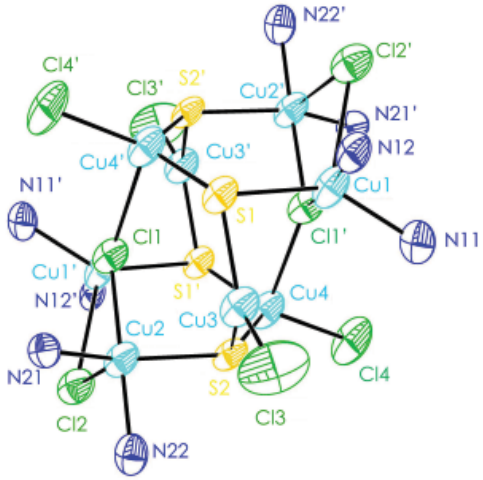

Fig. 3. Core structure of of $[Cu^{I}_4Cu^{II}_4(peampt)_4Cl_8]\cdot 2H_2O$ (2).

The Cu3 (Cu3') atom is coordinated to the thiolato S1 and S2 (S1' and S2') atoms to connect the Cu1(peampt) and Cu2(peampt) (the Cu1'(peampt)' and Cu2'(peampt)') moieties. Similarly, the Cu4 (Cu4') atom is coordinated to the thiolato S2 and S1' (S2' and S1) atoms to connect the Cu2(peampt) and Cu1'(peampt)' (the Cu2'(peampt)' and Cu1(peampt)) moieties. The octanuclear core is shown in Fig. 3.

The octanuclear copper core is made up of four trigonal-bipyramidal $Cu^{II}N_2SCl_2$, two trigonal $Cu^{I}S_2Cl$, and two tetrahedral $Cu^{I}S_2Cl_2$ moieties and has adjacent six-membered rings [-Cu-S-Cu-S-Cu-Cl-] containing three of the trigonal-bipyramidal (Cu1, Cu2, Cu1', and Cu2'), trigonal (Cu3 and Cu3'), and tetrahedral (Cu4 and Cu4') copper atoms. Charge consideration requires a formal $Cu^{I}_4Cu^{II}_4$ description of this core and thus we can assign the Cu1 and Cu2 (Cu1' and Cu2') atoms to copper(II) oxidation state and the Cu3 and Cu4 (Cu3' and Cu4') atoms to copper(I) oxidation state, respectively. The Cu^{II}-Cu^{II} separations, the Cu1'-Cu2 and Cu1-Cu2 distances, are 3.703(3) and 5.708(3)

Å, respectively, forming a rectangurar array of the four copper(II) ions in the octanuclear core. The Cu^{I}-Cu^{I} (Cu3-Cu4) distance is 4.016(3) Å. As for the Cu^{I}-Cu^{II} separations, the Cu2-Cu3, Cu2-Cu4, Cu1-Cu4, and Cu1'-Cu4 distances are 3.184(3), 3.968(3), 4.485(3), and 3.961(3) Å, respectively. It is to be noted that the Cu^{I}-S bond distances [2.273(6)—2.296(6) Å] are comparable to the Cu^{II}-S bond lengths [2.296(6), 2.298(6) Å]. Such a small difference is also found in **1** and both the Cu^{I}-S and Cu^{II}-S distances are comparable to the values found in thiolato-bridged mixed-valent $Cu^{I}Cu^{II}$ complexes [12-14].

The diffuse reflectance spectra of **2** (Fig. 4) contains broad features at 266, 330sh, 425, 554, 628, 736 nm.

Table 2

Selected bond distances (Å) and angles (°), with esds in parentheses for $[Cu^{I}_4Cu^{II}_4(peampt)_4Cl_8]\cdot 2H_2O$

2			
Cu(1)−N(12)	2.008(18)	Cu(1)−N(11)	2.082(19)
Cu(1)−S(1)	2.296(6)	Cu(2)−N(22)	1.993(19)
Cu(2)−N(21)	2.031(17)	Cu(2)−S(2)	2.298(6)
Cu(3)−S(1)	2.273(6)	Cu(3)−S(2)	2.279(7)
Cu(4)−Cl(4)	2.268(7)	Cu(4)−S(1)'	2.292(6)
Cu(4)−S(2)	2.296(6)	Cu(4)−Cl(1)	2.683(7)
Cu(1)-Cl(1)'	2.338(6)	Cu(1)-Cl(2)'	2.740(7)
Cu(2)-Cl(1)	2.351(6)	Cu(2)-Cl(2)	2.767(8)
Cu(3)-Cl(3)	2.225(7)		
N(12)−Cu(1)−N(11)	93.6(8)	N(12)−Cu(1)−S(1)	88.5(5)
N(11)−Cu(1)−S(1)	142.0(6)	N(12)−Cu(1)−Cl(1)'	171.1(5)
N(11)−Cu(1)−Cl(1)'	91.5(6)	S(1)−Cu(1)−Cl(1)'	92.0(2)
N(12)−Cu(1)−Cl(2)'	87.3(5)	N(11)−Cu(1)−Cl(2)'	110.5(6)
S(1)−Cu(1)−Cl(2)'	107.6(2)	Cl(1)'−Cu(1)−Cl(2)'	84.2(2)
N(22)−Cu(2)−N(21)	94.5(8)	N(22)−Cu(2)−S(2)	87.2(5)
N(21)−Cu(2)−S(2)	143.8(6)	N(22)−Cu(2)−Cl(1)	169.6(5)
N(21)−Cu(2)−Cl(1)	92.4(6)	S(2)−Cu(2)−Cl(1)	91.9(2)
N(22)−Cu(2)−Cl(2)	87.1(5)	N(21)−Cu(2)−Cl(2)	108.9(6)
S(2)−Cu(2)−Cl(2)	107.3(2)	Cl(1)−Cu(2)−Cl(2)	83.3(2)
Cl(3)−Cu(3)−S(1)	122.7(3)	Cl(3)−Cu(3)−S(2)	121.3(3)
S(1)−Cu(3)−S(2)	116.0(2)	Cl(4)−Cu(4)−S(1)'	119.8(3)
Cl(4)−Cu(4)−S(2)	121.0(3)	S(1)−Cu(4)−S(2)	115.8(2)
Cl(4)−Cu(4)−Cl(1)'	100.4(3)	S(1)'−Cu(4)−Cl(1)'	93.9(2)
S(2)−Cu(4)−Cl(1)'	93.7(2)	Cu(3)−S(1)−Cu(4)'	125.0(3)
Cu(3)−S(1)−Cu(1)	84.9(2)	Cu(4)'−S(1)−Cu(1)	119.4(2)
Cu(3)−S(2)−Cu(4)	122.8(3)	Cu(3)−S(2)−Cu(2)	88.2(2)
Cu(4)−S(2)−Cu(2)	119.5(3)	Cu(1)−Cl(1)'−Cu(2)'	104.3(2)
Cu(1)−Cl(1)'−Cu(4)	126.4(2)	Cu(2)−Cl(1)−Cu(4)	125.9(2)
Cu(1)'−Cl(2)−Cu(2)	84.5(2)		

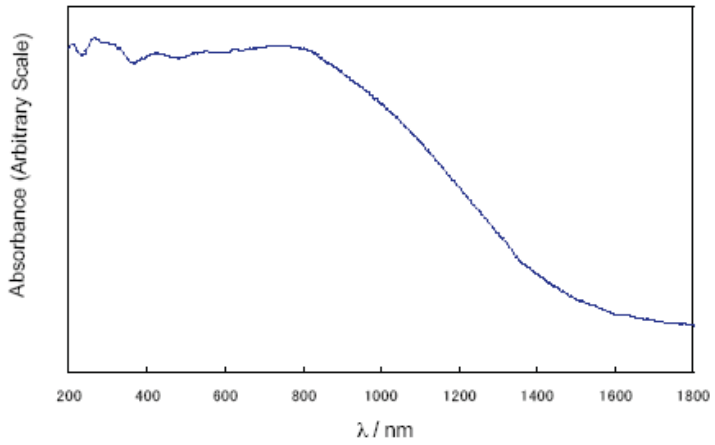

Fig. 4. Diffuse reflectance spectra of $[Cu^{I}_4Cu^{II}_4(peampt)_4Cl_8]\cdot 2H_2O$ (2).

The former two absorption bands in the UV region can be attributed to chloro-to-Cu^{II} and thiolato-to-Cu^{II} charge transfer transitions, respectively [13]. The absorption bands in the visible region can be assigned to the d-d transitions of the $Cu^{II}N_2SCl_2$ chromophores. The mixed-valence state of **2** may be considered to be fully localized because of no observation of the IT band in the near IR region.

The magnetic moment of **2** is 2.98 μ_B at 300 K per $[Cu^{I}_4Cu^{II}_4(peampt)_4Cl_8]\cdot 2H_2O$ unit, which is lower than the spin-only value of 3.46 μ_B. Temperature dependence of the magnetic susceptibilities and moments are shown in Fig. 5.

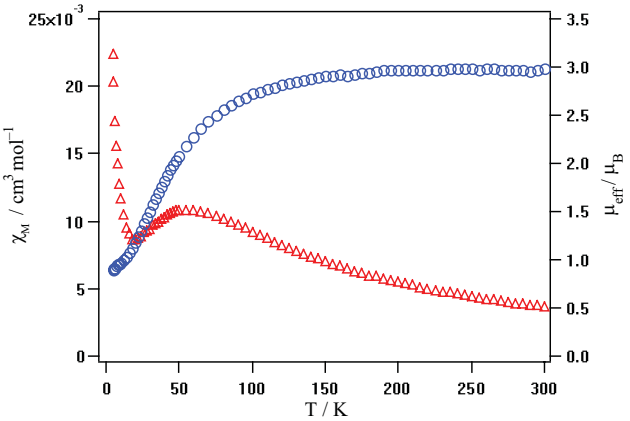

Fig. 5. Temperature dependence of magnetic susceptibilities and moments of $[Cu^{I}_4Cu^{II}_4(peampt)_4Cl_8]\cdot 2H_2O$ (2).

The magnetic moment is decreased with lowering the temperature. Thus, we can expect an antiferromagnetic interaction is operating between the four copper(II) ions. Although some attempts of fitting the magnetic data by using the van Vleck equation based on the Heisenberg model $H = -2[J_1(S_1 \bullet S_2 + S_3 \bullet S_4) + J_2(S_1 \bullet S_4 + S_2 \bullet S_3)]$ considering the location of the four copper(II) ions [15], where J_1 and J_2 correspond to the magnetic interactions between the Cu1' and Cu2 (Cu1 and Cu2') and the Cu1 and Cu2 (Cu1' and Cu2') ions, respectively, were made, reasonable magnetic parameters were not obtained because of the serious influence of the paramagnetic impurity at low temperature.

CONCLUSIONS

N,N,S-donor tridentate thiol, 1-[(2-pyridylethyl)amino]methylpropane-2-thiol (Hpeampt), was synthesized and proved to be worked to prepare a thiolato-bridged mixed valent complex. Analytical data, IR and UV-vis spectroscopic data, and magnetic susceptibility data as well as X-ray crystal structure support a localized mixed-valent $Cu^{I}Cu^{II}$ state of the thiolato-bridged complex with $peampt^-$. The formation of the octanuclear cluster may be achieved by the protection from oxidation reaction and solvent attack through the steric hindrance of the β-methyl groups of the present thiolic ligand.

EXPERIMENTAL

Synthesis: Syntheses of tholic ligand and metal complex were carried out by using standard Schlenk techniques under argon. The thiolic ligand Hpeampt was synthesized as follows. A toluene solution (70 mL) of isobutylene sulfide (11.8 g, 0.13 mol) was added dropwise to a toluene solution (50 mL) containing 2-(2-aminoethyl)pyridine. The solution was refluxed for 24 h. Then, the solvent was removed by distillation and the product was fractionally distilled at reduced pressure. Bp. 138-140°C/5 mmHg.

$[Cu^{I}_4Cu^{II}_4(peampt)_4Cl_8]\cdot 2H_2O$ (**2**). To a solution of Hpeampt (42 mg, 0.2 mmol) in methanol (5 mL) was added a solution (5 mL) of copper(II) chloride dihydrate (17 mg, 0.1 mmol) in methanol (5 mL). The reaction mixture was stirred at 80°C for 10 min. The resulting dark brown solution was allowed to stand several days at room temperature. The black plates deposited were collected by filtration. Found: C, 32.15; H, 4.39; N, 6.33%. Calcd for $C_{44}H_{72}Cl_8Cu_8N_8O_2S_4$, C, 31.73; H, 4.36; N, 6.73%. IR (KBr, cm^{-1}): ν_{as}(OH) 3449, ν_s(NH) 3254, 3205, $\nu(CH_3)$ 2960, $\nu(CH_2)$ 2860. Diffuse reflectance spectra (λ_{max}/nm): 266, 330, 425sh, 554, 628, 736. Magnetic moment (μ_{eff}/μ_B (T/K)): 2.98 (300).

Measurements: Elemental analyses for carbon, hydrogen, and nitrogen were done using a Thermo-Finnigan FLASH EA1112 analyzer. Infrared spectra were measured with a JASCO MFT-2000 FT-IR Spectrometer in the 4000—600 cm^{-1} region. Electronic spectra were measured with a Shimadzu UV-vis-NIR Recording Spectrophotometer (Model UV-3100). Variable-temperature magnetic susceptibilities were measured with a Quantum Design MPMS-5S SQUID susceptometer operating at a magnetic field of 0.5 T over a range of 4.5—300 K. The susceptibilities were corrected for the diamagnetism of the constituent atoms using Pascal's constants. The effective magnetic moments were calculated from the equation $\mu_{eff} = 2.828\sqrt{\chi_M T}$, where χ_M is the molar magnetic susceptibility.

X-Ray Crystallography: A preliminary examination was made and data were collected on a Bruker CCD X-ray diffractometer (SMART APEX) using graphite-monochromated Mo-*K*α radiation at 20±2 °C. The structure was solved by direct methods and refined by full-matrix least-squares methods. All non-hydrogen atoms were refined with anisotropic thermal parameters. The hydrogen atoms were inserted at their calculated positions and fixed at their positions. All of the calculations were carried out on a Pentium III Windows NT computer utilizing the SHELXTL software package. CCDC 632152 (**2**) contains supplementary crystallographic data for this paper. These data can be obtained free of charge at www.ccdc.cam.ac.uk/conts/retrieving.html [or from the Cambridge Crystallographic Data Centre, 12 Union Road, Cambridge CB12 1EZ, UK; fax: (internet.) +44-1223/336-033; E-mail: deposit@ccdc.cam.ac.uk].

ACKNOWLEDGEMENTS

The present work was partially supported by the "Open research Center" Project for private Universities: matching fund subsidy and Grants-in-Aid for Scientific research Nos. 16550062 and 19550074 from the Ministry of Education, Culture, Sports, Science and Technology (Japan).

REFERENCES

[1] Fleischer, H. Coord. Chem. Rev. 2005, 249, 799-827.
[2] Andrew, C. R.; Sanders-Loehr, J. Acc. Chem. Res. 1996, 29, 365-372.
[3] Mandal, S.; Das, G.; Singh, R.; Shukla, R.; Bharadwaj, P. K. Coord. Chem. Rev. 1997, 160, 191-235.
[4] Handa, M.; Mikuriya, M; Zhuang, J.-Z.; Okawa, H.; Kida, S. Bull. Chem. Soc. Jpn. 1988, 61, 3883-3887.
[5] Kawahashi, T.; Mikuriya, M.; Nukada, R.; Lim, J.-W. Bull. Chem. Soc. Jpn. 2001, 74, 323-329.
[6] Mikuriya, M.; Xiao, J.; Ikemi, S.; Kawahashi, T.; Tsutsumi, H. Bull. Chem. Soc. Jpn. 1998, 71, 2161-2168.
[7] Mikuriya, M.; Adachi, F.; Iwasawa, H.; Handa, M.; Koikawa, M.; Okawa, H. Bull. Chem. Soc. Jpn. 1994, 67, 3263-3270.
[8] Mikuriya, M.; Kotera, T.; Adachi, F.; Handa, M.; Koikawa, M.; Okawa, H. Bull. Chem. Soc. Jpn. 1995, 68, 574-580.
[9] Mikuriya, M.; Xiao, J.; Ikemi, S.; Kawahashi, T.; Tsutsumi, H.; Nakasone, A.; Lim, J.-W. Inorg. Chim. Acta 2001, 312, 183-187.
[10] Kotera, T.; Fujita, A.; Mikuriya, M.; Tsutsumi, H.; Handa, M. Inorg. Chem. Commun. 2003, 6, 322-324.
[11] Mikuriya, M.; Tsutsumi, H.; Nukada, R.; Handa, M.; Sayama, Y. Bull. Chem. Soc. Jpn. 1996, 69, 3489-3498.
[12] Kotera, T.; Fujita, A.; Mikuriya, M.; Handa, M. Materi. Sci. 2003, 21, 171-179.
[13] Kotera, T.; Mikuriya, M. Chem. Lett. 2002, 654-655.
[14] Dunaj-Jurco, M.; Ondrejovic, G.; Melnik, M. Coord. Chem. Rev. 1988, 83, 1-28.
[15] Alzuet, G.; Real, J. A.; Borras, J.; Santiago-Garcia, R.; Garcia-Granda, S. Inorg. Chem. 2001, 40, 2420-2423.

STEROIDAL GLYCOSIDES FROM THE SEEDS OF HYOSCYAMUS NIGER L. AND THEIR ANTIFUNGAL ACTIVITY

Irina Lunga,[a]* Pavel Chintea,[a] Stepan Shvets,[a] Anna Favel[b] and Cosimo Pizza[c]

[a] *Institute of Genetics and Physiology of Plants, Academy of Sciences of Moldova,Padurii 20, 2004, Chisinau, Moldova*
[b]*Laboratory of Botany, Cryptogamy and Cellular Biology, Faculty of Pharmacy, 27 Bd. J. Moulin 13385 Marseille Cedex 5, France*
[c]*Department of Pharmaceutical Sciences, University of Salerno, Ponte Don Melillo, 84084, Fisciano, Salerno, Italy*
* lunga_irina@yahoo.com, tel. 373 22 555259, fax 373 22 556180

Abstract: Phytochemical analysis of the seeds of *Hyocyamus niger L.* (Solonaceae) resulted in the isolation of six steroidal glycosides, two furostanol (**1**, **2**) and four spirostanol saponins (**3, 4, 5, 6**), which were found in this plant for the first time. The structures of these compounds were determined by detailed analysis of their spectral data, including two-dimensional NMR spectroscopy and MS spectroscopy. The antifungal activity of a crude steroidal glycoside extract, fractions of spirostanoles and individual glicosides was investigated *in vitro* against a panel of human pathogenic fungi, yeasts as well as dermatophytes and filamentous species.

Keywords: *Hyoscyamus niger L.*, steroidal glycosides, antifungal activity**.**

INTRODUCTION

The genus *Hyocyamus* belongs to the family Solonaceae and is widely distributed in Europe and Asia [1]. As a weed of cultivation it now grows also in North America and Brazil. The leaves or roots eaten produce maniacal delirium, if nothing worse. It is poisonous in all its parts, and neither drying nor boiling destroys the toxic principle.

Previously this plant never has been studied on steroidal glycosides. The chief constituent of *Hyoscyamus niger L.* (black henbane) was earlier reported by us [2]. The antifungal activity of steroidal saponins, particularly against agricultural pathogens, has been known for a long time [3-6], while other reported activities for this class of compounds include antitumor, hypoglycemic, immunoregulatory, and cardiovascular disease prevention and treatment [7].

Since several steroidal glycosides exhibit fungistatic or fungicidal activity [8,9], extract of seeds has been included in our screening programme for novel antifungal agents of plant origin. Its activity has been investigated *in vitro* against a panel of human pathogenic fungi, yeasts as well as dermatophytes and filamentous species. The antifungal activity of a spirostanoid fraction and of the individual glycosides, has been also evaluated to identify the bioactive compound.

RESULTS AND DISCUSSION

The ^{1}H NMR spectrum of **1** showed signals for four steroidal methyl groups at δ0.89 (3H, s, Me-19), 0.84 (3H, s, Me-18), 1.02 (3H, d, Me-21), 0.98 (3H, d, Me-27), two methine proton signals at δ 3.68 (1H, m, H-3) and 4.39 (1H, m, H-16) indicative of secondary alcoholic functions, two methylene proton signals at δ3.41 (1H, m, H-26a) and 3.29 (1H, m, H-26b), ascribable to a primary alcoholic function, and four anomeric protons at δ 4.40 (1H, d, J = 7.5 Hz), 4.56 (1H, d, J = 7.5 Hz), 4.69(1H, d, J = 7.5 Hz) and 4.26 (1H, d, J = 7.5 Hz). The ^{13}C NMR spectrum displayed signals ascribable to a hemiketal function at δ 113.8, two secondary carbons bearing alcoholic functions at δ 79.2 and 82.4, and one primary carbon bearing the same functionality at δ 75.9, suggesting the occurrence of a glycoside furostanol skeleton. It was evident from the ^{1}H and ^{13}C NMR data that the sugar chain at C-3 of **1** consisted of three sugar units. The chemical shifts of all the individual protons of the three sugar units were ascertained from a combination of 1D-TOCSY and DQF-COSY spectral analysis, and the ^{13}C chemical shifts of their corresponding carbons could be assigned unambiguously from the HSQC spectrum. These data showed the presence of one β-galactopyranosyl unit (δ 4.40) and two β-glucopyranosyl unit (δ 4.56 and 4.69). A glycosidation shifts were observed for C-4_{gal} (δ 80.3) and for C-2_{glc}(δ 85.9). The HMBC spectrum showed key correlation peaks between the proton signal at δ 4.40 (H-1_{gal}) and the carbon resonance at δ 79.2 (C-3 of the aglycon), the proton signal at δ 4.56 (H-1_{glc}) and the carbon resonance at δ 80.3 (C-4_{gal}), the proton signal at δ 4.69 (H-1_{glcI}) and the carbon resonance at δ 85.9 (C-2_{glc}), the proton signal at δ 4.26 (H-1_{glcII}) and the carbon resonance at δ 75.9 (C-26 of the aglycon).

Table 1

^{13}C NMR spectral data (300 MHz, CD_3OD) of saponins (1-3)

Carbon	1	2	3
1	37.9	38.3	38.2
2	30.4	30.5	30.6
3	79.2	78.9	79.3
4	34.9	34.8	35.2
5	46.0	46.0	45.6
6	32.9	33.0	32.9
7	32.7	32.7	32.6
8	34.6	34.7	36.3
9	55.7	55.7	55.6
10	36.0	36.0	36.4
11	30.9	22.0	21.8
12	40.8	40.8	40.7
13	55.9	55.9	41.5
14	57.3	57.4	57.4
15	32.4	32.8	32.4
16	82.4	82.2	82.0
17	64.9	64.9	63.5
18	16.5	16.5	16.9
19	12.3	12.8	12.7
20	41.0	41.0	42.5
21	16.0	16.6	14.6
22	113.8	113.8	110.4
23	37.4	37.3	32.5
24	28.9	30.9	29.5
25	34.8	36.4	31.1
26	75.9	75.8	67.4
27	16.8	16.2	16.6
1′	102.7	102.3	102.7
2′	73.0	72.8	73.1
3′	75.3	75.1	75.4
4′	80.3	79.0	79.0
5′	79.3	79.3	75.0
6′	60.6	62.6	60.9
1"	105.0	105.7	105.7
2"	85.9	75.2	75.4
3"	78.0	78.2	78.0
4"	75.6	78.0	71.8
5"	71.6	71.6	78.0
6"	63.0	62.9	63.0
1‴	106.3		
2‴	76.4		
3‴	75.8		
4‴	77.9		
5‴	70.5		
6‴	61.4		
1⁗	104.7	104.1	
2⁗	74.9	74.8	
3⁗	78.4	78.0	
4⁗	71.5	71.4	
5⁗	71.6	71.2	
6⁗	62.8	63.0	

On the basis of this evidence, the structure of compound **1** was established as 3-*O*-β-D-glucopyranosyl-(1→2)-*O*-β-D-glucopyranosyl-(1→4)-*O*-β-D-galactopyranoside-[(25*R*)- 5α- furostan- 3β, 22α, 26-triol]- 26-*O*-β-D-glucopyranoside.

Comparison of the ^{1}H and ^{13}C NMR spectra of **1** and **2** indicated an identical aglycon moiety. Compound **2** was shown to contain three sugar residues from the HSQC spectrum. The anomeric protons at δ 4.39 (1H, d, *J* = 7.5 Hz), 4.54 (1H, d, *J* = 7.5 Hz) and 4.27 (1H, d, *J* = 7.5 Hz) giving correlations with carbon signals at δ 102.3, 105.7, and 104.1, respectively, were assigned to anomeric protons of β-galactopyranose and two molecules of β-glucopyranose, respectively.

Table 2

***In vitro* antifungal activity of extract, spirostanoid fraction, individual glicosides, given as minimum fungicidal concentrations (μg/mL)**

Species	Extract	Spirost. fraction	Compounds						Ref. Drug.*
			1	2	3	4	5	6	
Yeast									
Candida albicans ATCC 90029	0.125	50	>100	>100	25	25	25	25	1.56
C.albicans 38248	0.125	50	100	100	12.5	12.5	12.5	12.5	1.56
C.albicans 40109	0.125	50	>100	>100	25	25	25	12.5	1.56
C. tropicalis IP 1275-81	0.06	25	>100	>100	12.5	12.5	12.5	12.5	12.5
C. parapsilosis ATCC 220	0.06	50	>100	>100	12.5	12.5	12.5	12.5	3.12
C. glabrata ATCC 90030	0.06	25	100	100	12.5	12.5	12.5	12.5	0.78
C. kefir Y0106	>1	>100	N.T.	N.T.	>100	>100	>100	100	0.78
C. kruse ATCC 6258	0.25	>100	>100	>100	25	25	25	25	3.12
C. lusitaniae CBS 6936	>1	>100	N.T.	N.T.	>100	>100	>100	100	1.56
Cryptococcus neoformans	0.06	25	>100	>100	12.5	12.5	12.5	12.5	0.78
Dermatophytes									
Trichophyton rubrum	0.5	7.8	>100	>100	6.25	6.25	6.25	3.12	1.56
Trichophyton mentagraphytes	0.5	15.6	>100	>100	6.25	6.25	6.25	6.25	1.56
Trichophyton soudanense	1.0	15.6	N.T.	N.T.	12.5	12.5	12.5	12.5	1.56
Microsporum canis	0.5	7.8	>100	>100	6.25	6.25	6.25	3.12	1.56
M. gypseum	0.5	7.8	>100	>100	6.25	6.25	6.25	3.12	1.56
Epidermophyton floccosum	0.5	7.8	>100	>100	6.25	6.25	6.25	6.25	1.56
Filamentous fungi									
Aspergillus funigatus	10	100	N.T.	N.T.	75	75	75	50	1.56
A. flavus	7.5	31.2	N.T.	N.T.	6.25	6.25	6.25	3.12	0.78
Scopulariopsiss brevicaulis	15	250	N.T.	N.T.	125	125	125	100	3.12

*The reference antifungal agents were amphotericin B and ketoconazole for yeasts and filamentous fungi, and dermatophytes, respectively.

The point of attachment of these sugars was then deduced from the HMBC of **2** which showed a cross peak between the H-1 Gal at δ 4.39 and C-3 of the aglycon at δ 78.9. Other correlations between H-1 GlcI at δ 4.27 and C-26 of the aglycon at δ 75.8; and between H-1 Glc at δ 4.54 and C-4 Gal at δ 79.0. On the basis of the above results the

structure of **2** was determined as 3-*O*-β-D-glucopyranosyl -(1→4)-*O*-β-D-galactopyranoside-[(25*R*) - 5α- furostan- 3β, 22α, 26-triol]-26-*O*-β-D-glucopyranoside. The presented chemical structures have been previously reported in *Petunia hybrida* by Shvets et al. in 1995 [10].

The ^{1}H NMR spectrum of **3** showed signals for four methyl groups at δ 0.89 (3H, s, Me-19), 0.82 (3H, s, Me-18), 1.00 (3H, d, Me-21), 1.12 (3H, d, Me-27). The HMBC correlation of methyl groups clearly showed that the aglycon moiety was similar of compound **1** and was identified as (25*R*)- 5α-spirostan-3β, 26-diol. Glycoside spirostanol skeleton is suggested according to the presence of primary alcoholic function at δ 67.7 (C-26). The ^{1}H NMR spectrum showed signals for two anomeric protons at δ 4.39 (1H, d, J = 7.5 Hz), 4.56 (1H, d, J = 7.5 Hz). The HMBC, 1D-TOCSY and DQF-COSY spectral analysis of the sugar moiety was similar to those of compound **2.** According to these data, compound **3** was assigned the structure 3-*O*-β-D-glucopyranosyl -(1→4) -*O*-β-D-galactopyranoside-(25*R*) - 5α- spirostan - 3β-ol, described with Gutsu et al. in year 1987 from *Capsicum annum* [11].

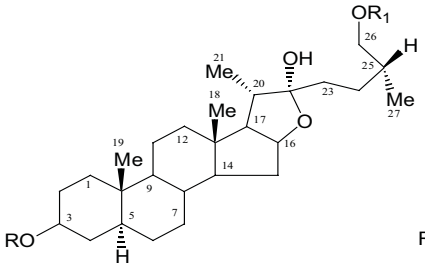

1: R=Glc(1-2)Glc(1-4)Gal; R_1=Glc
2: R=Glc(1-4)Gal; R_1=Glc

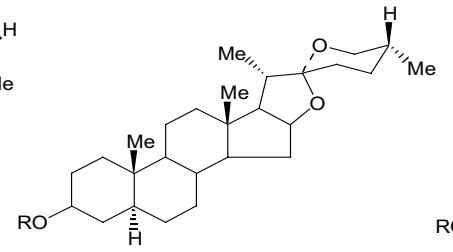

3: R=Glc(1-4)Gal
4: R=Rha(1-2)Glc
6: R=Glc(1-2)Glc(1-4)Gal

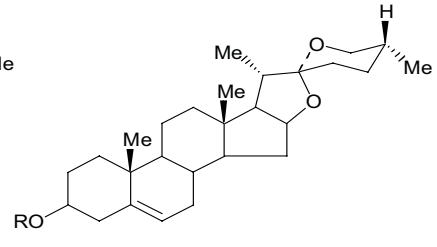

5: R=Rha(1-2)Glc

The structures of compounds **4**, **5** and **6** were elucidated by us earlier [2]. For compound **4** -3-*O*-α-L-rhamnopyranosyl-(1→2) - β - D-glucopyranoside-(25*R*) - 5α- spirostan - 3β-ol; for compound **5-** *O*-α-L-rhamnopyranosyl-(1→2) - β - D-glucopyranoside -(25*R*)- 5-ene -spirostan -3β-ol and for compound **6** -3-*O*-β-D-glucopyranosyl-(1→2)-β-D-glucopyranosyl -(1→4)-*O*-β-D-galactopyranoside-(25*R*) - 5α- spirostan - 3β-ol.

Table 2 shows that extract had a broad spectrum of antifungal activity *in vitro*. It was active against all the tested strains except for two (*C. lusitaniae* and *C. kefir*). The best antifungal activity was observed against dermatophytes and against yeasts, to a lesser extent. The least sensitive yeast species were *C.tropicalis, C. parapsilosis, C. glabrata* and *Cryptococcus neoformans*. Its activity against filamentous fungi was weak to moderate. The furostanol glycosides were devoid of any antifungal activity. The antifungal activity was found to reside entirely in the spirostanol fraction and individual glycosides with minimum inhibitory concentrations (MIC) from 7.8 to 250 μg/mL. The MICs for the dermatophytes were between 3.12 and 125 μg/mL. The most sensitive filamentous species was *A. flavus* (MIC = 3.12 μg/ mL).

EXPERIMENTAL

The seeds of *Hyoscyamus niger L*. have been collected in the scientific research field of the Institute of Scientific Researches and Technological Constructions for Tobacco and Tobacco Products of Moldova in November 2001 year. The voucher specimen has been deposited in laboratory of botanic by leading of Doctor in Biology Kalkei E.D. The air-dried seeds were extracted three times in 50°C with water saturated n-buthanol. After evaporation of n-buthanol, water extract was purified with chloroform and finally the steroidal glycosides were crystallised in acetone. The sum of steroidal saponins has been obtained in yellow powder in the yield 3,7%. Extract has been chromatographied on silica gel column (30-500mm, 60-100μm, Merck). The column was eluted with the system of solvents chloroform-methanol-water (8:2:0→20:10:1). The polar subfractions were obtained, which was further separated on a C_{18} column (7,8x300mm, LiChroprep RP18, 25-40μm, XTerra Waters) using a MeOH/H_2O (60-65% MeOH) gradient. Three single compounds were obtained.

Structures were determined by 1D- (^{1}H, ^{13}C, TOCSY), 2D (COSY, HSQC, HMBC) NMR, ESIMS and HRMS experiments. Samples were analyzed by matrix assisted laser desorption ionization (MALDI) mass spectrometry. ESIMS analyses were performed using a ThermoFinnigan (San Josè, CA, USA) LCQ Deca XP Max ion trap mass spectrometer equipped with Xcalibur software. NMR experiments in CD_3OD were performed on a Bruker DRX-600 spectrometer at 300 K. Column chromatography was performed over Silica gel (Merck). HPLC separations were carried out on a Waters 590 system equipped with a Waters R401 refractive index detector, a Waters XTerra Prep MSC_{18} column, and a U6K injector. TLC was performed on silica gel F254 (Merck) plates, and reagent grade chemicals (Carlo Erba) were used throughout.

1. HRMS, *m/z* 1081.643 [calculated for $C_{51}H_{84}O_{24}$ $(M)^+$]; 919.6 $[M-162]^+$**;** 757 $[M-2x162]^+$**;** ^{1}H NMR (aglycon)

δ 4.39 (1H, m, H-16), 3.68 (1H, m, H-3), 3.41 (1H, m, H-26a), 3.29 (1H, m, H-26b), 0.89 (3H, s, Me-19), 0.84 (3H, s, Me-18), 1.02 (3H, d, H-21), 0.98 (3H, d, Me-27). (sugars) δ4.40 (d, *J*=7.4 Hz, H-1Gal), 3.60 (dd, *J*=7.4 and 9.0 Hz, H-2Gal), 3.53 (dd, *J*=4.0 and 9.0 Hz, H-3Gal), 4.02 (dd, *J*=2.5 and 4.0 Hz, H-4Gal), 3.69 (ddd, *J*=2.5, 2.5 and 4.5 Hz, H-5Gal), 3.62 (dd, *J*=4.5 and 12.0 Hz, H-6aGal), 3.95 (dd, *J*=2.5 and 12.0 Hz, H-6bGal), 4.56 (d, *J*=7.5 Hz, H-1Glc), 3.55 (dd, *J*=7.5 and 9.0 Hz, H-2Glc), 3.60 (dd, *J*=9.0 and 9.0 Hz, H-3Glc), 3.35 (dd, *J*=9.0 and 9.0 Hz, H-4Glc), 3.25 (ddd, *J*=2.5, 4.5 and 9.0 Hz, H-5Glc), 3.60 (dd, *J*=4.5 and 11.5 Hz, H-6aGlc), 3.93 (dd, *J*=2.5 and 11.5 Hz, H-6bGlc), 4.69 (d, *J*=7.5 Hz, H-1GlcI), 3.29 (dd, *J*=7.5 and 9.0 Hz, H-2GlcI), 3.36 (dd, *J*=9.0 and 9.0 Hz, H-3GlcI), 3.40 (dd, *J*=9.0 and 9.0 Hz, H-4GlcI), 3.42 (ddd, *J*=2.5, 4.5 and 9.0 Hz, H-5GlcI), 3.69 (dd, *J*=4.5 and 11.5 Hz, H-6aGlcI), 3.82 (dd, *J*=2.5 and 11.5 Hz, H-6bGlcI), 4.26 (d, *J*=7.5 Hz, H-1GlcII), 3.20 (dd, *J*=7.5 and 9.0 Hz, H-2GlcII), 3.37 (dd, *J*=9.0 and 9.0 Hz, H-3GlcII), 3.33 (dd, *J*=9.0 and 9.0 Hz, H-4GlcII), 3.28 (ddd, *J*=2.5, 4.5 and 9.0 Hz, H-5GlcII), 3.69 (dd, *J*=4.5 and 11.5 Hz, H-6aGlcII), 3.85 (dd, *J*=2.5 and 11.5 Hz, H-6bGlcII). For ^{13}C NMR see Table 1.

2. HRMS, *m/z* 919.342 [calculated for $C_{45}H_{74}O_{19}$ $(M)^+$]; 757.53 $[M-162]^+$**;** 595 $[M-2x162]^+$**;** ^{1}H NMR (aglycon) δ 4.38 (1H, m, H-16), 3.68 (1H, m, H-3), 3.41 (1H, m, H-26a), 3.29 (1H, m, H-26b), 0.89 (3H, s, Me-19), 0.84 (3H, s, Me-18), 1.02 (3H, d, H-21), 0.98 (3H, d, Me-27). (sugars) δ4.39 (d, *J*=7.4 Hz, H-1Gal), 3.52 (dd, *J*=7.4 and 9.0 Hz, H-2Gal), 3.53 (dd, *J*=4.0 and 9.0 Hz, H-3Gal), 4.08 (dd, *J*=2.5 and 4.0 Hz, H-4Gal), 3.69 (ddd, *J*=2.5, 2.5 and 4.5 Hz, H-5Gal), 3.70 (dd, *J*=4.5 and 12.0 Hz, H-6aGal), 3.92 (dd, *J*=2.5 and 12.0 Hz, H-6bGal), 4.54 (d, *J*=7.5 Hz, H-1Glc), 3.55 (dd, *J*=7.5 and 9.0 Hz, H-2Glc), 3.38 (dd, *J*=9.0 and 9.0 Hz, H-3Glc), 3.35 (dd, *J*=9.0 and 9.0 Hz, H-4Glc), 3.24 (ddd, *J*=2.5, 4.5 and 9.0 Hz, H-5Glc), 3.69 (dd, *J*=4.5 and 11.5 Hz, H-6aGlc), 3.89 (dd, *J*=2.5 and 11.5 Hz, H-6bGlc), 4.27 (d, *J*=7.5 Hz, H-1GlcI), 3.20 (dd, *J*=7.5 and 9.0 Hz, H-2GlcI), 3.37 (dd, *J*=9.0 and 9.0 Hz, H-3GlcI), 3.32 (dd, *J*=9.0 and 9.0 Hz, H-4GlcI), 3.29 (ddd, *J*=2.5, 4.5 and 9.0 Hz, H-5GlcI), 3.69 (dd, *J*=4.5 and 11.5 Hz, H-6aGlcI), 3.84 (dd, *J*=2.5 and 11.5 Hz, H-6bGlcI). For ^{13}C NMR see Table 1.

3. HRMS, *m/z* 741.452 [calculated for $C_{39}H_{64}O_{13}$ $(M)^+$]; 579.3 $[M-162]^+$; ^{1}H NMR (aglycon) δ 4.41 (1H, m, H-16), 3.68 (1H, m, H-3), 3.46 (1H, m, H-26a), 3.33 (1H, m, H-26b), 0.88 (3H, s, Me-19), 0.81 (3H, s, Me-18), 0.98 (3H, d, H-21), 1.10 (3H, d, Me-27). (sugars) δ4.38 (d, *J*=7.4 Hz, H-1Gal), 3.51 (dd, *J*=7.4 and 9.0 Hz, H-2Gal), 3.53 (dd, *J*=4.0 and 9.0 Hz, H-3Gal), 4.08 (dd, *J*=2.5 and 4.0 Hz, H-4Gal), 3.58 (ddd, *J*=2.5, 2.5 and 4.5 Hz, H-5Gal), 3.63 (dd, *J*=4.5 and 12.0 Hz, H-6aGal), 3.90 (dd, *J*=2.5 and 12.0 Hz, H-6bGal), 4.53 (d, *J*=7.5 Hz, H-1Glc), 3.29 (dd, *J*=7.5 and 9.0 Hz, H-2Glc), 3.39 (dd, *J*=9.0 and 9.0 Hz, H-3Glc), 3.24 (dd, *J*=9.0 and 9.0 Hz, H-4Glc), 3.31 (ddd, *J*=2.5, 4.5 and 9.0 Hz, H-5Glc), 3.62 (dd, *J*=4.5 and 11.5 Hz, H-6aGlc), 3.93 (dd, *J*=2.5 and 11.5 Hz, H-6bGlc). For ^{13}C NMR see Table 1.

Antifungal assays. Whatever the tested product (extract, spirostanol fraction, individual glycosides) and the test microorganisms (yeasts, dermatophytes, filamentous fungi), the antifungal activity was evaluated with an agar dilution method, as previously described [12]. Yeast nitrogen base (Difco, Becton Dickinson, Sparks, MD) supplemented with 2% agar (Difco) was used as a test medium for yeasts. For dermatophytes and filamentous species, the tests were performed on Sabouraud dextrose agar (Difco). Eight reference yeast strains were used: *Candida albicans* ATCC 90029, *Candida albicans* Y0109, *Candida albicans* 38248*, Candida tropicalis* IP 1275-81, *Candida parapsilosis* ATCC 22019, *Candida glabrata* ATCC 90030, *Candida kefyr* Y 0106, *Candida krusei* ATCC 6258 and *Candida lusitaniae* CBS 6936. Dermatophytes (one isolate of each species: *Trichophyton mentagrophytes*, *Trichophyton rubrum*, *Trichophyton soudanense*, *Microsporum canis*, *Microsporum gypseum*, *Epidermophyton floccosum*) and *Cryptococcus neoformans* were all clinical isolates. Filamentous fungi (one isolate of each species: *Aspergillus fumigatus*, *Aspergillus flavus, Scopulariopsis brevicaulis*) were environmental isolates. All samples were dissolved in dimethyl sulphoxide (DMSO). The tested concentrations were 0.03 mg/mL for extract, and from 0.0625 to 10 μg/mL for pure compounds and the fractions. The final concentration of DMSO never exceeded 1%. The minimum inhibitory concentration was defined as the first concentration showing no visible growth after the incubation time (48 h for the yeasts, 5–15 days for the dermatophytes and the filamentous fungi according to the species). The tests were performed in duplicate and in two separate experiments. Amphotericin B and ketoconazole (Sigma Chemical Co., St Louis, MO) were included in the assays as reference antifungal agents, for yeasts and filamentous fungi, and dermatophytes, respectively.

CONCLUSION

During the investigation six steroidal glycosides have been isolated from the seeds of *Hyoscyamus niger L.* for the first time. In this work the following structures have been suggested for three of them: compound **1** - 3-*O*-β-D-glucopyranosyl-(1→2)-*O*-β-D-glucopyranosyl-(1→4)-*O*-β-D-galactopyranosyl-[(25*R*)- 5α- furostan- 3β, 22α, 26-triol]- 26-*O*-β-D-glucopyranoside; compound **2 -** 3-*O*-β-D-glucopyranosyl -(1→4)-*O*-β-D-galactopyranosyl-[(25*R*) - 5α- furostan- 3β, 22α, 26-triol]-26-*O*-β-D-glucopyranoside; compound **3 -** 3-*O*-β-D-glucopyranosyl -(1→4) -*O*-β-D-galactopyranoside-(25*R*) - 5α- spirostan - 3β-ol. Structural determination of steroidal glycosides **4, 5** and **6** have been reported in previous work.

The results of biological tests revealed that antifungal steroidal glycosides are present in *Hyoscyamus niger* seeds. *In vitro* spirostanol fraction and glycosides showed a broad spectrum of antifungal activity. Only slight differences in their fungicidal profiles were observed. Not surprisingly, these compounds are monodesmosidic spirostanol glycosides

like the majority of biologically active steroid saponins [9]. The antifungal properties of saponins are usually ascribed to their ability to complex with sterols in fungal membranes, thereby causing pore formation and loss of membrane integrity [13]. Interestingly, the tested extracts and compounds were inactive against *C. lusitaniae* ATCC 6936 although its sterol composition was shown to be similar to that of *C. albicans* ATCC 90029 [14]. Because antifungal agents must pass through the polysaccharidic cell wall first before reaching the target, this finding could be related to an unusual cell wall structure of this emerging yeast pathogen.

Thus, our study revealed the therapeutic potential of some spirostanol glycosides from *Hyoscyamus niger* seeds. Extract, which showed good activity against dermatophytes and which is readily available in large quantities, is a promising active principle for the topical treatment of dermatophytosis. Therefore, it is wortwhile to further study these antifungal compounds and, in a broad sense, the structure-activity relationships of more steroidal saponins to explore the therapeutic potential of this important class of natural products as antifungal leads for drug discovery.

ACKNOWLEDGMENTS

Financial support from INTAS (The International Association for the Promotion of Co-operation with Scientists from the New Independent States) is gratefully acknowledged. Also we are grateful to Prof. Carla Bassarello and Prof. Paola Montoro from the Department of Pharmaceutical Sciences, University of Salerno for the measurements of the mass spectra and NMR analysis.

REFERENCES

[1] Kirtikar, K.R.; Basu, B.D.; Indian Medicinal Plants, Reprint ed., Periodical Experts, New Delhi, 1975, 3, pp 1794-1795.

[2] Lunga, I.; Kintia, P.; Shvets, S.; Bassarello, C.; Pizza, C.; Piacente, S. Three spirostanol glycosides from the seeds of Hyoscyamus niger L., Chemistry Journal of Moldova, 2006, 1, pp 123-127.

[3] Dimoglo, A. S.; Choban, I. N.; Bersuker, I. B.; Kintia, P. K.; Balashova, N. N. Structure-activity correlations for the antioxidant and antifungal properties of steroid glycosides. Bioorg. Khim., 1985, 11, pp 408–413.

[4] Imai, S.; Fujioka, S.; Murata, E.; Goto, M.; Kawasaki, T.; Yamauchi, T. Bioassay of crude drugs and oriental crude drug preparations. XXII. Search for biologically active plant ingredients by means of antimicrobial tests: 4. Antifungal activity of dioscin and related compounds. Takeda Kenkyusho Nenpo, 1967, 26, pp 76–83.

[5] Wolters, B. The share of the steroid saponins in the antibiotic action of *Solanum dulcumata*. Planta Med, 1965, 13, pp 189–193.

[6] Wolters, B. Antimicrobial activity of plant steroids and triterpenes. Planta Med, 1966, 14, pp 392–401.

[7] Sparg, S. G.; Light, M. E.; Staden J. V. Biological activities and distribution of plant saponins. J. Ethnopharmacol. 2004, 94, pp 219–243.

[8] Lacaille-Dubois, M. A.; Wagner, H. A review of the biological and pharmacological activities of saponins. Phytomedicine, 1996, 2, pp 363–386.

[9] Hostettman, K. A.; Marston, A. Saponins. Cambridge University Press: Cambridge, 1995.

[10] Shvets, S. A.; Naibi, A. M.; Kintia, P. K. Steroidal glycosides from Petunia hybrida seeds. II. Structure of petuniosides I, L and N. Inst. Genet., AN Respub. Moldova, Chisinau, Moldova. Khimiya Prirodnykh Soedinenii, 1995, 2, pp 247-52.

[11] Gutsu, E.V.; Kintia, P.K.; Lazur'evskii, G.V. Steroidal glycosides of Capsicum annuum root. Part II. Structure of capsicosides. Khimia Prirodnykh Soedinenii, 1987, 2, pp 242-246.

[12] Favel, A,; Steinmetz, M.D.; Regli, P. et al. In vitro antifungal activity of triterpenoid saponins. Planta Med, 1994, 60, pp 50–53.

[13] Morrissey, J.P.; Osbourn, A. E. Fungal resistance to plant antibiotic as a mechanism of athogenesis. Microbiol. Mol., Biol. Rev., 1999, 63, pp 708–724.

[14] Peyron, F.; Favel, A.; Calaf, R. et al. Sterol and fatty acid composition of Candida lusitaniae clinical isolates. Antimicrob Agents Chemother, 2002, 46, pp 531–533.

SYNTHESIS OF 7α- AND 17-BROMONORAMBREINOLIDES FROM NORAMBREINOLIDE

Pavel F. Vlad,[a*] Alexandru G. Ciocarlan,[a] Grigore N. Mironov,[a] Mihai N. Coltsa,[a] Yurii A. Simonov,[b] Victor Ch. Kravtsov[b] and Janusz Lipkowski[c]

[a]*Institute of Chemistry, Academy of Sciences of Moldova, Academiei str. 3, MD-2028 Chisinau, Republic of Moldova*
[b]*Institute of Applied Physics, Academy of Sciences of Moldova, Academiei str. 5, MD-2028 Chisinau, Republic of Moldova*
[c]*Institute of Physical Chemistry of the Polish Academy of Sciences, Kasprzaka 44/52, Warzawa,PL-01224, Poland*
**E-mail: vlad_p@mail.md; Phone: 373 22 739775; Fax: 373 22 739775*

Abstract: A mixture of 7α- and 17-bromonorambreinolides was obtained on treatment of the mixture of isomeric methyl bicyclohomofarnesenoates, the norambreinolide transformation product, with NBS and H_2O_2. The structure of 7α- and 17-bromonorambreinolides was elucidated on the basis of spectral data. The structure of 17-bromonorambreinolide was confirmed by its reduction with $LiAlH_4$ into sclaradiol, and that of 7α-bromonorambreinolide by X-ray analysis.

Keywords: 7α- and 17-bromonorambreinolides, synthesis, X-rays analysis.

INTRODUCTION

Norambreinolide [sclareolide, 8α,12-epoxi-14,15,16,17-tetranorlabdane-12-one] (1) is a valuable, commercially available chirone, formed on oxidative degradation of a series of labdanic diterpenoides [1]. It served as starting compound in the synthesis of many drimanic sesquiterpenoids [2-5] and some higher terpenoids [6,7]. However, to a certain extent, synthetic possibilities of the norambreinolide are limited because in its molecule there are only two functional groups, at C(8) and C(12). In connection with this it was of interest to obtain its derivatives with functional groups at other carbon atoms of cycle B and especially at hardly accessible position C(17).

RESULTS AND DISCUSSIONS

Herein, we describe a short synthesis of the mixture of 7α- and 17-bromonorambreinolides (2) and (3) from norambreinolide (1). The latter was transformed according to the known procedure [8] in high yield into the mixture of methyl bicyclohomofarnesenoates (4) (scheme 1). On treatment of this esters mixture in mild conditions with NBS and an aqueous solution of hydrogen peroxide a mixture of two products was formed which were separated by column chromatography on SiO_2. Their structure was determined on the bases of analytical and spectral data and for the more polar compound was also confirmed by X-ray analysis.

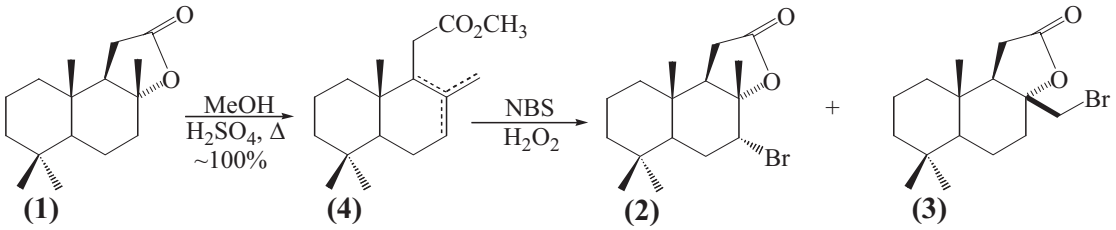

Scheme 1.

The less polar product according to the elemental analysis has the composition $C_{16}H_{25}BrO_2$. Its IR spectrum exhibits absorption bands of the C-Br-bond at 653 cm^{-1} and a γ-lactone at 1793 cm^{-1}. In the ^1H NMR spectrum of this compound three-protons singlet signals of three tertiary methyl groups are presented, one methyl group less then in the starting compound (1). In the low field region of its ^1H NMR spectrum besides the signals of $–CH-CH_2CO$-group, there are at 3.36 and 3.37 ppm two one protone doublets belonging to the AB-system of the group $≡C-CH_2Br$. Since the signal of C(10)-CH_3 group in the ^1H NMR spectrum of investigated bromolactone was not shifted downfield in comparison with its signal in the spectrum of norambreinolide (1) [9], the $–CH_2Br$ group is placed on the β-side of molecule and has axial configuration. This conclusion was confirmed also by chemical data: on the reaction of investigated bromolactone with $LiAlH_4$ in THF the known diol (5) was obtain (scheme 2). Thus, on this treatment not only the lactone group, but also the CH_2Br group were reduced. The summary of the above mentioned data proved that the studied bromolactone is the 17-bromonorambreinolide (3). It contains the bromine atom at a hardly accessible position and can served for the synthesis of terpenoids in which the C(17) carbon atom is functionalized (see, for example, the articles [10-15]).

Further elution with the same solvent yielded the major reaction product, having the same elemental composition as compound (3) (scheme 1). Its IR spectrum contains absorption bands characteristic of a C-Br bond at 657 cm^{-1} and a

γ-lactone group at 1791 cm^{-1}. In the low field portion of ^1H NMR spectrum besides the signals of $C(11)H_2$-group there are the signals of the proton at C(7) carbon atom, bonded with the bromine atom. In such a way the major reaction product is the 7α-norambreinolide (2). The structure of this compound was confirmed not only by spectral data but also by X-ray analysis.

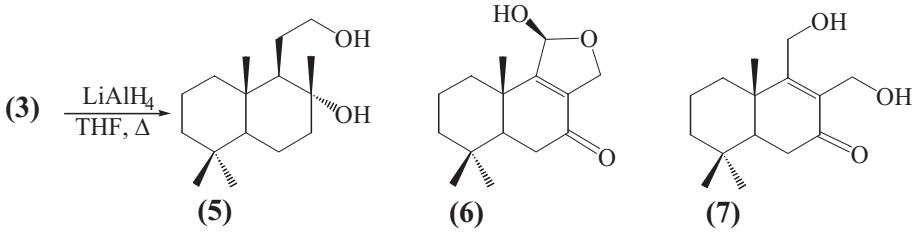

Scheme 2.

Crystal structure determination

The structure of compound (2) has been confirmed by X-ray single crystal method. X-Ray data were collected on a KUMA Diffraction KM4 at 100 K using graphite-monochromated Cu-Kα radiation. Lattice parameters were obtained from least-squares refinement of 25 reflections with 22°≤ 2Θ≤52°. There was no intensity decay during data collection. Structure was solved by direct methods (SHELXS-97) and refined by full-matrix least-squares methods based on F^2 (SHELXL–97) [16]. Lorentz and polarization corrections were applied for diffracted reflections. The non–hydrogen atoms were refined anisotropically and hydrogen atoms isotropically. The crystallographic data and details of structure refinement are listed in Table1. Crystallographic data for the structural analysis have been deposited with the Cambridge Crystallographic Data Center, CCDC NO. 646964 . Copy of this information may be obtained free of charge from The Director, CCDC, 12 Union Road, Cambridge CB2 1EZ, UK (fax:+44-1223-336-033; e-mail: deposit@ccdc.cam.ac.uk or http://www.ccdc.cam.ac.uk).

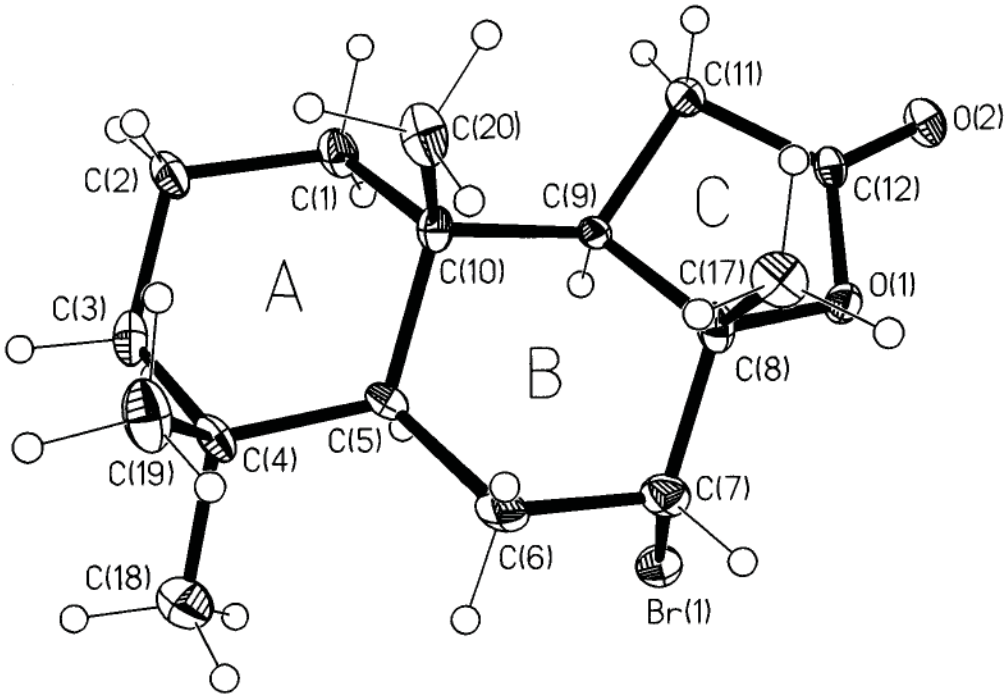

Figure 1.

View of molecule in two projections with numbering scheme is shown in Figure 1 and 2. X-ray study unambiguously proves the molecular structure of (2). Both cyclohexyl rings, A and B have chair conformation. Atoms C(1), C(2), C(4), C(5) are coplanar within ±0.018Å.. The displacement of atoms C(3) and C(10) from this plane are -0.625(9) and 0.700 Å respectively. The Cremer-Pople (CP) parameters [17] for cycle A: Θ=4.9(6)º, φ = -11(8) º and Q=0.567(7)Å. In cycle B the atoms C(8) and C(5) displace at 0.695(10) and –0.683(9)Å out of the plane of C(6)C(10)C(9)C(7) atoms, which are coplanar within ±0.013Å. CP parameters for cycle B are Θ=2.4(6)º, φ=-101(16)º and Q=0.592(7)Å. Methyl groups at atoms C(8) and C(10) reside axial position and at C(4)-axial C(19) and equatorial C(18) positions. Such arrangement of methyl groups lead to stressed 1,5-intramolecular contacts C(19)···C(20)=3.23(1)

and C(20)···C(17)=3.14Å. The similar stressed intramolecular contacts have been found in related compounds having the same skeleton, namely in the structures of 11,12-epoxydrim-8-en-11β-ol-7-one (6) [18] and 11,12-dihydroxydrim-8-en-7-one (7) [19], where such intramolecular contacts equal 3.32 and 3.35Å, respectively. One can suppose that such contacts always take place in molecules of this type and cause the slight distortion of tetrahedral angles at carbon atoms of molecular skeleton. Bromine atom reside axial position at C(7) opposite to axial methyl groups (Fig. 2). The distance C(7)-Br(1) equals 1.973(7)Å. The carbon-carbon distances in cyclohexyl rings are in the range 1.521(8)-1.575(9)Å, C-CH_3 - 1.517(9)-1.535(9)Å. Tetrahydrofuran cycle C has an envelop conformation. Displacement of atoms C(9) and O(2) from the mean plane of coplanar within ±0.048Å remaining atoms of five membered cycle equal –0.655(10) and –0.16(10)Å, respectively. The puckering parameters (CP) of cycle C φ=-118.1(7)º and q2 =0.430(7)Å close to value φ=108º for ideal envelop. The distances in cycle C C(12)-O(2)=1.215(8)Å, O(1)-C(12)=1.354(8)Å, O(1)-C(8)=1.468(8) Å, C(12)-C(11)=1.508(8)Å indicate π-conjunction in the fragment O(2)C(12)O(1). Endo-cyclic angle at O(1) equals 108.2(6)º.

The majority of intermolecular contacts in crystal are Van-der-Waals type. The shortest contacts are Br(1)···C(11)=3.798(8)Å, Br(1)···C(17)=3.843(9)Å, O(1)···C(7)=3.435(9)Å, O(1)···C(17)Å and O(2)···C(20)=3.342Å. The last described contacts may be rate as C-H···O hydrogen bond [20], H···O =2.50Å and angle C-H···O=144º. The shortened contacts take place between two-fold screw axis and translations *a* and *b* related molecules.

The nearest contacts between the neighboring in molecules of the crystal have basically Van-der-Waals character. The shortest among them are distances Br(1)…C(11) = 3.798(8) Å, Br(1)…C(17) = 3.843(9) Å, O(1)…C(7) = 3.435(9) Å, O(1)…C(17) = 3.527 Å and O(2)…C(20) = 3.342 Å. Last value can be considered as C-H…O hydrogen bond [20] with the distance H…O = 2.50 Å and an angle at H atom equals to 144°. The short intermolecular contacts are observed for the molecules connected by an 2_1 axis with basic, and also with distant from her on translation on axes X and Y.

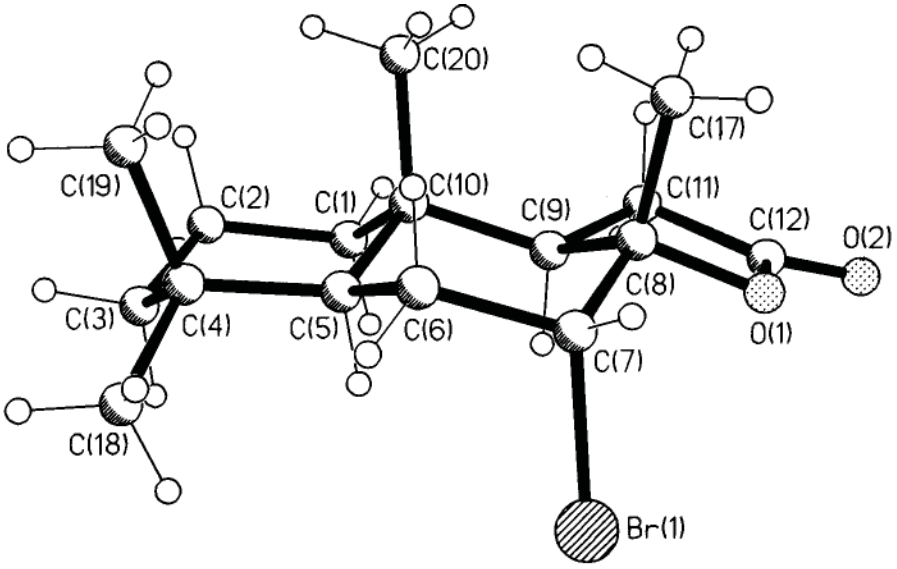

Figure 2

EXPERIMENTAL SECTION

Melting points (mp) were determined on a Boetius hot stage. IR spectra were obtained on a Specord 74 spectrometer in CCl_4. NMR ^1H and ^{13}C spectra were recorded on a Bruker WM (300.13 and 75.32 MHz) spectrometers in $CDCl_3$. Chemical shifts are given in parts per million values in δ scale with $CHCl_3$ as reference (set δ_H at 7.24 ppm and δ_C 77.00 ppm) and coupling constants in Hertz. Optical rotations were determined on a Perkin-Elmer 241 polarimeter using $CHCl_3$ as solvent. For analytical TLC the "Сорбфил" plates were used. Column chromatography was carried out on Across silica gel (60-200 mech).

Synthesis of 7α- and 17-bromonorambreinolide (2) and (3). To the solution of 300 mg (1.14 mmol) of esters mixture (4), prepared according to the procedure [8], in 3 mL of $CHCl_3$, was added on stirring at 22°C 410 mg (2.27 mmol) of NBS and then was dropped 0.2 mL of 30% H_2O_2. The mixture was stirred at the same temperature up to the finish of the reaction (24 hours, controlled by TLC). Then the reaction mixture was diluted with water (10 mL) and extracted with diethyl ether (3x15 mL). The extract was washed with 0.1 N solution of $Na_2S_2O_3$ (20 mL), water (20 mL), dried with anhydrous Na_2SO_4, filtered and concentrated in vacuo. The oil residue (400 mg) was chromatographied

on a column with silica gel (40 g). Elution with the mixture of benzene : ethylacetate 96:4 gave 82.2 mg (yield 22 %) of 17-bromonorambreinolide (3), mp 107-108°C (from petroleum ether), $[a]_D^{22}$ - 11.3° (c 0.97), Found (%): C, 58.08; H, 8.12; Br, 24.39. $C_{16}H_{25}BrO_2$. Requires (%): C, 58.36; H, 7.65; Br, 24.27. IR, ν/cm^{-1}: 653 (Br), 1793 (γ-lactone). ^{1}H NMR, *δ*: 0.87 (s, 3H, C(20)H_3), 0.89 (s, 3H, C(18)H_3), 0.90 (s, 3H, C(19)H_3), 1.10-2.23 (m, 12H), 2.39 (dd, 1H, J=1.2, 18.4 Hz), 2.68 (dd, 1H, J=8.8; 18.4 Hz, C(11)H_2), 3.36 (d, 1H, J=10.88 Hz) and 3.37 (d, 1H, J=10.88 Hz, AB-system, C(17)H_2). ^{13}C NMR, δ): 14.98, 17.86, 18.03, 21.91, 30.60, 31.48, 33.11, 33.22, 35.98, 40.17, 40.99, 41.62, 50.15, 50.99, 85.97, 176.56.

Further elution with the same solvent afforded 179.4 mg (yield 48.1%) of 7α-bromonorambreinolide (2), mp 187-188°C (from petroleum ether), $[a]_D^{22}$ - 31.3° (c 0.8). Found (%): C, 58.34; H, 8.10; Br, 24.32. $C_{16}H_{25}BrO_2$. Requires (%): C, 58.36; H, 7.67; Br, 24.27. IR, ν/cm^{-1}: 657 (Br), 1791 (γ-lactone). ^{1}H NMR, *δ*: 0.87 (s, 3H, C(20)H_3), 0.92 (s, 3H, C(18)H_3), 0.94 (s, 3H, C(19)H_3), 1.58 (s, 3H, C(17)H_3), 1.00-2.30 (m, 10H), 2.49 (dd, 1H, J=3.96, 18.4 Hz), 2.75 (dd, 1H, J=10.44, 18.4 Hz, C(11)H_2), 4.61 (dd, 1H, J=7.53, 9.90 Hz, C(7)). ^{13}C NMR, δ): 16.74, 18.01, 21.13, 27.95, 30.50, 31.15, 32.19, 33.49, 36.53, 41.48, 41.99, 49.76, 55.80, 55.89, 87.35, 175.44.

Reduction of 17-bromonorambreinolide (3) with $LiAlH_4$. To the solution of 10 mg (0.03 mmol) of 17-bromonorambreinolide (3) in 2 mL of anhydrous THF 4.6 mg (0.012 mmol) of $LiAlH_4$ was added, and the reaction mixture was refluxed for 1 h (control by TLC). The excess of $LiAlH_4$ was destroyed by ethyl acetate, the mixture was treated with 5% solution of H_2SO_4 and extracted with diethyl ether (3x5mL). The extract was washed with water (2x10 mL), dried with anhydrous Na_2SO_4, filtered and solvent removed under reduced pressure. The residue was recrystallized from the mixture of petrol ether and AcOEt (4:1), to give 5 mg of known diol (5), m.p. 130-131°C, which was identified by comparison with the authentic sample.

Table 1

Crystal data and structure refinement for 7α- bromonorambreinolide (2)

Empirical formula	$C_{16}H_{25}BrO_2$
Formula weight	329.27
Temperature, K	100(2)
Wavelength, Å	1.5418
Crystal system, space group	Monoclinic, $P2_1$
Unit cell dimensions	
a, Å	7.871(1)
b, Å	7.773(2)
c, Å	12.471(2)
β, deg.	91.00(1)
V, Å^3	762.9(3)
Z, Calculated density, Mg/m^3	2, 1.433
Absorption coefficient, mm^{-1}	3.634
F(000)	344
Crystal size, mm	0.50 x 0.10 x 0.10
θ-range for data collection, deg.	3.54 - 72.24
Limiting indices	$-9 \le h \le 0$, $0 \le k \le 9$, $-15 \le l \le 15$
Reflections collected / unique, [R_{int}]	1707 / 1595, [0.0541]
Completeness to θ =72.24deg.	97.7 %
Data / restraints / parameters	1595 / 1 / 176
Goodness-of-fit on F^2	1.030
Final *R* indices [$I>2\sigma(I)$]	$R1$ = 0.0365, $wR2$ = 0.0867
R indices (all data)	$R1$ = 0.0607, $wR2$ = 0.0956
Absolute structure parameter	-0.05(4)
Largest diff. peak and hole, e·Å^{-3}	0.540 and -0.645

REFERENCES

[1] Vlad, P.F.; Koltsa, M.N.; *Synthesis and Application of Odorous Compounds from Labdane Diterpenoids, Kishinev, Shtiintsa*, 1988, 184 p. (In Russian).
[2] Jansen, B.J.M.; de Groot A.. *Nat. Prod. Rep.,* 1991, 8, 319-337.
[3] Vlad, P.F.; Koltsa, M.N.; Mironov, G.N. Russ. Chem. Bull., 1997, 46, 855-873.
[4] Jansen, B.J.M.; de Groot A.. *Nat. Prod. Rep.* 2004, 21, 449-477.
[5] Vlad, P.F. Synthetic investigation in the field of drimanic sesquiterpenoids in „*Studies of Natural Products Chemistry, Bioactive natural products"* (Part II); Elsevier: Amsterdam, 2006, 33, pp 393-432.
[6] Corey, E.J.; Sauers, R.R. *J. Am. Chem. Soc.* 1959, 81, 1739-1743.
[7] Vlad, P.F.; Kuchkova, K.I.; Aryku, A.N.; Deleanu, K. *Russ. Chem. Bull.* 2005, 54, 2656-2658.
[8] Stoll, M.; Hinder, M. *Helv. Chim. Acta.* 1954, 37, 1859-1866.
[9] Weyerstahl, P.; Marschall, H.; Weirauch, M.; Thefeld, K.; Surburg, H. *Flavour. Fragr. J.* 1998, 13, 295-318.
[10] De Pascual Teresa J.; Urones, J. G.; Marcos, I.S.; Martin, D.D.; Alvarez, V.M. *Phytochemistry,* 1986, 25, 711-713.
[11] Jakupovic, J.; Schuster, A.; Wasshausen, D.C. *Phytochemistry,* 1991, 30, 2785-2787.
[12] Urones, J.G.; Marcos, I.S.; Basabe, P.; Diez, D.; Garrido, N.M.; Alonso, C.; Oliva, I.M.; Lithgow, A.M.; Moro, R.F.; Sexmero, M J.; Lopez, C. *Phytochemistry,* 1994, 35, 713-719.
[13] Lee, I.-S.; Ma, X.; Chai, H.-B.; Madulid, D.A.; Lamont, R.B.; O'Neill, M.J.; Besterman, J.M.; Farnsworth, N.R.; Soejarto, D.D.; Cordell, G.A.; Pezzuto, J.M.; Kinghorn, A.D. *Tetrahedron,* 1995, 51, 21-28.
[14] Joshi, B.S.; Hegde, V.R.; Kamat, V.N. *Phytochemistry,* 1996, 42, 761-766.
[15] Zoretic, Ph.A.; Fang, H.; Ribeiro, A.A.; Dubay, G. *J.Org.Chem*., 1998, 63, 1156-1161.
[16] Sheldrick, G.M. SHELXL-93, *Program for refining crystal structure,* Univ. of Gottingen, 1993.
[17] Cremer, D.; Pople, J.A. *J. Am. Chem. Soc.,* 1975, 97, 1354-1358.
[18] Kravtsov, V.Ch.; Simonov, Yu.A.; Gorinchoi, E.K.; Koltsa, M.N.; Vlad, P.F. *Crystallogr. Rep.*, 2000, 45, 789-791.
[19] Kravtsov, V.Ch.; Gorinchoi, E.K.; Mironov, G.N.; Koltsa, M.N.; Simonov, Yu.A.; Vlad, P.F. *Crystallogr. Rep.*, 2000, 45, 258-260.
[20] Steiner, T. *Cryst. Rev.* 1996, 6, 1-51.

NEW ROOM TEMPERATURE LIQUIDS: SYNTHESIS AND CHARACTERIZATION

Macaev Fliur, Munteanu Viorica, Stingaci Eugenia, Barba Alic, Pogrebnoi Serghei
Institute of Chemistry of the Academy of Sciences of Moldova, Academiei str. 3, MD-2028 Chişinău, Republic of Moldova
E-mail : flmacaev@cc.acad.md, Phone (+373-22) 73-97-54, Fax (+373-22) 73-99-54

Abstract: New functionalized imidazolium salts that can be classified as ionic liquids were synthesized.

Keyword: organic synthesis, ionic liquids, epoxides, nitriles, allylimidazoles.

1. INTRODUCTION

Room temperature ionic liquids (ILs) have been recognized as a new generation of solvents for "green chemistry" and represent remarkably promising classes of technologically useful and fundamentally interesting materials [1-6]. Most of them are quaternary imidazolium cations with inorganic counterions. Cation in these salts is appended to the organic group (usually saturated hydrocarbon fragments). However, some problems regarding the functionalization [2,7], coordination properties [4] of ILs still remain to be solved. It seems to us that functionalization of imidazoles by ethylcarbonitrile, allyl, 2,3-epoxypropyl fragments will lead to new properties of synthesized ILs. There are no literature data on use of 2-(1*H*-1-imidazolyl)ethylcarbonitrile **4** for synthesis of imidazolium salts with ILs properties.

2. RESULTS AND DISCUSSION

In continuation of our investigations [8,9] on the chemistry of intramolecular reaction of conjugate acceptors, we carried out the cyanoethylation of imidazole **1** into **4** via Michael addition of acrylonitrile. Taking into account the simplicity of the discussed reaction, no bis-product formation, it is possible to carry out the process technologically on large scale.

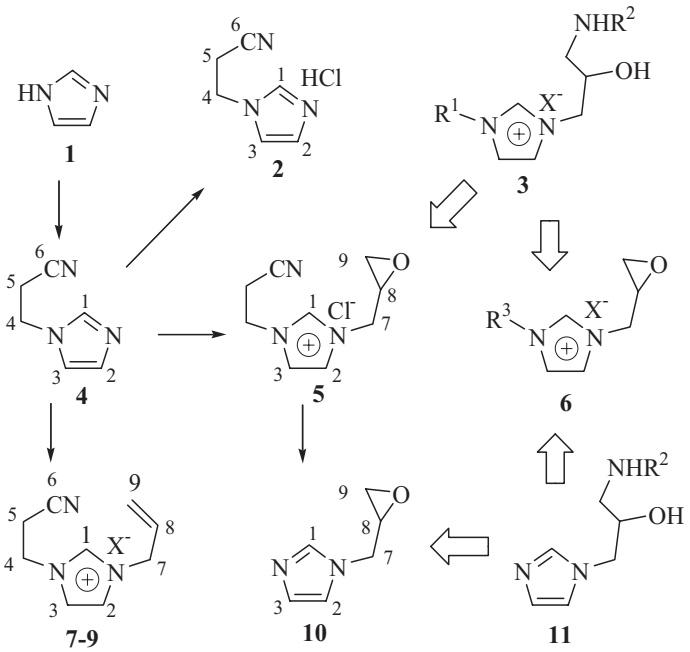

7: X= Br^-, **8**: X= BF_4^-, **9**: X= PF_6^-

Most used ILs are based on 1,3-dialkylimidazolium cations and large anions (BF_4^-, PF_6^-, $CF_3SO_3^-$, etc), but not halides, due to their relatively high melting point (MP). For example, 1-butyl-3-methylimidazolium chloride has MP 67^{0}C. Although some imidazolium halide salts having long alkyl chains are known to form super-cooled liquids, but they show high viscosity [1-6]. There are also reports that some of allylimidazolium halide could be obtained as liquids [10].

We have synthesized new allylimidazolium compounds for the study of relation between structure and physical-chemical properties.

Table 1

Characteristic Data of Synthesized Compounds

Compound/ Molecular formula	Aggregation/ color	Metod[a]/ Yield (%)	IR (Nujol) ν, cm^{-1}	Elemental analysis Calculated /Found		
				C	H	N
2 $C_6H_8ClN_3$	Oil/White	C/66 D/95	3130, 1520, 1450, 1520 (CH=C); 2260 (CN); 670 (Cl)	45.72/ 45.66	5.11/ 4.98	26.66/ 26.51
4 $C_6H_7N_3$	Oil/Yellow	99	3130, 1455, 1525 (CH=C); 2250 (CN)	59.49/ 59.33	5.82/ 5.99	34.69/ 34.98
5 $C_9H_{12}ClN_3O$	Oil/Yellow	B/75	3130, 1520, 1450 (CH=C); 2260 (CN); 670 (Cl)	50.59/ 50.46	5.66/ 5.64	19.67/ 19.87
7 $C_9H_{12}BrN_3$	Oil/Yellow	A/98	3195 1560, 1420 (CH=C); 2260 (CN); 630 (Br)	44.65/ 44.43	5.00/ 4.88	17.36/ 17.39
8 $C_9H_{12}BF_4N_3$	Oil/Yellow	A/87 B/94	3100 1560, 1420 (CH=C); 2250 (CN)	43.41/ 43.32	4.86/ 4.76	16.87/ 16.88
9 $C_9H_{12}F_6PN_3$	Oil/ Pale-yellow	A/53 B/97	3185, 3120, 1570, 1450 (CH=C); 2260 (CN)	35.19/ 35.26	3.94/ 4.15	13.68/ 13.49
10[b] $C_6H_8N_2O$	Oil/Colourless	A/70* A/75**	3130, 1550, 1450 (CH=C)	58.05/ 58.00	6.50/ 6.73	22.57/ 22.46

[a]Method: **A** – Reaction in Water; **B** - Reaction in Acetone; **C -** Reaction in MeCN; **D -** Reaction in MeOH.
[b]Method* - Use KPF_6 in Water; Method** - Use KBF_4 in Water.

Quaternization of **4** with allyl bromide yielded 1-allyl-3-(2-cyanoethyl)-1*H*-imidazolium bromide **7** as yellow liquid.

The next step was the metathesis of **7** with the appropriate inorganic salt ($NaBF_4$ or KPF_6) in water or acetone. Notable, caring out reaction in acetone leads to the highest yields of room temperature liquids **8, 9** (See Tab. 1).

After developing successfully the synthesis of ionic liquids **7-9**, our interest was switched to evaluation of the usefulness of **4** for selective synthesis of salts, functionalized by 2,3-epoxypropyl chain. There are several advantages and reasons to synthesize the ionic liquids with a glycidyl group. The epoxides in the cation of glicidyl ionic liquids can react with different kind of nucleophiles, electrophiles and other reactants, resulting in the production of new ILs **3**, **6** with different groups [11]. We shall emphasize, that derivatives like **11**, could be applied in the cycloaddition of CO_2 as well as in medicinal chemistry studies by introduction imidazolium and other ammonium group to different aminosacharides**.**

Table 2

NMR Spectroscopic Data of Synthesized Imidazolium Derivatives

№	Me-thod	The chemical shifts (δ, ppm, *J*/Hz)								
		1	2	3	4	5	6	7	8	9
2	^{1}H	7.72 [a]s, 1H	9.41 s, 1H	7.94 s, 1H	4.57 [c]t, 2H, *J*=6.4	3.30 t, 2H *J*=6.4	-	-	-	-
	^{13}C	128.79	137.5	118.59	41.83	19.72	119.43	-	-	-
4	^{1}H	6.95 s, 1H	7.43 s, 1H	6.95 s, 1H	4.13 t, 2H, *J*=6.94	2.69 t, 2H *J*=6.95	-	-	-	-
5	^{1}H	7.27 s, 1H	7.73 s, 1H	6.94 s, 1H	4.27 t, 2H, *J*=6.4	3.20 t, 2H, *J*=6.62	-	3.81-4.19 m, 2H	3.5-3.86 m, 1H	3.63-3.69 m, 2H
	^{13}C	128.57	137.29	118.35	69.56	19.49	119.18	46.26	68.67	41.26
7	^{1}H	7.91 s, 1H	9.56 s, 1H	8.05 s, 1H	4.61 t, 2H, *J*=6.4	3.35 t, 2H, *J*=6.4	-	4.94 [b]d, 2H, *J*=5.71	5.8-6.21 [d]m, 1H	5.14-5.35 m, 2H
	^{13}C	122.67	136.5	120.3	44.46	18.89	117.53	50.85	131.37	122.68

8	^{1}H	7.77 s, 1H	9.24 s, 1H	7.84 s, 1H	4.50 t, 2H, *J*=6.27	3.20 t, 2H, *J*=6.27	-	4.87 d, 2H, *J*=5.53	5.6-6.3 m, 1H	5.15-5.42 m, 2H
	^{13}C	122.77	136.59	120.41	44.53	18.89	117.62	50.95	131.43	122.61
9	^{1}H	7.73 s, 1H	9.26 s, 1H	7.84 s, 1H	4.52 t, 2H, *J*=6.62	3.20 t, 2H, *J*=6.62	-	4.86 d, 2H, *J*=5.75	5.8-6.21 m, 1H	5.15-5.39 m, 2H
	^{13}C	122.86	137.0	120.38	44.56	18.65	117.67	51.02	131.45	122.65
10	^{1}H	7.82 s, 1H	9.30 s, 1H	7.82 s, 1H		-			3.15-4.57 m, 5H	

[a]s-singlet, [b]d-doublet, [c]t-triplet, [d]m-multiplet

Chloride **5** was obtained by simple mixing of **4** and 2-chloromethyloxirane at room temperature. We tried to carry out anion exchange by similar manner as discribed above. However, compound **10** has isolated as main product.

It is known that dequaternization of 1-(2-cyanoethyl)-3-alkylazolium salts can be achieved by the addition of a strong base to the azolium salts [12]. During such reaction, formation of the cyanoethylated byproducts is possible, but we didn't observe any by-product.

It was worth to note that the mixture of **4** and epichlorohydrin refluxed in MeCN leaded to hydrochloride **2**. This result shows that other type of elimination takes place and is preferable. Additionally, **2** was prepared by treatment of **4** with a HCl solution in dry MeOH.

The structures of new salts were established based on their spectral data and elemental analysis. The chemical shifts of the imidazole ring protons strongly depend on anion nature (δ ppm = 9.41, 7.94 and 7.72 for **2**; 9.56, 8.05 and 7.91 for **7**; 9.24, 7.84, 7.77 for **8**; 9.26, 7.84 and 7.75 for **9**). Similar phenomenon was observed for ^{13}C-chemical shifts for discussed fragment (δ ppm = 137.5, 128.79 and 118.59 for **2**; 136.5, 120.3 and 117.5 for **7**; 136.5, 131.43, 122.77 for **8**; 137.0, 131.45 and 122.88 for **9**) (See Table 2). Notable, chemical shifts of protons of cyanoethyl chain depend on anion nature, too (δ ppm = 3.30 and 4.57 for **2**; 2.69 and 4.13 for **4**; 3.20 4.27 for **5**; 3.35 and 4.61 for **7**; 3.20 and 4.50 for **8**; 3.20 and 4.52 for **9**). Small difference for ^{13}C-chemical shifts (δ ppm = 119.43 for **2**; 119.18 for **4** and 117.53 for **7**; 117.62 for **8** and 117.67 for **9**, respectively) as well as IR absorption band of carbonitrile group were observed also (See Tab. 1 and 2).

The solvent's properties of the synthesized imidazolium salts are under investigation, and will be published soon.

It should be menthioned that during the preparation of current paper, the development of nitrile-functionalized ionic liquids for C-C coupling reaction was reported [13].

4. EXPERIMENTAL

All the solvents used were reagent quality, and all commercial reagents were used without additional purification. Removal of all solvents was carried out under reduced pressure. Melting points (uncorrected) were determined on a Boetius apparatus. Physical and analytical data of the synthesized compounds are given in Table 1. Analytical TLC plates were Silufol® UV-254 (Silpearl on aluminium foil, Czecho-Slovakia). IR spectra were recorded on a Specord 75 IR instrument. ^{1}H and ^{13}C NMR spectra were recorded for d_6-DMSO 2-3% solution on a Bruker AC-80 (80 and 20 MHz) and on a Varian XL-400 spectrometer (399.95 MHz) apparatus and are given in Table 2.

Synthesis of 3-(1*H*-1-imidazolyl)propanenitrile hydrochloride 2.

Method A): To a solution of **4** (2.18 g, 0.018 mol) in MeCN (10 ml) was added 2-chloromethyloxirane (1.63 g, 0.018 mol). The mixture was refluxed for 18 hours, concentrated under reduced pressure and dried under vaccuum. Yield 1.87 g of **2**.

Method B): A mixture of **4** (1.45 g, 0.012 mol) and 18% solution of HCl in MeOH (5 ml) was stirred with for 2 days. The same workup as for method A was followed. Yield 1.85 g salt **2**.

Synthesis of 3-(1*H*-1-imidazolyl)propanenitrile 4.

The mixture of imidazole **1** (40 g, 0.59 mol), acrylonitrile (33.85 g, 0.59 mol) and Et_3N (0.1 ml) in 80 ml toluene was refluxed for 30 hours. Solvent was removed under high vacuum to yield 71g (pure according spectral and TLC data) of compound **4**.

Synthesis of 1-(2-cyanoethyl)-3-(2-oxiranylmethyl)-1*H*-imidazolium chloride 5. To a solution of **4** (2.13 g (0.018 mol) in 10 ml acetone 2-chloromethyloxirane (1.63 g, 0.018 mol) was added dropwise. The reaction mixture was stirred for a 25 hours. Solvent was removed in vacuum to give 2.84 g of viscously yellow oil **5**.

Synthesis of 1-allyl-3-(2-cyanoethyl)-1*H*-imidazolium bromide 7.

Product **7** (4.19 g) has prepared from **4** (2.13 g, 0.018 mol) and allyl bromide (2.13 g, 0.018 mol) by the same procedure as for preparation of **5**.

Synthesis of 3-allyl-1-(2-cyanoethyl)-1*H*-imidazolium tetrafluoroborate 8.

Method A): A solution of imidazolium bromide **7** (1.57 g, 0.0065 mol) in water (2 ml) containing (0.82 g, 0.0065 mol) KBF_4 was stirring at room temperature for 60 hours. The insoluble oily material was separated. It was then dissolved in CH_2Cl_2, washed with H_2O and brine, dried over Na_2SO_4, filtered, and concentrated to dryness. Salt **8** (1.4 g) was obtained as a pale yellow oil.

Method B): To a solution of bromide **7** (1.57 g, 0.0065 mol) in acetone (2 ml) was added KPF_6 (0.82 g, 0.0047 mol). The reaction mixture was stirred for a total 60 hours. Solids were filtered, and the solvent removed to give 1.51 g of oil **8**.

Synthesis of 3-allyl-1-(2-cyanoethyl)-1*H*-imidazolium hexafluorophosphate 9.

Method A): Bromide **7** (1.57 g, 0.0065 mol) has reacted with KPF_6 (1.19 g, 0.0065) according to the procedure described for the preparation of tetrafluoroborate **8** (See method A) to give salt **9** (1 g) as a pale yellow oil. Method B): Salt **9** (1.97 g) was prepared by use **7** (1.57 g, 0.0065 mol) and KPF_6 (1.19 g, 0.0065 mol) in acetone by the same procedure as for **8** (See method B).

Synthesis of 1*H*-imidazolyl(2-oxiranyl)methane 10

Metod A): A solution of KPF_6 (0.86 g, 0.0047 mol) in 5 ml H_2O was added to **5** (1 g, 0.0047 mol). The reaction mixture was stirred for a total 35 hours. The insoluble oily material was separated. It was then dissolved in CH_2Cl_2, washed with H_2O and brine, dried over Na_2SO_4, filtered, and concentrated to dryness to give 0.40 g of viscously colorless oil **10**. Method B): Use of chloride **5** (1.2 g, 0.0056 mol) and solution of KBF_4 (0.7 g, 0.0056 mol) in water (5 ml) analogously Method A) afforded 0.46 g of oxirane **10**.

5. CONCLUSIONS

This work presents results of the synthesis and analyses of the effect of nature of C3 groups on imidazolium ring to aggregation of Br^-, Cl^-, BF_4^- and PF_6^- imidazolium salts.

6. ACKNOWLEDGMENTS

The authors gratefully acknowledge funding though a grant 06.21 CRF from the Moldavian-Russian Grants Program. We also acknowledge Professor Gavrilov K., Ryazan State Pedagogical University (Russia), for providing NMR Spectroscopic Data.

7. REFERENCES

[1] Chowdhury, S.; Mohan, R.S.; Scott, J.L. *Tetrahedron*, **2007,** 63, 2363-2389.
[2] Binnemans, K. *Chem. Rev*. **2005**, 105, 4148-4204.
[3] Jain, N.; Kumar, A.; Chauhan, S.; Chauhan, S.M.S. *Tetrahedron*, **2005,** 61, 1015-1060.
[4] Lin, I. J. B.; Vasam, C. S. *J. Organomet. Chem.*, **2005**, 690, 3498-3512.
[5] Davis, J. H. *Chemistry Lett.*, **2004**, 33, 1072-1077.
[6] Baudequin, C.; Baudoux, J.; Levillan, J.; Cahard, D.; Gaumont, A.C.; Plaquevent, J.C. Tetrahedron: *Asymmetry*, **2003**, 14, 3081-3093.
[7] Braunstein, P. *J. Organomet. Chem.*, **2004**, 689, 3953-3967.
[8] Meulemans, T.M.; Stork, G.A.; Macaev, F.Z.; Jansen, B.J.M.; De Groot, A. *J.Org.Chem*. **1999**, 64, 9178-9188.
[9] Jansen, B.J.M.; Hendrikx, C.C.J.; Masalov, N.; Stork, G.A.; Meulemans, T.M.; Macaev, F.Z.; De Groot, A. *Tetrahedron*. **2000**, 56, 2075-2094.
[10] Mizumo, T.; Marwanta, E.; Matsumi, N.; Ohno, H. *Chemistry Lett.* **2004**, 33, 1360-1361.
[11] Demberelnyamba, D.; Yoon, S.J.; Lee, H. *Chemistry Lett.* **2004**, 33, 560-561.
[12] Horvath, A. *Synthesis*, **1994**, 102-105.
[13] Fei, Z.; Zhao, D.; Pieraccini, D.; Ang, W.H.; Geldbach, T.J.; Scopelliti, R.; Chiappe, C.; Dyson, P.J. *Organomettallics*. **2007**, 26, 1588-1598.

DUMITRU BATIR: THE INFINITE ROAD OF THE HOURGLASS

The great thinker and enlighten writer Voltaire had said: "The day of a great spiritual revolution will come doubtless. A man of my age will not see it, but he will pass away hoping that people will become more enlighten and milder". This day can be brought nearer through an assiduous work of each human being. These thoughts came into my mind when I tried to remind the image of the professor Dumitru Batir, whom I had always around me for better, for worse, having his generosity and competence, tact and kindheartedness along my formation and affirmation on the scientific, didactic, cultural and public fields. For he was the promoter of my good fate.

Reaching the time of balance-sheet, Dumitru Batir is a distinct personality in the contemporary scientific landscape, who asserted himself through the wide variety of concerning and the diversity of the fields to which he contributed: an outstanding chemistry researcher, a highly appreciated university professor, a faithful chronicler of the science and culture evolution, the creator of terminology and nomenclature in chemistry, a plenary engaged citizen in the public life, a man of the completed duty.

By his formation,Dumitru Batir is inorganic chemist, specialized in coordinative, biocoordinative and ecologic chemistry. He was born on the 1st April 1927 in Budesti village, Balti district, he graduated from The Pedagogic University from Chishinau (1947-1951), obtained his doctor degree at the Inorganic Chemistry Department of The State University of Moldova (1952-1956), worked as lecturer at The Pedagogic University from Tiraspol (1956-1959). After these, his life and activity is ceaselessly connected to the Institute of Chemistry of The Academy of Sciences of Moldova, where he by turn occupies the position of superior scientific researcher (1959-1960), scientific secretary (1960-1963) and assistant director for scientific problems (1964-1974), the chief of the Bioinorganic Chemistry Laboratory (1975-1987). Beginning with 1988 he is the principal scientific researcher at the same institution, being simultaneously university professor, having special course initiated by him. He obtained the degree of doctor (1958) and doctor habilitat (1974) in chemistry, the didactic title of university professor (1984) and was the laureate of the State Prize of the Republic of Moldova (1996).

His researchers are focused on the research of the physical-chemical structure-properties relations which lead to the discovery of the ways of building biologically active compounds with expected features, as well as to the prospecting of the toxicophores which determines the noxiousness of the substances. Via the contribution of the scholar there have been elaborated original methods of synthesis, there have been studied the properties, there has been explained the structure and proved the possibility to implement the synthesized compounds in industry, medicine and agriculture. The obtained results made possible to perform refuseless technologies with a significant economic efficiency.

The bibliography of Dumitru Batir counts over 900 titles, inclusive 18 books and 22 patents that have been applied as biopharmaceutical preparations, stimulative fodder ingredients, stabilizers, rigiditive agents. The results of scientific investigations had been presented within different congresses, conferences, national and international symposia, being highly appreciated the outstanding contribution of the scholar in the development of fundamental sciences, plenary involvement in social and human problems, creative spirit.

Being the founder and the chief of Bioinorganic Chemistry Laboratory (1975) and of the Interdepartmental Laboratory of Veterinary Biotechnology (1980), he introduced in the scientific circuit new conceptions and elaborated new performing technologies, prepared 9 doctors and habilitate doctors in chemistry, who activate nowadays in education, research and production, continuing the tradition of Scientific School of Chemistry and Biocoordinative Ecochemistry launched by him. Along the years he published around 500 analytical articles, essays, sketches medallions and other materials that contributed to the round of his image of professor and modern researcher, of animator of scientific and cultural life, of publisher. The professor Dumitru Batir works permanently as a member of the Councils of encyclopaedically works , as well as editorial board of the of academicals journals.

Dumitru Batir asserts that he had great luck in his life to have around him teachers, masters, disciples and friends of elite. In the early childhood, beginning with primary school he had a lot of rare books that his openhearted teacher Theodor Purch provided to him. After this, he enjoyed the library of the highly erudite Alexandru Cosmescu, from which he read almost the books. In the field of chemistry he had been initiated and guided by such unrepeatable scholars

as the large-hearted Eugeniu Nirca and the famous Antonie Ablov. He was encouraged by the outstanding researchers as Nicolai Javoroncov and Yurii Zolotov from Moscow, Yacov Fialkov from Kiev, Petru Spacu from Bucharest and many others. He shared his bread with the great artist and thinker Igor Vieru who gave him as presents two memorable portraits; he had near him Ion Vatamanu, Nicolae Testimitsanu, Sergiu Radutsanu.

Probably he had luck. Still a whole world knows that if at night at the Institute of Chemistry there is a light, than this comes from the laboratory in which Dumitru Batir works hard. A human life changed into hard work! For Dumitru Batir hard work appears as a necessity, a work from the deep soul, with the open heart and bore on wings of enthusiasm and which nobody would be able to do instead of him. For him work is a blessing which gives sense to life and strength to man, beauty to human nature and nobles. Not at random we called him "A man of work" 10 years ago in a warm word of homage addressed to the celebrated. Because only the creative work as a social and moral process ensure the progress, confer to man the supreme happiness, prolonging his life after his death. Because his life does not melt in yesterday, but becomes the symbol of that tomorrow that is to come.

But which are the origins, where from comes the passion for research and rounding up the things that have been started, the interest to reveal the things that are lived through books? We can find the answer in a confess of the master Vasile Vasilache who was writing in the days of inauguration of the Academy of Sciences, on 3rd August 1961 in "Moldovan Culture" that Dumitru Batir is "full of power, as the vain of cornel tree. He is on a vigorous parent stock, nourished with the must of wormwood wine from the follow-grounds of Glodeni and bears in his soul the odor of the ground from the homeland Budesti". Years on, in 1996, the poet and publisher Ion Anton came to round up this portrait with the words:" Both the zeal of the bee and the masterliness of the jeweller are fully proper to the researcher Dumitru Batir… Being one of the chemistry researcher who masters both the chemical formula and the written word, he was selected by the His Excellency Providence to be the author of exceptional books".

We will stop briefly on the recently appeared book "Restless of memory. The development of chemistry in Moldova and the avatar of the life. Synthesis. Portraits. Medallions. Reflections." signed by Dumitru Batir – a monographic study about the evolution, within Moldovan area, from the origins to the present, of one of the fundamental science, chemistry, considered the almighty queen of the life. Based on concrete archive materials, the author tried to reconstitute and define the profile of some educational institutions, research and application, involved directly in the given process. It happened that came together many synthesized articles about tens of educational and research, academic, university and interdepartmental institutions, interested in this field of science, as well as thousands portraits of savants, researchers and professors, founders of well known schools worldwide and home, who through their ambitions and hard work could promote the science and chemistry education in a difficult medium, managing to include the chemistry into the scientific concerns in our country.

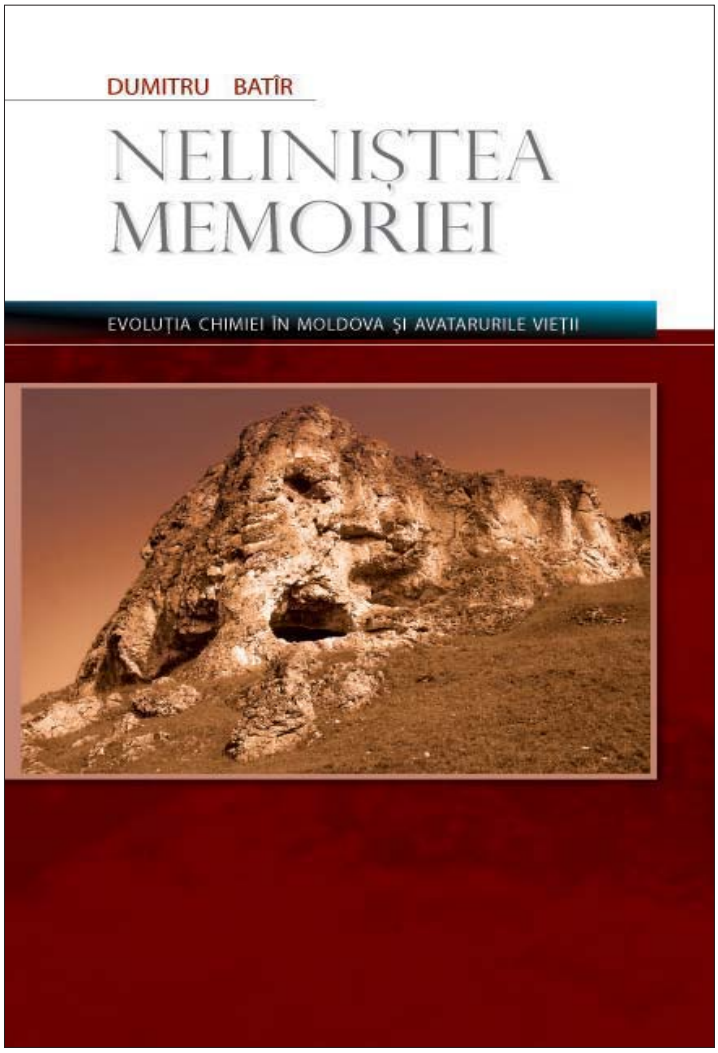

Beside the strictly chronological, concrete informational, fully comprehensive aspect of studied materials arranged very carefully on the book page, the work has a character of affective history, in which a tone of confession, evocation, sometimes lyrics dominates. Factual material of almost incommensurable dimensions has been collected by the author with a healthy pedantry that is proper to a chemist-experimenter, but this material has a peculiar style of expression as like the author would touch with his soul and his breath some past times and some people that are always alive in his memory, because he lived among them the most difficult and the most beautiful moments of the evolution of a fascinating domain.

In the "Restless of Memory" there are

presented pieces of minds, attitudes – sometimes harsh, but always benevolent – passing easily from a domain to another, from an event to another, approaching sometimes names and events that do not refer to the chemistry but are part of the triangle Education-Science-Life, all in a logical, consistent and persistent chain with much daring, inspiration and mastery. Retrospective memory, especially in the case of a life experience like that of the savant Dumitru Batir, places us in a relation with yesterday's, today's, tomorrow's time, placing us in the middle of life facts, bringing sometimes pleasure, but in many cases dramatic and even tragic facts. This free flight of author through the space and time, with his meditations and reflections, affirmations and negations, could seem to us as unacceptable, but doubtless it would incite the public.

On the forth page of the book we find an author's confession full of significance, in fact a credo to which he remained faithful during all his life: "Our faith and conviction is that in order to thrive we should know our past. The past is the lever that is able to transform the good into something better. The same way the strength of a tree resides in its root system, the human might is based on his past. Only a human affective archive, carefully gathered along the time like a priceless thesaurus would guarantee the unforgettable ness, would identify or recover the bridges between generations, projecting image after image a full marathon of endless life, it could be the certificate of maturity for the passers throughout the mornings and the evenings of this life, because it is an authentic document of a community caught in the nets of a deep sentiment of restless memory"

At one of his latest launch of the book our famous professor and colleague Dumitru Batir had confessed that every book is like a precious child for him that appeared as a result of the love for the books of that who is writing it, a longing tear for present and future searchers of truth, a truth admired as majesty, a drop of dew fallen from heavens via a divine inspiration in which like in a mirror is reflecting the figure of the author with all the present, past and forever aspirations with his signs on the tally of time.

At the end of reading the pages of this book we are lead to the idea that it would be wonderful if every academic profile institution could analyse their steps and would try to do a reconstitution of the long and difficult way passed by the given institution presenting to us the people and their actions that cannot be left to pass into an anonymous or forgotten world; that would be unforgivable. In fact this is another message of the book "The Restless of the Memory", that we presented with understanding and appreciation to the reader.

Academician Gheorghe DUCA
President of the Academy of Sciences of Moldova

THE HORIZONS OF KNOWLEDGE AND THE POWER OF SYNTHESIS

The father of Russian science, Mihailo Lomonosov, in one of his most beautiful works, "Words on the Use of Chemistry" – an embodiment of his philosophy of life and work – wrote that: "Science discovers and and explains the hidden features of things, as well as the hidden reasons for their inner function; in its turn invention facilitates a better use of science in man's life…". In modern terms, Lomonosov's assertion can be interpreted somewhat like this: Discovery is the supreme form of scientific creation, but inventions that are formally legitimized with legal patents are mainly the result of the creative synthesis in daily life. The ratio between discoveries and inventions is one to several thousands. It can be said that one of our greatest discoverers, the famous Isaac Bersuker – an outstanding scholar, and the founder of the internationally known School of Quantum Chemistry and Chemical Physics of the Republic of Moldova – is a giant of thought.

Born on the 12th of February 1928 to the family of a Chishinau carpenter named Boruh, he together with his father dreamed of becoming a first-rate locksmith, but his destiny was another – he chose to unlock the subtleties of electrons and atomic nucleus "respiration", which could be explained only by his discovery of the pulsating movement of molecules.

After graduating from the Faculty of Physics and Mathematics at The State University of Moldova in 1952, he wrote a PhD thesis on the topic, "Optical transitions in atoms and molecules with a polarizable structure" (Saint Peterburg, 1957). His second thesis for the title of Doctor Habilitat in physical-mathematical sciences, was titled, "Contributions in the field of quantum theory of transitional metal complexes" (the same place, 1964). He became a University Professor (1967), a corresponding member (1972), a full member (academician) of the Academy of Sciences of Moldova (A.S.M.) (1989). Subsequently he became a member of the Chemical Society of the United States.

He was the first from the Institute of Chemistry of A.S.M. to organize a laboratory for the study of Quantum Chemistry (1964), which, along with careful research allowed him to register his first discovery, number 202 (1978). Thus, he became the first laureate of the State Prize of the Republic of Moldova in the field of science and technology (1979).

The fruitful development of quantum chemistry – a composite discipline, being at the interface between physics and chemistry – led to explanation of some fundamental questions of chemistry such as the nature of chemical bonds and the relationship between molecular structure and physical-chemical properties, which may also explain how to build biologically active compounds with programmable proprieties. The contributions of the Bersukerian School have been important for promoting research in the field of integrated chemistry by using fundamental principles and equations of quantum mechanics to reveal the difficult problems regarding the reactivity of chemical bonds, electronic structure of reactant molecules, as well as the transition state in catalysis, the modeling of molecular systems containing transitional metals, and the regulation of processes specific to life. The scholar introduced and developed the concept of vibronic interactions applicable in chemistry, biology and physics and developed the vibronic theory of seignetto-electricity, which allows prediction and discovery of new phenomena. Professor Isaac Bersuker has published over 600 scientific works, including 13 widespread monographs (6 in Russian and 7 in English). He has been scientific advisor to 50 doctors and 10 habilitate doctors in science.

All these accomplishments have been the result of hard work and perspiration, common to minds, inspired by the demon of creation and discovery. Maybe the most subtle and surprising description of the exceptional mind and nature of Isaac Bersuker was written by Victor Polingher, one of his disciples, in his work, "The Chemist", written in January 1988, (during the "Perestroika" period, when things began to have names.): "His cheerful disposition and constant optimism helped him face many hardships in his difficult work as a theoretical scholar. Frankly speaking, we have to mention that public scientific opinion was initially critical of almost all that Isaac Bersuker had published. Thus, the vibronic theory of seignetto-electricity – which today is recognized and appreciated – needed almost 20 years before being accepted by the scientific community. Some of his research results still provoke great debates even today. In paraphrasing a well-known poem it could be said: "… how many roads I've taken and how few mistakes I've made".

Isaac Bersuker is a man who is not too flattered by complements. At the same time he is a man who understands and does not hesitate to consider real and honest work on an idea proposed by his close or occasional colleagues. So, looking through my modest contributions in newspapers and specialized reviews, especially those in which I'm trying

to reconstruct the inner life of our academic and university life, the tireless Isaac Bersuker sends me a letter full of optimism even from the University of Texas, in which he encourages me by saying: "My dear colleague, you've taken a very noble task of "chronicling" the great achievements from the Academy of Sciences and the scientific community of Moldova. I think that not only the present generation, but also the future one will be very grateful for this work. Persevere, even if you meet with difficulties and impediments".

A more detailed analysis of, Isaak. Bersukers' personality would require more space, while our goal is to emphasize the most important contributions of his life and work. We met at the Institute of Chemistry of A.S.M. the same day as its inauguration (April 1959): I came from the Tiraspol University of Pedagogy where I was holding Chemistry lectures. He came from the Balti University of Pedagogy where he was a physics lecturer. I - doctor in Chemistry, and he – doctor in physics-mathematics; both were members of the first scientific Council of April 1959. In 1961 we both received apartments on the same floor and in the same building at 63 Gheorghe Asachi Street. We both held the position of deputy director for scientific work, and we both settled new laboratories – he of quantum chemistry, I of bioinorganic chemistry. We both were favored with a happy destiny shaped by our spiritual father, the late Antonie Ablov, a destiny that perpetuates the tradition. So, I consider myself qualified to confirm the remarkable spirit of this brilliant expert in the modern concepts of physics and chemistry, Isaac Bersuker. My collaboration and communication with him have always been a real delight.

The laboratory of Quantum Chemistry at the Institute of Chemistry of A.S.M. in its first years succeeded in transforming itself into a "pearl of the Soviet Union" (Mihail Veselov), recognized later all over the world. Specialists from the four corners of the world came to him either to recognize the laboratory's achievements, to participate in the many conferences and symposia focused on the laboratory's area of research, or for long-term training. A professor from Marburg University, D. Reinen, who participated in the 10th International Symposium dedicated to the Jahn-Teller effect (Chisinau, 26-29 September 1989), wrote in a news article that he greatly appreciated the high standards of scientific research by the scientists from Chisinau and that "the research group of Isaac Bersuker, the academician of the Academy of Sciences of Moldova, approaches international standards. This is due to the fact that professor Bersuker and his disciples maintain outstanding cooperation with scientific centers from abroad. In science it is impossible to compete with others when one is isolated".

Academician Isaac Bersuker understood this truth very well. Thus he entered into an employment contract with the University of Texas, at Austin, where for two and half years he worked intensively on developing and improving a method of modeling molecular systems containing transitional metals. To get a sense of the conditions and intellectual forces of this institution it should be mentioned that the University of Texas houses two Nobel Prize laureates, 50, 000 students and 10, 000 doctoral candidates. As a result of his diligent research it is possible to regulate metal-containing biological systems. These include hemoglobin, vitamin B12, cytochrome, peroxydase, as well as other forms of medicine These results can be used in biology and medical biology, for the development of new medicines.

Isaac Bersuker together with his closest collaborators – including seven Doctors Habilitat. Moisei Belinski, Serghei Borsci, Anatol Dimoglo, Mihail Kaplan, Victor Polingher, Boris Tukerblat, Beniamin Vehter, became involved in the universal science, which attracted them to the most famous scientific centers from Belgium, France, Israel, Italy, Spain, the U.S.A., Turkey, and other countries.

My friend, Professor Isaac Bersuker tohether with his lovely wife, Lilia, his talented son, Ghenadie and two admirable grandsons has settled in Austin, Texas. The scholar himself has declared that this place is not a permanent home, but an extended scientific journey that has lasted more than 10 years so far. Isaac Bersuker carries on his activity at the University of Texas, where he has all the necessary facilities for his fundamental research and where his creative work is highly appreciated. From the beginning of the 1990's the American Biographical Institute included him in the group of the 500 international scientific leaders, assigning to him the title of the world's most imposing and honored scholar of the 9th decade. In 1992 the International Biographical Centre from Cambridge, England conferred on him the title of "The Man of The Year".

As an ambassador during the difficult times when the fate of science in Moldova was at stake, he responded promptly with useful suggestions for "The Concept of Reformation of the Research-Development Sphere of the Republic of Moldova," which has now been accepted by the parliament. As always, he knew how to explain things and to contribute to the cessation of the process of ruining the fundaments of our academic scientific research. During his stay Chisinau in July 2002, in a relevant interview given on 29 August 2002 ("Kishinevskii obozrevateli", he tried to explain the difficult situation faced by our academic science and proposed some solutions which would allow us to overcome the critical situation, making some surprising remarks that we might take seriously::«In destroying science we sentence ourselves to poverty….In the Republic of Moldova serious mistakes against science have been committed. We need decades to correct them. The old mentality of the national leadership did not permit solving this problem at the proper time, as it was occurring throughout the world. Elsewhere money is granted for the development of science, while in our country money is granted for wages". Isaac Bersuker pays a great deal of attention to the support that the state gives for scientific development. Only through active cooperation between the authorities and the fundamental research

process can we move science toward an acceptable level of performance. How can the fair-minded ideas of this famous architect of science be ignored?

Lately Isaac Bersuker has focused his knowledge meticulously accumulated during the last half century on the most important problem of the present times – Ecotoxicology. Thisis the right time and the right place for this initiative . At present the scholar has been invited to participate in the highest international forums focused on ecological issues. At the 2nd International Conference of Ecologic Chemistry held in Chisinau (11- 12 October 2002), Isaac Bersuker was appointed the chairman of the Scientific Committee. At the same meeting he read a highly acclaimed paper regarding the utilization of Computer Based Chemistry in testing and predicting toxicity in Industrial Ecology (see "The Environment". 2002. N.3 (3). P. 10).

Being deeply concerned with industrial ecology, a distinct branch of ecology whose objective is to reduce emission of toxic substances in water, air and soil, Isaac Bersuker proposes to use the so-called electrono-conformatioal, computer-based method to identify pharmacophores and predict bioactivity in pharmaceutics. This method was developed earlier to identify toxicophores and predict their toxicity. In this case, computer-based chemistry serves to analyze data concerning the specific toxic character of different structures in industry in order to detect the toxicophore groups in these molecules, and the spatial position and electronic structure which determines their toxicity. The method is fast, cheap and efficient, ensuring a high level of prediction with 90% accuracy.

I think, as I describe, with considerable emotion, the man's life and biography, that it would be good to have as many fellow country men like Isaac Bersuker as possible,, who serve as ambassadors throughout the world to ensure permanent effective and affective contacts with the great scientific centers from abroad. Isaac Bersuker is a man and a scholar who in fact promotes the image of the Earth and of our Academy on the globe, an earth that he loves and will never leave, and an Academy that he wants to see among the modern institutions of the world. An Earth, which, bless the Lord, appreciates the scholar. In February 2004, Isaac Bersuker was favored with the "Order of Honor" of the Republic, as a sign of great appreciation for his outstanding contribution to the development of academic relations between the Republic of Moldova and the United States of America.

Today as never before, we have a real need for such great messengers and promoters as Isaac Bersuker.

Dumitru BATÎR
Dr. hab. in chemistry, University professor
State Prize Laureate

CHEMISTRY JOURNAL OF MOLDOVA.
General, Industrial and Ecological Chemistry

Instructions for authors

Please follow these instructions carefully to ensure that the review and publication of your paper are as swift and efficient as possible. These notes may be copied freely.

Journal policy

"Chemistry Journal of Moldova. General, Industrial and Ecological chemistry" seeks to publish experimental or theoretical research results of outstanding significance and timeliness in all fields of Chemistry, including Industrial and Ecological Chemistry. The main goal of this edition is strengthening the Chemical Society of Moldova, following development of research in Moldovan chemical institutions and promotion of their collaboration with international chemical community. Publications may be in the form of *Short Communications*, *Full Papers and Review Papers*.

The contents of papers are the sole responsibility of the authors, and publication shall not imply the concurrence of the Editors or Publisher.

Short Communications should describe preliminary results of an investigation and for their significance are due to rapid communication. For this kind of publications, experimental confirmation is required only for the final conclusion of the communication. Maximum allowed length – 2 pages.

Full Papers should describe original research in chemistry of high quality and timeliness. Experimental work should be accompanied by full experimental details. Priority will be given to those contributions describing scientific work having as broad appeal as possible to the diverse readership. Maximum allowed length – 6 pages.

Review Papers are specially commissioned reviews of research results of topical importance. Maximum allowed length – 20 pages.

The language of submission is English, articles in other languages will not be considered. Papers are submitted on the understanding that the subject matter has not been previously published and is not being submitted elsewhere. Authors must accept full responsibility for the factual accuracy of the data presented and should obtain any authorization necessary for publication. All papers are sent to referees who advise the Editor on the matter of acceptance in accordance with the high standards required.

Referees' names are not disclosed, but their views are forwarded by the Editor to the authors for consideration. Authors are strongly encouraged to suggest the names and addresses of suitable referees.

Journal conventions

Nomenclature: Authors will find the following reference books and websites useful for recommended nomenclature. It is the responsibility of the author to provide correct chemical nomenclature.

- IUPAC Nomenclature of Organic Chemistry; Rigaudy, J.; Klesney, S. P., Eds; Pergamon: Oxford, 1979.
- A Guide to IUPAC Nomenclature of Organic Compounds (Recommendations 1993); Panico, R.; Powell, W. H.; Richer, J. C., Eds; Blackwell Publishing: Oxford, 1993.
- http://www.acdlabs.com/iupac/nomenclature
- http://www.chem.qmul.ac.uk/iupac/

X-ray crystallographic data: Prior to submission of the manuscript, the author should deposit crystallographic data for organic and metal-organic structures with the Cambridge Crystallographic Data Centre. The data, without structure factors, should be sent by e-mail to: deposit@ccdc.cam.ac.uk, as an ASCII file, preferably in the CIF format. Hard copy

data should be sent to CCDC, 12 Union Road, Cambridge CB2 1EZ, UK. A checklist of data items for deposition can be obtained from the CCDC Home Page on the World Wide Web (http://www.ccdc.cam.ac.uk/) or by e-mail to: fileserv@ccdc.cam.ac.uk, with the one-line message, send me checklist. The data will be acknowledged, within three working days, with one CCDC deposition number per structure deposited. These numbers should be included with the following standard text in the manuscript: Crystallographic data (excluding structure factors) for the structures in this paper have been deposited with the Cambridge Crystallographic Data Centre as supplementary publication numbers CCDC … . Copies of the data can be obtained, free of charge, on application to CCDC, 12 Union Road, Cambridge CB2 1EZ, UK [fax: 144-(0)1223-336033 or e-mail: deposit@ccdc.cam.ac.uk]. Deposited data may be accessed by the journal and checked as part of the refereeing process. If data are revised prior to publication, a replacement file should be sent to CCDC.

Experimental: Authors should be as concise as possible in experimental descriptions. The Experimental section must contain all the information necessary to guarantee reproducibility. An introductory paragraph containing information concerning solvents, sources of less common starting materials, special equipment, etc. should be provided. The procedures should be written in the past tense and include the weight, mmol, volume, etc. in brackets after the names of the substances or solvents. General reaction conditions should be given only once. The title of an experiment should include the chemical name and compound number of the product prepared: subsequently, these compounds should be identified by their number. Details of the work up procedure must be included. An experimental procedure is not normally required for known compounds prepared by a literature procedure; in such cases, the reference will suffice. For known compounds prepared by a novel procedure, comparative data together with the literature reference are required (e.g. m.p. and published m.p. with a reference to the latter).

Characterization of new compounds: All new compounds should be fully characterized with relevant physical and spectroscopic data, normally including compound description, m.p./b.p. if appropriate, IR, NMR, MS and $[a]_D$ values for enantiopure compounds. In addition, microanalyses should be included whenever possible (normally ±0.4%). Under appropriate circumstances, and at the Editor's discretion, high resolution mass data (normally to ±5 ppm) may serve in lieu of microanalyses; in this case a statement must be included regarding the purity of the products and how this was determined [e.g. all new compounds were determined to be >95% pure by HPLC (or GLC or ^{1}H NMR spectroscopy)]. For compound libraries prepared by combinatorial methods, a significant number of diverse examples must be fully characterized (normally half of the members for libraries up to 40 compounds, 20 representative examples for bigger libraries). Resin-bound intermediates do not have to be fully characterized if acceptable characterization of released products is provided. No supplementary data are accepted in addition to the basic material.

Manuscript preparation

Please follow these guidelines for manuscript preparation. An example of manuscript formatting is provided after the descriptive part of the document.

General requirements: Manuscripts will be accepted only in electronic form in A4 format, one column layout, single-spaced, margins 2.5 cm on top and bottom and 2 cm on left and right sides (see the sample formatting page). Pages must be numbered. The corresponding author's full mailing address, plus phone and fax numbers and e-mail address should be included. The manuscript should be compiled in the order depending on the paper type.

A theoretical or physicochemical paper normally contains the *Title, Authors, Affiliations, Abstract, Keywords,* a brief *Introduction* and formulation of the problem, an *Experimental Section* (or methodical part), *Results and Discussion, Conclusion*, followed by *Acknowledgments and References.*

A paper devoted to synthesis contains the *Title, Authors, Affiliations, Abstract, Keywords, Introduction, Results and Discussion, Conclusion, Experimental, Acknowledgments and References.*

Graphical Abstracts: Authors must supply a graphical abstract at the time the paper is first submitted. It will include the article title and authors with the same formatting as in the article. The abstract body should summarize the contents of the paper in a concise, pictorial form designed to capture the attention of a wide readership and for compilation of databases. Carefully drawn chemical structures are desired that serve to illustrate the theme of the paper. Authors may also provide appropriate text, not exceeding 50 words. The whole graphical abstract should be kept within an area of 5cm by 17cm. Authors must supply the graphical abstract on a separate page integrated in the article file. The graphics which is a part of the graphical abstract should be sent separately in its original format.

*Title***:** The title should be brief, specific and rich in informative words; it should not contain any literature references or compound numbers. The title is in size 14 pt Bold (all capital letters).

Authors and affiliations: Where possible, supply given names, middle initials and family names for complete identification. Indicate all the authors in order of their affiliation and provide affiliation address after the author's names. Addresses should be as detailed as possible and must include the country name. The corresponding author should be indicated with an asterisk, and contact details (fax, e-mail) should be placed after nomination of the authors. There should be only one corresponding author. The names of the authors are in size 12 pt Normal and the name of the organization and its address are in size 9 pt Italic.

Abstract: Authors must include a short abstract of approximately four to six lines that states briefly the purpose of the research, the principal results and major conclusions. References and compound numbers should not be mentioned in the abstract unless full details are given. The abstract body is 9 pt in size with the heading in bold.

Keywords: Authors are expected to provide maximum 5 keywords using 10 pt font size with the heading in bold.

Text: Text should be subdivided in the simplest possible way consistent with clarity. Headings should reflect the relative importance of the sections. Ensure that all tables, figures and schemes are cited in the text in numerical order. The graphics and artworks should be integrated in the paper. Trade names should have an initial capital letter, and trademark protection should be acknowledged in the standard fashion, using the superscripted characters TM and ® for trademarks and registered trademarks respectively (although not for words which have entered common usage, e.g. pyrex). All measurements and data should be given in SI units where possible. Abbreviations should be used consistently throughout the text, and all nonstandard abbreviations should be defined on first usage. Authors are requested to draw attention to hazardous materials or procedures by adding the word CAUTION followed by a brief descriptive phrase and literature references if appropriate. The experimental information should be as concise as possible, while containing all the information necessary to guarantee reproducibility. The text body is 10 pt in size with the heading in bold.

Acknowledgments: This is an optional section. The authors have to decide acknowledgement of certain collaborators, funds or programs who contributed in a way to the research described in the paper.

References: In the text, references should be indicated by Arabic numerals taken in square brackets, which run consecutively through the paper and appear before any punctuation; ensure that all references are cited in the text and vice versa. The reference list should preferably contain only literature references; other information (e.g. experimental details) should be placed within the body of the text. Preferably, each reference should contain only one literature citation. Authors are expected to check the original source reference for accuracy. Journal1 titles should be abbreviated according to American Chemical Society guidelines (The ACS Style Guide; Dodd, J. S., Ed.: American Chemical Society: Washington, DC, 1997). Inclusive pagination is strongly recommended. Book references [2,3] should cite author(s), chapter title (if applicable), editor(s), book title, edition/volume, publisher name, publisher location, date and pages. Examples, including a thesis citation, 4 are shown below.

[1] Barton, D. H. R.; Yadav-Bhatnagar, N.; Finet, J.-P.; Khamsi, J. Tetrahedron Lett. 1987, 28, 3111–3114.
[2] Katritzky, A. R. Handbook of Organic Chemistry; Pergamon: Oxford, 1985; pp 53–86.
[3] Smith, D. H.; Masinter, L. M.; Sridharan, N. S. In Heuristic DENDRAL: Analysis of Molecular Structure;
[4] Wipke, W. T.; Heller, S. R.; Feldmann, R. J.; Hyde, E., Eds. Computer representation and manipulation of chemical information. John Wiley: New York, 1974; pp 287–298.
[5] Cato, S. J. Ph.D. Thesis, University of Florida, 1987.

Footnotes: Footnotes should appear at the bottom of the appropriate page and be indicated by the following symbols: *, †, ‡, §, ¶, *k*.

Tables: All tables should be cited in the text, and numbered in order of appearance with Arabic numerals. All table columns should have a brief explanatory heading and where appropriate, units of measurement. Vertical lines should not be used. Footnotes to tables should be typed below the table, each on a separate line, and should be referred to by superscript letters.

Artwork: Only black and white artwork will be accepted. Figures, schemes and equations must be cited in the text and numbered in order of appearance with Arabic numerals; other graphics should be placed at a particular position in the text but not specifically referenced. All graphics (including chemical structures) must be supplied in digital format integrated into the paper. If graphics are created using ChemDraw the preferred settings is RSC-1997.cds set

(File/Apply settings/RSC-1997.cds): font 7 pt Arial, chain angle 120^o, bond spacing 20% of length, fixed length 0.43 cm, bold width 0.056 cm, line width 0.016 cm, margin width 0.044 cm and hash spacing 0.062 cm. Compound numbers should be in bold face. Computer-generated illustrations, halftones and line/tones should also be provided where possible. The following points should be taken into consideration when preparing electronic graphic files:

Preferred graphics programs: ChemDraw, CorelDraw 6 and 7, Photoshop

Restricted use: ChemWindow, ISIS-Draw

Unusable: *.doc files, Excel graphics, C-Design, Origin, ClarisDraw, ChemIntosh, MacDraw Pro

Acceptable formats of all graphics programs: TIFF, WMF, BMP, CDX, CDR.

Files of scanned line graphics can be accepted at a minimum resolution of 1000 dpi, for scanned halftones, 300 dpi, and scanned line/tones.

Copyright guidelines

Upon acceptance of an article, Authors will be asked to transfer copyright. This transfer will ensure the widest possible dissemination of information. A letter will be sent to the corresponding Author confirming receipt of the manuscript. A form facilitating transfer of copyright will be provided. If excerpts from other copyrighted works are included, the Author(s) must obtain written permission from the copyright owners and credit the source(s) in the article. Authors will be provided preprinted forms for use by Authors in these cases.

Submission of manuscripts

Please send your contribution as an e-mail attachment to:

Journal Editor, Academician Gheorghe DUCA
e-mail: chemjm@cc.acad.md

using Microsoft Word (Office 97 or higher for PCs) word processing soft.

Please prepare a single file (allowed formats: *.doc or *.rtf) containing on a separate page a short accompanying letter to the Editor, justifying why your article should appear in "Chemistry Journal of Moldova. General, Industrial and Ecological Chemistry", followed by the article body with all schemes, figures, tables integrated in the text (though not crystallographic CIF files). On the last page of this file please provide the Graphical Abstract. Submission of figures and artwork in separate files is mandatory in their native formats.

Authors should indicate the field of chemistry of their paper (see below) as well as the nature of contribution (Short Communication, Full Paper or Review Article) in their accompanying letters, along with their mailing address, daytime phone number and fax if available. Authors will be notified by email if their contribution is received and accepted.

Editorial office:

Institute of Chemistry, Academy of Sciences of Moldova, Str. Academiei, 3, MD-2028, Chisinau, Republic of Moldova.
e-mail: chemjm@cc.acad.md
Fax: +373 22 739954
Tel: + 373 22 725490

Proofs: Proofs will be dispatched via e-mail and should be returned to the publisher with corrections as quickly as possible, normally within 48 hours of receipt.

Fields of research:

1. Analytical chemistry
2. Ecological chemistry
3. Food chemistry
4. Industrial chemistry
5. Inorganic and coordination chemistry
6. Natural product chemistry and synthesis
7. Organic chemistry
8. Physical chemistry and chemical physics
9. Supramolecular chemistry

A CONTRIBUTION TO "CHEMISTRY JOURNAL OF MOLDOVA. GENERAL, INDUSTRIAL AND ECOLOGICAL CHEMISTRY" (14 pt Bold, All CAPITALS)

First Author[a], Second Author[a]*, and Third Author[b] (12 pt Normal) (no titles please)

[a]*First Organization, First Address (9 pt, Italic)*

[b]*Second Organization; Second Address (9 pt, Italic)*

** E-mail, phone and fax numbers of the corresponding author*

Abstract: This document is an example of a contribution to be submitted to "Chemistry Journal of Moldova. General Industrial and Ecological Chemistry". This is the abstract in font size: 9 pt with the heading in bold. Please use the Times New Roman font. The title is in size 14 pt Bold (all capital letters), the names of the authors are in size 12 pt Normal and the name of the organization and its address are in size 9 pt Italic. The rest of the text is in single-space, typed in a one column layout and font size 10 pt.

Keywords: Insert a maximum of 5 keywords that will facilitate database searching.

1. Introduction (Headings - 10 pt Bold)

Contributions should comprise an even number of pages**.** There are no limits to the contribution size. Authors are also kindly requested to adhere to the formatting instructions for font size and layout.

2. How to prepare your paper

In MS Word, under the *File* menu, choose *Page setup* and set the *Top, Bottom, Left* & *Right Margins* as 2.5 cm, the *Gutter* as 0 cm, and the *Header* and *Footer* to 1.2 cm and choose *Apply to: Whole Document.* Then select the *"Paper Size"* tab and set the *Paper Size: A4* and *Orientation: Portrait.*

3. Figures and Tables

Figure and table titles must be typed in bold and should appear below the figures and above the tables.

4. Equations

Please use *italics* for symbols, bold face for vectors and normal fonts for standard functions (i.e. log, In, exp) and subscripts (i.e. I_{app}).

5. Acknowledgments (optional)

You can acknowledge certain collaborators, funds or programs who contributed in a way to the research described in the paper.

6. References

References should be numbered in the text in the order they are cited [1]. Multiple consecutive references may be abbreviated as [2-5]. The following style must be used for all contributions:

[1] Barton, D. H. R.; Yadav-Bhatnagar, N.; Finet, J.-P.; Khamsi, J. Tetrahedron Lett. 1987, 28, 3111–3114.
[2] Katritzky, A. R. Handbook of Organic Chemistry; Pergamon: Oxford, 1985; pp 53–86.
[3] Cato, S. J. Ph.D. Thesis, University of Florida, 1987.

7. Graphical Abstract

Please, supply a graphical abstract that will include title, authors (with the same formatting as in the article) and graphical abstract body. The whole graphical abstract should be kept within an area of 5cm by 17cm. The graphical abstract must be on a separate page integrated in the article file.

8. How to submit your document

Please send your contribution as an e-mail attachment to Journal Editor, Academician Gheorghe DUCA (e-mail: chemjm@cc.acad.md), using Microsoft Word (Office 97 or higher for PCs).
Please prepare a single file (allowed formats: *.doc or *.rtf) containing all schemes, figures, tables integrated in the text (though not crystallographic CIF files). In this file, please include on a separate page an accompanying letter justifying why your article should appear in "Chemistry Journal of Moldova. General, Industrial and Ecological Chemistry". Submission of figures and artwork in separate files is mandatory in their native formats.

ISNN 1857-1727

No. 1, 2007
Volume 2